Understanding the Role of Mitochondrial Remodeling during Myogenesis, Post-natal Muscle Growth, and Disuse Atrophy

By

Fasih Ahmad Rahman

A thesis

presented to the university of Waterloo

in fulfillment of the

thesis requirement for the degree of

Doctor of Philosophy

in

Kinesiology

Waterloo, Ontario, Canada, 2024

© Fasih Ahmad Rahman 2024

Examining Committee Membership

The following served on the Examining Committee for this thesis. The decision of the Examining Committee is by majority vote.

External Examiner	Dr. Keir Menzies Professor – Interdisciplinary School of Health University of Ottawa, Ottawa, Ontario, Canada
Supervisor	Dr. Joe Quadrilatero Professor – Department of Kinesiology and Health Sciences University of Waterloo, Waterloo, Ontario, Canada
Internal Members	Dr. Russ Tupling Professor – Department of Kinesiology and Health Sciences University of Waterloo, Waterloo, Ontario, Canada
	Dr. Michaela Devries-Aboud Associate Professor – Department of Kinesiology and Health Sciences University of Waterloo, Waterloo, Ontario, Canada
Internal-external Member	Dr. Paul Craig Associate Professor – Department of Biology University of Waterloo, Waterloo, Ontario, Canada

Author's Declaration

This thesis consists of data, all of which I authored or co-authored: see **Statement of Contributions** included in the thesis. This is a true copy of the thesis, including any required final revisions, as accepted by my examiners.

I understand that my thesis may be made electronically available to the public.

Statement of Contribution

Chapter 1 was written by Fasih Rahman as part of his comprehensive examination in September 2020 and edited by Joe Quadrilatero.

Chapter 2 experiments were designed by Fasih Rahman and Joe Quadrilatero. Fasih performed the experiments, analyzed data, and generated figures. Darin Bloemberg generated the *Bnip3*$^{-/-}$ cell line used for these experiments. Jasmine Yap and Tyler Joseph assisted with confocal imaging. Amanda Adams assisted with immunoblotting. Sarah Chapman assisted with cell staining. This chapter was written by Fasih Rahman and edited by Joe Quadrilatero.

Chapter 3 experiments were designed by Fasih Rahman and Joe Quadrilatero. Fasih performed the experiments, analyzed data, and generated figures. Mackenzie Graham assisted with fiber type analyses. Amanda Adams assisted with immunoblotting. This chapter was written by Fasih Rahman and edited by Joe Quadrilatero.

Chapter 4 experiments were designed by Fasih Rahman and Joe Quadrilatero. Fasih performed the experiments, analyzed data, and generated figures. Mackenzie Graham assisted with fiber type analyses. Emma Juracic assisted with *ex vivo* muscle contractility measurements. This chapter was written by Fasih Rahman and edited by Joe Quadrilatero.

Chapter 5 was written by Fasih Rahman and edited by Joe Quadrilatero.

Abstract

Mitochondria are characterized as the chemical factory of cells. This organelle is fundamental to life and death, by generating chemical energy (i.e., ATP) and regulating cellular stress responses. Importantly, mitochondria have evolved elegant mechanisms to respond to numerous stressors/stimuli. These stressors/stimuli including metabolic and oxidative stress elicit differential responses at the mitochondria level, which is accompanied by a change in its structure and function. Collectively, the change in mitochondrial structure and function is termed mitochondrial remodeling. At the organelle level, the dynamic balance of mitochondrial morphology (i.e., fission/fusion balance) coupled with mitochondrial turnover (i.e., biogenesis and mitophagy) is required for appropriate mitochondrial remodeling. These remodeling processes must occur in a controlled manner to prevent excessive activation of downstream mitochondrial apoptotic signaling events. Although the primary function of mitochondria is to produce energy; their behaviour and response to stressors/stimuli can vary between different tissues. This is particularly relevant in tissues with high metabolic demand, such as skeletal muscle. Within skeletal muscle, there are phenotypically distinct myofibers (e.g., slow-twitch and fast-twitch), and within each myofiber, there are distinct pools of mitochondria (e.g., subsarcolemmal and intermyofibrillar). Given the uniqueness and complexity of skeletal muscle mitochondria, there are several unknowns with respect to mitochondrial remodeling in skeletal muscle. Therefore, the studies in this thesis were designed to better understand mitochondrial remodeling during three important stages: skeletal muscle formation (myogenesis), postnatal muscle growth, and disuse muscle atrophy. **Chapter 1** provides a literature review of

mitochondria, mitochondrial quality control, skeletal muscle mitochondria and mitochondrial remodeling during myogenesis, postnatal muscle growth, and disuse atrophy.

Chapter 2 is focused on understanding the interaction between mitochondrial dynamics and turnover during myogenesis *in vitro*. Overexpression of the fission protein DNM1L increased mitochondrial network fragmentation and enhanced mitophagic flux during myogenic differentiation of C2C12 cells, resulting in smaller myotubes without impairing the myogenesis. Despite these morphological changes, DNM1L overexpression did not affect the levels of mitochondrial turnover proteins. In contrast, DNM1L knockdown reduced mitochondrial fragmentation and mitophagic flux, significantly impairing myogenesis and increasing mitochondrial apoptotic signaling. This knockdown also diminished mitochondrial biogenesis and mitophagy signaling. Overexpression of BNIP3 in fission-deficient (DNM1L knockdown) cells promoted mitophagic flux and reduced mitochondrial apoptotic signaling without impacting myogenesis. BNIP3 overexpression also suppressed PPARGC1A levels but did not affect other mitochondrial or mitophagy-related proteins. Finally, PPARGC1A overexpression worsened myogenic defects in fission-deficient cells, independent of changes in mitophagy or mitochondrial protein levels. These findings demonstrate that optimal mitochondrial fission is crucial for regulating both mitophagy and biogenesis during myogenesis.

Chapter 3 then explored the role of mitochondrial remodeling on postnatal skeletal muscle growth. RNA sequencing analyses identified BNIP3 as the only gene differentially expressed and associated with mitochondrial remodeling during postnatal development, which was characterized by an upregulation of metabolic genes and a downregulation of those involved in cell growth and differentiation. *In vivo* experiments revealed significant increases in body mass,

muscle mass, and myofiber cross-sectional area, with mass doubling between P21 and P42. Mitochondrial maturation during this period was evidenced by increased maximal respiration, reduced electron leak, and elevated mitophagic flux, along with increased mitochondrial localization of autophagy and mitophagy proteins. Cellular signaling revealed an increase in anabolic signaling, which was accompanied by enhanced mitophagy and fusion signaling and a simultaneous decrease in mitochondrial biogenesis signaling. In skeletal muscle-specific *Atg7* knockout mice, there were no changes in body or muscle mass, nor in mitochondrial function; however, compensatory hypertrophy of type IIX fibers was observed despite ablated mitophagic flux. These mice exhibited compensatory activation of alternative degradative enzymes, including mitochondrial apoptotic signaling and ubiquitin-proteasome signaling, suggesting a shift in degradative pathways to preserve muscle mass and function in young mice. These findings demonstrate that postnatal development is marked by increased mitochondrial activity and mitophagy. Furthermore, while constitutive autophagy deficiency abolishes mitophagic flux, it does not impair muscle growth in young mice.

Chapter 4 examined the role of mitochondrial remodeling with an emphasis on mitophagy during disuse atrophy of mature skeletal muscle. RNA sequencing analyses reveal an upregulation of genes associated with protein degradation, particularly those linked to the ubiquitin-proteasome system and apoptosis, while downregulating genes involved in muscle development and mitochondrial components. Immobilization-induced muscle atrophy affected the large muscles of the hindlimb, with partial recovery following remobilization. Notably, type IIA fibers regained mass after remobilization, whereas type IIX and IIB fibers did not recover. Immobilization increased mitophagic flux, which remained elevated following remobilization,

alongside a reduction in mitochondrial function, evidenced by decreased maximal respiration and increased reactive oxygen species (ROS) emission. The mitophagy receptor BNIP3 localized to mitochondria during both immobilization and remobilization phases. Immobilization also enhanced mitochondrial apoptotic signaling, with increased mitophagy and suppressed mitochondrial biogenesis signaling. Treatment with N-acetylcysteine during immobilization exacerbated atrophy in type IIX and IIB fibers, yet suppressed mitophagic flux, enhanced mitochondrial function, and reduced ROS emission without significantly altering markers of mitochondrial remodeling or the localization of autophagy/mitophagy-related proteins. Colchicine treatment during immobilization also led to atrophy in type IIX and IIB fibers, inhibiting mitophagic flux without affecting mitochondrial tagging with mitophagy or apoptosis-related molecules. Colchicine treatment was accompanied by suppressed mitochondrial function, likely due to the accumulation of dysfunctional mitochondria. Together, these findings suggest that mitophagy protects against excessive atrophy is muscle due to immobilization.

Finally, **Chapter 5** integrates and summarizes the findings from all the studies and highlights the physiological implications. Overall, these insights suggest that targeted therapeutic strategies aimed at enhancing the coordination of mitochondrial remodeling processes could optimize skeletal muscle function. Such strategies would focus on stabilizing the balance between mitochondrial fission and fusion, ensuring efficient mitophagic clearance of damaged or dysfunctional mitochondria, and promoting mitochondrial biogenesis to maintain a healthy mitochondrial network in skeletal muscle cells and tissues.

Acknowledgements

To my supervisor and mentor, Dr. Joe Quadrilatero, my gratitude extends far beyond what words can express. The work I have accomplished in the Skeletal Muscle Biology and Cell Death Lab would not have been possible without your unwavering support. I am deeply thankful for our many conversations, which not only provided direction but also helped me "see the bigger picture." Thank you for offering me a rigorous training experience, the necessary resources, and the freedom to explore my interests in this field. I hope to carry these lessons forward as I develop my own research program and pass this knowledge on to the next generation of scientists.

Thank you to my examination committee members, Drs. Keir Menzies, Paul Craig, Russ Tupling, and Michaela Devries-Aboud, for your thoughtful insights and detailed feedback.

I am also incredibly fortunate to have worked alongside many talented students in the Quad Lab, including Mackenzie Graham, Alex Truong, Amanda Adam, Jasmine Yap Friedrich, Tyler Joseph, Sarah Chapman, Emma Teszner, Autumn Lif, James Thoms, Dylan Hian-Cheong, and Zinnia Cheung. Thank you all for your support in the lab, for helping generate data, assisting with analyses, and enriching my overall experience.

I also want to thank my collaborators from the SERCA Lab (Tupling Lab: Emma Juracic, Paige Chambers, Adi Brahmbhatt, and Mark Valentim), METS Lab (Devries-Aboud Lab: Vito Pipitone, Jennifer Wilkinson), Lipid Discovery Lab (Duncan Lab: John Chan, Michelle Tomczewski, Antonia Berdeklis, Musa Musa, Alex Cocco and Ash Hashemi), Biomechanics (Callaghan Lab: Jessa Davidson, Jackie Zehr, Jeff Barrett, and Dan Viggiani) Physics (Leonenko Lab: Irina Bukhteeva), Engineering (Poudineh Lab: Fatemeh Keyvani, Hanjia Zheng, and Sadegh Sadeghzadeh), York University (Perry Lab: Catherine Bellissimo, Luca Delfinis, Shivam Gandhi, and Shahrzad Khajehzadehshoushtar), and Queen’s University (Gurd Lab: Hashim Islam, Eveline

Menezes, and Lauren Pacitti) for all the great conversations and opportunity to expand my knowledge.

I would like to express my gratitude to the Natural Sciences and Engineering Research Council Canada Graduate Scholarship Program, the Ontario Graduate Scholarship Program, and the University of Waterloo President's Graduate Scholarship Program for collectively funding my doctoral studies.

Beyond academia, I am deeply thankful for the unwavering support of my wonderful wife, Sarah, my mother (the original Dr. Rahman), and my sister, Natasha. Without their love and encouragement, I wouldn't be where I am today.

Table of Contents

Examining Committee Membership ii

Author's Declaration iii

Statement of Contribution iv

Abstract v

Acknowledgements ix

List of Figures xiv

List of Abbreviations xvi

Chapter 1: Introduction and Literature Review *1*

The Mitochondria 2

Mitochondrial Structure 2

Mitochondrial Function 4

Mitochondrial Quality Control and Life Cycle 5

Mitochondrial Biogenesis 7

Mitochondrial Fission and Fusion 9

Mitochondrial Degradation 11

Mitochondrial Regulation of Apoptosis 14

Mitochondria in Skeletal Muscle 16

Mitochondrial Subpopulations in Skeletal Muscle 16

Fiber type Differences in Mitochondrial Profile 18

Understanding Mitochondrial Remodeling in Skeletal Muscle 19

Mitochondrial Remodeling During Myogenesis 19

Mitochondrial Remodeling Regulates Skeletal Muscle Growth 21

Mitochondrial Remodeling During Skeletal Muscle Atrophy 24

Overall Purpose and Objectives 27

Chapter 2: Role of Mitochondrial Remodeling During Myogenesis *30*

Project Rationale and Objectives 31

Introduction 34

Material and Methods 36

Cell culture 36

Adenovirus Amplification and Precipitation 37

Adenoviral Transduction of Myoblasts 37

Immunoblotting 38

Immunocytochemistry 38

Flow Cytometry 39

Confocal Microscopy 40

Mitochondrial Network Analysis 40

Caspase and Calpain Activity Assay 41

Statistics 41

Results 42

Discussion 66

Conclusion 74

Chapter 3: Role of Mitochondrial Remodeling During Postnatal Muscle Development ***75***

Project Rationale and Objectives 76

Introduction 78

Material and Methods 80

RNA Sequencing Analysis 80
Animals 80
Isolation of Skeletal Muscle 81
Live Myofiber Imaging and Mitophagy Flux Analyses 82
High-Resolution Respirometry with Simultaneous ROS Measurements 82
Mitochondrial Fractionation 83
Immunoblotting 84
Caspase, Calpain, and Proteasomal Activity Assay 85
Immunofluorescence Fiber Type Analysis 85
Grip Strength Measurement 86
Statistics 86

Results 87

Discussion 105

Conclusion 114

Chapter 4: Role of Mitochondrial Remodeling During Immobilization-induced Muscle Atrophy ***115***

Project Rationale and Objectives 116

Introduction 119

Material and Methods 121

RNA Sequencing Analysis 121
Animals 121
Hindlimb Immobilization and Drug Treatment 122
Isolation of Skeletal Muscles 122
Live Myofiber Imaging and Mitophagy Flux Analysis 123
High-Resolution Respirometry with Simultaneous ROS Measurements 123
Mitochondrial Fractionation 124
Immunoblotting 125
Caspase, Calpain, and Proteasomal Activity Assay 126
Immunofluorescence Fiber Type Analysis 126
Skeletal Muscle Contractility 127
Statistics 127

Results 128

Discussion 150

Conclusion 161

Chapter 5: Summary and Conclusion ***162***

Perspective 163
Chapter 2 Summary 164

Chapter 3 Summary ____ 165
Chapter 4 Summary ____ 166
Broad Summary ____ 167
Mitochondrial Fission Regulates Mitophagy and Biogenesis ____ 171
Temporal Modulation of Mitochondrial Remodeling in Skeletal Muscle ____ 173
Apparent Elevation of Mitophagy in Muscle Growth and Atrophy ____ 176
The Recurring Role of BNIP3 in Muscle Growth and Atrophy ____ 178
Relevance to Human Physiology ____ 180
Limitations ____ 183
Future Directions ____ 184
Conclusion ____ 186

References ____ 188

List of Figures

Chapter 1:

Figure 1: Structure of the mitochondria. 4
Figure 2: Mitochondria life cycle. 7
Figure 3: Conceptual image of study design. 29

Chapter 2:

Method Figure 1: Study design for Project 1, Objective 1. 32
Method Figure 2: Study design for Project 1, Objective 2. 33
Method Figure 3: Study design for Project 1, Objective 3. 33

Figure 1: DNM1L OE induces mitochondrial fragmentation and upregulation of mitophagy during myogenesis. 43
Figure 2: DNM1L OE does not modify myogenesis but reduces myotube size. 45
Figure 3: Molecular changes in mitochondrial remodeling proteins in response to DNM1L OE. 46
Figure 4: DNM1L KD suppresses mitochondrial fission and mitophagy during myogenesis. 48
Figure 5: DNM1L KD impairs myogenic differentiation. 50
Figure 6: Molecular changes in mitochondrial remodeling proteins in response to DNM1L KD. 51
Figure 7: BNIP3 OE activates mitophagy and suppresses CASP activity in fission-deficient cells. 53
Figure 8: BNIP3 OE in fission-deficient cells does not modify myogenic differentiation. 55
Figure 9: Molecular changes in mitochondrial remodeling proteins in response to BNIP3 OE in fission-deficient cells. 56
Figure 10: PPARGC1A OE in fission deficient cells exacerbates myogenic defects associated with fission-deficiency. 58
Figure 11: Molecular changes in mitochondrial remodeling proteins in response to PPARGC1A OE in fission-deficient cells. 60
Figure 12: DNM1L OE in *Bnip3*$^{-/-}$ cells increases mitochondrial fragmentation and mitophagy. 62
Figure 13: DNM1L OE in *Bnip3*$^{-/-}$ cells does not modify myogenic differentiation. 64
Figure 14: Molecular changes in mitochondrial remodeling proteins in response to DNM1L OE in *Bnip3*$^{-/-}$ cells. 65

Chapter 3:

Method Figure 1: Study design for Project 2, Objectives 1 and 2. 77

Figure 1: RNA sequencing analysis of gastrocnemius-plantaris muscle during development. 89
Figure 2: Changes in skeletal muscle during postnatal development of mt-Keima mice. ..91

Figure 3: Postnatal development-associated changes in mitophagy and mitochondrial function. 93
Figure 4: Quantitative analysis of upstream kinases in skeletal muscle during development. 95
Figure 5: Quantitative analysis of mitochondrial remodeling proteins in skeletal muscle during development. 97
Figure 6: Developmental changes in muscles from young CTRL (*Atg7*$^{f/f}$) and skmKO (*Atg7*$^{f/f}$:ACTA1-Cre) mice. 99
Figure 7: Postnatal development-associated changes in mitophagy and mitochondrial function in young autophagy-deficient skeletal muscle. 101
Figure 8: Quantitative analysis of upstream kinases in young autophagy-deficient skeletal muscle. 103
Figure 9: Quantitative analysis of mitochondrial remodeling proteins in young autophagy-deficient skeletal muscle. 104

Chapter 4:

Method Figure 1: Study design for Project 3, Objective 1. 117
Method Figure 2: Study design for Project 3, Objective 2. 117
Method Figure 2: Study design for Project 3, Objective 3. 118

Figure 1: RNA sequencing analysis of control (CTRL) and immobilized (IM) gastrocnemius muscle. 130
Figure 2: Immobilization- and remobilization-induced changes in skeletal muscle structure and mitophagic flux. 133
Figure 3: Quantitative analysis of autophagy and mitophagy proteins in IM and RM muscles. 135
Figure 4: Quantitative analysis of mitochondrial remodeling proteins in IM and RM muscles. 139
Figure 5: Effect of N-acetyl cysteine (NAC) treatment on immobilized muscles. 141
Figure 6: Quantitative analysis of autophagy and mitophagy proteins in VEH and NAC treated immobilized muscles. 142
Figure 7: Quantitative analysis of mitochondrial remodeling proteins in VEH and NAC treated immobilized muscles. 144
Figure 8: Effect of colchicine (COL) treatment on immobilized muscles. 146
Figure 9: Quantitative analysis of autophagy and mitophagy proteins in VEH and COL treated immobilized muscles. 148
Figure 10: Quantitative analysis of mitochondrial remodeling proteins in VEH and COL treated immobilized muscles. 149

List of Abbreviations

4HNE	4-Hydroxynonenal
ADP	Adenosine diphosphate
AIFM1	Apoptosis inducing factor mitochondria associated 1
AKT1	AKT Serine/Threonine Kinase 1
AMPK	AMP-activated protein kinase
ANT1	Adenine Nucleotide Translocator 1
APAF1	Apoptosis peptidase activating factor 1
ATG5	Autophagy-related gene 5
ATG7	Autophagy-related gene 7
ATP	Adenosine triphosphate
BAK1	BCL2 Antagonist/Killer 1
BAX	BCL2 Associated X
BBC3	BCL2 binding component 3
BCL2	BCL2 Apoptosis Regulator
BCL2L1	BCL2 like 1
BECN1	Beclin 1
BID	BH3 interacting domain death agonist
BNIP3	B-cell lymphoma 2 interacting protein 3
BNIP3L	BNIP3-like
CAPN	Calpain
CASP	Caspase
COX4	Cytochrome C oxidase subunit 4
CYCS	Cytochrome C
DEG	Differentially expressed genes
DFFA	DNA fragmentation factor alpha
DFFB	DNA fragmentation factor beta
DMD	Dystrophin
DNM1L	Dynamin 1-like
$\Delta\Psi_m$	Mitochondrial membrane potential
EDL	Extensor Digitorum Longus
ENDOG	Endonuclease G
ER	Endoplasmic Reticulum
ERR	Estrogen related receptor
ETC	Electron transport chain
FBXO32	F-box protein 32
FIB-SEM	Focus ion beam scanning electron microscopy
FIS1	Mitochondrial fission 1
FOXO3A	Forkhead box O3

GADD45A	Growth arrest and DNA damage inducible alpha
GAS	Gastrocnemius
GFP	Green fluorescent protein
GO	Gene Ontology
GS	Gastrocnemius-soleus complex
IMF	Intermyofibrillar
IMM	Inner mitochondrial membrane
MAP1LC3	Microtubule-associated protein 1 light chain 3
MCAT	Mitochondrial Catalase
MFF	Mitochondrial fission factor
MFN	Mitofusin
mH2O2	Mitochondrial Hydrogen Peroxide
MICOS	Mitochondrial contact site and cristae organizing system
MID49/51	Mitochondrial dynamics protein of 49/51kDa
MOI	Multiplicity of Infection
MOMP	Mitochondrial outer membrane permeability
MRF	Myogenic regulatory factor
mtDNA	Mitochondrial DNA
MTFP1	Mitochondrial fission process 1
MTG	Mitotracker Green
MYOD1	Myogenic differentiation 1
MYOG	Myogenin
nDNA	Nuclear DNA
NRF	Nuclear respiratory factor
OCR	Oxygen Consumption Rate
OMA1	OMA1 zinc metalloproteinase
OMM	Outer mitochondrial membrane
OPA1	Optic-atrophy 1
OXPHOS	Oxidative phosphorylation
P70S6K	70 KDa Ribosomal Protein S6 Kinase 1
PARL	Presenilin-associated rhomboid-like
PAX3	Paired box 3
PAX7	Paired box 7
Pi	Inorganic phosphate
PINK1	PTEN-induced kinase 1
PPARGC1A	Peroxisome proliferator-activated receptor (PPAR)-gamma coactivator-1 alpha
PPARGC1B	Peroxisome proliferator-activated receptor (PPAR)-gamma coactivator-1 beta
PRKN	Parkin
QUAD	Quadriceps
RHEB	Ras homolog, MTORC1 binding

RNASeq	RNA Sequencing
ROS	Reactive oxygen species
SOD	Superoxide Dismutase
SQSTM1	Sequestosome 1
SR	Sarcoplasmic reticulum
SS	Subsarcolemmal
TA	Tibialis Anterior
TFAM	Mitochondrial transcription factor A
TFBM	Mitochondrial transcription factor B
TMRE	Tetramethylrhodamine, ethyl ester
TRIM63	Tripartite motif containing 63
ULK1	Unc-51 like autophagy activating kinase 1
UPR^{mt}	Mitochondrial unfolding protein response
UPS	Ubiquitin proteasome system
VDAC1	Voltage dependent anion channel 1
YME1L1	YME1 like 1 ATPase

Chapter 1: Introduction and Literature Review

The Mitochondria

Mitochondria have long been characterized as a chemical factory of the cell. Since its first description as "bioblasts" in 1894 by Richard Altmann (Altmann, 1894), tremendous strides have been made over the last century to better understand this organelle. Mitochondria are primarily responsible for producing ATP, the main chemical energy source, through oxidative phosphorylation (OXPHOS). This process involves the transfer of electrons from coenzymes across a series of membrane-bound complexes, culminating in the reduction of oxygen to water. The generated membrane potential ($\Delta\Psi_m$) from this electron transport is essential for synthesizing ATP from ADP and inorganic phosphate (Pi). Beyond energy production, mitochondria are involved in several other critical processes, including the synthesis of amino acids, heme groups, iron-sulfur clusters, and phospholipids (Kühlbrandt, 2015; Spinelli & Haigis, 2018). They also play key roles in calcium signaling and stress responses, making them vital signaling hubs and central components in both physiology and pathology.

Mitochondrial Structure

Mitochondria are separated from the cytoplasm by two membranes – the outer mitochondrial membrane (OMM) and the inner mitochondrial membrane (IMM) (Kühlbrandt, 2015). The OMM is porous and allows for transport of ions and neutrally charged molecules through channel proteins called porins (Figure 1). One well characterized porin is the voltage-dependent anion channel (VDAC) that is a major integral protein found on the OMM and serves as a gatekeeper for the entry and exit of mitochondrial metabolites (Camara et al., 2017). Given its porous nature, the OMM does not hold a membrane potential. In contrast to the OMM, the regulation of ions and molecules across the IMM is tightly regulated. As a result, transport proteins

are required to assist the movement of these molecules, including members of the SLC25A superfamily of proteins (Ruprecht & Kunji, 2020). Furthermore, the selectivity of the IMM enables the generation of a transmembrane potential (~180mV) that is generated primarily with the help of the respiratory chain (discussed later). OXPHOS protein complexes are primary located along the invaginations of the IMM, called cristae. Mitochondrial contact site and cristae organizing system (MICOS) proteins are needed to anchor the cristae junctions to contact sites on the OMM to maintain normal cristae morphology (Khosravi & Harner, 2020). Interestingly, the cristae density and morphology can vary between tissues. For instance, tissues with high metabolic demand, such as the heart and skeletal muscle, form “stacked” cristae (Kappler et al., 2019; Kühlbrandt, 2015). In contrast to tissues with highly structured mitochondria, organs such as the liver and kidneys have mitochondria with less "stacked" cristae. This results in a larger mitochondrial matrix, which is crucial for the biosynthetic processes unique to these tissues (Kappler et al., 2019; Kühlbrandt, 2015). Consequently, any defects in the IMM architecture can lead to misdistribution of respiratory complexes and potential loss of mitochondrial function (Friedman et al., 2015).

While mitochondria are often depicted as static "jellybean"-shaped structures within cells, they are in fact highly dynamic and continuously undergoing fission and fusion. The extent of these processes can vary depending on the tissue type and cellular conditions. For example, mitochondria may experience increased fission in response to mitochondrial toxins, such as chemotherapy drugs. A key function of mitochondrial fusion is to facilitate communication and complementation between organelles, likely serving to protect the mitochondrial pool (Friedman & Nunnari, 2014). Nonetheless, the dynamic nature of the mitochondria is associated with changes in mitochondrial function. For instance, mitochondrial fusion allows for an elongated

mitochondrial network, with more complex cristae, and is associated with the preservation of mitochondrial bioenergetics (Sgarbi et al., 2014). Conversely, mitochondrial fission results in smaller, less functional mitochondria that exhibit lower respiration rates, and lower $\Delta\Psi_m$. Together, the precise balance of mitochondrial morphology plays a central role in regulating its function within cells.

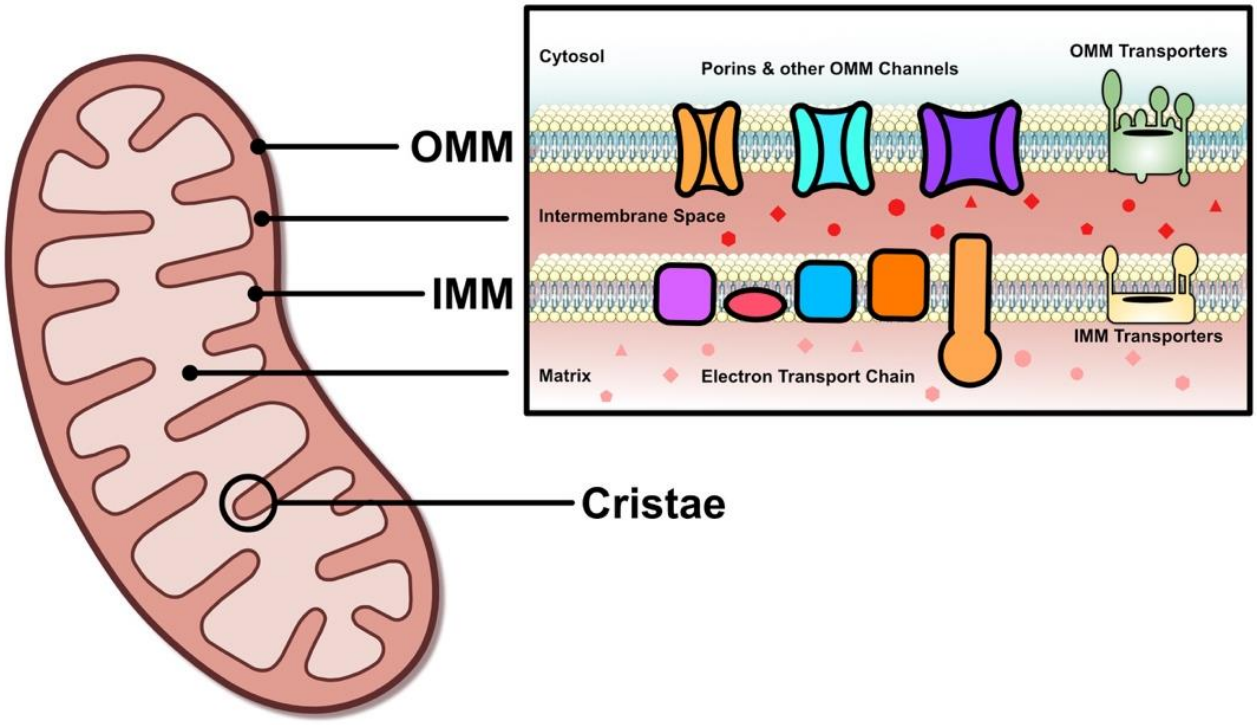


Figure 1: Structure of the mitochondria. The outer mitochondrial membrane (OMM) separates the mitochondria from the cytosol and is comprised of porins, channels, and ion/protein transporters. The OMM surrounds the inner mitochondrial membrane (IMM) with the space in between being defined as the intermembrane space. The IMM also separates the mitochondrial matrix from the intermembrane space. The electron transport chain is found on the IMM along with other transporters.

Mitochondrial Function

Mitochondria generate energy through OXPHOS. A proton gradient is produced across the IMM by three major membrane-bound complexes known as complex I (NADH/ubiquinone oxidoreductase), complex III (cytochrome c reductase), and complex IV (cytochrome c oxidase) (Garcia-Vallve, 2004). The transfer of electrons from complex I begins with the oxidation of

NADH (Garcia-Vallve, 2004; Schultz & Chan, 2001). The energy from this reaction enables the pumping of four protons into the IMS/cristae lumen. The electrons are transferred and reduce ubiquinone (Trumpower, 1990). Complex III takes the electrons from the reduced ubiquinone and transfers them to a small molecule called cytochrome c (CYCS) while pumping two protons into the IMS (Trumpower, 1990). In doing so, the oxidized ubiquinone can cycle back to complex I to continue this process (Trumpower, 1990). Nonetheless, complex IV transfers the electrons from the reduced CYCS to molecular oxygen and pumps four additional protons into the IMS (Berry et al., 2000). Compared to these complexes, complex II (succinate dehydrogenase) transfers electrons from succinate directly to ubiquinone, without contributing to the proton gradient (Garcia-Vallve, 2004; Schultz & Chan, 2001). Together, the respiration through complexes I-III-IV pumps 10 protons, while complex II-III-IV pumps 6 protons into the IMS. This generates a membrane potential, which is essential for ATP production, ROS generation, ion/substrate transport, and mitochondrial quality control mechanisms (Alexandre et al., 1978; Kühlbrandt, 2015; Madeira, 2012).

Mitochondrial Quality Control and Life Cycle

Mitochondria have evolved elegant mechanisms to respond to various stressors. Quality control of mitochondria can occur at various levels (Tatsuta & Langer, 2008). For example, mitochondria can regulate cellular quality control by inducing apoptosis in defective cells to protect neighboring cells/tissues. At the organelle level, the dynamic balance of fission/fusion and mitochondrial turnover (biogenesis and mitophagy) ultimately dictates the health of the mitochondrial pool within cells (Tatsuta & Langer, 2008). At the molecular level, mitochondrial quality control can be regulated through other mechanisms like the antioxidant pathways and

mitochondrial unfolding protein response (UPR^{mt}) to maintain mitochondrial integrity and limit the extent of quality control at the organelle level (Fischer et al., 2012; Franco-Iborra et al., 2018; Kumar & Reichert, 2021; Tatsuta & Langer, 2008). The collective purpose of mitochondrial quality control mechanisms is to preserve mitochondrial integrity, including maintaining normal $\Delta\Psi_m$ and bioenergetic function.

Mitochondria exist as a dynamic network that is govern by the four major processes: biogenesis, fission, fusion, and mitophagy. The expansion of the mitochondrial pool, termed biogenesis, is accompanied by increased respiration, metabolic processes, and ATP production, while autophagic degradation of mitochondria (mitophagy) is needed to remove damaged or unnecessary mitochondria (Figure 2). The balance between biogenesis and mitophagy is important in modulating cell survival and cell fate in various physiological and pathological states (Baechler et al., 2019; Bernardini et al., 2017; Bloemberg & Quadrilatero, 2019; LeBleu et al., 2014; Rimbaud et al., 2009; Salem et al., 2012; Schumacker et al., 2014; Zhou et al., 2015). The elongation (fusion) and division (fission) of mitochondria serve as a bridge between biogenesis and mitophagy. For instance, mitochondrial fusion prevents mitophagy while fission is an important preceding step needed for mitophagy (Burman et al., 2017; Lee et al., 2011). Furthermore, mitochondrial fusion can promote the survival of damaged mitochondria through complementation of mitochondrial DNA (mtDNA), whereas fission can remove damaged parts of the mitochondrial network, thereby preventing the entire network from sustaining major damage (Bloemberg & Quadrilatero, 2019).

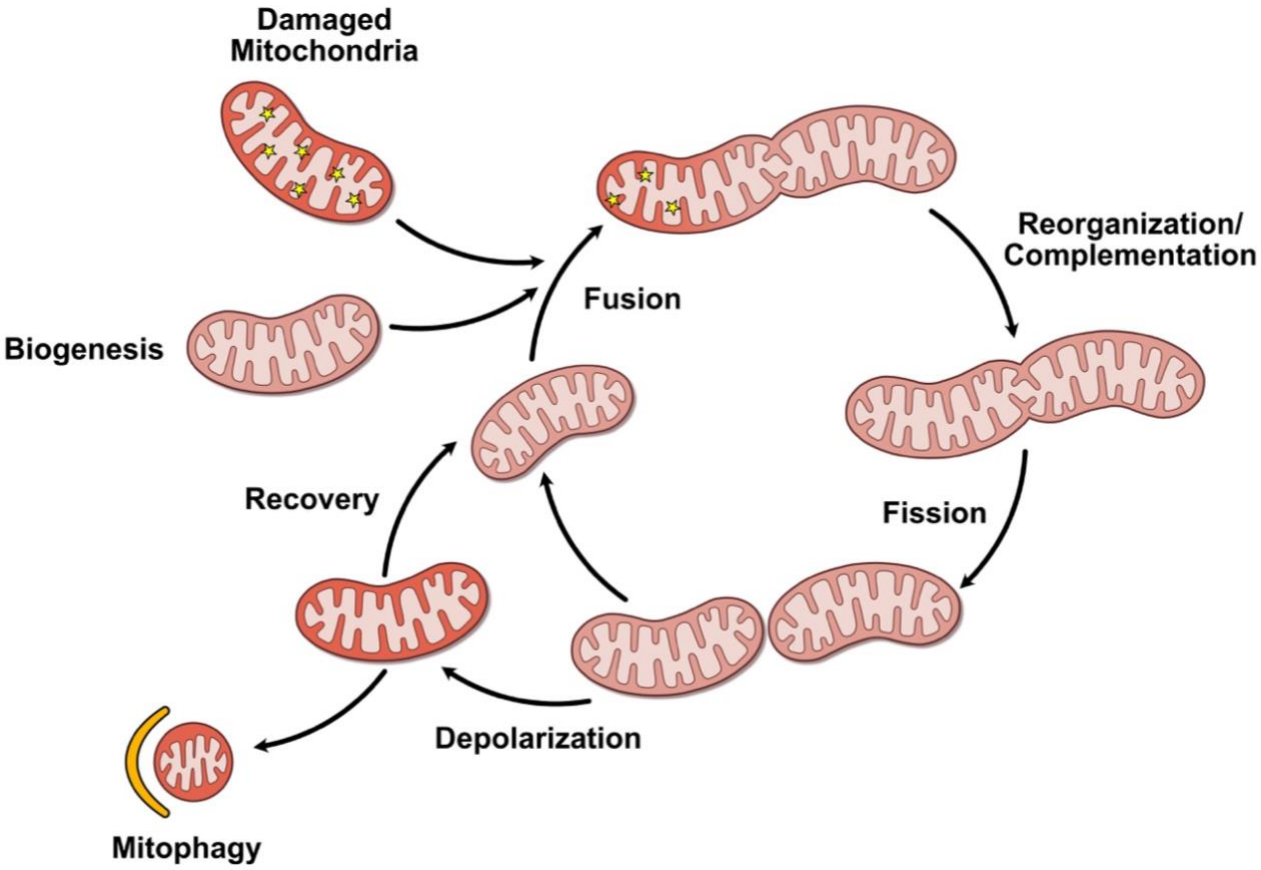


Figure 2: Mitochondria life cycle. The mitochondrial pool is expanded through mitochondrial biogenesis. Healthy mitochondria may fuse with other healthy mitochondria or damaged mitochondria to allow complementation and reorganization of the mitochondrial network. In response to stimuli, such as depolarization, the mitochondrial network may split via mitochondrial fission to ultimately undergo mitophagy. In some cases, the mitochondria may recover and fuse back to the existing network.

Mitochondrial Biogenesis

Mitochondrial biogenesis is a regulated process that occurs in response to a number of mitochondrial and nuclear factors. Over the last two decades, several regulators of mitochondrial biogenesis have been found. The peroxisome proliferator-activated receptor (PPAR)-gamma coactivator-1 (PPARGC1) family of transcriptional coactivators has emerged as the main components of mitochondrial biogenesis. Within this family of proteins, PPARGC1A has received the greatest attention, and thus, has been termed the "master regulator" of mitochondrial

biogenesis. PPARGC1A and other members of the PPARGC1 family interact with nuclear receptors and transcription factors to upregulate the expression of mitochondrial-related genes (Gleyzer & Scarpulla, 2011; Liang & Ward, 2006; Sonoda et al., 2007). It should be noted that mitochondrial biogenesis can occur independent of PPARGC1A; however, the extent to which alternative mechanisms are involved is still being explored.

Mechanism of PPARGC1A-dependent Mitochondrial Biogenesis

PPARGC1A is a co-transcriptional regulatory factor that is highly inducible under various physiological/pathological conditions including exercise, starvation, cold, and hypoxic stress (Liang & Ward, 2006). These conditions activate several molecular sensors, including nutrient/energy sensors and stress sensors (Rahman & Quadrilatero, 2021b), to aid in the upregulation of PPARGC1A and promote mitochondrial biogenesis (Popov et al., 2015; Rowe et al., 2010, p. 20).

The canonical mechanism of PPARGC1A-induced mitochondrial biogenesis occurs by its binding to nuclear respiratory factors (NRFs) and estrogen related receptors (ESRRs). NRFs are key components in regulating mitochondrial biogenesis, with NRF1 and nuclear factor erythroid 2 like 2 (NFE2L2 or NRF2) being the major downstream targets of PPARGC1A. The knockout of either of these factors results in embryonic lethality (Chan et al., 1998; Ristevski et al., 2004). NRF1 forms homodimers on DNA to target a broad range of genes related to the electron transport, mitochondrial membrane transport, detoxification pathway (i.e., glutathione pathway), heme biogenesis, and mitochondrial DNA replication (Ploumi et al., 2017). In contrast, NFE2L2 appears to be mitochondrial specific. NFE2L2 can transcriptionally regulate mitochondrial transcription

factor A (TFAM), mitochondrial transcription factor B (TFBM), and electron transport genes (Bruni et al., 2010).

Compared to NRFs, the physiological function of ESRRs and its relationship with PPARGC1A is less studied. PPARGC1A can target, bind, and activate ESRRA to regulate the expression of genes involved in OXPHOS, fatty acid oxidation, mitochondrial membrane transport, and mitochondrial DNA replication (Schreiber et al., 2003, 2004). Chemical inhibition of ESRRA impaired the ability of PPARGC1A to promote mitochondrial biogenesis as evidenced by a lower mtDNA:nDNA ratio (Schreiber et al., 2003, 2004). Overall, these seminal studies suggest that mitochondrial biogenesis largely occurs through a defined PPARGC1A-related mechanism that may differentially interact with other downstream transcriptional regulators.

Mitochondrial Fission and Fusion

The dynamic nature of the mitochondria occurs by the continuous cycling of fission and fusion. These processes are required in maintaining the appropriate morphology, which subsequently regulates its function. On one hand, mitochondrial fission is required for cell division to ensure equal distribution of mitochondria in daughter cells (Yamano & Youle, 2011). The fragmentation of the mitochondrial network into small puncta enables the efficient removal of damaged mitochondria via selective autophagy (mitophagy) (Twig & Shirihai, 2011; Youle & Karbowski, 2005). On the other hand, mitochondrial fusion plays an essential role in mtDNA inheritance and mitigates mitochondrial damage through complementation (H. Chen et al., 2010; Ramos et al., 2019). Given the importance of mitochondrial dynamics, it is unsurprising that impairments in these processes are associated with several diseases. Nonetheless, the following section discusses the molecular mechanism of mitochondrial fission and fusion.

Mechanism of Mitochondrial Fission and Fusion

At its core, mitochondrial fission occurs through the constriction and cutting of the mitochondrial membranes, which results in two mitochondrion (Kraus & Ryan, 2017; Ramachandran, 2018). The major player for this process is a dynamin-like GTPases protein, called dynamin 1-like protein (DNM1L or DRP1). DNM1L localizes in the cytosol but translocates to the mitochondria and interacts with several adaptor proteins found on the OMM. These include mitochondrial fission 1 (FIS1), mitochondrial fission factor (MFF), and mitochondrial dynamics protein of 49/51 kDa (MID49/51)(Kraus & Ryan, 2017; Ramachandran, 2018). Alterations in DNM1L function and/or its adaptor molecules can significantly alter the balance of mitochondrial fission and fusion. For example, the loss of these adaptor proteins, particularly MID49/51, have been shown to reduce mitochondrial fission, while favouring mitochondrial fusion (Osellame et al., 2016). Nonetheless, once bound to the adaptor molecules, DNM1L oligomerizes around the mitochondria and utilizes GTP to change its conformation and constrict the OMM (Fröhlich et al., 2013; Mears et al., 2011). In contrast to the OMM, the constriction of the inner mitochondrial membrane (IMM) is not fully understood. IMM constriction may be due to a mitochondrial fission process 1 (MTFP1) has been shown to enhance mitochondrial fission whereas the depletion of this protein results in hyperfusion (Morita et al., 2017; Tondera et al., 2005). The untethering of the mitochondrial membranes may also facilitate the IMM fission (Cho et al., 2017). Taken together, it is well understood that DNM1L mediates fission through its interaction with adaptor proteins found on the OMM, whereas the mechanism of IMM fission has yet to be fully determined.

Mitochondrial fusion is mediated by three major dynamin-like GTPase proteins: mitofusin 1 (MFN1), MFN2, and optic-atrophy 1 (OPA1). The location of these proteins on the mitochondria

dictates their function. MFN1/2 are found on the OMM while OPA1 is found on the IMM. MFN1 forms homomultimers or heteromultimers with MFN2 and undergo oligomerization to fuse the OMM (H. Chen et al., 2003). The MFN1/2 platform utilizes GTP hydrolysis to pull two OMMs together (Ishihara et al., 2004). After this, the long isoform of OPA1 (L-OPA1) mediates the fusion of the IMM through heteromultimer interaction with cardiolipin (Ban et al., 2017). The function of OPA1 extends beyond just mitochondrial fusion alone. The enzymatic conversion of L-OPA1 to its short isoform (S-OPA1) via OMA1 or YME1L1 peptidase has also been shown to aid in the dissociation of the IMM; favouring fission over fusion (Cho et al., 2017).

Mitochondrial Degradation

Mitochondria can change their structure and subsequent function to promote survival in response to cellular stress. Under high stress conditions, the mitochondria become damaged or dysfunctional; therefore, the efficient removal of damaged/dysfunctional mitochondria is require to protect cells from death (Kubli & Gustafsson, 2012). Although several mitochondrial quality control processes exist, the selective degradation of mitochondria by autophagy (i.e., mitophagy) appears to be the last line of defence before cell death (Baechler et al., 2019; Bloemberg & Quadrilatero, 2019). A lack of mitophagy has been implicated in numerous pathological conditions (Bravo-San Pedro et al., 2017, p.; Kerr et al., 2017; J. Liu et al., 2019; VanderVeen et al., 2017). Emerging evidence supports the notion that mitochondria can undergo mitophagy through various mechanisms. These redundant pathways further demonstrate the evolutionary importance of the removal of damaged mitochondria. The following section discusses the mechanism of two major categories of mitophagy.

PINK1/PRKN-mediated Mitophagy

The most studied mechanism of mitophagy is orchestrated by two proteins: a Ser/Thr kinase, PTEN-induced kinase 1 (PINK1), and the E3-ubitquitin ligase parkin (PRKN) (Matsuda et al., 2010; Narendra et al., 2010). PINK1 serves as a molecular sensor of mitochondrial depolarization by targeting and forming a complex with translocase of outer mitochondrial membrane (TOMM) (Matsuda et al., 2010; Narendra et al., 2010). Under normal conditions where membrane potential is maintained, PINK1 is partially imported into the mitochondrial matrix and undergoes initial cleavage by mitochondrial processing peptidase (MPP) (Greene et al., 2012). Following this, PINK1 is cleaved again by the IMM protein presenilin-associated rhomboid-like protein (PARL), which ultimately results in the dissociation of PINK1 from TOMM (Deas et al., 2011; Greene et al., 2012; Jin et al., 2010; Meissner et al., 2011; G. Shi et al., 2011). The double cleaved PINK1 is broken down within the cytosol via N-end rule pathway (Yamano & Youle, 2013). In damaged/depolarized mitochondria, PINK1 once again associates with TOMM; however, reduced $\Delta\Psi_m$ limits the degree of internalization (Lazarou et al., 2012; Okatsu et al., 2013). As a result, double cleavage of PINK1 does not take place and it accumulates on the OMM. As PINK1 accumulates, it becomes highly active after dimerization and autophosphorylation (Aerts et al., 2015), and recruits PRKN to the OMM (Okatsu et al., 2012, 2013).

Under resting conditions, PRKN is in an inactive/closed conformation (Chaugule et al., 2011). Upon phosphorylation of PRKN by PINK1, it changes to an active/open conformation (Chaugule et al., 2011; Iguchi et al., 2013; Kondapalli et al., 2012; Shiba-Fukushima et al., 2012). The activated PRKN can tag multiple OMM proteins with ubiquitin chains, allowing the damaged mitochondria to be recognized by the autophagic machinery (Sarraf et al., 2013; Youle & van der Bliek, 2012). Autophagic cargo proteins, such as sequestosome 1 (SQSTM1), can interact with the

ubiquitin chains found on the OMM. These cargo proteins contain a microtube-associated protein 1 light chain 3 (MAP1LC3 or LC3) interacting region (LIR) motif that work together to enable the recognition, efficient recruitment of the autophagosome, and degradation of mitochondria (Heo et al., 2015; Lazarou et al., 2015; Yamano et al., 2016).

Mitophagy Through Multifunctional Receptors

The second most common mechanism for mitophagy involves the direct interaction of multifunctional receptor molecules and are induced under different conditions. B-cell lymphoma 2 (BCL2) interacting protein 3 (BNIP3) and sister protein BNIP3-like (BNIP3L or NIX) are two such molecules that play an important role in receptor-mediated mitophagy. Similar to PINK1 and PRKN, these proteins exist in the cytosol and translocate to the mitochondria upon depolarization. BNIP3 and BNIP3L also contain a LIR motif, allowing its direct interaction to LC3 decorated autophagosomes to induce mitophagy. Some studies suggest that interaction between BNIP3/BNIP3L and LC3 is weak under normal conditions but is enhanced when the LIR motif is phosphorylated (Novak et al., 2010; Zhu et al., 2013). These multifunctional receptors can also interact with other mitophagy related proteins. In particular, BNIP3 was found to inhibit the breakdown of mitochondrial-bound PINK1, causing its accumulation and promoting PINK1/PRKN-mediated mitophagy (T. Zhang et al., 2016, p. 3). On the other hand, BNIP3L has been shown to improve mitochondrial turnover in cells from Parkinson's disease patient to compensate for lack of functional PINK1/PRKN (Koentjoro et al., 2017).

Mitochondrial Regulation of Apoptosis

As previously mentioned, autophagy is essential for protecting cells against the accumulation of damaged material. When autophagy is compromised, or when the level of damage exceeds the capacity of the autophagic machinery to efficiently target and remove this material, pathways leading to programmed cell death (i.e., apoptosis) can be activated. This serves as a safeguard to prevent damaged cells from potentially harming the organism. Apoptosis is a conserved physiological mechanism responsible for the degradation of dysfunctional, damaged, and/or unnecessary cells (Galluzzi et al., 2018; Gustafsson & Gottlieb, 2007; Kroemer et al., 2007; Saikumar et al., 1999). Apoptotic signaling is partially mediated by the mitochondria in response to stress stimuli, such as the lack of growth factors, DNA damage, and oxidative stress (Galluzzi et al., 2018; Gustafsson & Gottlieb, 2007; Kroemer et al., 2007; Saikumar et al., 1999). At the mitochondrial level, apoptotic stimuli lead to bioenergetic deficits (i.e., impaired membrane potential, reduced oxidative phosphorylation (OXPHOS), and reduced ATP production) and initiate a multi-step signaling cascade leading to cell death. The BCL2 family, consisting of pro- and anti-apoptotic proteins, plays a major role in regulating mitochondrial apoptotic signaling. Within the BCL2 family, there are generally three categories of proteins: pro-apoptotic initiators, pro-apoptotic effectors, and anti-apoptotic proteins. Pro-apoptotic initiators such as BCL2 binding component 3 (BBC3/PUMA) and BH3 interacting domain death agonist (BID) function to directly activate pro-apoptotic effectors while simultaneously inhibiting anti-apoptotic proteins (H.-C. Chen et al., 2015; H. Kim et al., 2006; Kuwana et al., 2005; Letai et al., 2002). This results in a shift towards a pro-apoptotic cellular response. Once stimulated, pro-apoptotic effectors including BCL2-associated X protein (BAX) and BCL2-antagonist/killer 1 (BAK1) translocate to the mitochondria and oligomerize, causing mitochondrial outer membrane permeabilization (MOMP)

(H.-C. Chen et al., 2015; H. Kim et al., 2006; Kuwana et al., 2005; Letai et al., 2002). Alternatively, mitochondrial permeability transition pores (MPTP) can form in response to oxidative stress or cytosolic ion overload through the assembly of channeling proteins, including voltage-dependent anion channel 1 (VDAC1) and adenine nucleotide translocase-1 (ANT1) (Bernardi et al., 2015; Beutner et al., 2017; Kroemer et al., 2007). MPTP opening can ultimately lead to mitochondrial swelling and mitochondrial membrane rupture (Bernardi et al., 2015; Beutner et al., 2017; Kroemer et al., 2007). A significant outcome of mitochondrial outer membrane permeabilization (MOMP) and OMM rupture is the liberation of CYCS. second mitochondria-derived activator of caspase (SMAC), apoptosis inducing factor mitochondria associated 1 (AIFM1) and endonuclease G (ENDOG), which directly mediate DNA fragmentation, are also released (Baker & Hepple, 2006; Kroemer et al., 2007). Key to counteracting these apoptotic processes are anti-apoptotic proteins, including BCL2 and BCL2-like 1 (BCL2L1/BCLXL), which actively suppress mitochondrial apoptotic signals. Nonetheless, the release of pro-apoptotic mitochondrial-derived molecules are crucial for the activation of caspases (CASPs), particularly CASP9 (Bloemberg & Quadrilatero, 2019). The interaction between CYCS, APAF1, and pro-CASP9 results in the formation of the apoptosome, which triggers the activation of CASP9 and CASP3 (Bratton et al., 2002; H. Dehkordi et al., 2020), ultimately leading to cleavage of several cellular targets, and DNA fragmentation via DNA fragmentation factors (DFFA/DFFB) (Enari et al., 1998; Sakahira et al., 1998). These events collectively govern the progression of the apoptotic signaling cascade (Rahman & Quadrilatero, 2022).

Mitochondria in Skeletal Muscle

The primary role of mitochondria across all tissues and cells is to produce energy; however, their behavior and responses can vary under different conditions. For example, mitochondria that are present in tissues with higher energy demands likely have greater OXPHOS protein content, a complex cristae structure, and a more intricate network (e.g., heart and skeletal muscle). In comparison, mitochondria in other tissues, like the liver, have less developed cristae and are more involved in biosynthetic pathways (Kappler et al., 2019). Interestingly, even within the same tissue, mitochondrial content and function can vary significantly, which may be attributed to the state of the tissue/cell (e.g., fiber types). Therefore, understanding the tissue and the state of the tissue are important for correct interpretations of findings.

Mitochondrial Subpopulations in Skeletal Muscle

The primary function of skeletal muscle cells (i.e., myofibers) is to produce mechanical force by converting substrates/fuel into chemical energy needed to perform work (Willingham et al., 2021). Skeletal muscle also functions as a metabolic sink, owing to its high metabolic demand. Skeletal muscle mitochondria occupy approximate 2-10% of the total muscle volume, but is capable of producing ATP at a higher rate compared to other tissues (Bleck et al., 2018; Holloszy, 1967; Ørtenblad et al., 2018; Schwerzmann et al., 1989; Willingham et al., 2021). As eluted to earlier, not all mitochondria are created equal; some mitochondria exhibit greater metabolic function compared to others. Within each myofiber, there are distinct populations of mitochondria, each with their individual function to support energy distribution for the cell. The intermyofibrillar mitochondria (IMF) subpopulation form an elongated and highly branched structures, reminiscent of a power grid, that extends between the individual myofibrils (around I-band of the sarcomere)

(Bleck et al., 2018; Glancy et al., 2015; Hoppeler et al., 1973; Picard et al., 2015; Picard, Gentil, et al., 2013; Picard, White, et al., 2013). The IMF mitochondria occupy a large proportion of the mitochondria within the muscle and are thought to play a major role in energy production for contraction. High resolution 3D electron microscopy analyses have demonstrated that virtually all IMF mitochondria are in contact with the sarcoplasmic reticulum, and therefore may be involved in Ca^{2+} signaling (Eisner et al., 2013; Tubbs et al., 2018). In contrast, the subsarcolemmal (SS) mitochondrial population are found around the nuclei in the periphery of the myofiber. SS mitochondria are larger, less branched, and densely packed around the nuclei. This population of mitochondria can extend and connect with IMF mitochondria, which was proposed as a mechanism for energy transport within the muscle (Bakeeva et al., 1978). Nonetheless, the localization of SS mitochondria may suggest its role in providing energy for transcription of nuclear DNA.

The subpopulations of the mitochondria are thought to be ubiquitous in mammalian skeletal muscle; however, their exact function may vary. For instance, isolated IMF mitochondria have greater ETC enzyme activity and respiration rates compared to SS mitochondria (Adhihetty et al., 2005; Cogswell et al., 1993; Seo et al., 2009; Triolo et al., 2022). IMF mitochondria also exhibit a 3-fold greater capacity to import substrates, such as malate, and a 10-fold greater release of pro-apoptotic factors in response to ROS-induced membrane damage (Adhihetty et al., 2005; Takahashi & Hood, 1996). In contrast, SS mitochondrial maximal State 3 respiration rates are ~10% lower (potentially due to lower CYCS levels), and they can generate significantly greater amounts of ROS compared to IMF mitochondria (Adhihetty et al., 2005). It is unclear whether a relationship between the dynamic balance of mitochondrial morphology and function exists between the IMF and SS subpopulations. Nonetheless, a recent study showed that LC3-II flux in

SS mitochondria occurs within days of denervation, whereas the same is not observed in IMF mitochondria (Triolo et al., 2022). Perhaps the contractile structure surrounding the IMF mitochondria limits their degradative potential. Alternatively, the lysosome may be localized in the periphery (Neel et al., 2015), and therefore translocate to the SS mitochondria at a faster rate.

Fiber type Differences in Mitochondrial Profile

Skeletal muscle is a heterogeneous tissue comprised of phenotypically distinct myofibers. These myofibers are defined by the rate at which they generate force and their metabolic characteristics. For example, type I (i.e., slow-twitch/oxidative) myofibers contract at a slower rate and generally have greater oxidative potential compared to type II (i.e., fast-twitch/glycolytic). Furthermore, type I myofibers have a more elaborate and densely mitochondrial network compared to type II myofibers. Studies investigating mitochondrial function have found greater respiration rates in permeabilized myofibers from type I muscles compared to type II muscles (Morales et al., 2021). Studies have identified similar cristae density between type I and II myofibers (Nielsen et al., 2017; Ørtenblad et al., 2018), which may suggest that the higher degree of mitochondrial respiration is a result of the greater overall mitochondrial content present in type I myofibers. Nonetheless, the heterogeneity of myofibers within skeletal muscle provides several benefits: the primary one being the balance between fatigue resistance (type I) and rapid force generation (type II).

The divergent profiles across myofibers may signify distinct quality control of mitochondria. Numerous studies have shown that slow/oxidative muscles have greater levels of some autophagy- and mitophagy-related proteins (i.e., BECN1, ATG7, LC3, BNIP3, and PRKN), but lower levels of others (i.e., ULK1 and ATG5) (Lira et al., 2013; McClung et al., 2010;

Mofarrahi et al., 2013; Paré et al., 2017). Our lab and others have found total autophagy flux to be greater in fast/glycolytic muscles (Mofarrahi et al., 2013; Paré et al., 2017). It is unclear how basal expression of autophagy/mitophagy markers and autophagy flux influences mitochondria quality control in different myofibers. It is also unclear whether changes in mitophagy simply reflects changes in mitochondrial content and skeletal muscle phenotype or represents the direct involvement of mitochondrial quality control processes (Rahman et al., 2024).

Understanding Mitochondrial Remodeling in Skeletal Muscle

Cellular remodeling has become a major topic of interest over the last three decades. Cellular remodeling is defined as the changing of cellular structure, and therefore function, that typically occurs in response to stimuli/stressor. This can result in gross changes in cellular morphology and behaviour and may also be important in facilitating cellular fate. The central theme for remodeling is the balance between growth and degradative signals. Cellular remodeling is often accompanied by remodeling of the mitochondria via fission/fusion and turnover. This is particularly relevant in post-mitotic cells/tissues, like skeletal muscle. As discussed earlier, skeletal muscle mitochondria are highly dynamic organelles that undergo remarkable remodeling in numerous physiological and pathological states. The controlled remodeling of the mitochondrial network plays an essential role in regulating muscle formation (i.e., myogenesis), muscle growth, and atrophy (Rahman & Quadrilatero, 2021b, 2021a).

Mitochondrial Remodeling During Myogenesis

Myogenesis is the formation of skeletal myofibers that occurs during embryonic development (Buckingham et al., 2003) and following injury in adult skeletal muscle tissue

(Dumont, Bentzinger, et al., 2015; Hawke & Garry, 2001). Cellular fate of myogenic cells is ultimately regulated by myogenic regulator factors (MRFs), including paired box 7 (PAX7), myogenic differentiation 1 (MYOD1), myogenin (MYOG), among others. During embryonic development, paired box 7 (PAX7+) muscle progenitor cells begin to activate into committed myogenic cells, called myoblasts (Buckingham et al., 2003). The appropriate temporal regulation of these MRFs is essential for these cells to facilitate proliferation, differentiation, and fusion to form multinucleated myofibers (Buckingham et al., 2003). A subset of these cells also enter a quiescent state and remain present on skeletal myofibers throughout adolescence and adulthood to aid in skeletal muscle growth and regeneration (Buckingham et al., 2003; Dumont, Bentzinger, et al., 2015; Hawke & Garry, 2001).

Myoblasts display lower bioenergetic demands compared to immature myofibers, called myotubes (Robinson et al., 2019). This change in metabolic profile is accompanied by the remodeling of the mitochondrial network. Myoblast mitochondria can be considered "underdeveloped", or "immature" compared to their myofiber counterparts. This is evident by their underdeveloped cristae morphology, low levels of beta-oxidation, and lower overall respiration compared to myotubes and myofibers (Barbieri et al., 2011; Robinson et al., 2019; Sin et al., 2016; Vertel & Fischman, 1977). Myoblasts must meet the increased metabolic demand associated with terminal differentiation. In doing so, differentiated myoblasts shift towards a more oxidative phenotype (Kraft et al., 2006; Moyes et al., 1997). The shift in metabolic phenotype is accompanied by mitochondrial fission and mitophagy that occurs within the first 24-48 hours after differentiation stimuli (Baechler et al., 2019; Bloemberg & Quadrilatero, 2016; B. Kim et al., 2013; Redpath et al., 2013; Sin et al., 2016). These processes are essential for the initiation of the differentiation program in myoblasts. Inhibition of mitochondrial fission (Bloemberg &

Quadrilatero, 2016; B. Kim et al., 2013) or the ablation of proteins related to autophagy/mitophagy (Baechler et al., 2019) concomitantly lead to impaired differentiation.

During the differentiation process, myoblasts start to differentially express MRFs. Among these, MYOD1 and MYOG are two key MRFs whose transient expression is essential for the progression of myoblast differentiation. Our lab and others show that the elevation of these MRFs is accompanied with elevated PPARGC1A, TFAM, cytochrome c oxidase subunit 4 (COX4), and mtDNA (Baechler et al., 2019; Baldelli et al., 2014; Barbieri et al., 2011; Remels et al., 2010). In particular, nuclear localization of PPARGC1A follows a similar trend to that of MYOG (Sin et al., 2016); however, a direct relationship between the two has not been established. As fission/mitophagy begin to decline and mitochondrial biogenesis machinery increases, so do the levels of fusion protein OPA1 (Sin et al., 2016). It is worth noting that the absence of autophagy/mitophagy during the early stages of myoblast differentiation results in a blunted PPARGC1A response, and decreased mitochondrial protein content (Baechler et al., 2019). This may emphasize a greater importance of mitophagy in modulating mitochondrial biogenesis. Nonetheless, mitochondrial biogenesis and fusion lead to increased basal and maximal respiration that is needed for the newly formed myotubes/myofibers (Remels et al., 2010).

Mitochondrial Remodeling Regulates Skeletal Muscle Growth

Skeletal muscle development is characterized by an increase in total size, mass, and contractile properties of myofibers. In rodent models, the postnatal developmental period typically extends until the weaning of the pups at about three weeks; however, remodeling continues even beyond this phase. The reorganization of contractile filaments, t-tubules, the SR and mitochondria must take place to ensure normal development of skeletal muscle (Luff & Atwood, 1971). The

mitochondria undergoes dramatic remodeling during this state (Y. Kim, Yang, et al., 2019; Y. Kim et al., 2024). Early studies have shown that mitochondria in developing muscle are organized parallel to the myofiber (Bakeeva et al., 1978; Y. Kim, Yang, et al., 2019; Y. Kim et al., 2024). As the muscle develops, the mitochondrial network changes and becomes perpendicular to the myofiber, which forms the classic "energy grid" morphology within mature the myofiber (Bakeeva et al., 1978). These findings have been further corroborated in a recent study that utilized MitoDendra reporter mice and found that the percentage of myofibers with the perpendicular mitochondrial morphology is present starting P14 (Y. Kim, Yang, et al., 2019).

This development of the mitochondrial network may be attributed to the natural changes in the dynamic balance of mitochondrial remodeling processes. The role of mitochondrial fission and fusion have been implicated during the developmental stage of skeletal muscle. Complete knockout of mitochondrial fission and fusion-related proteins, including DNM1L, OPA1, and MFN1/2, results in embryonic lethality or death shortly after birth (Caffin et al., 2013; H. Chen et al., 2010; Ishihara et al., 2004). As a result, studies have utilized constitutive muscle-specific knockout models to investigate the role of these proteins during muscle development. It is consistently found that although muscle-specific knockout of DNM1L, OPA1, and MFN1/2 are viable, their lifespan is dramatically reduced (H. Chen et al., 2010; Favaro et al., 2019; Tezze et al., 2017). For instance, muscle-specific DNM1L knockout animals only live for 30 days, have lower body mass and smaller type II myofibers (Favaro et al., 2019). Furthermore, muscle-specific OPA1 knockout results in lethality at P9 (Tezze et al., 2017), whereas MFN1/2 knockout are viable for up to 6-8 weeks but present severe defects in muscle growth, mitochondrial dysfunction, and accumulation of point mutations (H. Chen et al., 2010). Based on these results, mitochondrial fission and fusion is required for normal skeletal muscle growth and development. Interestingly,

the overexpression of DNM1L does not impair skeletal muscle growth, but significantly altered the mitochondrial network (Touvier et al., 2015). Muscle-specific DNM1L overexpression present very few IMF mitochondria, lower mtDNA content, and higher UPR^{mt}, without any alterations in the bioenergetic profile of their mitochondria (Touvier et al., 2015). Nonetheless, a balance between mitochondrial fission and fusion is essential for postnatal skeletal muscle development.

Given the change in mitochondrial morphology during postnatal development, there is a strong possibility that mitochondrial turnover processes may also be playing a role in its remodeling. There is some evidence that suggest an upregulation of mitochondrial content, as measured by mtDNA during postnatal development (Minai et al., 2008); however, another study showed no changes in mtDNA or ETC protein content (Y. Kim, Yang, et al., 2019). The extent to which the remodeling takes place is largely unclear during postnatal development, particularly in relation to mitophagy and biogenesis. For instance, total PRKN knockout animals have been shown to lower muscle force production, lower respiration, mitochondrial uncoupling, and greater susceptibility to MPTP opening (Gouspillou et al., 2018). More recent work has found elevated PINK1, PRKN, ATG7, LC3B and SQSTM1 levels at the neonatal stage (P1 and P7) that declines as the mice continue to develop (Y. Kim, Yang, et al., 2019). Interestingly, BNIP3 levels were found to rise throughout the developmental period in skeletal muscle, suggesting the activation of diverse mitophagy-related pathways at different stages of muscle development. However, it remains unclear whether these changes in autophagy and mitophagy signaling correlate with flux, and if this is important for the maturation of the mitochondrial network.

Studies that have investigated the role of PPARGC1A knockout have reported minimal phenotypic change in skeletal muscle development (Lelliott et al., 2006; Leone et al., 2005; J. Lin et al., 2004; Sonoda et al., 2007; Vianna et al., 2006; Zechner et al., 2010). Similar to the PRKN

knockout, this is likely due to redundancies in the molecular pathways that lead to mitochondrial biogenesis. For instance, double knockout of PPARGC1A and PPARGC1B leads to heart failure and fatality shortly after birth (Lai et al., 2008). Global knockout of PPARGC1A and muscle-specific constitutive knockout of PPARGC1B results in altered mitochondrial morphology, lower state 3 respiration, a profound decrease in exercise performance, and a greater distribution of slow-twitch myofibers (Zechner et al., 2010). Importantly, PPARGC1A levels have been shown to increase by 60% during P14-P21, which seems to occur after elevations in mitophagy proteins from P7 to P14 (Y. Kim, Yang, et al., 2019). It is postulated that as the myofibers develop, there is a need for greater mitochondrial content to support the growing skeletal muscle; however, investigation is needed to fully elucidate the "metabolic demand" of the developing skeletal muscle.

Mitochondrial Remodeling During Skeletal Muscle Atrophy

Mitochondria in mature myofibers are characteristically distinct from mitochondria from other cells. Elevated mitochondrial respiration, increased cristae formation, and greater mitochondrial networking are hallmarks of mature myofiber (Barbieri et al., 2011; Robinson et al., 2019; Vertel & Fischman, 1977). This provides myofibers with the framework to meet the metabolic demand of muscular contraction (Barbieri et al., 2011; Robinson et al., 2019; Vertel & Fischman, 1977). Moreover, the energy demands are met by the distribution of the mitochondria in a reticular fashion.

An increasing number of studies have signified the implication of mitochondrial turnover in the maintenance of skeletal muscle mass. Reduced autophagy and subsequent mitophagy was previously shown to cause mitochondrial dysfunction, accompanied with skeletal muscle loss

(Carnio et al., 2014; Demontis & Perrimon, 2010; Distefano et al., 2017; Masiero et al., 2009; Ogborn et al., 2015; Russ et al., 2012, p. 201; Wohlgemuth et al., 2010; Yeo et al., 2019). More recent work has demonstrated that major atrophic stimuli, such as disuse, are associated with mitochondrial remodeling in the form of mitochondrial fragmentation and elevations in mitophagic signaling (Borgia et al., 2017; Cannavino et al., 2015; Graham et al., 2018; C. Kang et al., 2016; Sandri et al., 2006; Triolo et al., 2022; Vainshtein et al., 2015; Yamashita et al., 2021). Disuse via immobilization or denervation of skeletal muscle is a major stimuli for atrophy by reducing muscle protein synthesis and increasing degradation (Brooks & Myburgh, 2014; Rudrappa et al., 2016). Additionally, atrophying skeletal muscle display decreased mitochondrial quantity and quality as evident by reduced mitochondrial content (i.e., mitochondrial-related protein content or mtDNA:nDNA ratio), mitochondrial biogenesis signaling (i.e., PPARGC1A-signaling), lower $\Delta\Psi_m$, and elevated ROS generation (Cannavino et al., 2015; C. Kang et al., 2016; S. W. S. Kang et al., 2016; P. Sakellariou et al., 2016; Sandri et al., 2006). Interestingly, the loss of mitochondrial mass and muscle mass can partly be rescues via overexpression of PPARGC1A and upregulation of mitochondrial biogenesis (Cannavino et al., 2015; C. Kang et al., 2016; Sandri et al., 2006).

Skeletal muscle atrophy can be observed within weeks of disuse. Early changes, noted as soon as 3-days following disuse, include reductions in *Opa1* and *Mfn1/2* transcripts, which may shift the dynamic nature of the mitochondrial network towards greater fission. These alterations are followed by the accumulation of PINK1, PRKN, and *Bnip3l* within 7-days, indicating the initiation of mitochondrial quality control mechanisms (Cannavino et al., 2015; Deval et al., 2020; C. Kang et al., 2016). A recent study utilizing the mito-QC mitophagy reporter mouse has confirmed elevations in mitophagic flux with disuse atrophy, likely attributed to elevations in *Bnip3, Bnip3l,* and *Prkn* transcripts (Yamashita et al., 2021). Another report observed elevated

mitophagy flux in mt-Keima mice as early as 1-day following denervation (Triolo et al., 2022). It is unclear whether mitophagy is the driving force for disuse atrophy. The upregulation of mitophagy may be complementary to atrophic conditions given the lack of energy demand placed on the mitochondria or perhaps due to the intrinsic dysfunction within the mitochondria. Alternatively, mitophagy may serve as an initiating step for atrophy; however, further investigation is required to delineate this relationship.

Overall Purpose and Objectives

Mitochondrial remodeling has been implicated in various skeletal muscle conditions. Although the mechanisms of mitochondrial remodeling have been well characterized in non-muscle cell types, their interaction in skeletal muscle is less understood. Moreover, the relationship between mitochondrial biogenesis, fission/fusion, and mitophagy in not entirely understood in the context of myogenesis, skeletal muscle growth, and atrophy. Previous work in our lab has shown that autophagy and subsequent mitophagy is an essential step for myogenic differentiation (Baechler et al., 2019; McMillan & Quadrilatero, 2014). Separately, we have also shown that inhibition of mitochondrial fission can limit myogenic differentiation (Bloemberg & Quadrilatero, 2016); however, the interaction between these mechanisms has yet to be explored in the context of differentiation. Additionally, our lab has demonstrated that constitutive knockout of *Atg7*, an important protein for the maturation of the autophagosome, leads to a reduction in muscle force production, and greater number of myofibers with centrally located nuclei (Paré et al., 2017). To date, the morphological changes in mitochondria during postnatal growth of skeletal muscle has been characterized (Y. Kim, Yang, et al., 2019; Y. Kim et al., 2024); however, the integration of mitochondrial remodeling processes during this essential stage in life is largely unknown and warrants further investigation. Additionally, mitochondrial remodeling, particularly mitophagy, has been linked to atrophic conditions (Triolo et al., 2022; F. Wang et al., 2023; Yamashita et al., 2021); however, the mechanism has not been explored. As a result, **the overarching theme was to investigate mitochondrial remodeling during myogenesis, postnatal skeletal muscle growth, and skeletal muscle atrophy**.

The first project investigated mitochondrial dynamics as a precursor to mitophagy during myogenesis *in vitro,* focusing on the interplay between DNM1L-mediated fission and BNIP3-mediated mitophagy. The second project explored mitochondrial remodeling and its role in the maturation of the mitochondrial network during postnatal development, employing mt-Keima mice and constitutive muscle-specific *Atg7* knockout mice. The third project assessed the role of mitophagy in immobilization-induced muscle atrophy, using mt-Keima mice treated with various agents to modify ROS signaling and autophagy signaling.

Therefore, the experiments comprising this thesis were aimed to improve our understanding of mitochondrial remodeling in three important stages: during myogenesis, during postnatal growth, and during atrophy.

In summary, the objectives of this thesis were:

1. To understand the interaction between mitochondrial remodeling processes during myogenesis.
2. To determine the role of mitochondrial remodeling during postnatal development of skeletal muscle.
3. To examine the role of mitochondrial remodeling, particularly mitophagy, during immobilization-induced atrophy of mature skeletal muscle.

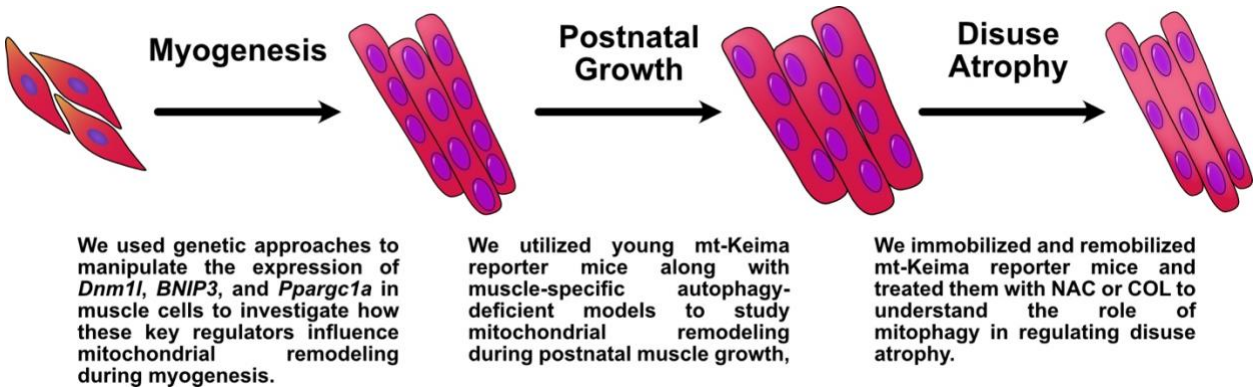


Figure 3: Conceptual image of study design. Different models are used to study mitochondrial remodeling during myogenesis, postnatal muscle growth, and disuse atrophy.

Chapter 2: Role of Mitochondrial Remodeling During Myogenesis

Project Rationale and Objectives

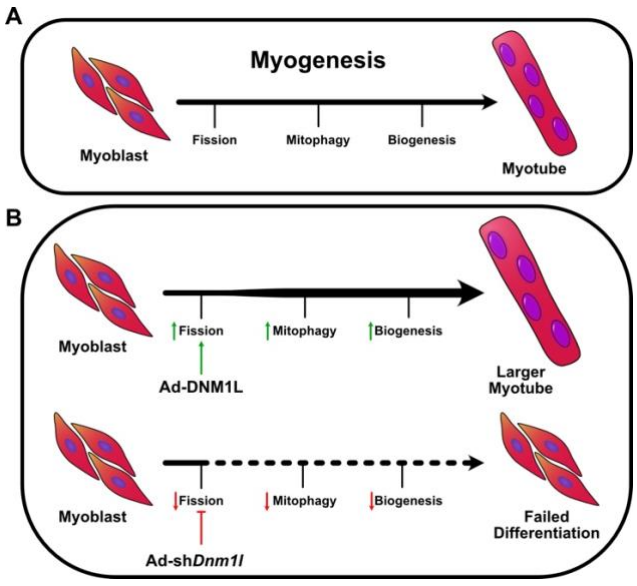
The remodeling of the mitochondria is essential for myogenic differentiation. Previous work from our lab has demonstrated that the activation of autophagy and mitophagy is needed for normal differentiation (Baechler et al., 2019; McMillan & Quadrilatero, 2014). The consequence of limited autophagy and/or mitophagy is oxidative stress and activation of apoptotic signaling cascades (Baechler et al., 2019; McMillan & Quadrilatero, 2014). Interestingly, the interaction of mitochondria dynamics, namely mitochondrial fission, on mitophagy has been previously implicated (Bloemberg & Quadrilatero, 2016; B. Kim et al., 2013). Emerging evidence also suggests that mitochondrial fission regulates mitophagy and biogenesis (Kleele et al., 2021). Based on these findings, it stands to reason that mitochondrial fission may be sufficient in inducing a change in the mitochondrial network that is required for myogenesis by signaling mitophagy and biogenesis.

Therefore, the main objectives of Project 1 were:

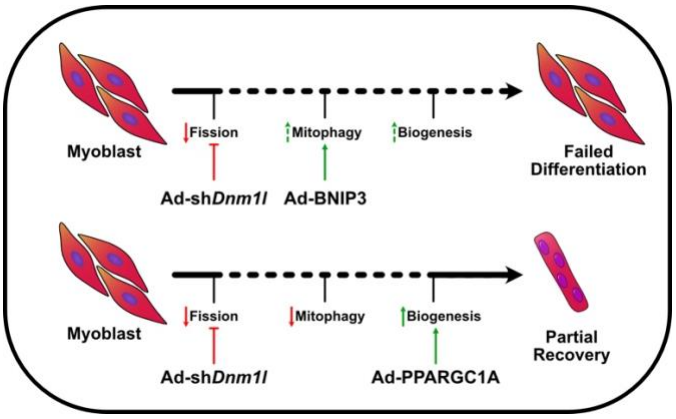
1. To determine the regulatory role of mitochondrial fission on mitophagy and biogenesis during myogenesis.
2. To determine if the overexpression of mitophagy (BNIP3) or biogenesis (PPARGC1A) markers sufficiently rescue defects in myogenesis that were accompanied by a lack of mitochondrial fission.
3. To determine if the overexpression of mitochondrial fission protein, DNM1L, signals mitochondrial biogenesis and restores myogenesis independent of BNIP3-mediated mitophagy.

I hypothesized that:

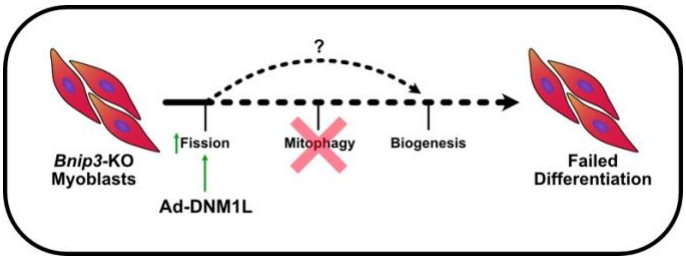
1. Upregulation of mitochondrial fission would accelerate mitophagy, which would signal for the activation of mitochondrial biogenesis to accelerate differentiation, while suppression of mitochondrial fission would reduce mitophagy and biogenesis, leading to impaired myogenic differentiation.
2. Overexpression of mitophagy receptor BNIP3 would fail to differentiate cells in a fission-deficient state, while overexpression of biogenesis protein PPARGC1A would partially restore myogenic differentiation in fission-deficient cells by enhancing mitochondrial content and function.
3. Overexpression of DNM1L would fail to signal mitochondrial biogenesis in BNIP3-deficient cells, leading to failed myogenic differentiation.



Method Figure 1: Study design for Project 1, Objective 1. A) Illustration of normal myogenesis. Mitochondrial fission is one of the first steps, which is followed by mitophagy and biogenesis. B) Illustration for Objective 1. Enhanced fission via Ad-DNM1L was hypothesized to improve mitophagy and biogenesis, leading to enhanced differentiation. Conversely, impairment of fission via Ad-sh*Dnm1l* was hypothesized to decrease mitophagy and biogenesis, leading to failed differentiation. Mitophagy, biogenesis, and differentiation were measured as described in the **Material and Methods** section.



Method Figure 2: Study design for Project 1, Objective 2. C2C12 myoblasts were transduced with Ad-sh*Dnm1l* to reduce fission and co-transduced with Ad-BNIP3 or Ad-PPARGC1A. It was hypothesized that Ad-BNIP3 may partially increase mitophagy and biogenesis in cells with hyperfused mitochondria, but they will fail to differentiate. Alternatively, it was hypothesized that Ad-PPARGC1A may improve mitochondrial biogenesis, which may partially recover differentiation as a result of improved mitochondrial function. Mitophagy, biogenesis, and differentiation were measured as described in the **Material and Methods** section.



Method Figure 3: Study design for Project 1, Objective 3. *Bnip3*-KO myoblasts were transduced with Ad-DNM1L to enhance fission. It was hypothesized that increased mitochondrial fission in BNIP3-deficient myoblasts will be unable to activate mitophagy or biogenesis and fail to differentiate. Mitophagy, biogenesis, and differentiation were measured as described in the **Material and Methods** section.

Introduction

Cellular differentiation is the process through which a precursor cell undergoes changes in its morphology and function into a specialized cell type. For cells to differentiate, they must carefully integrate numerous extracellular and intracellular signals to facilitate the elimination of unspecialized cellular material and repurpose the basic macromolecules to synthesize more specialized cellular material (Chang, 2020). This process is typically referred to as "remodeling". One of the major mechanisms of cellular remodeling is autophagy (i.e., self-eating). Autophagy is a degradative process that is used to eliminate damaged proteins, organelles, and other cellular components (Bloemberg & Quadrilatero, 2019; Chang, 2020; Rahman & Quadrilatero, 2021b). Interestingly, autophagy can occur in bulk or select form. For instance, the degradation of mitochondria, termed mitophagy, has classically been implicated in the context of cellular differentiation (Baechler et al., 2019; Sin et al., 2016).

Various mechanisms of mitophagy have been identified over the last decade. One of the first mechanisms identified is the PINK1/PRKN pathway, which is involved in the removal of damaged/depolarized mitochondria (Durcan & Fon, 2015). Alternatively, mitophagy-receptors have also been identified, and are implicated in the removal of mitochondria during cellular differentiation (Baechler et al., 2019; Sandoval et al., 2008; Schweers et al., 2007). The removal of the mitochondria is particularly relevant is specialized cells that have a high metabolic demand, such as muscle cells (i.e., myoblasts). Recent evidence from our lab (Baechler et al., 2019; McMillan & Quadrilatero, 2014), and others (Sin et al., 2016) demonstrates that a lack of autophagy or mitophagy severely inhibits myogenic differentiation. Furthermore, the lack of degradation of "immature" mitochondria is one of the major culprits that prevents the rebuilding

of the mitochondrial network needed for myogenic differentiation (Baechler et al., 2019; Sin et al., 2016).

The role of mitophagy is apparent during myogenic differentiation; however, emerging evidence suggests that the state of the mitochondrial network may be a regulatory mechanism for mitophagy. For instance, hyperfusion of mitochondria severely halts mitophagy, whereas the fragmentation of mitochondria plays an important preceding step for mitophagy (Twig & Shirihai, 2011). Additionally, the fragmentation of mitochondria results in smaller, less functional mitochondria that exhibit lower membrane potential, which is a major signal for mitophagy (Twig & Shirihai, 2011). Conversely, hyperfusion of mitochondria present physical limitation for the autophagy machinery, and therefore, limiting mitophagic flux (Twig & Shirihai, 2011). Nevertheless, the regulation of the mitochondrial network and its regulatory role over mitophagy is only starting to be unraveled. Previous work from our lab has demonstrated that the inhibition of fission protein DNM1L significantly impairs myogenic differentiation (Bloemberg & Quadrilatero, 2016); however, it is unclear whether this is a result of reduced mitophagy. Moreover, the regulatory role of DNM1L on other mitochondrial remodeling processes remains elusive.

Therefore, the purpose of the present study was to determine the regulatory role of DNM1L on mitochondrial remodeling processes during myogenic differentiation. We further questioned whether the overexpression of mitophagy or biogenesis markers can restore myogenic differentiation in a fission-deficient state. We also questioned whether increased mitochondrial fission could facilitate differentiation independent of BNIP3-mediated mitophagy.

Material and Methods

Cell culture

C2C12 murine myoblasts were cultured is similar conditions as previously described (Baechler et al., 2019; Bloemberg & Quadrilatero, 2016; McMillan & Quadrilatero, 2014). Cells were maintained in growth media consisting of low-glucose Dulbecco's Modified Eagles Medium (DMEM) supplemented with 5% fetal bovine serum, 5% Serum Plus II, and 1% penicillin/streptomycin on polystyrene culture dishes. Differentiation was induced at 80% confluency with the addition of differentiation medium consisting of low-glucose DMEM supplemented with 2% horse serum and 1% penicillin/streptomycin. Cells were collected by trypsinization, centrifugation at 1000 x g, and stored at -80°C until analyses.

Knockout of *Bnip3* in C2C12 was achieved with CRISPR/Cas9 vectors targeting mouse *Bnip3*. Guide RNA (gRNA) targets were identified using the following tools: Zhang Lab, MIT (https://zlab.bio/guide-design-resources), CCTop (https://cctop.cos.uni-heidelberg.de:8043/), and Off-Spotter (https://cm.jefferson.edu/Off-Spotter/). Two gRNA sequences were identified: First: 5′GAGCCACCATGTCGCAGAGC(GGG), and 5′GGAGGAGAACCTGCAGGGTG(AGG). The following scramble sequence was used as a control vector: 5′GCACTACCAGAGCTAACTCA. Corresponding oligonucleotides were constructed (Sigma) to allow cloning into the CRISPR/Cas9 vector pSpCas9(BB)-2A-puro (PX459) V2.0 (Addgene, 62988), which uses a single gRNA. Cloning was confirmed by sequencing constructs (Center for Applied Genomics, Sick Kids Hospital, Toronto, Canada).

Adenovirus Amplification and Precipitation

Adenoviruses were amplified using HEK-293 cells in a similar manner as previously described (Baechler et al., 2019). Briefly, HEK-293 cells were grown until 60% confluency. Growth medium was refreshed, and the following adenoviruses were added at an MOI of 5: Ad-GFP, Ad-LacZ, Ad-sh*Dnm1l*, Ad-DNM1L, Ad-BNIP3, Ad-GFP-PPARGC1A, and Ad-CMV-COXVIII-EGFP-mCherry. Cells were incubated until 90% cytopathic effect (CPE) was observed and cells detached from the plate. The cell suspension was collected, centrifuged at 1000 x g for 15 minutes and the supernatant was transferred to a fresh tube. The remaining cell pellet was resuspended in a small volume of PBS, freeze/thawed three times, and centrifuged at 3000 x g for 15 minutes to pellet cellular debris. The resulting supernatant was pooled into the previously collected supernatant. Adenoviruses were precipitated using polyethylene glycol/NaCl (10% PEG-8000 / 0.625M NaCl final concentration) or protamine sulfate-chondroitin sulfate C (100μg/ml each) overnight on a rocker. The following day, tubes were centrifuged at 3000 x g for 30 minutes to pellet the adenovirus and the supernatant was discarded. All viruses were stored in PEG-PBS at -80°C with no loss in viral titers after multiple freeze/thaw cycles.

Adenoviral Transduction of Myoblasts

All adenovirus experiments were performed in 24-well plates. C2C12 myoblasts were plated at $2x10^4$ per well. On the subsequent day, cells were washed in PBS and adenoviruses were added at an MOI of 30-100 in serum-free DMEM supplemented with 8μg/ml polybrene for 1-2 hours at 37°C. Following incubation, cells were washed in PBS to remove residual virus, and growth media was added to allow cells to recover from viral load. Cells were differentiated on the following day as described earlier.

Immunoblotting

Immunoblotting was performed as previously described (Baechler et al., 2019; Bloemberg & Quadrilatero, 2016; McMillan & Quadrilatero, 2014; Paré et al., 2017). Pelleted cells were incubated in ice-cold lysis buffer (20mM HEPES, 10mM NaCl, 1.5mM $MgCl_2$, 1mM DTT, 20% glycerol, 0.1% Triton-X100, pH 7.4) containing protease inhibitor and sonicated at 40 Hz for 10 seconds. Protein content was determined using a BCA protein assay. Equal protein was loaded and separated using 8-12% SDS-PAGE, transferred on to PVDF membranes, and blocked with 2-5% non-fat milk powder in TBS-T at room temperature for 1 hour. Membranes were briefly rinsed and incubated overnight in primary antibodies against: BNIP3 (#3769, Cell Signaling), BNIP3L (#12396, Cell Signaling), MAP1LC3B/LC3B (#2775, Cell Signaling), GAPDH (#2118, Cell Signaling), OPA1 (#80471, Cell Signaling), MFN2 (#9482, Cell Signaling), DNM1L (#8570, Cell Signaling), SQSTM1 (PM045, MBL), PINK1 (sc-33796, Santa Cruz), VDAC1 (sc-390996, Santa Cruz), ANT1 (sc-9299, Santa Cruz), CYCS (sc-13256, Santa Cruz), ACT (S2066; Sigma), PPARGC1A (ST1202, Sigma), SOD1 (SOD-101, Stressogen), SOD1 (SOD-110, Stressogen), myosin heavy chain (MYH; MF-20, DSHB), and myogenin (MYOG; F5D, DSHB). Following incubation, membranes were washed, and appropriate horseradish peroxidase-conjugated secondary antibody was applied at room temperature for 1 hour. Bands were visualized using ECL substrate on a ChemiDoc Imaging System.

Immunocytochemistry

Myosin heavy chain (MYH) was stained to determine differentiation capacity of myoblasts. Briefly, cells were differentiated for 5-days (D5), fixed in 4% formaldehyde, and blocked in 5% goat serum in PBS containing 0.1% Triton-X100 (PBS-T) at room temperature.

Anti-MYH (1:400; DSHB; MF-20) was applied for 2 hours at room temperature. Cells were washed with PBS-T prior to adding the appropriate Alexa Fluor secondary antibody and counterstaining with 300nM DAPI for 1 hour at room temperature. Cells were washed several times and 0.5ml of PBS added to each well prior to imaging. All images were collected using the Cytation 5 Imaging Multi-mode Reader at 20X magnification.

Flow Cytometry

Myoblasts were cultured on 24-well plates, treated with appropriate adenoviruses, and grown until confluent. Cells were differentiated for 24-hours (i.e., D1), collected, centrifuged, washed in PBS, and resuspended in PBS containing 1 g/L glucose with 50nM TMRE and 50nM MitoTracker Green (MTG) to determine mitochondrial membrane potential and content, respectively. Mitochondrial permeability transition pore (MPTP) formation was assessed by resuspending cells in PBS with 1g/L glucose containing 1μM Calcein AM and 1mM $CoCl_2$. $CoCl_2$ quenches Calcein fluorescence and is permeable to the plasma membrane but not the IMM (Ying et al., 2021). Therefore, healthy cells co-loaded with Calcein-AM and $CoCl_2$ results in quenching of cytosolic Calcein Florescence without affecting mitochondrial fluorescence. In contrast, MPTP opening facilitates permeability of $CoCl_2$, allowing it to pass the IMM and enter the mitochondrial matrix to quench Calcein fluorescence (i.e., reduces fluorescence). All samples were incubated at 37°C with gentle rocking for 30 minutes before being diluted in PBS with 2% BSA and analyzed using a BD FACSCalibur flow cytometer equipped with Cell Quest Pro software (BD Bioscience).

Confocal Microscopy

C2C12 myoblasts were grown on Cultrex-coated coverslips in a 24-well plate and transduced in the same manner with the addition of Ad-CMV-COXVIII-EGFP-mCherry. The growth media was refreshed, and other adenoviruses were added as previously indicated. Cells were grown until 80% confluency, differentiated, and fixed in 4% formaldehyde. Coverslips containing cells were briefly washed in PBS and mounted on microscope slides using Fluoromount mounting medium. Ten to thirty cells were imaged on a Zeiss LSM 800 confocal microscope at 63X magnification. Mitophagic area was determined using the threshold function on ImageJ.

Mitochondrial Network Analysis

Confocal microscopy images were exported and subsequently analyzed using a custom macro developed for ImageJ. Firstly, merged channel images were converted to 8-bit grayscale format to standardize intensity values across all samples. These images underwent a deconvolution process using the Iterative Deconvolution 3D plugin, which applies a theoretical point spread function over ten iterations to correct for inherent optical distortion. To enhance the detectability of network features, the contrast of these images was increased. Following contrast enhancement, images were processed through a Gaussian Blur filter to reduce noise, enhancing feature extraction during subsequent analysis steps. The images were then converted into binary masks to isolate and define structural elements within the mitochondrial network. The refined images were analyzed using the Skeleton 2D/3D plugin to quantitatively assess network morphology. Quantitative data extracted from this analysis were compiled and saved into a spreadsheet format. A custom Python script was used to synthesize data from multiple spreadsheets.

Caspase and Calpain Activity Assay

To measure caspase (CASP) and calpain (CAPN) activities, whole-cell lysates were collected at D1 as described above in the absence of protease inhibitors. Samples were incubated in duplicates with 20μM of Ac-DEVD-AFC for CASP3 or Ac-LEHD-AFC for CASP9 in assay buffer (20 mM HEPES pH 7.4, 10 mM DTT, and 10% glycerol). For CAPN activity, samples were incubated in duplicates with 20μM of Suc-LLVY-AMC and Z-LL-CHO inhibitor in assay buffer for 2 hours at 30°C. Fluorescence measurements were performed at room temperature using a Cytation 5 Imaging Multi-Mode Reader. The AFC probe was measured with excitation and emission wavelengths at 400 and 505 nm, respectively. The AMC probe was measured with excitation and emission wavelengths at 360 and 440 nm, respectively. The fluorescence values were normalized to protein concentration of samples and expressed as fold changes in fluorescence.

Statistics

Statistical analyses were performed in GraphPad PRISM in a similar manner as previously described (Baechler et al., 2019; Bloemberg & Quadrilatero, 2016; McMillan & Quadrilatero, 2014). T-tests were performed to assess differences in treatment within a given time-point. An alpha value of 0.05 was assigned for all analyses.

Results

Overexpression of DNM1L promotes mitochondrial fragmentation, increased mitophagic flux, and reduced myotube size

Dynamin 1 like protein (DNM1L) is a key regulator of myogenesis, playing a pivotal role in mitochondrial fission (Bloemberg & Quadrilatero, 2016; B. Kim et al., 2013). Its proper expression is crucial for ensuring normal myotube formation and mitochondrial function by also regulating mitophagy. We aimed to investigate the role of DNM1L and its impact on other mitochondrial remodeling parameters during myogenesis. To fully understand the role of DNM1L during myogenesis, we first questioned whether the targeted genetic overexpression (OE) of DNM1L would alter the mitochondrial network during myogenesis. To address this question, we transduced cells with Ad-DNM1L or control virus (Ad-LacZ) and examined several mitochondrial and myogenic parameters. Furthermore, we also transduced cells with Ad-CMV-COXVIII-GFP-mCherry, a dual-fluorescence reporter virus used to accurately measure mitophagic flux.

DNM1L OE resulted in early elevations in mitophagic flux (+75% at D0 and +58% at D1; $p < 0.05$) coinciding with marked mitochondrial fragmentation, as shown by reduced total mitochondrial network branch number (-27% at D0 and -14% at D1; $p < 0.05$) and junction number (-28% at D0 and -18% at D1; $p < 0.05$; Figure 1A-D). The mitochondrial network appeared to normalize by D2, accompanied by a non-significant reduction in mitophagic flux (-30%; $p = 0.08$; Figure 1B-D). This temporal pattern suggests a transient impact of DNM1L OE on mitochondrial dynamics and mitophagy. DNM1L OE did not alter MTG (i.e., mitochondrial mass) or normalized TMRE (i.e., mitochondrial membrane potential) fluorescence measures but reduced mitochondrial retention of Calcein-AM fluorescence (-23%; $p < 0.05$) suggesting the induction of mitochondrial permeability transition pore (MPTP) opening at D1 (Figure 1E-J). Interestingly, this was

accompanied by reduced caspase 9 (CASP9; -9%; $p < 0.05$) activity, without affecting caspase 3 (CASP3) or calpain (CAPN) activity at D1 (Figure 1K-M). This shows that DNM1L-mediated fission also influences mitochondrial apoptotic signaling, perhaps independent of MPTP opening.

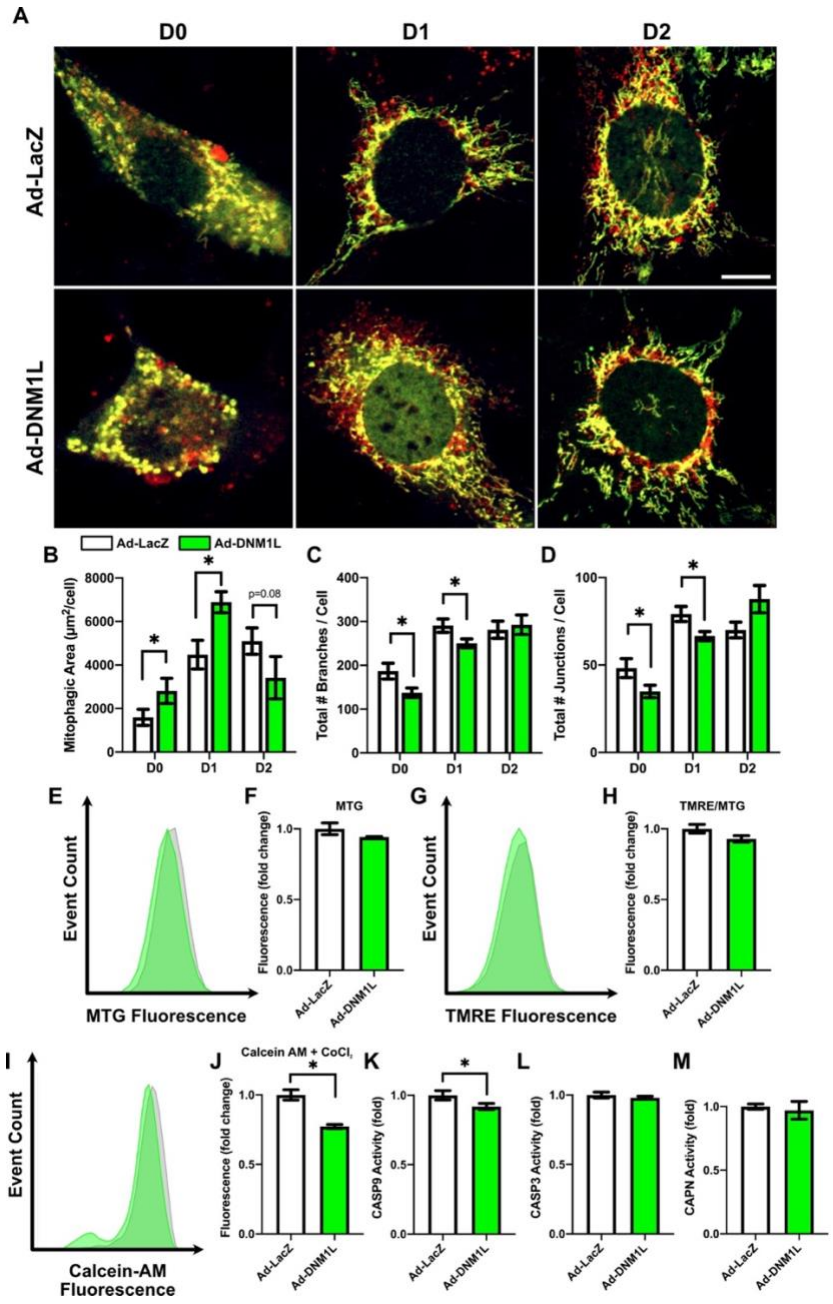


Figure 1: DNM1L OE induces mitochondrial fragmentation and upregulation of mitophagy during myogenesis. A) Representative images of myoblasts transduced with Ad-CMV-COXVIII-EGFP-mCherry to detect mitophagic flux. Mitochondria are dual-labeled EGFP and mCherry (i.e., yellow). EGFP is degraded during the breakdown of the mitochondria resulting in red fluorescence only (i.e., red puncta) and is indicative of mitophagic flux. Scale bar indicates 5 μm. Quantification of B) mitophagic area, C) total mitochondrial branch count, and D)

total mitochondrial junction count per cell. Representative histograms and quantification of E-F) MitoTracker Green (MTG) fluorescence, G-H) TMRE fluorescence, and I-J) Calcein-AM + $CoCl_2$ fluorescence. Quantification of K) caspase 9 (CASP9), L) caspase 3 (CASP3), and M) calpain (CAPN) activities at D1. * $p < 0.05$ compared to Ad-LacZ group within the same time point. n = 4-30 per group.

DNM1L OE led to a significant reduction in myotube size at D5 (-23%; $p < 0.05$) without affecting the differentiation or fusion indices (Figure 2A-D). This suggests that while DNM1L plays a critical role in myotube formation, its overexpression primarily impacts cell size rather than the differentiation process itself. Additionally, we observed no changes in SQSTM1 but early elevations in LC3B-II levels (+100% at D0 and +24% at D3; $p < 0.05$), likely signaling an initial increase in autophagic activity (Figure 2E-H). Although there was a decline in LC3B-II:I ratio by D5, this change was not statistically significant ($p = 0.08$) (Figure 2I). Despite these changes, there were no alterations in proteins related to mitochondrial biogenesis (i.e., PPARGC1A) or mitophagy (i.e., BNIP3, BNIP3L, and PINK1) (Figure 3A-E). However, DNM1L OE was associated with reductions in key mitochondrial molecules including cytochrome c (CYCS), and superoxide dismutase 2 (SOD2) at D3 and D5 ($p < 0.05$; Figure 3K & 3M), perhaps indicating impairments in mitochondrial electron transport efficiency and antioxidant capacity in the newly formed myotubes.

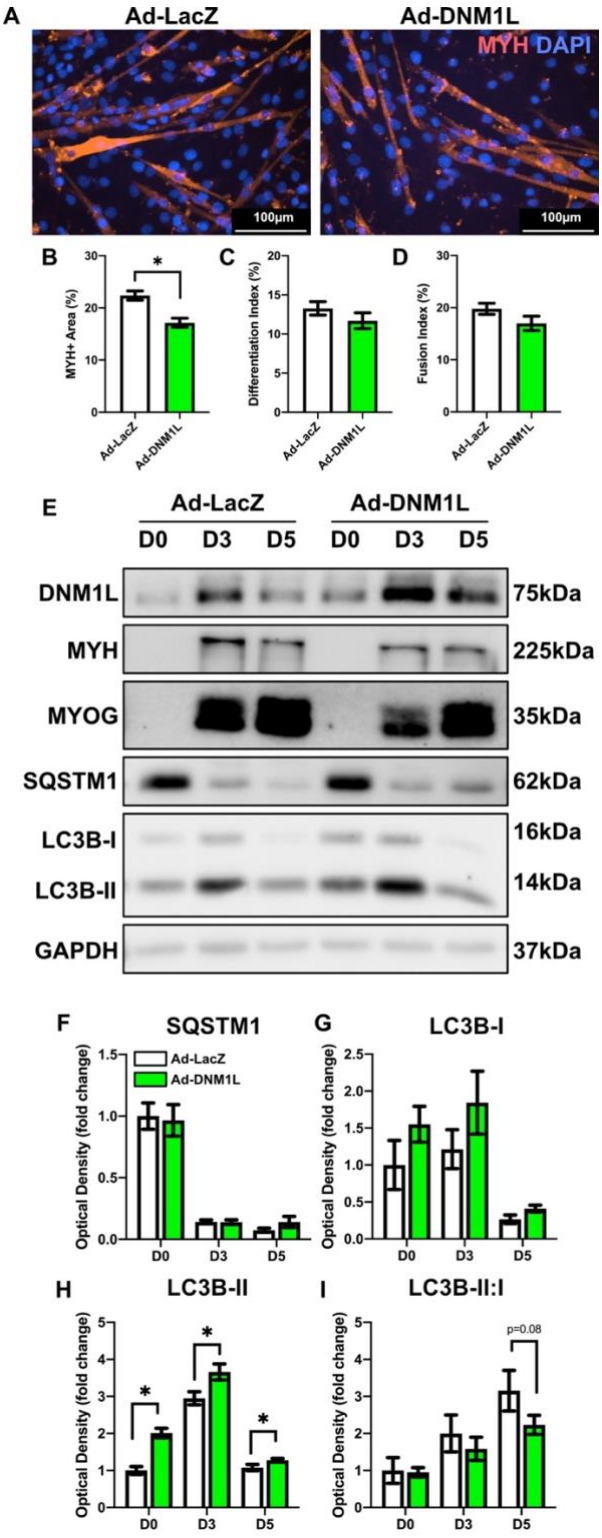


Figure 2: DNM1L OE does not modify myogenesis but reduces myotube size. A) Representative myosin heavy chain (MYH; red) and DAPI (blue) stain of D5 myotubes. Scale bar indicates 100 μm. Quantification of B) MYH+ area, C) differentiation index, and D) fusion index. Representative immunoblot E) and quantification of F) SQSTM1, G) LC3B-I, H) LC3B-II, and I) LC3B-II:I. * $p < 0.05$ compared to Ad-LacZ group within the same time point. n = 4-12 per group.

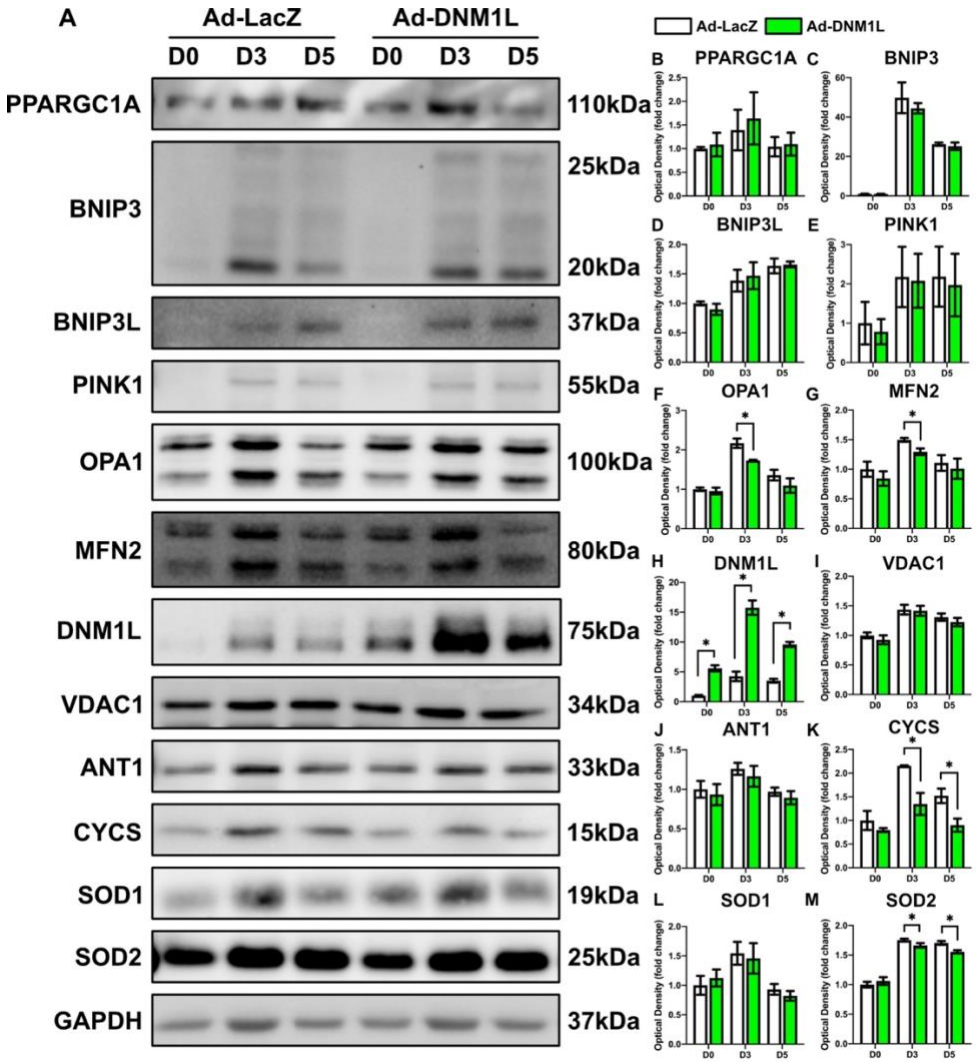


Figure 3: Molecular changes in mitochondrial remodeling proteins in response to DNM1L OE. Representative immunoblots A) and quantification of B) PPARGC1A, C) BNIP3, D) BNIP3L, E) PINK1, F) OPA1, G) MFN2, H) DNM1L, I) VDAC1, J) ANT1, K) CYCS, L) SOD1, and M) SOD2. * $p < 0.05$ compared to Ad-LacZ group within the same time point. n = 4 per group.

Loss of DNM1L impairs mitophagic flux, limits myogenesis and increases mitochondrial apoptotic signaling

Previous work has utilized pharmacological and genetic approaches to limit DNM1L-mediated mitochondrial fission via treatment of cells with mdivi-1 or dominant negative

DNM1L^{K38A} (Bloemberg & Quadrilatero, 2016; B. Kim et al., 2013). To further understand the regulatory role of DNM1L on mitochondrial remodeling during myogenesis, we used an adenovirus approach to knockdown (KD) DNM1L. Utilizing the dual-fluorescence reporter virus in Ad-LacZ and Ad-sh*Dnm1l* transduced cells, we showed that DNM1L KD suppressed mitophagic flux at D0 (-63%; $p < 0.05$) and D1 (-57%; $p < 0.05$; Figure 4A-B). This correlated with increased in mitochondrial branch number (+25% at D0 and +15% at D2; $p < 0.05$; Figure 4C) and junction number (+36% at D0, +26% at D1, and +21% at D2; $p < 0.05$; Figure 4D). Moreover, DNM1L KD was associated with increased MTG fluorescence (+19%; $p < 0.05$) and no changes in normalized TMRE fluorescence (Figure 4E-H). These data suggest that DNM1L KD alters mitochondrial dynamics, shifting towards a hyperfused morphology. The hyperfused morphology appears to limit mitochondrial degradation without significantly affecting the mitochondrial membrane potential. Interestingly, DNM1L KD resulted in increased Calcein-AM retention in mitochondria (+69%; $p < 0.05$), suggestive of reduced MPTP opening (Figure 4I-J). We also observed reduced CAPN activity (-25%; $p < 0.05$), while significantly elevated CASP9 (+87%; $p < 0.05$) and CASP3 (4-fold increase; $p < 0.05$) activities at D1 in DNM1L KD cells (Figure 4K-M). These findings indicate that DNM1L KD affects apoptotic pathways, potentially shifting the balance towards increased CASP activity in response to failed mitochondrial fragmentation and/or mitophagic flux.

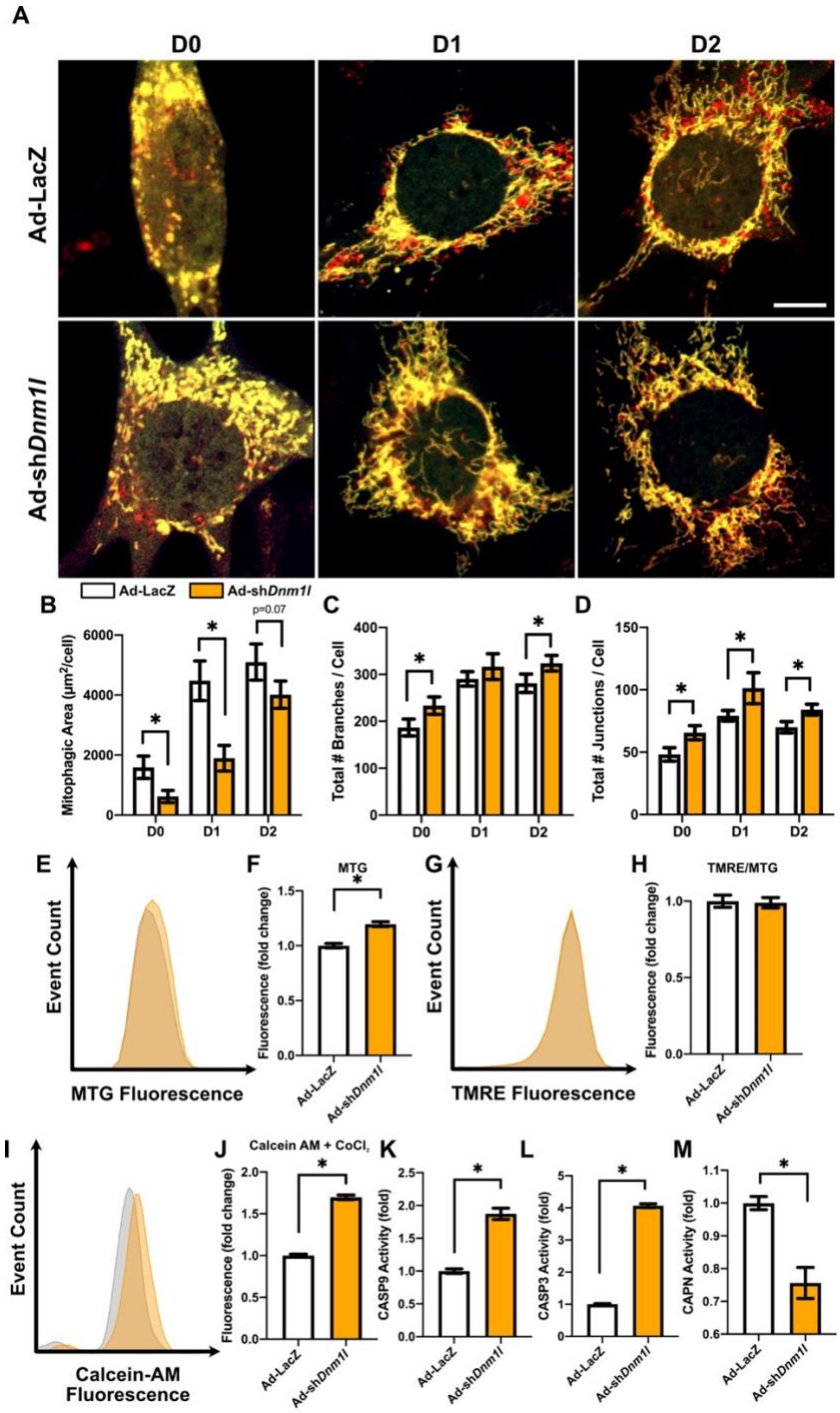


Figure 4: DNM1L KD suppresses mitochondrial fission and mitophagy during myogenesis. A) Representative images of myoblasts transduced with Ad-CMV-COXVIII-EGFP-mCherry to detect mitophagic flux. Mitochondria are dual-labeled EGFP and mCherry (i.e., yellow). EGFP is degraded during the breakdown of the mitochondria resulting in red fluorescence only (i.e., red puncta) and is indicative of mitophagic flux. Scale bar indicates 5 μm. Quantification of B) mitophagic area, C) total mitochondrial branch count, and D) total mitochondrial junction count per cell. Representative histograms and quantification of E-F) MitoTracker Green (MTG) fluorescence, G-H) TMRE fluorescence, and I-J) Calcein-AM + $CoCl_2$ fluorescence. Quantification of K) caspase 9 (CASP9), L) caspase 3 (CASP3), and M) calpain (CAPN) activities at D1. * $p < 0.05$ compared to Ad-LacZ group within the same time point. n = 4-30 per group.

Similar to previous findings (Bloemberg & Quadrilatero, 2016; B. Kim et al., 2013), we showed that DNM1L KD significantly reduces myotube size (-55%; $p < 0.05$), differentiation (-40%; $p < 0.05$) and fusion (-45%; $p < 0.05$) indices at D5 (Figure 5A-D). Accompanying this reduction, we observed depressed LC3B-II levels at D3 (-28%; $p < 0.05$) and a decline in the LC3B-II:I ratio at D5 (-36%; $p < 0.05$) in DNM1L KD cells, perhaps hinting at impaired autophagosome formation (Figure 5E-I). This indicates that DNM1L is crucial for proper myotube formation, and its reduction disrupts the formation and growth of myotubes. Additionally, DNM1L KD led to approximately 50% reduction in key remodeling molecules including PPARGC1A and BNIP3 throughout the differentiation time course ($p < 0.05$; Figure 6A-C), although PINK1 levels increased at D5 (+64%; $p < 0.05$; Figure 6E). We also observed other changes in signaling like reduced MFN2 levels at D5 (-31%; $p < 0.05$; Figure 6G), reduced SOD2 at D3 (-13%; $p < 0.05$; Figure 6M), and increased SOD1 at D0 (+90%; $p < 0.05$; Figure 6L) in DNM1L KD cells; however, the changes in these molecules remain largely ambiguous.

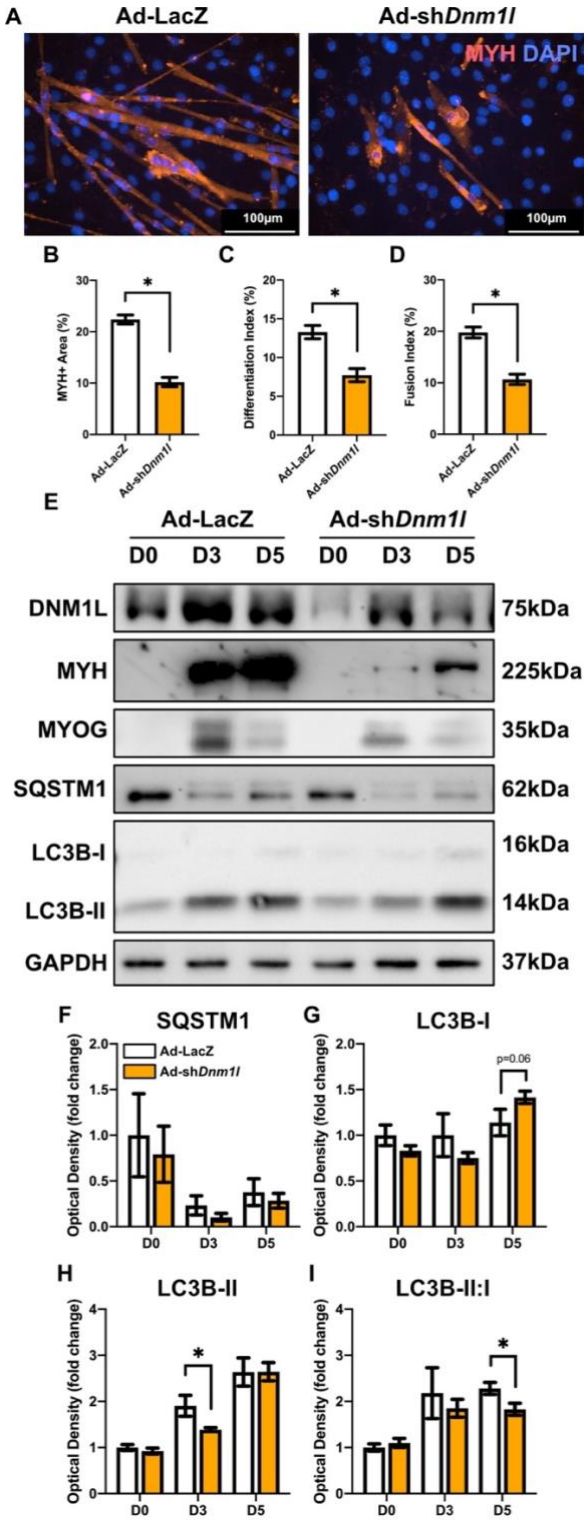


Figure 5: DNM1L KD impairs myogenic differentiation. A) Representative myosin heavy chain (MYH; red) and DAPI (blue) stain of D5 myotubes. Scale bar indicates 100 μm. Quantification of B) MYH+ area, C) differentiation index, and D) fusion index. Representative immunoblot E) and quantification of F) SQSTM1, G) LC3B-I, H) LC3B-II, and I) LC3B-II:I. * $p < 0.05$ compared to Ad-LacZ group within the same time point. n = 4-12 per group.

Collectively, these data underscore the complex role of DNM1L in regulating myotube size, myoblast differentiation, mitochondrial dynamics, and apoptosis. The observed alterations in mitochondrial structure and function provide new insights into the cellular mechanisms regulated by DNM1L and highlight the importance of balanced DNM1L expression for maintaining mitochondrial function and myogenesis.

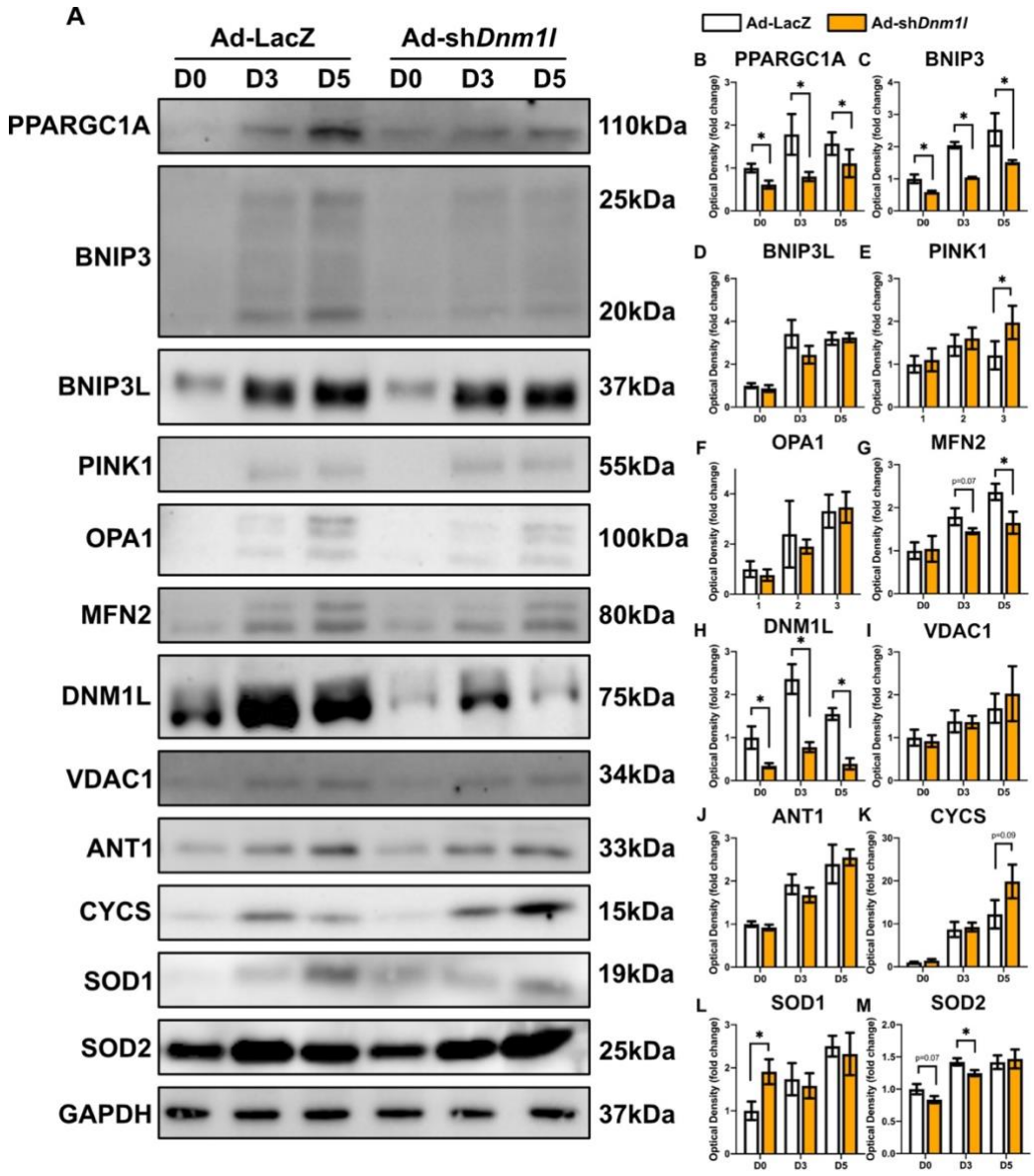


Figure 6: Molecular changes in mitochondrial remodeling proteins in response to DNM1L KD. Representative immunoblots A) and quantification of B) PPARGC1A, C) BNIP3, D) BNIP3L, E) PINK1, F) OPA1, G) MFN2, H) DNM1L, I) VDAC1, J) ANT1, K) CYCS, L) SOD1, and M) SOD2. * $p < 0.05$ compared to Ad-LacZ group within the same time point. n = 4 per group.

Overexpression of BNIP3 promotes mitophagic flux and suppresses mitochondrial apoptotic signaling in fission-deficient myoblasts during differentiation

Given the role of DNM1L in regulating mitophagy and myogenesis, we questioned whether OE of the critical mitophagy receptor BNIP3, which we have previously shown to be important in myogenesis (Baechler et al., 2019), would enhance mitophagy and modify the myogenic response to fission deficiency. Despite the known dependence of BNIP3-induced mitophagy on fission (Lee et al., 2011), BNIP3 OE was sufficient to promote mitophagy in DNM1L KD cells (+320% at D0, +75% at D1, and +42% at D2; $p < 0.05$; Figure 7A-B). Additionally, BNIP3 OE resulted in a slight reduction in the number of mitochondrial branches per cell were observed at D0 ($p = 0.08$) and D1 ($p = 0.09$), hinting the potential role of BNIP3 on mitochondrial fragmentation independent of DNM1L (Figure 7C). This slight morphological change was accompanied by increased MTG fluorescence (+29%; $p < 0.05$; Figure 7E-F), suggesting greater mitochondrial mass, while the normalized TMRE fluorescence was reduced at D1 (-19%; $p < 0.05$; Figure 7G-H). Furthermore, BNIP3 OE in fission-deficient cells reduced CASP3 (-29%; $p < 0.05$) and CASP9 (-15%; $p < 0.05$) activities, without affecting mitochondrial Calcein-AM retention (i.e., MPTP opening) or CAPN activity at D1 (Figure 7I-M). Collectively, these findings indicate that the upregulation of mitophagy, mediated by BNIP3 OE, may attenuate apoptotic pathways by facilitating the degradation of dysfunctional mitochondria.

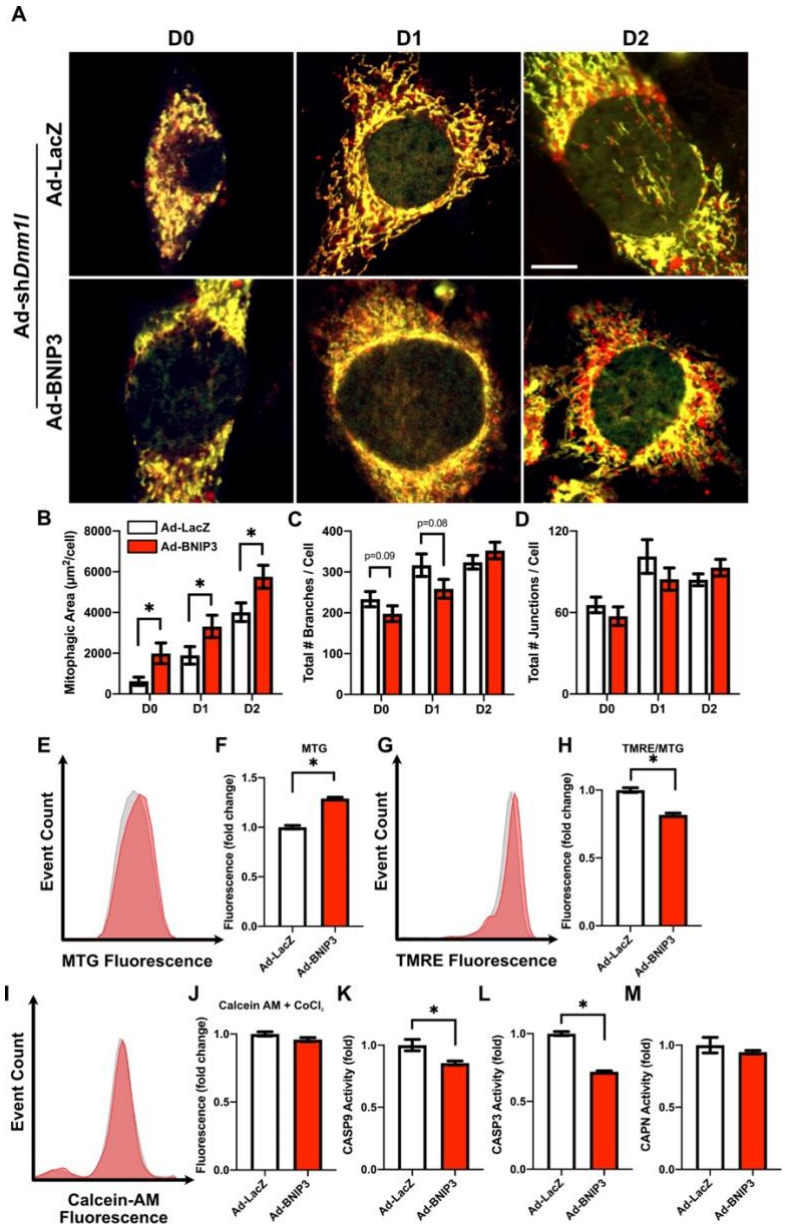


Figure 7: BNIP3 OE activates mitophagy and suppresses CASP activity in fission-deficient cells. A) Representative images of myoblasts transduced with Ad-CMV-COXVIII-EGFP-mCherry to detect mitophagic flux. Mitochondria are dual-labeled EGFP and mCherry (i.e., yellow). EGFP is degraded during the breakdown of the mitochondria resulting in red fluorescence only (i.e., red puncta) and is indicative of mitophagy. Scale bar indicates 5 μm. Quantification of B) mitophagic area, C) total mitochondrial branch count, and D) total mitochondrial junction count per cell. Representative histograms and quantification of E-F) MitoTracker Green (MTG) fluorescence, G-H) TMRE fluorescence, and I-J) Calcein-AM + $CoCl_2$ fluorescence. Quantification of K) caspase 9 (CASP9), L) caspase 3 (CASP3), and M) calpain (CAPN) activities at D1. * $p < 0.05$ compared to Ad-LacZ group within the same time point. n = 4-30 per group.

BNIP3 OE in fission-deficient cells did not affect myotube size, differentiation, or fusion indices (Figure 8A-D). Additionally, BNIP3 OE did not alter parameters of bulk autophagy, as

evidenced by unchanged levels of SQSTM1 and LC3B (Figure 8E-I). These data indicate that the role of BNIP3 on progressing myogenesis and signaling general autophagic pathways is limited in the absence of mitochondrial fission. Additionally, BNIP3 OE resulted in decreased levels of PPARGC1A at the mid/late stages of differentiation (-60% at D3, -90% at D5; $p < 0.05$; Figure 9A-B), while simultaneously increasing PINK1 levels but not to a significant degree (Figure 9E). BNIP3 OE in fission-deficient cells did not alter other markers of mitochondrial dynamics (OPA1 and MFN2) or mitochondrial proteins (Figure 9F-M). This highlights that while BNIP3 can enhance mitophagy in fission-deficient cells, its OE alone is not sufficient to compensate for the deficiencies in mitochondrial fission, nor to broadly impact myogenesis in these cells.

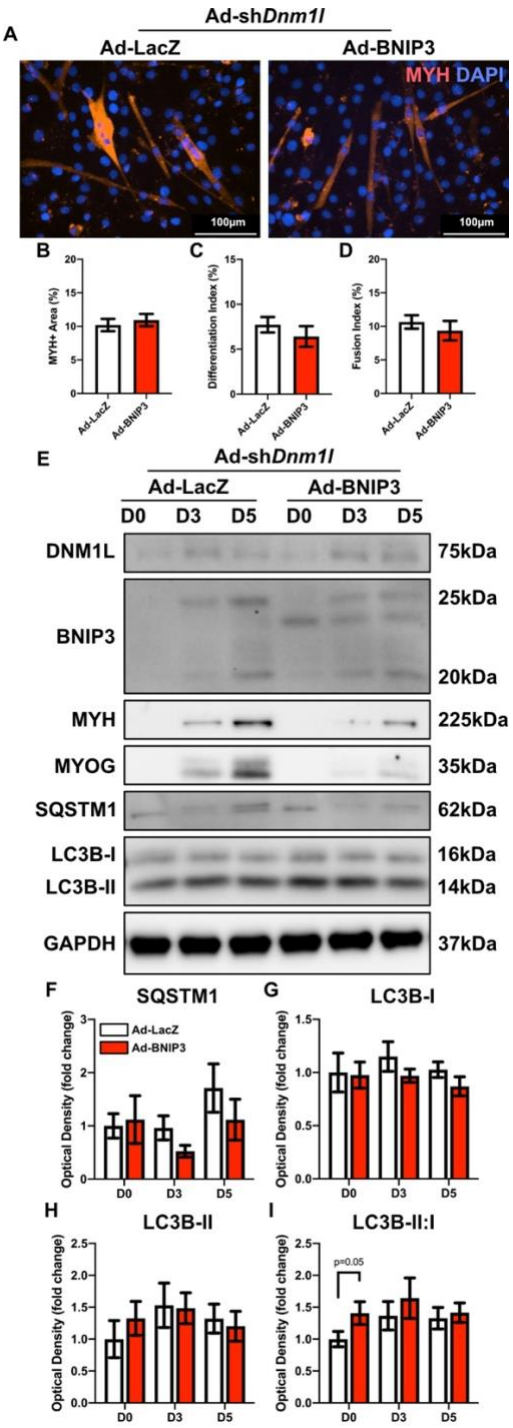


Figure 8: BNIP3 OE in fission-deficient cells does not modify myogenic differentiation. A) Representative myosin heavy chain (MYH; red) and DAPI (blue) stain of D5 myotubes. Scale bar indicates 100 μm. Quantification of B) MYH+ area, C) differentiation index, and D) fusion index. Representative immunoblot E) and quantification of F) SQSTM1, G) LC3B-I, H) LC3B-II, and I) LC3B-II:I. * $p < 0.05$ compared to Ad-LacZ group within the same time point. n = 4-12 per group.

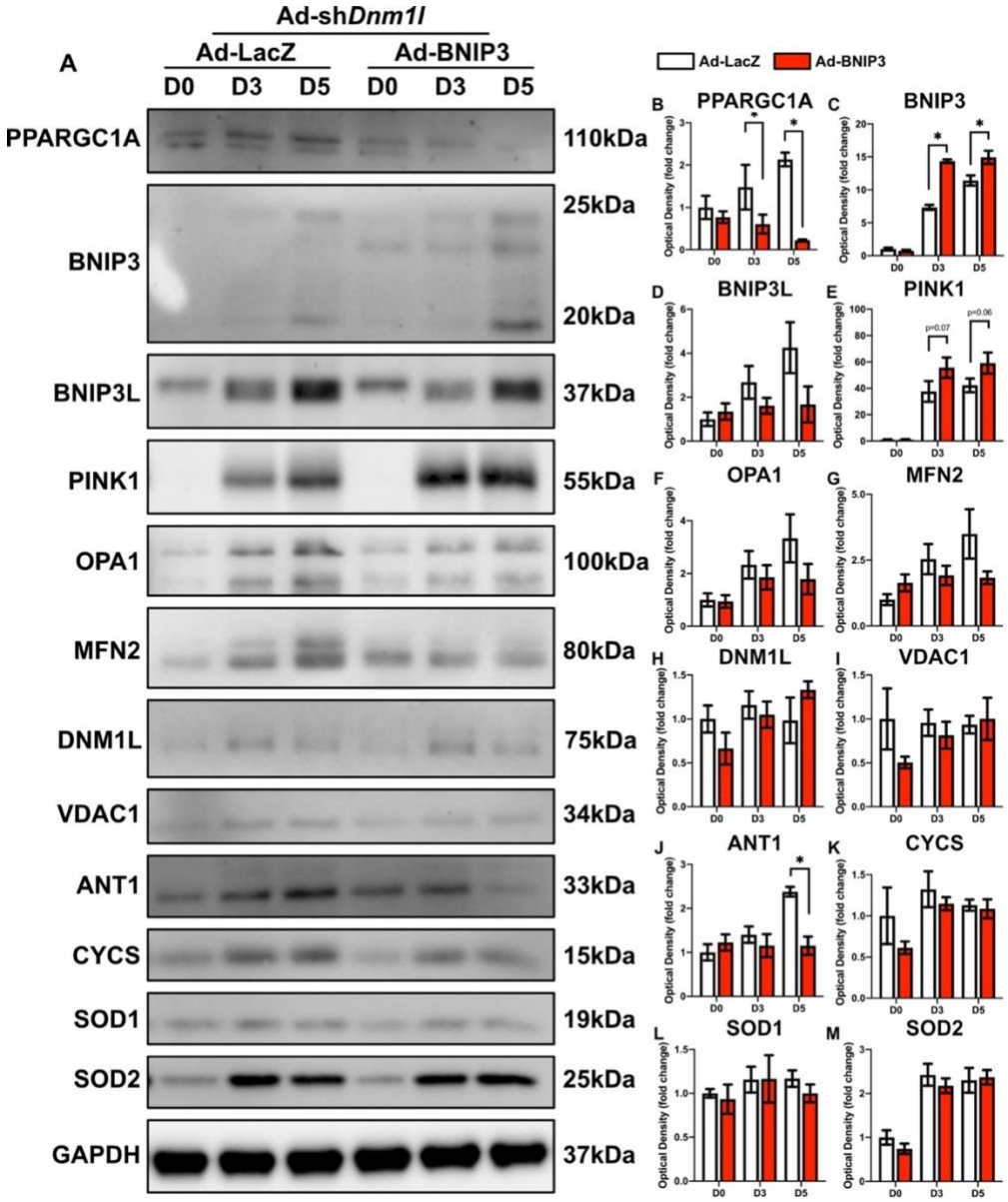


Figure 9: Molecular changes in mitochondrial remodeling proteins in response to BNIP3 OE in fission-deficient cells. Representative immunoblots A) and quantification of B) PPARGC1A, C) BNIP3, D) BNIP3L, E) PINK1, F) OPA1, G) MFN2, H) DNM1L, I) VDAC1, J) ANT1, K) CYCS, L) SOD1, and M) SOD2. * $p < 0.05$ compared to Ad-LacZ group within the same time point. n = 4 per group.

PPARGC1A OE exacerbates myogenic defects in fission-deficient cells

Myogenesis is accompanied by significant mitochondrial remodeling, the result of which is a mitochondrial network that is adept to provide energy at a high enough level to meet the demands of the newly formed myotube (Rahman & Quadrilatero, 2021b, 2021a). As a result, we

questioned whether the OE of the master regulator of mitochondrial biogenesis PPARGC1A could overcome the need for mitochondrial fission and mitophagy to aid in maturation of the mitochondrial network to meet the increased energetic demand of myogenesis.

To our surprise, PPARGC1A OE in fission-deficient cells significantly exacerbates myogenic defects, leading to reduced myotube size (-20%; $p < 0.05$), differentiation (-33%; $p < 0.05$), and fusion indices (-34%; $p < 0.05$; Figure 10A-D). This was accompanied by initial elevations in LC3B-I (+75% at D0, +117% at D3; $p < 0.05$) and LC3B-II (210% at D0, 150% at D3; $p < 0.05$); however, SQSTM1 levels were only reduced at D0 ($p = 0.07$), and the overall LC3B-II ratio was elevated only at D0 ($p = 0.06$; Figure 10E-I). This indicates that while PPARGC1A generally supports mitochondrial mass/function, its OE disrupts myogenesis when fission is impaired, highlighting the need for sequential activation of mitochondrial remodeling processes during myogenesis. The results may also suggest a temporary autophagic response that is not sustained over time in fission-deficient cells.

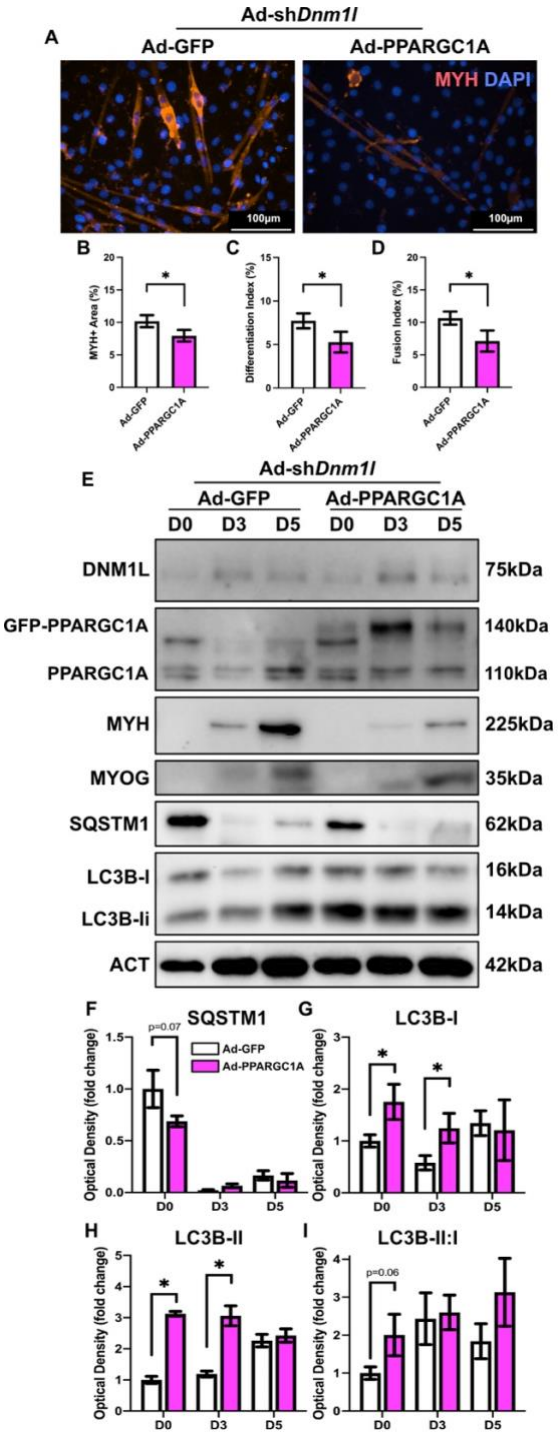


Figure 10: PPARGC1A OE in fission deficient cells exacerbates myogenic defects associated with fission-deficiency. A) Representative myosin heavy chain (MYH; red) and DAPI (blue) stain of D5 myotubes. Scale bar indicates 100 μm. Quantification of B) MYH+ area, C) differentiation index, and D) fusion index. Representative immunoblot E) and quantification of F) SQSTM1, G) LC3B-I, H) LC3B-II, and I) LC3B-II:I. * $p < 0.05$ compared to Ad-GFP group within the same time point. n = 4-12 per group.

PPARGC1A OE in fission-deficient cells resulted in increased levels of mitophagy receptors, such as BNIP3 (+148% at D0, +278% at D3; $p < 0.05$) and BNIP3L (+227% at D0, 101% at D3; $p < 0.05$; Figure 11A-D). In addition to these changes, PPARGC1A OE was associated with elevated levels of mitochondrial dynamic proteins OPA1 and MFN2, along with increased levels of mitochondria-related proteins including VDAC1, ANT1, CYCS, and SOD1/2 in fission-deficient cells (Figure F-M). Elevated mitophagy receptor levels may suggest the cells are attempting to remove damaged mitochondria more efficiently. Alternatively, increased levels of mitophagy receptors may be a consequence of a larger mitochondrial pool and could simply be a by-product of mitochondrial biogenesis.

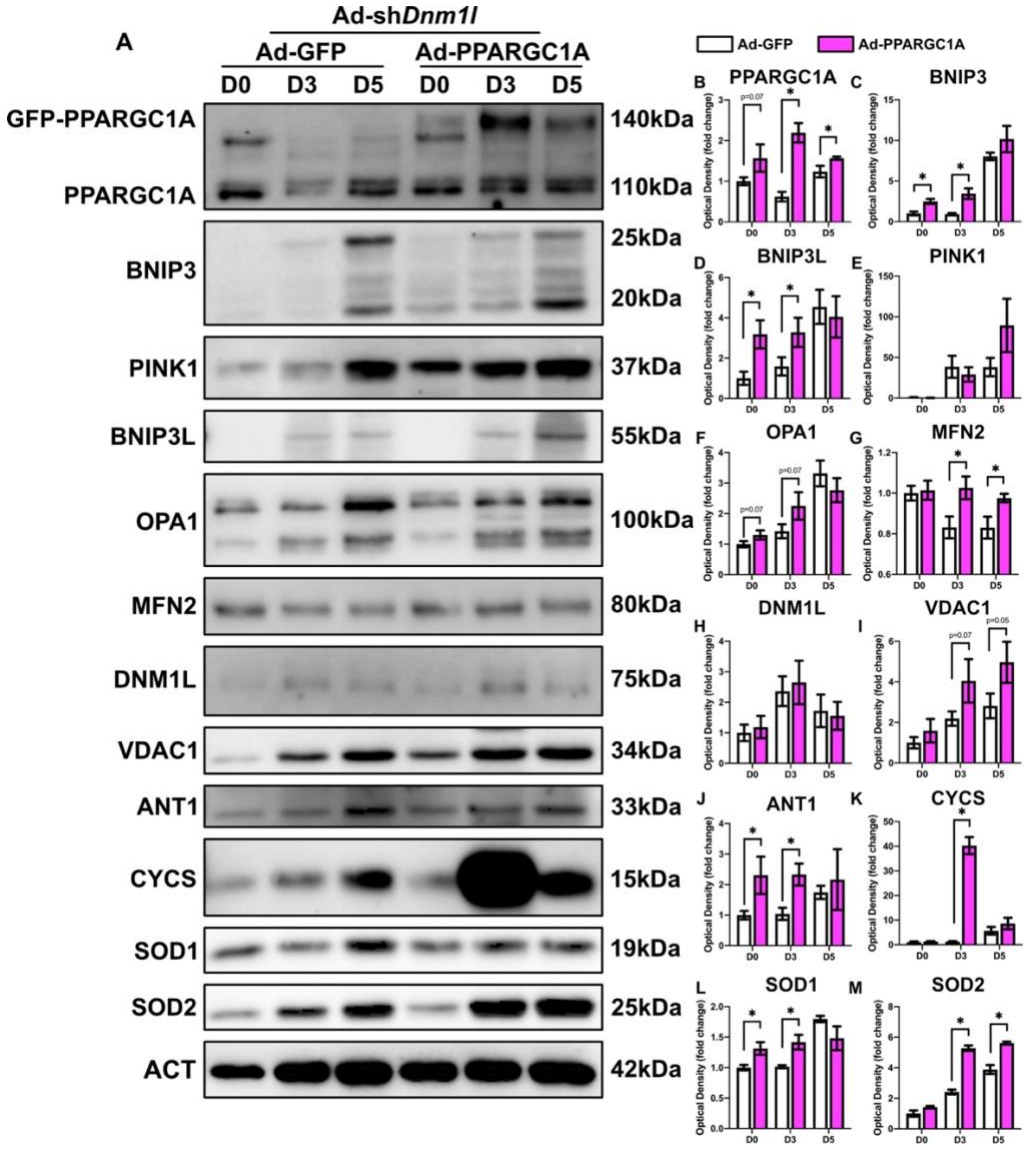


Figure 11: Molecular changes in mitochondrial remodeling proteins in response to PPARGC1A OE in fission-deficient cells. Representative immunoblots A) and quantification of B) PPARGC1A, C) BNIP3, D) BNIP3L, E) PINK1, F) OPA1, G) MFN2, H) DNM1L, I) VDAC1, J) ANT1, K) CYCS, L) SOD1, and M) SOD2. * $p < 0.05$ compared to Ad-GFP group within the same time point. n = 4 per group.

Enhanced mitophagic flux and fission are insufficient to recover myogenesis in Bnip3$^{-/-}$ cells

To further understand the complex interaction between mitochondrial remodeling processes, we questioned whether DNM1L OE could signal mitochondrial remodeling and recover myogenesis independent of BNIP3-mediated mitophagy. We found that DNM1L OE in *Bnip3*$^{-/-}$ cells increased mitophagic flux in differentiating myoblasts at D1 (+42%; $p < 0.05$) and D2 (+41%;

$p < 0.05$), concomitant with a reduction in the total number of mitochondrial branches (-13% at D0 and 14% at D1; $p < 0.05$; Figure 12A-D). This coincides with our earlier results demonstrating enhanced mitophagic flux in DNM1L OE cells (Figure 1); however, this is unique because the enhanced mitophagic flux independent of BNIP3 suggests alternative mitophagy mediated mechanisms that are active in these cells. Furthermore, DNM1L OE in *Bnip3*$^{-/-}$ cells led to decreased MTG fluorescence (-22%; $p < 0.05$), TMRE fluorescence (-27%; $p < 0.05$), and activities of CASP3 (-40%; $p < 0.05$), CASP9 (-27%; $p < 0.05$), and CAPN activities (-38%; $p < 0.05$), while also reducing mitochondrial MPTP opening at D1 (+15%; $p < 0.05$; Figure 12E-M). These findings collectively indicate a role of DNM1L in modulating mitochondrial function and downstream mitochondrial apoptotic signaling during myogenic differentiation independent of BNIP3-mediated mitophagy.

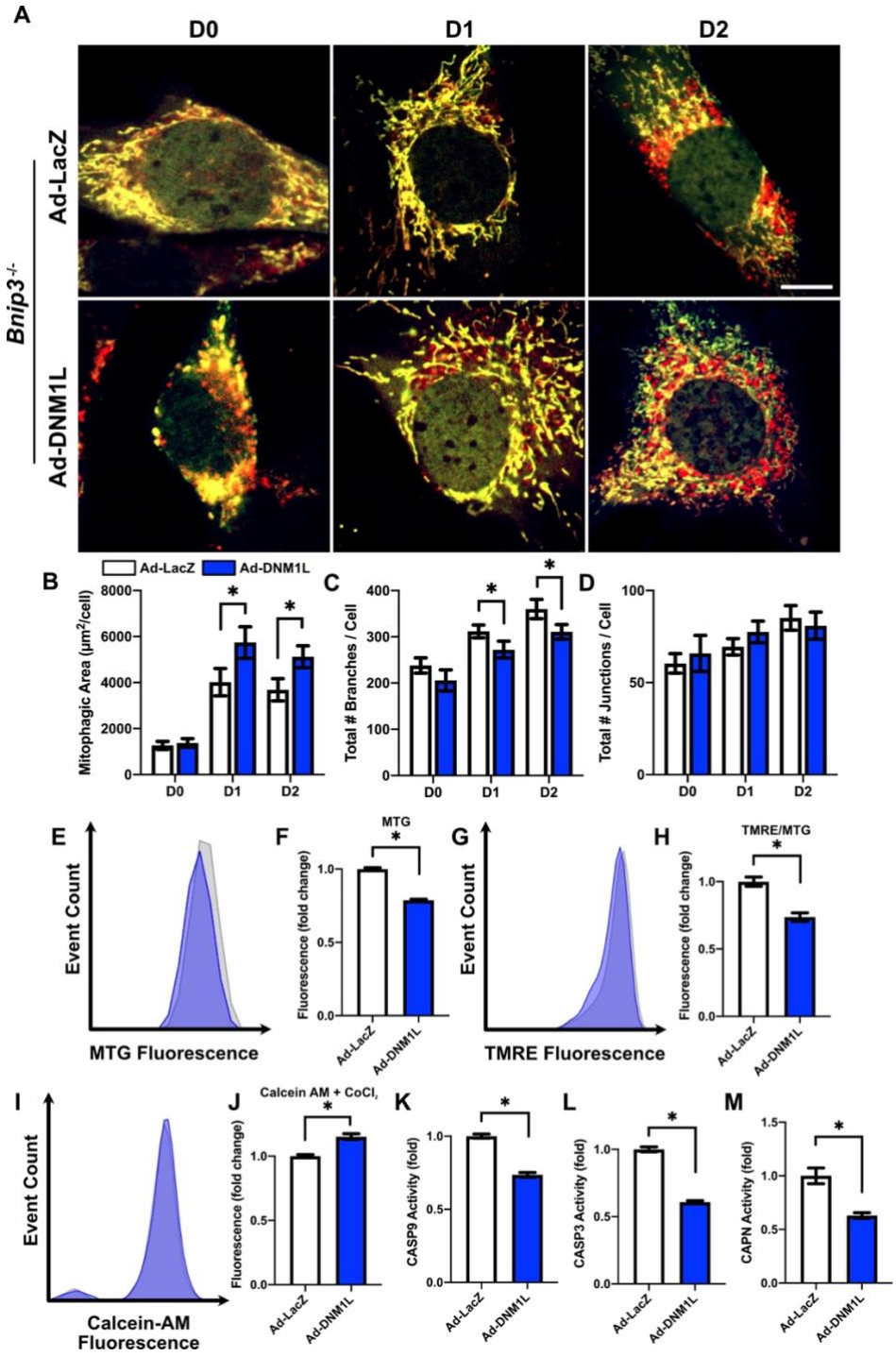


Figure 12: DNM1L OE in *Bnip3*$^{-/-}$ cells increases mitochondrial fragmentation and mitophagy. A) Representative images of myoblasts transduced with Ad-CMV-COXVIII-EGFP-mCherry to detect mitophagic flux. Mitochondria are dual-labeled EGFP and mCherry (i.e., yellow). EGFP is degraded during the breakdown of the mitochondria resulting in red fluorescence only (i.e., red puncta) and is indicative of mitophagy. Scale bar indicates 5 μm. Quantification of B) mitophagic area, C) total mitochondrial branch count, and D) total mitochondrial junction count per cell. Representative histograms and quantification of E-F) MitoTracker Green (MTG) fluorescence, G-H) TMRE fluorescence, and I-J) Calcein-AM + $CoCl_2$ fluorescence. Quantification of K) caspase

3 (CASP3), L) caspase 9 (CASP9), and M) calpain (CAPN) activities at D1. * $p < 0.05$ compared to Ad-LacZ group within the same time point. n = 4-30 per group.

We also show that DNM1L OE in *Bnip3*$^{-/-}$ cells does not recover defects observed in myotube size, differentiation, or fusion indices (Figure 13A). This suggests that BNIP3 plays a crucial role in myogenesis, with its influence possibly extending beyond its known function in mitophagy. Alternatively, the direct targeting of mitophagic flux in *Bnip3*$^{-/-}$ cells could be the key to restoring myogenesis. Nonetheless, we show that DNM1L OE in *Bnip3*$^{-/-}$ cells was associated with reduced levels of LC3B-I (-50% at D3 and -47% at D5; $p < 0.05$) and alterations in LC3B-II (+80% at D0, -35% at D3 and -50% at D5; $p < 0.05$) during differentiation, indicating rapid changes in autophagosome formation (Figure 13B-F). Interestingly, DNM1L OE in *Bnip3*$^{-/-}$ cells does not alter the levels of key proteins related to mitochondrial biogenesis (i.e., PPARGC1A), mitophagy (i.e., BNIP3L, PINK1), mitochondrial dynamics (i.e., OPA1, MFN2), or other mitochondrial-related molecules (i.e., VDAC1, ANT1, CYCS, SOD1, and SOD2) (Figure 14A-L). This suggests that DNM1L may specifically affect mitochondrial quality control mechanisms rather than broader aspects of mitochondrial remodeling including mitochondrial biogenesis in *Bnip3*$^{-/-}$ cells.

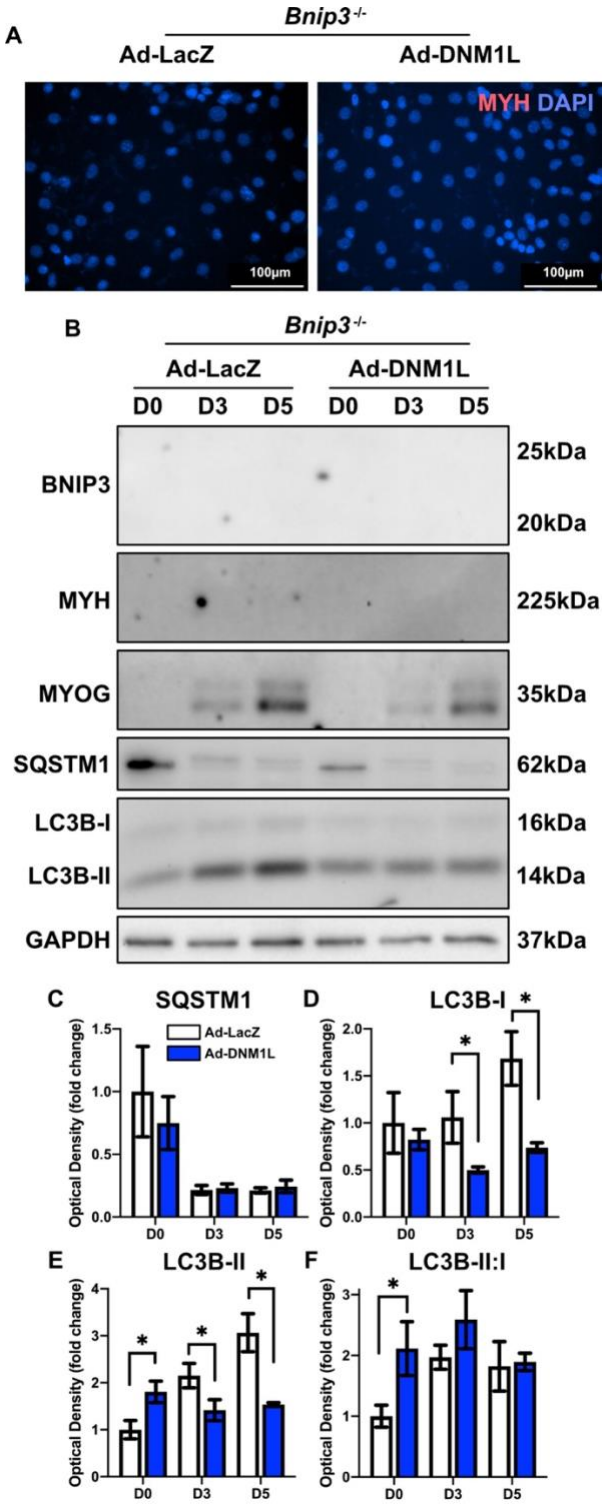


Figure 13: DNM1L OE in *Bnip3*$^{-/-}$ cells does not modify myogenic differentiation. A) Representative myosin heavy chain (MYH; red) and DAPI (blue) stain of D5 cells. Scale bar indicates 100 μm. Representative immunoblot B) and quantification of C) SQSTM1, D) LC3B-I, E) LC3B-II, and F) LC3B-II:I. * $p < 0.05$ compared to Ad-LacZ group within the same time point. n = 4 per group.

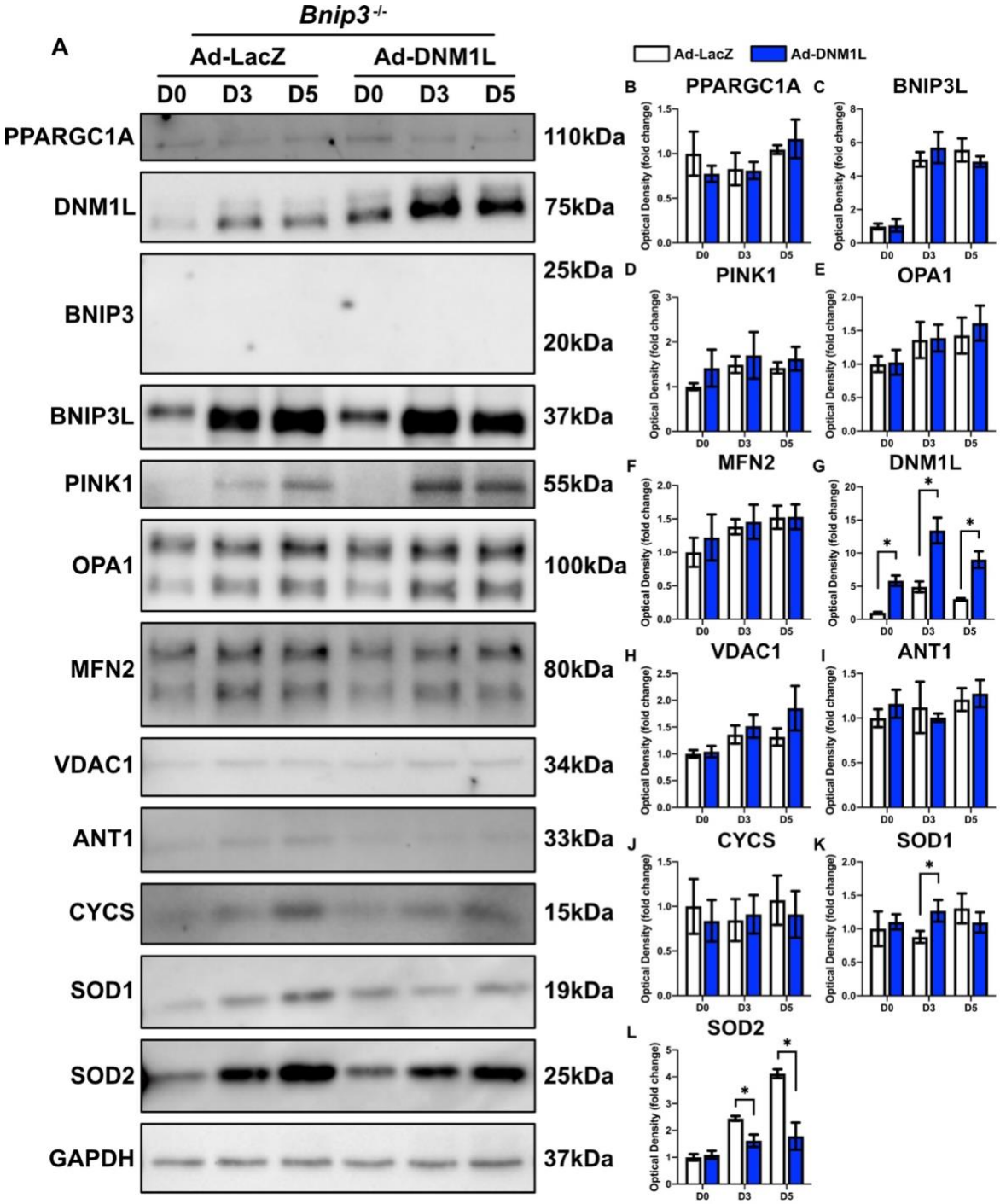


Figure 14: Molecular changes in mitochondrial remodeling proteins in response to DNM1L OE in *Bnip3*$^{-/-}$ cells. Representative immunoblots A) and quantification of B) PPARGC1A, C) BNIP3L, D) PINK1, E) OPA1, F) MFN2, G) DNM1L, H) VDAC1, I) ANT1, J) CYCS, K) SOD1, and L) SOD2. * $p < 0.05$ compared to Ad-LacZ group within the same time point. n = 4 per group.

Discussion

Robust cellular remodeling is a fundamental aspect that underpins myogenesis. A critical component of this remodeling process is mitochondrial remodeling, which is crucial in ensuring the energy demands of newly formed myotubes are met to fully support its physiological functions. Despite the recognized importance of mitochondrial remodeling in myogenesis (Rahman & Quadrilatero, 2021b, 2021a), the precise mechanisms and interactions within this process remain inadequately understood. In the present study, we provide evidence that mitochondrial remodeling processes must occur in a specific, sequential order for effective myogenesis. Our findings indicate that: 1) alterations in mitochondrial fission regulates mitophagy and the progression of myogenesis, 2) the overexpression of mitophagy or biogenesis-related molecules alone does not compensate for defects associated with fission-deficiency, underscoring the necessity of proper mitochondrial fission during myogenesis, and 3) the overexpression of DNM1L in BNIP3-deficient cells fails to rescue differentiation or signal other mitochondrial remodeling processes. These data highlight the intricate balance required among mitochondrial dynamics processes for successful muscle cell differentiation. This sequential coordination of mitochondrial remodeling processes is required for the efficient progression of myogenesis, providing new insights into the cellular mechanisms underlying *in vitro* myotube formation.

Alterations in mitochondrial fission modulate mitophagy and progression of myogenesis

Mitochondrial fission is a critical process that ensures proper mitochondrial distribution and function within cells, playing a vital role in maintaining cellular energy balance and homeostasis. This dynamic remodeling of mitochondria facilitates the removal of damaged mitochondria through mitophagy and supports the generation of higher functioning mitochondria

(Barbieri et al., 2011; Rahman & Quadrilatero, 2021b, 2021a; Robinson et al., 2019; Sin et al., 2016; Vertel & Fischman, 1977). Changes in mitochondrial dynamics can significantly affect the differentiation of various cell types by disrupting mitochondrial function and energy production. In certain cell types, a shift towards mitochondrial fusion is essential for efficient differentiation, such as in induced pluripotent stem cells (iPSCs) and immune cells (Buck et al., 2016; Hoque et al., 2018). In this context, the fusion of the mitochondrial network is necessary to reprogram the cells and enhance OXPHOS (Buck et al., 2016; Hoque et al., 2018). A similar form of metabolic reprogramming is observed in muscle cells during differentiation. However, there appears to be a greater need for mitochondrial fission, especially during the early stages of the differentiation program, to support the metabolic reprogramming of these cells (Schwarten et al., 2009). The need for mitochondrial fission is also corroborated by more recent work in muscle stem cells (i.e., satellite cells) that lack DNM1L (Hong et al., 2022). This study demonstrated that *in vivo* regeneration is accompanied by a temporal increase in DNM1L to aid in satellite cell proliferation via activation of mitophagy (Hong et al., 2022). Conversely, the loss of DNM1L-mediated fission in satellite cells significantly limits mitophagy and activation of satellite cells; thereby, leading to an impaired regenerative response (Hong et al., 2022). Taken together, it is clear that mitochondrial dynamics are important in cellular differentiation.

There is strong evidence indicating that impaired mitochondrial fission is detrimental to myogenic differentiation. (Bloemberg & Quadrilatero, 2016; B. Kim et al., 2013); however, there is less direct evidence linking the role of mitochondrial hyper-fragmentation during myogenesis. By extrapolating results from developmental studies utilizing a DNM1L OE mouse model, we can gain insights into the role of DNM1L in regulating muscle formation. Previous studies have demonstrated that DNM1L OE impaired muscle development in young mice by preventing the

maturation of the mitochondrial network (Giovarelli et al., 2020; Touvier et al., 2015). Our data indicate a similar pattern, showing a reduction in MYH+ area in DNM1L OE cells, suggesting a decrease in myotube size without affecting the differentiation or fusion of muscle cells. We show that the reduction in myotube size appears to be linked to the increased fragmentation of the mitochondrial network, particularly during the early phase of the differentiation program, which is also associated with enhanced mitophagic flux. Interestingly, although previous studies suggest that mitochondrial fission is a preceding step to cell death (Suen et al., 2008), our findings indicate that DNM1L OE reduces CASP9 activity; albeit while increasing MPTP opening. The reasons behind this paradox are not fully understood. One possibility is the persistence of "dysfunctional" mitochondria that have not been effectively targeted for mitophagy. Alternatively, MPTP opening may be sensitive to changes in the overall mitochondrial network morphology. Supporting this idea, previous research has demonstrated that inhibition of mitochondrial fission can prevent MPTP opening, whereas ablation of MFN2, leading to increased mitochondrial fragmentation, heightens the susceptibility to MPTP opening in cardiomyocytes (Ong et al., 2010; Papanicolaou et al., 2011). Nonetheless, DNM1L OE decreased OPA1 and MFN2 levels during the mid-stage of myotube formation (i.e., Day 3), while also reducing mitochondrial-specific molecules like total CYCS and SOD2 during the mid/late stage of myogenesis (i.e., Days 3 and 5). We found no changes in the mitochondrial biogenesis marker PPARGC1A or other mitophagy-related molecules in DNM1L OE cells, suggesting a lack of crosstalk between these mechanisms. Nonetheless, our DNM1L OE data indicates that mitochondrial fission directly impacts mitophagic flux in differentiating cells; however, it is unknown if DNM1L actively promotes recruitment of mitophagy-related molecules to the mitochondria following fission.

Previous studies have investigated the role of mitochondrial fission in regulating myogenesis through the chemical inhibition of DNM1L or transfection using a dominant negative $DNM1L^{K38A}$ *in vitro* (Bloemberg & Quadrilatero, 2016; B. Kim et al., 2013). These studies have consistently shown significant defects in myogenesis and the activation of cellular apoptosis (Bloemberg & Quadrilatero, 2016; B. Kim et al., 2013). For instance, increasing concentrations of mdivi-1 resulted in a stepwise decline in myogenic markers, including MYOG, and reduces MYH formation in C2C12 cells and primary myoblasts (Bloemberg & Quadrilatero, 2016; B. Kim et al., 2013). Transfection of cells with dominant negative $DNM1L^{K38A}$ showed an identical reduction in myotube formation as mdivi-1 treatment (B. Kim et al., 2013). Our findings are in direct alignment with these studies, demonstrating impaired differentiation, fusion, and overall myotube size in DNM1L KD cells. These defects appear to be coupled with a hyperfused mitochondrial network and suppressed mitophagic flux. Furthermore, we observed consistent activation of CASP9 and CASP3, suggesting the activation of intrinsic apoptotic signaling. These results are consistent with previous work from our lab (Bloemberg & Quadrilatero, 2016) and others (Inoue-Yamauchi & Oda, 2012; B. Kim et al., 2013), which link impaired mitochondrial fission to the activation of CASP3 and elevated TUNEL+ nuclei in cells. Unlike the earlier results from the present study showing little to no change in mitochondrial remodeling proteins with DNM1L OE (Figure 3), DNM1L KD significantly suppresses several molecules, including PPARGC1A, BNIP3, MFN2, and SOD2. This suggests that the lack of mitochondrial fission can signal, probably indirectly, several other mitochondrial remodeling processes. Collectively, these data indicate that mitochondrial fission is crucial not only for the progression of myogenesis but also for maintaining mitochondrial and cellular function, potentially by regulating key signaling pathways and protein degradation mechanisms.

Overexpressing molecules involved in mitophagy or biogenesis are insufficient to rescue myogenic defects due to fission-deficiency

In the present study, we have established the necessity of mitochondrial fission for myogenesis. We then aimed to determine if modifying other mitochondrial remodeling processes, particularly mitophagy and biogenesis, could improve differentiation in DNM1L-independent mechanisms. As discussed earlier, mitophagy is at the center of the myogenic differentiation program such that the activation of mitophagy is required for downstream activation of other processes like biogenesis (Baechler et al., 2019). Furthermore, cellular defects and a loss of differentiation potential are observed when mitophagy is either directly or indirectly suppressed, as seen in aged cells or autophagy-deficient cells (Baechler et al., 2019; García-Prat et al., 2016; Hong et al., 2022). Therefore, it stands to reason that suppression of mitophagy in a fission-deficient state could be countered with the OE of mitophagy-related molecules. Since previous work from our lab has emphasized the importance of the mitophagy receptor BNIP3, we questioned if BNIP3 OE could counter the defects observed in fission-deficient cells by enhancing mitophagy. Overexpressing BNIP3 in fission-deficient cells enhanced mitophagic flux but failed to recover myogenic defects. Interestingly, BNIP3 OE in these cells also led to decreased activity of CASP3 and CASP9, potentially due to improvements in the mitochondrial network stemming from the enhanced mitophagic flux. However, these findings contrast with prior studies in cardiomyocytes, where BNIP3 OE did not activate mitophagy in either fission-deficient cells or cells with hyperfused mitochondria (Lee et al., 2011). Interestingly, BNIP3 OE in fission-deficient cells led to a reduction in PPARGC1A levels and nonsignificant increases in PINK1. This observation may suggest potential crosstalk between BNIP3 and other signaling pathways, including those involved in mitochondrial biogenesis and alternative mitophagy mechanisms.

To date, no studies have specifically investigated PPARGC1A OE in fission-deficient cells. Nevertheless, previous work has established a relationship between autophagy and PPARGC1A during myogenic differentiation (Baechler et al., 2019; Sin et al., 2016). For example, our group has observed decreased PPARGC1A levels in autophagy-deficient and *Bnip3*$^{-/-}$ cells, indicating that impaired autophagy or mitophagy may disrupt mitochondrial biogenesis signaling pathways (Baechler et al., 2019). This finding is supported by other studies that demonstrate enhanced nuclear localization of PPARGC1A during the later stages of myogenesis (Sin et al., 2016). Additionally, inhibition of autophagy by bafilomycin A has been shown to restrict the nuclear translocation of PPARGC1A (Sin et al., 2016). The current study further supports these observations by documenting reduced PPARGC1A expression in fission-deficient cells, suggesting an interaction between mitochondrial fission and biogenesis signaling pathways. Previous findings have also shown that mitochondrial biogenesis facilitates the renewal of the mitochondrial network following mitophagy, thereby producing more functionally efficient mitochondria that meet the energetic demands of myotubes (Sin et al., 2016). In our experiments, overexpressing PPARGC1A in fission-deficient cells significantly hindered myogenic differentiation, a process associated with increased levels of autophagosome proteins, mitophagy receptors, dynamics proteins, and other mitochondrial-related molecules. These results indicate that while PPARGC1A OE can enhance biogenesis, it may negatively impact myogenesis in the absence of proper mitochondrial fission and subsequent mitophagy.

BNIP3 governs myogenic differentiation beyond its role in mitophagy

Based on the data presented, it appears that efficient mitochondrial fission and mitophagy are essential for myogenesis. In the absence of mitochondrial fission, significant defects in

mitophagy occur, leading to impaired myogenesis. Previous research from our group has demonstrated that disruptions in autophagic flux or the absence of the mitophagy receptor BNIP3 impedes the myogenic program of cells, and suppresses the expression of fission-related proteins such as DNM1L (Baechler et al., 2019). Consequently, we investigated whether elevating DNM1L levels in *Bnip3*$^{-/-}$ cells could influence myogenesis parameters, and if enhanced mitochondrial mitophagy could trigger additional mechanisms, such as mitochondrial biogenesis, to promote myogenesis in these cells. Although prior studies have established that fission is necessary for BNIP3-mediated mitophagy (Lee et al., 2011); to our knowledge, the effect of DNM1L OE on enhancing mitophagy independently of BNIP3 has not been examined. Contrary to expectations, we observed that *Bnip3*$^{-/-}$ cells continued to show mitophagic activity but failed to differentiate into myotubes. This finding aligns partially with earlier findings from our group, which noted differentiation defects in *Bnip3*$^{-/-}$ cells; however, mitophagic flux was not explored (Baechler et al., 2019). In the present study, DNM1L OE led to increased mitochondrial network fragmentation (i.e., reduced branching) and enhanced mitophagic flux, yet it did not restore myogenic differentiation in these cells. This observation suggests a potential requirement for BNIP3 in regulating myogenic differentiation, possibly through its roles in mitophagy or the modulation of other signaling cascades. Interestingly, the persistence of mitophagic flux in *Bnip3*$^{-/-}$ cells indicates the activation of alternative mitophagy pathways. Moreover, this observation aligns with existing knowledge that multiple redundant mitophagy pathways exist, which can compensate for the loss of a single molecule (Lampert et al., 2019; K. Liu et al., 2022). This redundancy highlights the complexity of studying mitophagy mechanisms.

Upon detailed examination of mitochondrial function, we noted a decline in mitochondrial membrane potential, previously associated with increased mitochondrial fragmentation.

Concurrently, we observed diminished MPTP opening and CASP9, CASP3, and CAPN activities. These findings imply a potential reduction in mitochondrial apoptotic signaling associated with alterations in the mitochondrial network. This alteration could potentially mitigate some network defects linked to the absence of BNIP3. Notably, the present study also demonstrates for the first time that DNM1L OE does not significantly affect mitochondrial biogenesis, the expression of mitochondrial fusion-related proteins, or other mitochondrial-associated proteins. Collectively, our results indicate that while DNM1L can enhance mitochondrial fragmentation, it is insufficient to modify other mitochondrial remodeling processes or to facilitate the differentiation of BNIP3-deficient myoblasts.

Conclusion

This study explored the complex interplay between mitochondrial remodeling processes and myogenesis, revealing that the orchestrated regulation of mitochondrial fission, mitophagy, and biogenesis is fundamental to efficient muscle cell differentiation. We show that mitochondrial fission acts as a pivotal gateway that facilitates subsequent cellular processes such as the efficient removal of damaged mitochondria through mitophagy and the renewal of mitochondrial networks via biogenesis. We demonstrate that genetic alterations in the expression of key mitochondrial remodeling proteins, such as BNIP3 and PPARGC1A, though critical, are insufficient on their own to address defects in myogenesis due to DNM1L KD. This suggests that a lack of proper fission disrupts the foundational architecture required for initiating effective mitochondrial remodeling processes, specifically mitophagy, which is needed for the progression of myogenesis. Insights from this study highlight a potential therapeutic angle, emphasizing the need for strategies that can restore or enhance the natural sequence of mitochondrial remodeling, ensuring that each phase contributes positively to myogenesis. These strategies could be particularly beneficial in treating muscular diseases where mitochondrial dysfunction is a contributing factor, offering a route to enhance muscle repair and functional recovery through targeted modulation of mitochondrial dynamics.

Chapter 3: Role of Mitochondrial Remodeling During Postnatal Muscle Development

Project Rationale and Objectives

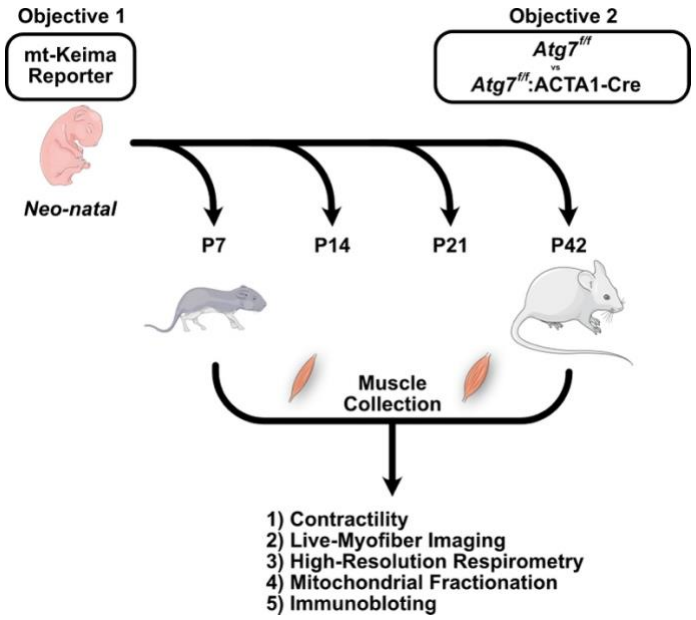
Skeletal muscle development is characterized by the rapid growth of muscle mass, and maturation of myofibers (i.e., greater myonuclei count, myonuclear domain, mitochondrial network complexity, etc.) (Bakeeva et al., 1978; Y. Kim, Yang, et al., 2019; Luff & Atwood, 1971). As skeletal muscle develops, the mitochondrial network changes dramatically. For instance, the mitochondrial network is parallel to the myofiber shortly after birth but changes to a perpendicular structure as the skeletal muscle develops (Y. Kim, Yang, et al., 2019). Although some studies have characterized aspects of mitochondrial remodeling during postnatal development (Bakeeva et al., 1978; Y. Kim, Yang, et al., 2019; Y. Kim et al., 2024; Luff & Atwood, 1971), the mechanism for this remodeling is unclear. Based on these findings alone, it remains unclear how mitophagy influences mitochondrial remodeling, a process we have previously demonstrated. This includes how autophagy and mitophagy signaling regulate differentiation and whether changes in other mitochondrial remodeling processes occur during postnatal development.

Therefore, the main objectives for Project 2 were:

1. To characterize mitochondrial remodeling during postnatal development of skeletal muscle.
2. To determine the role of autophagy/mitophagy-deficiency on mitochondrial remodeling during postnatal development.

I hypothesized that:

1. Postnatal development would be accompanied by an initial stage of mitochondrial turnover via mitophagy followed by biogenesis and formation of higher functioning mitochondria in skeletal muscle.
2. *Atg7*-deficiency would prevent the initiation of mitophagy and biogenesis during postnatal development, leading to incomplete maturation of the mitochondrial network and significant mitochondrial dysfunction.



Method Figure 1: Study design for Project 2, Objectives 1 and 2. Young mice from the mt-Keima purebred line (Objective 1) were collected at the following postnatal time-points: P7, P14, P21, and P42. *Atg7*$^{f/f}$:ACTA1-Cre line (Objective 2) were collected at P42. White muscles were collected and analyzed as outlined in the **Material and Methods** section. Results from these experiments characterized mitochondrial remodeling during development, and the influence of the autophagy machinery in regulating the mitochondrial network.

Introduction

The development of skeletal muscle occurs at different stages of life. During embryonic development, the dermomyotome gives rise to $PAX3^{+}/PAX7^{+}$ muscle progenitor cells that proliferate and activate into committed myogenic cells, called myoblasts (Buckingham et al., 2003). Following birth, skeletal muscle continues to grow (i.e., hypertrophy) and is accompanied by the proliferative activity of myogenic cells (Gattazzo et al., 2020). These cells can donate their nuclei to the growing myofibers to increase the overall number of myonuclei and expanding their myonuclear domain (Bachman & Chakkalakal, 2022; White et al., 2010). In mice, the first three weeks of postnatal development is accompanied by rapid increase in body weight up to 8-fold, half of which is due to the increase in muscle mass (Gokhin et al., 2008). Unsurprisingly, postnatal development of skeletal muscle is also accompanied by a robust increase in mitochondrial protein content (Y. Kim, Yang, et al., 2019), signifying an increase in energy demand. Importantly, there is a change in mitochondrial morphology during postnatal development. For example, the mitochondrial network changes from a parallel to a perpendicular morphology relative to the myofiber (Bakeeva et al., 1978; Y. Kim, Yang, et al., 2019).

The development of the mitochondrial network may be attributed to the dynamic balance of mitochondrial remodeling processes, including mitochondrial dynamics and turnover. The importance of these processes has been signified during skeletal muscle development using experimental models. For instance, the muscle-specific knockout of *Dnm1l*, *Opa1*, and *Mfn1/2*, proteins involved in mitochondrial fission and fusion, exhibit a dramatically reduced lifespan and is associated with defects in muscle growth and mitochondrial dysfunction (H. Chen et al., 2010; Favaro et al., 2019; Tezze et al., 2017). Although there is a clear change in mitochondrial morphology during postnatal development, the same is not entirely understood with respect to

mitochondrial turnover (i.e., mitophagy and biogenesis). To date, there are no studies investigating muscle-specific mitophagy deficiency and its implications on muscle development. Previous work from our lab has demonstrated that constitutive knockout of *Atg7*, an important autophagy protein, can result in smaller and weaker muscles (Paré et al., 2017); however, its link to mitophagy and the mitochondrial network is unknown. Additionally, there is emerging evidence suggesting the role of mitophagy as an initiator of mitochondrial biogenesis in myoblasts (Baechler et al., 2019; Sin et al., 2016), albeit more work is needed to fully understand this mechanism with respect to postnatal muscle development.

The purpose of this study was to investigate the role of mitochondrial remodeling during postnatal skeletal muscle development. The current study explored the role of constitutive autophagy-deficiency and its implication on mitochondrial remodeling processes during postnatal muscle development.

Material and Methods

RNA Sequencing Analysis

Publicly available RNA sequencing datasets were retrieved from the Gene Expression Omnibus (GEO) database (accession number GSE1025). Initial quality control was based on exclusion criteria including adapter contamination and low-quality bases. Gene-level expression was quantified and analyzed using the DESeq2 package in RStudio. Differential expression was determined with an adjusted p-value of <0.05 and a minimum log2 fold change of >1, identifying significantly differentially expressed genes. Enrichment of biological processes and pathways was assessed using the clusterProfiler package, with tests against Gene Ontology (GO) terms. Pathways were considered significantly enriched at a corrected p-value of <0.05. Visualization of the results, including volcano plots, heatmaps, and barplots, was conducted using GraphPad PRISM software.

Animals

Mt-Keima animals with a FVB background were kindly gifted by Torin Finkel (Sun et al., 2015, 2017). These animals are a valuable tool for studying mitophagy since they express the fluorescent Keima protein conjugated to the COX8 subunit found within complex IV in the IMM. The unique feature of the Keima molecule is its dual-excitation, single-emission fluorescence, which changes depending on the pH of its environment. Under neutral pH conditions, as found in the cytosol, Keima is excited at 488 nm. In the acidic conditions of the lysosome, where mitochondria are degraded, the excitation shifts to 561 nm. This shift allows for precise monitoring of mitophagy. Additionally, the resistance of this molecule to lysosomal degradation enhances the accuracy of mitophagic flux measurements. Pure-bred mt-Keima pups from were examined at several postnatal timepoints (P7, P14, P21, and P42) during the initial characterization. Weaning

took place at P21, and as a result it was difficult to determine biological sex using anogenital distance at the earlier timepoints. All pups were randomly selected at P7 and P14 timepoints. Equal number of male and female animals were collected at P21 and P42.

In additional experiments, C57BL/6 homozygous for the floxed Atg7 allele (*Atg7*$^{f/f}$; kindly gifted by Dr. Herbert Virgin) were crossed with carriers of the constitutive skeletal muscle-specific Cre recombinase under the control of the actin alpha 1 promotor (i.e., ACTA1-Cre; kindly gifted by Dr. Karyn Esser). Breeding of these animals ultimately generated a constitutive skeletal muscle-specific *Atg7* knockout model (i.e., *Atg7*$^{f/f}$:ACTA1-Cre; hereby called skmKO). *Atg7*$^{f/f}$ littermates were used as controls (i.e., CTRL). Given the low ACTA1 levels and lack of early developmental defects observed in previous work until P40 (Masiero et al., 2009), we decided to collect these animals at P42 to understand the effect of *Atg7*-deficiency on young skeletal muscle. Furthermore, mt-Keima animals were also bred with *Atg7*$^{f/f}$ animals to generate a *Atg7*$^{f/f:mt\text{-}Keima}$ line. These animals were once again crossed with ACTA1-Cre to ultimately generate *Atg7*$^{f/f:mt\text{-}Keima}$:ACTA1-Cre that were used to measure mitophagic flux.

Animals were given free access to food and water. All animal procedures were conducted in accordance with the standards set by the Canadian Council on Animal Care (CCAC) and were approved by the Animal Care Committee (ACC) at the University of Waterloo.

Isolation of Skeletal Muscle

The tibialis anterior (TA), gastrocnemius (GAS), quadricep (QUAD), and triceps brachii muscles were rapidly excised from animals. One TA was stored in BIOPS buffer (2.77mM CaK_2EGTA, 7.23mM K_2EGTA, 5.77mM Na_2ATP, 6.56mM $MgCl_2$-$6H_2O$, 20mM taurine, 15mM Na_2PCr, 20mM imidazole, 0.5mM DTT, 50mM K-MES) on ice for respirometry and confocal

microscopy. The contralateral TA was embedded in OCT and frozen in isopentane cooled by liquid nitrogen for histological analyses. One GAS and QUAD muscle from each animal was snap frozen in liquid nitrogen for immunoblot analyses of whole tissues, while the others were stored in PBS-EDTA solution (10mM EDTA in 1X PBS, pH 7.4) for mitochondrial fractionation. Triceps were only used for mass measurements.

Live Myofiber Imaging and Mitophagy Flux Analyses

The tibialis anterior (TA) muscle was manually separated into bundles in BIOPS buffer on ice. Bundles were rapidly transferred to #1 coverslips and carefully separated to allow maximal contact of muscle bundle to the coverslip. A thin layer of 0.8% agarose gel was placed on top of the bundles to prevent movement during imaging. Five to ten fields consisting of 3-5 myofibers were imaged on a Zeiss LSM 800 confocal microscope at 40X magnification. Individual excitation wavelengths were used to minimize overlap between fluorescent channels. An excitation wavelength of 488nm was used to determine healthy mitochondria (pH ~7; green), whereas an excitation wavelength of 561nm was used to determine mitochondria undergoing mitophagy (pH ~4; red). Emission wavelengths remained the same at 620nm. Puncta count and size were determined in each field using the automated Particle Analysis function in ImageJ.

High-Resolution Respirometry with Simultaneous ROS Measurements

The TA muscle was separated under a stereomicroscope into bundles using very fine tipped forceps in ice-cold BIOPS buffer. Bundles were permeabilized in 50μg/ml of saponin in 1.5ml BIOPS buffer for 30 minutes on ice with gentle rocking. Muscle bundles (1-3mg) were then transferred to 1.5ml of buffer Z (105mM K-MES, 30mM KCl, 1mM EGTA, 10mM K_2HPO_4, 5mM

$MgCl_2$-$6H_2O$, 5mg/ml BSA, pH 7.1) to wash prior to respirometry experiments. Oxygen consumption and mitochondrial hydrogen peroxide (mH_2O_2) emission was measured in buffer Z supplemented with 10μM blebbistatin, 10μM Amplex Red, 5U/ml horseradish peroxidase, and 10U/ml superoxide dismutase using an Oxygraph-2K equipped with a LED2 fluorometry module. Experiments were conducted at 37°C in a 2ml chamber that was hyperoxygenated to ~350uM. Reverse electron flow was determined with the addition of 10mM succinate, followed by 5mM pyruvate and 2.5mM malate. Maximal coupled respiration was stimulated with the addition of 5mM ADP. Cytochrome C was added to ensure outer membrane integrity. mH_2O_2 emission was calibrated from a standard curve established with the same reaction conditions.

Mitochondrial Fractionation

GAS and QUAD muscles were chopped on a stainless-steel board using a razor for one minute. The tissue was transferred back into the same tube containing 5ml of PBS with 10mM EDTA (PBS-EDTA solution) and centrifuged at 500g for 5 minutes. The supernatant was discarded, and the muscles were digested in 0.05% trypsin in PBS-EDTA solution for 5 minutes on ice. The trypsin solution was removed by centrifugation at 500g for 5 minutes. Digested muscles were resuspended in mitochondrial isolation buffer (100mM KCl, 50mM MOPS, 5mM $MgSO_4$-$7H_2O$, 1mM EGTA, 2mg/ml BSA, pH 7.4) and homogenized using a Teflon homogenizer equipped on a drill press set to 200rpm for 5-10 strokes. The homogenized tissue was subjected to low-speed centrifugation (~700 x g) to pellet large debris and the supernatant was transferred to ultracentrifuge tubes and spun at 10,000g for 15 minutes at 4°C. The resulting pellet constituted the mitochondrial pellet and was resuspended in mitochondrial isolation buffer without BSA before being transferred to 1.5ml microcentrifuge tubes and spun at 10,000g for 5 minutes. The

resulting pellet was washed and centrifuged three times in mitochondrial isolation buffer without BSA to remove any cytosolic protein. After the final spin, the supernatant was aspirated, and the pellets were frozen in liquid nitrogen.

Immunoblotting

Snap frozen muscle samples were divided into 20-30mg portions and stored in separate tubes. Muscle samples were crushed into a powder using a liquid nitrogen-cooled pestle and mortar, and transferred to 1.5ml tubes containing 5 volumes of lysis buffer (20mM HEPES, 10mM NaCl, 1.5mM $MgCl_2$, 1mM DTT, 20% glycerol, 0.1% Triton-X100, pH 7.4) with protease inhibitor. Mitochondrial enriched fractions were resuspended in lysis buffer with protease inhibitor and sonicated at 40 Hz for 10 seconds on ice to dissolve any membranal structures. Protein content was determined using a BCA protein assay. Equal protein was loaded and separated using 8-12% SDS-PAGE, transferred on to PVDF membranes, and blocked with 2-5% non-fat milk powder in TBS-T at room temperature for 1 hour. Membranes were briefly rinsed and incubated overnight in primary antibodies against: BNIP3 (#3769, Cell Signaling), BNIP3L (#12396, Cell Signaling), ATG7 (#8558, Cell Signaling), MAP1LC3B/LC3B (#2775, Cell Signaling), GAPDH (#2118, Cell Signaling), OPA1 (#80471, Cell Signaling), MFN2 (#9482, Cell Signaling), DNM1L (#8570, Cell Signaling), FOXO3A (#9467, Cell Signaling), p-FOXO3A (#9465, Cell Signaling), AMPK (#2532, Cell Signaling), p-AMPK (#2535, Cell Signaling), P70S6K (#2708, Cell Signaling), p-P70S6K (#9204, Cell Signaling), AKT1 (#9272, Cell Signaling), p-AKT1 (#9275, Cell Signaling), SQSTM1 (PM045, MBL), PINK1 (sc-33796, Santa Cruz), PRKN (sc-32282, Santa Cruz), VDAC1 (sc-390996, Santa Cruz), ANT1 (sc-9299, Santa Cruz), CYCS (sc-13256, Santa Cruz), TFAM (sc-166965, Santa Cruz), PPARGC1A (ST1202, Sigma), SOD1 (SOD-101, Stressogen),

SOD1 (SOD-110, Stressogen), and 4HNE (ab46545). Following incubation, membranes were washed, and appropriate horseradish peroxidase-conjugated secondary antibody was applied at room temperature for 1 hour. Bands were visualized using ECL substrate on a ChemiDoc Imaging System.

Caspase, Calpain, and Proteasomal Activity Assay

To measure caspase (CASP), calpain (CAPN) and proteasomal activities, whole-cell lysates were collected as above in the absence of protease inhibitors. Samples were incubated in duplicates with 20μM of Ac-DEVD-AFC for CASP3 or Ac-LEHD-AFC for CASP9 in assay buffer (20 mM HEPES pH 7.4, 10 mM DTT, and 10% glycerol). For CAPN activity, samples were incubated in duplicates with 20μM of Suc-LLVY-AMC and Z-LL-CHO inhibitor in assay buffer for 2 hours at 30°C. For 20S proteasomal activity, samples were incubated in duplicates with 20μM of Suc-LLVY-AMC and MG-132 inhibitor in proteasome assay buffer (50mM Tris/HCl, 25mM KCl, 10mM NaCl, 1mM $MgCl_2$; pH 7.5) for 1 hour at 30°C. Fluorescence measurements were performed at room temperature using a Cytation 5 Imaging Multi-Mode Reader. The AFC probe was measured with excitation and emission wavelengths at 400 and 505 nm, respectively. The AMC probe was measured with excitation and emission wavelengths at 360 and 440 nm, respectively. The fluorescence values were normalized to protein concentration of samples and expressed as fold changes in fluorescence.

Immunofluorescence Fiber Type Analysis

Following collections, TA muscles were embedded in OCT compounds (Tissue Tek), frozen in isopentane cooled by liquid nitrogen and stored at -80°C until analysis. Ten-micron

cryosections were cut, mounted onto microscope slides and maintained at -20°C until staining. For staining, slides were dried at room temperature, circumscribed with a hydrophobic pen and blocked using 10% goat serum in PBS. Slides were incubated at room temperature with antibodies against type IIA (SC-71, DSHB), type IIX (6H1, DSHB), and dystrophin (MANDYS1, DSHB) for 2 hours. Slides were washed three times with PBS and incubated at room temperature with appropriate secondary antibodies. Following incubation with secondary antibodies, slides were washed three times and mounted with Fluoromount mounting medium. Fiber cross-sectional area (CSA) and fiber counts was quantified using ImageJ.

Grip Strength Measurement

Grip strength was assessed as an indicator of muscle strength using a custom-built grip apparatus. The grip apparatus featured a custom 3D-printed design using PLA filament and incorporated a micro load cell connected to an HX711 amplifier, all managed by an Arduino Uno microcontroller. The microcontroller was programmed using the Arduino IDE to record peak grip efforts at 3-second intervals. Data were saved to a spreadsheet for subsequent analysis. Maximal forelimb grip strength was determined from 3-5 trials per animal. Data are presented in gram-force (*g*f).

Statistics

Statistical analyses were performed in GraphPad PRISM. T-tests were performed to compare developmental changes from all groups compared to P7. T-tests were also performed to compare CTRL to skmKO. An alpha value of 0.05 was considered statistically significant.

Results

Postnatal muscle development exhibits significant changes in the genetic signature related to mitochondria

Postnatal muscle growth and development is a complex physiological process characterized by both hypertrophy of existing myofibers and the remodeling of muscle architecture. Postnatal remodeling is crucial for accommodating larger myofibers and adapting to new functional demands, ensuring that muscle growth during postnatal development enhances functionality and resistance to stress. Due to the limited number of studies on postnatal muscle development, we aimed to adopt a comprehensive approach to investigate this process. We performed RNA sequencing (RNAseq) analyses on developing skeletal muscle from the GEO database (GSE1025). These data were collected from the gastrocnemius-soleus complex (GS) of young mice ranging from postnatal day 7 (P7) to postnatal day 112 (P112). Our RNAseq analysis of approximately 12,000 genes identified 950 differentially expressed genes (DEGs) during this developmental period. Among the DEGs, we found several genes related to extracellular remodeling, muscle growth, metabolism and overall cellular signaling (Figure 1A-C). It is interesting to note that among the top 950 DEG, only two of them are directly related to remodeling process of autophagy and mitophagy, namely *Atg7* (rank 222/950) and *Bnip3* (rank 21/950; highlighted in Figure 1C), respectively. It is interesting to note that *Atg7* expression declined approximately 5-fold during postnatal muscle development between P7 and P112, whereas *Bnip3* expression increased approximately 8-fold.

Further analysis of the RNAseq dataset using Gene Ontology (GO) analyses revealed 7402 upregulated genes and 5992 downregulated genes (Figure 1D) related to major biological processes involved in growth related remodeling processes (i.e., muscle-specific, metabolism,

apoptosis, mitochondria-related, autophagy, and UPS). Specifically, we observed the upregulation of genes associated with biological processes related to metabolism and mitochondrial components during development (Figure 1E-F). Conversely, there was a downregulation of genes involved in *de novo* muscle formation, cellular growth, and other cellular remodeling components (Figure 1E-F). Together, these data establish that postnatal development was marked by significant mitochondrial remodeling, as indicated by the upregulation of genes related to metabolic processes and mitochondrial components. This suggests that changes at the mitochondrial level play a crucial role in the overall development of skeletal muscle during the postnatal period.

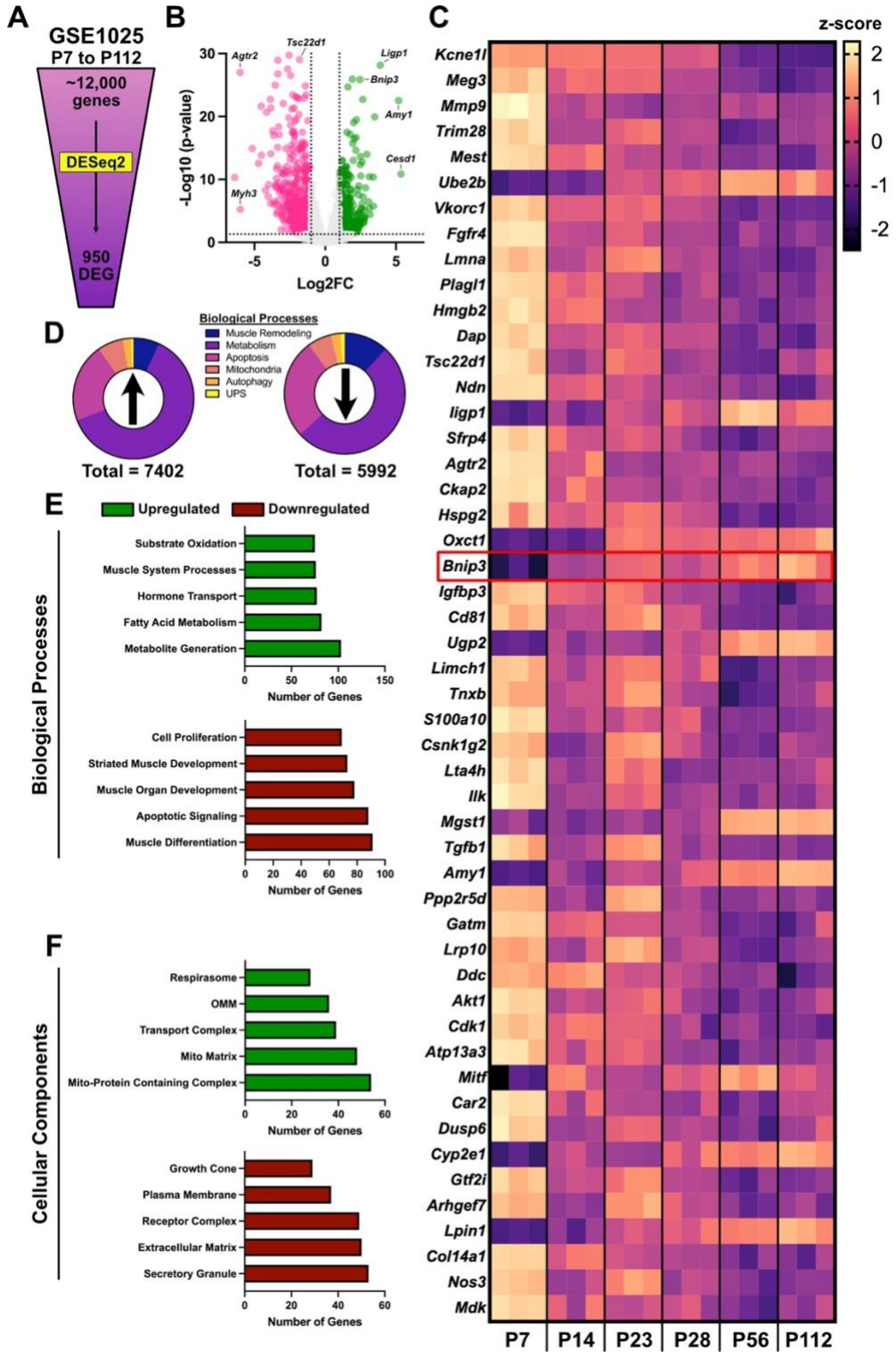


Figure 1: RNA sequencing analysis of gastrocnemius-plantaris muscle during development. A) Representative visualization of genes analyzed from the publicly available Gene Expression Omnibus database (Accession ID: 1025). B) Volcano plot displaying differential gene expression in skeletal muscle. The horizontal line delineates a significance threshold of $p < 0.05$. Vertical lines mark a z-score change greater than Log2. Green labels indicate upregulated differentially expressed genes (DEGs), while red labels indicate downregulated DEGs. C) List of top

50 DEGs identified by DESeq2 analysis. D) Gene ontology analyses and donut graph outputs summarizing changes in genes associated with five major remodeling processes: muscle remodeling, metabolism, apoptosis, mitochondria, autophagy, and the ubiquitin proteasome system (UPS). A total of 7402 genes related to these processes are upregulated while 5992 genes related to these processes are downregulated. E) Gene ontology analyses output of the number of genes linked to the top five upregulated (green) and downregulated (red) biological processes. F) Gene ontology analyses output of the number of genes linked to the top five upregulated (green) and downregulated (red) cellular components. CTRL indicates control animals. IM indicates animals collected following 7-days of immobilization. n = 3 per group.

Postnatal muscle development is accompanied by greater mitophagic flux and enhanced mitochondrial function

Given the fact that significant changes to mitochondrial-related gene profiles from the RNASeq analyses, we were interested in understanding the changes that occur at the mitochondrial level and their relation to muscle development. To further investigate these physiological changes, we collected muscles from neonatal pure-bred mt-Keima mice from P7 to P42 to understand the muscle growth pattern (Figure 2A). We observed a steady rate of growth with respect to body mass and muscle mass from P7 to P21 (Figure 2B-F). Importantly, we found a 2-fold increase in body mass and muscle mass from P21 to P42 (Figure 2B-F). This increased muscle mass and CSA were also accompanied by enhanced grip strength during development (Figure 2G). Closer analyses revealed significant myofiber hypertrophy within the TA, as shown by increased mean CSA of type IIA, IIX and IIB fibers. Once again, the most significant change observed was approximately a 2-fold increase in myofiber CSA between P21 and P42 (Figure 2H-I). Myofiber type distribution remained identical in IIX and IIB fibers; however, relative proportion of IIA fibers decreased at P42 compared to P7 in TA muscles (Figure 2J).

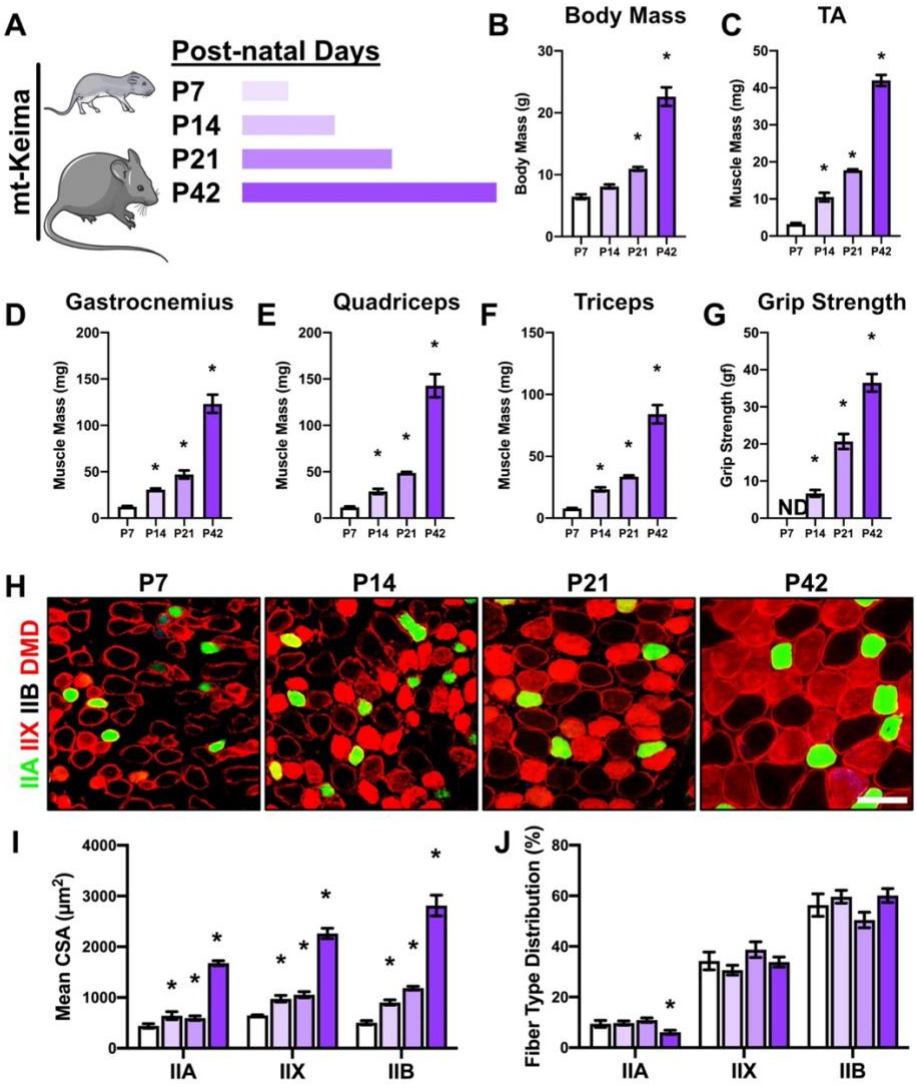


Figure 2: Changes in skeletal muscle during postnatal development of mt-Keima mice. A) Representative visualization of collection timepoints. Quantification of B) Body mass, relative muscle mass of C) tibialis anterior (TA), D) gastrocnemius, E) quadriceps, and F) triceps, and G) peak forelimb grip strength. H) Representative immunofluorescent images of TA muscles from P7 to P42 animals. Samples were stained with antibodies specific for individual myosin heavy chain isoforms: type IIA (green), type IIX (red), type IIB (unstained), and dystrophin (DMD; red). Scale bars indicate 50 μm. I-J) Quantification of mean cross-sectional area (CSA) and distribution of type IIA, IIX, and IIB myofibers. * $p < 0.05$ compared to P7 group. n = 4-8 per group.

To link the changes in postnatal muscle growth to mitochondrial remodeling, we performed live imaging of bundles collected from the TA muscle of mt-Keima reporter mice. We observed greater mitophagic flux throughout the developmental time course (Figure 3A). Specifically, we

found increased mitophagic (i.e., red) puncta count at P21 that remained elevated at P42 (Figure 3B), while the average red puncta size only increased at P42 compared to P7 (Figure 3C). Further investigation into mitochondrial function using high-resolution respirometry with simultaneous fluorometry measurements of reactive oxygen species (ROS) revealed a consistent pattern during postnatal development. We detected greater maximal oxygen consumption rate (OCR) at P21 and P42 compared to P7 (Figure 3D). Interestingly, succinate-stimulated (S-stimulated) and succinate plus pyruvate/malate-stimulated (S+PM-stimulated) mH_2O_2 emission was only elevated at P21 (~2-fold) compared to P7 and returned to similar levels by P42 (Figure 3E-F). The fraction of electron leak steadily declined and was significantly depressed at P42 compared to P7 (-50%; Figure 3G), suggesting improved electron transport efficiency. To further dissect the mechanism of mitophagy in developing muscles, we collected mitochondrial-enriched fractions and probed for select autophagy and mitophagy markers. We found mitochondrial localization of LC3B-II increased alongside BNIP3, PINK1, and PRKN during the developmental period (Figure 3I-N). Interestingly, mitochondrial BNIP3L declined rapidly after P7 and was virtually undetectable from P14 onwards (Figure 3L). These findings suggest that the developmental increase in muscle mass involves hypertrophic growth that may be driven by divergent changes in multiple signaling pathways. Additionally, the fractionation data align with the mitophagic flux data, indicating a coordinated regulation of mitochondrial remodeling during postnatal muscle development. Together, these data suggest that changes at the mitochondrial level may play a crucial role in the overall development of skeletal muscle during the postnatal period.

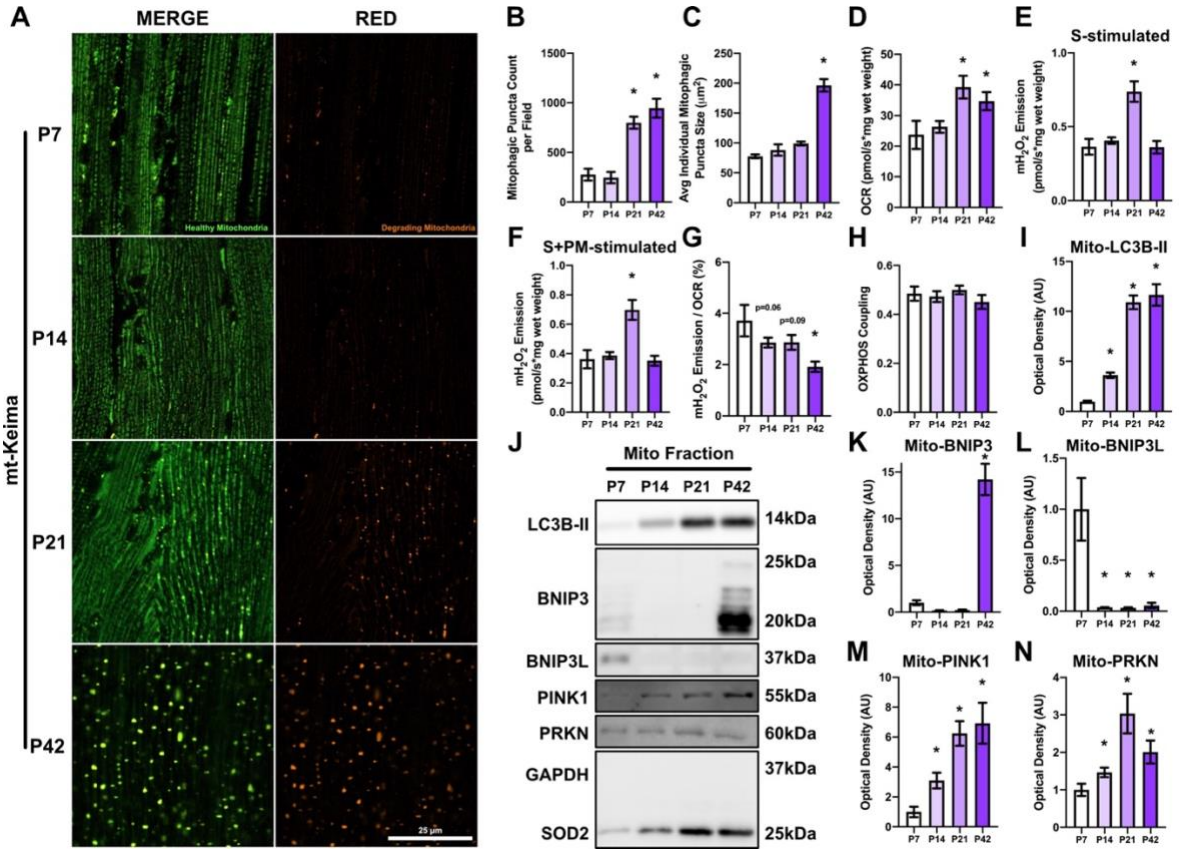


Figure 3: Postnatal development-associated changes in mitophagy and mitochondrial function. A) Representative confocal images of mitophagic flux from TA muscles of mt-Keima reporter mice. Green fluorescence indicates healthy mitochondria. Red fluorescence indicates degrading mitochondria. Scale bar indicates 25 μm. B) Quantification of mitophagic (i.e., red) puncta count per field. C) Quantification of average individual mitophagic puncta size. D) Quantification of maximal oxygen consumption rate (i.e., respiration) of permeabilized bundles from TA muscles. Simultaneous quantification of E) succinate-stimulated hydrogen peroxide (H_2O_2) production, and F) succinate + pyruvate/malate-stimulated H_2O_2 production in permeabilized TA muscle bundles. G) Quantification of mitochondrial fraction of electron leak. H) Quantification of oxidative phosphorylation (OXPHOS) coupling. I) Quantification of LC3B-II from mitochondrial-enriched fractions. J) Representative immunoblots of mitochondrial fractions derived from GAS. Quantification of K) BNIP3, L) BNIP3L, M) PINK1, and N) PRKN from mitochondrial-enriched fractions. * $p < 0.05$ compared to P7 group. n = 4-8 per group.

Changes in mitochondrial remodeling processes complement postnatal muscle development

As noted in the above results, we observe a direct link between muscle growth and mitophagic flux. Although these signals are intuitively opposed (i.e., growth signal vs. degradative signal), we questioned whether there were any changes in upstream signaling kinases that regulate muscle growth (i.e., anabolic) and degradative (i.e., catabolic) pathways. Upon closer examination of the major kinases involved in anabolic and catabolic signaling pathways, an interesting pattern

emerged. The levels of total and phosphorylated FOXO3A (Ser318/321) exhibited a gradual decrease from P7 to P42, leading to no significant change in the ratio of phosphorylated to total FOXO3A in mt-Keima mice (Figure 4A-D). In contrast, total AMPK showed a notable increase throughout the developmental period from P7 to P42, accompanied by a decrease in phosphorylated AMPK (Thr172), resulting in an overall reduction in the ratio of phosphorylated to total AMPK (Figure 4E-G). While the total protein levels of the growth signaling kinase P70S6K declined only at P42, phosphorylated P70S6K (Thr421/424) levels were elevated at P21 and P42, resulting in higher ratios of phosphorylated to total P70S6K at these time points in mt-Keima mice (Figure 4H-J). Interestingly, we observed a consistent increase in total and phosphorylated AKT1 (Thr308), particularly at P21 and P42. However, this increase did not translate into a higher ratio of phosphorylated to total AKT1 at P21; instead, there was a decrease in this ratio (Figure 4K-M). These data suggest that the ability of muscle to balance growth and degradation processes may involve fine-tuning of signaling pathways beyond mere upregulation of anabolic signaling.

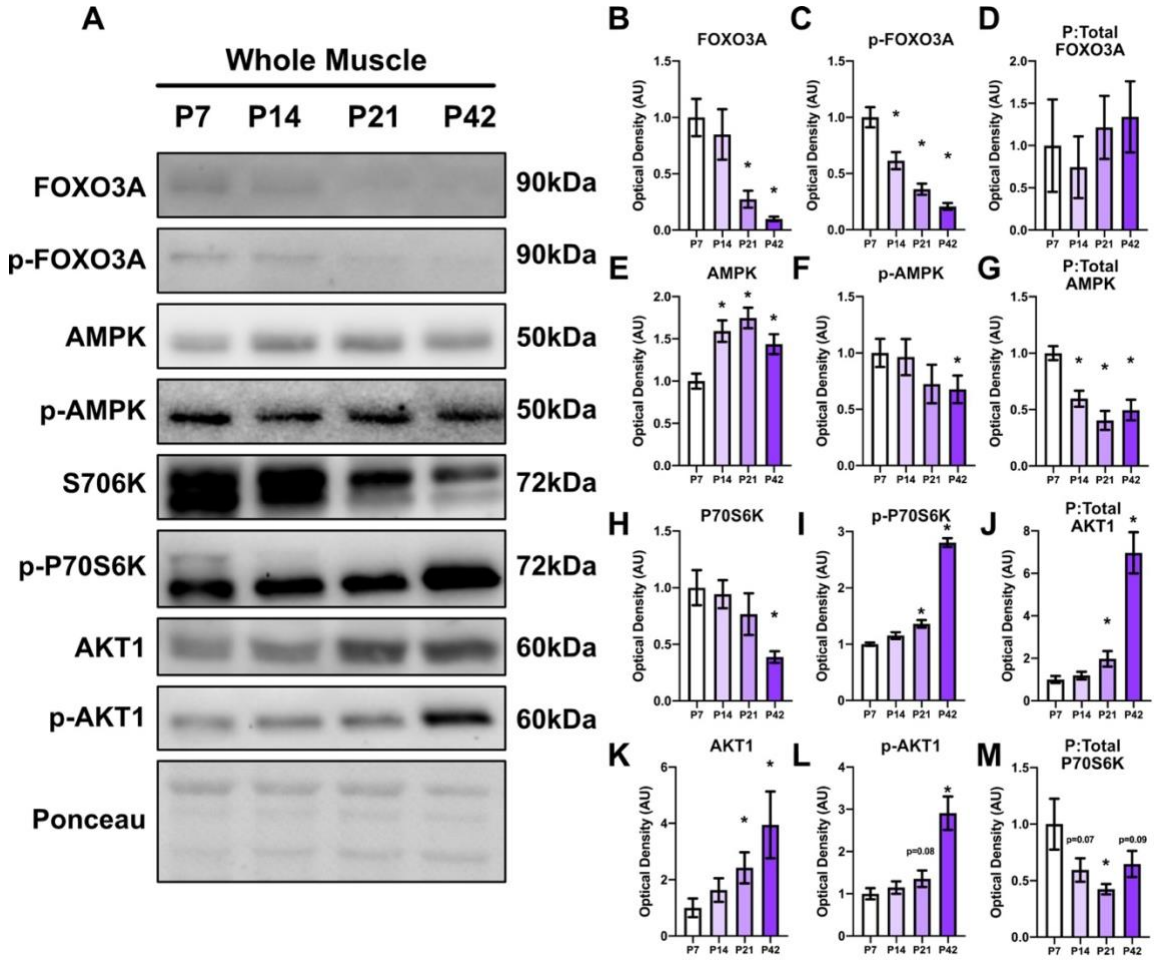


Figure 4: Quantitative analysis of upstream kinases in skeletal muscle during development. A) Representative immunoblots of whole muscle lysate derived from GAS of mt-Keima mice. Quantitative analysis of B) FOXO3A, C) p-FOXO3A (Ser318/321), D) p:total FOXO3A, E) AMPK, F) p-AMPK (Thr172), G) p:total AMPK, H) P70S6K, I) p-P70S6K (Thr421/424), J) p:total P70S6K, K) AKT1, L) p-AKT1 (Thr308), and M) p:total AKT1 * $p < 0.05$ compared to P7. n = 6 per group.

Next, we measured protein levels of major molecules related to mitochondrial remodeling. We found a steady decline in markers of mitochondrial biogenesis (PPARGC1A and TFAM; Figure 5A-C) and select mitophagy-related molecules (BNIP3L and PRKN; Figure 5E & 5G) during postnatal muscle development from P7 to P42. Interestingly, we observed significant elevations in the mitophagy receptor BNIP3 (> 2-fold) and no changes in PINK1 (Figure 5D & 5F). Changes in mitochondrial remodeling also include changes in mitochondrial dynamics. Upon assessing levels of OPA1, MFN2, and DNM1L, we observed a slight shift towards mitochondrial

fusion (Figure 5H-J). OPA1 was elevated at P14 and P21 compared to P7 before returning to baseline levels by P42 (Figure 5H). In contrast, DNM1L significantly decreased at P21 and remained depressed at P42 compared to P7 (Figure 5J), suggesting potential changes in mitochondrial dynamics that may modulate mitochondrial structure and function. Furthermore, we found reductions in the OMM molecule VDAC1, particularly at P21 and P42, whereas the IMM molecule ANT1 significantly increased from P14 to P42 (Figure 5K-L). Additionally, an elevation in CYCS was observed at P14, which returned to P7 levels by P21 (Figure 5M). We also observed mild yet significantly elevated levels of SOD1 and SOD2 at P42 (Figure 5N-O), along with a steady increase in the lipid peroxidation molecule 4-hydroxynonenal (4HNE; Figure 5P). Autophagy molecules SQSTM1 and LC3B-I declined steadily throughout the postnatal development periods, with no changes in LC3B-II (Figure 5Q-S). The overall LC3B-II:I ratio increased dramatically throughout the developmental period, suggesting increased autophagy activation (Figure 5T). These results suggest a complex interplay between growth processes and mitochondrial dynamics, potentially mediated by nuanced alterations in both mitophagic and biogenesis pathways.

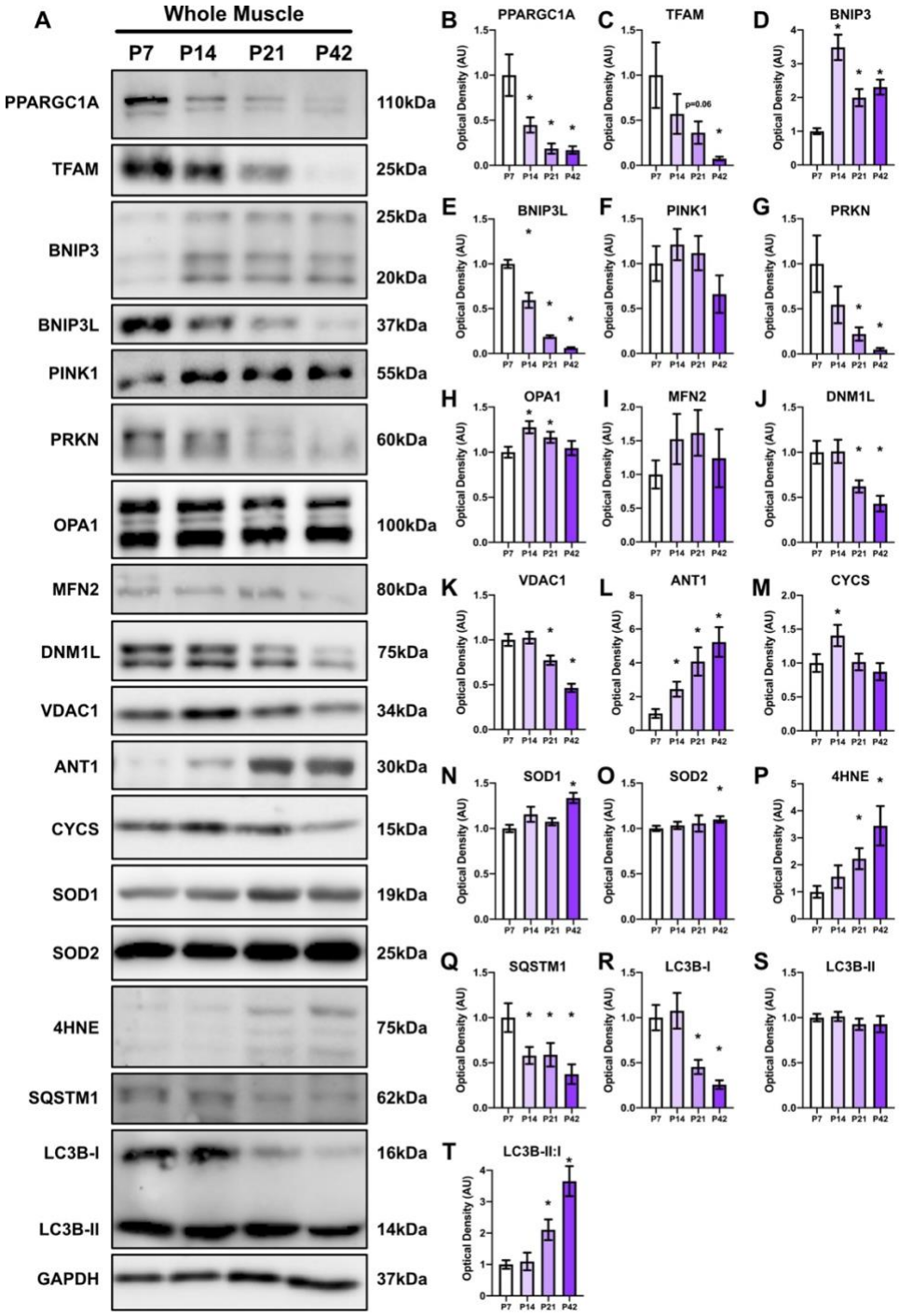


Figure 5: Quantitative analysis of mitochondrial remodeling proteins in skeletal muscle during development. A) Representative immunoblots of whole muscle lysate derived from GAS of mt-Keima mice. Quantitative analysis of B) PPARGC1A, C) TFAM, D) BNIP3, E) BNIP3L, F) PINK1, G) PRKN, H) OPA1, I) MFN2, J) DNM1L, K) VDAC1, L) ANT1, M) CYCS, N) SOD1, O) SOD2, P) 4HNE, Q) SQSTM1, R) LC3B-I, S) LC3B-II, and T) LC3B-II:I. * $p < 0.05$ compared to P7. n = 6 per group.

Autophagy-deficiency abolishes mitophagic flux, modifies mitochondrial remodeling signals, yet spares overall muscle development

Given the observed increase in autophagy/mitophagy-related molecules during muscle development, we sought to investigate this further. Recognizing that mitophagy can occur through various mechanisms, we broadened our approach to study changes in autophagy-deficient mice. We questioned whether autophagy-deficiency would negatively affect muscle growth by altering mitochondrial remodeling processes. In doing so, we generated a constitutive skeletal muscle-specific knockout (skmKO) mice by crossing *Atg7*$^{f/f}$ mice with ACTA1-Cre mice, while *Atg7*$^{f/f}$ mice were also used as controls (CTRL) (Figure 6A). Despite no differences in body mass or muscle mass (i.e., TA, gastrocnemius, quadriceps, or triceps) between P42 CTRL and skmKO mice (Figure 6B-F), we observed a reduction in grip strength in skmKO animals (Figure 6G), consistent with our previous findings (Paré et al., 2017). Fiber type analyses revealed compensatory hypertrophy in type IIX fiber CSA without changes in type IIA or IIB fiber CSA and no shift in fiber type distribution (Figure 6H-J).

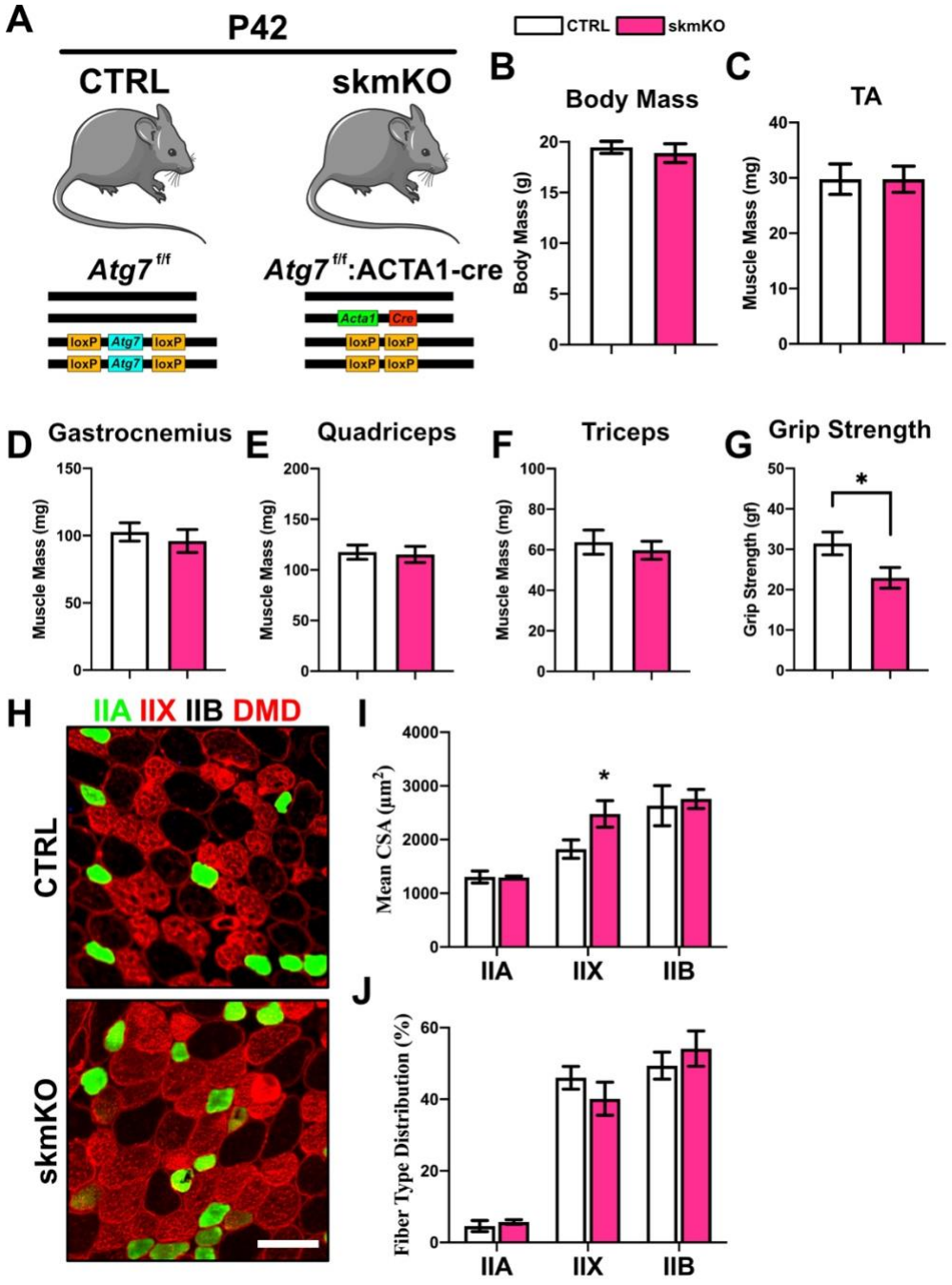


Figure 6: Developmental changes in muscles from young CTRL (*Atg7*$^{f/f}$) and skmKO (*Atg7*$^{f/f}$:ACTA1-Cre) mice. A) Representative visualization of genotypes collected at P42. Quantification of B) Body mass, relative muscle mass of C) tibialis anterior (TA), D) gastrocnemius, E) quadriceps, and F) triceps, and G) peak forelimb grip strength. H) Representative immunofluorescent images of TA muscles from P42 CTRL and skmKO animals. Samples were stained with antibodies specific for individual myosin heavy chain isoforms: type IIA (green), type IIX (red), type IIB (unstained), and dystrophin (DMD; red). Scale bars indicate 50 μm. I-J) Quantification of mean cross-sectional area (CSA) and distribution of type IIA, IIX, and IIB myofibers. * $p < 0.05$ compared to CTRL group. n = 4-8 per group.

Autophagy-deficiency completely ablated skeletal muscle mitophagic flux in young P42 skmKO crossed with mt-Keima reporter mice (Figure 7A). In this autophagy-deficient model, we observed no changes in maximal respiration, mH_2O_2 emission, or electron leak fraction, suggesting normal mitochondrial function (Figure 7B-E). Changes in the mitochondrial localization of autophagy and mitophagy molecules showed a significant reduction in LC3B-II (-90%; Figure 7F & 7H) without impacting mitochondrial localization of BNIP3, PINK1, or PRKN (Figure 7I-L). Moreover, this shows that tagging of mitochondria by BNIP3, PINK1, and PRKN occurs independently of autophagy.

The absence of phenotypic changes in young skmKO mice despite total ablation of mitophagic flux led us to question whether alternative degradative pathways are compensating for the lack of autophagy. To investigate this, we measured the enzymatic activities associated with various degradation pathways. We found significant elevation of enzymes related to mitochondrial apoptotic signaling, including CASP9 (+36%; $p < 0.05$) and CASP3 (+40%; $p < 0.05$) activities in skmKO mice compared to CTRL (Figure 7M-N). Additionally, we identified elevated CAPN (+74%; $p < 0.05$) and 20S proteasome (+87%; $p < 0.05$) activities in skmKO mice compared to CTRL (Figure 7O-P). The observed elevation in activities of enzymes involved in mitochondrial apoptotic signaling, calpain signaling, and UPS suggests a compensatory mechanism potentially serving as an adaptive response in the absence of autophagy. This is supported by previous work from our group that reported compensatory activation of CASPs in autophagy-deficient myoblasts, and increased proteasomal activity in autophagy-deficient muscles (Baechler et al., 2019; McMillan & Quadrilatero, 2014; Paré et al., 2017). Collectively, these results point to an adaptive response involving alternative degradative pathways when autophagy is impaired.

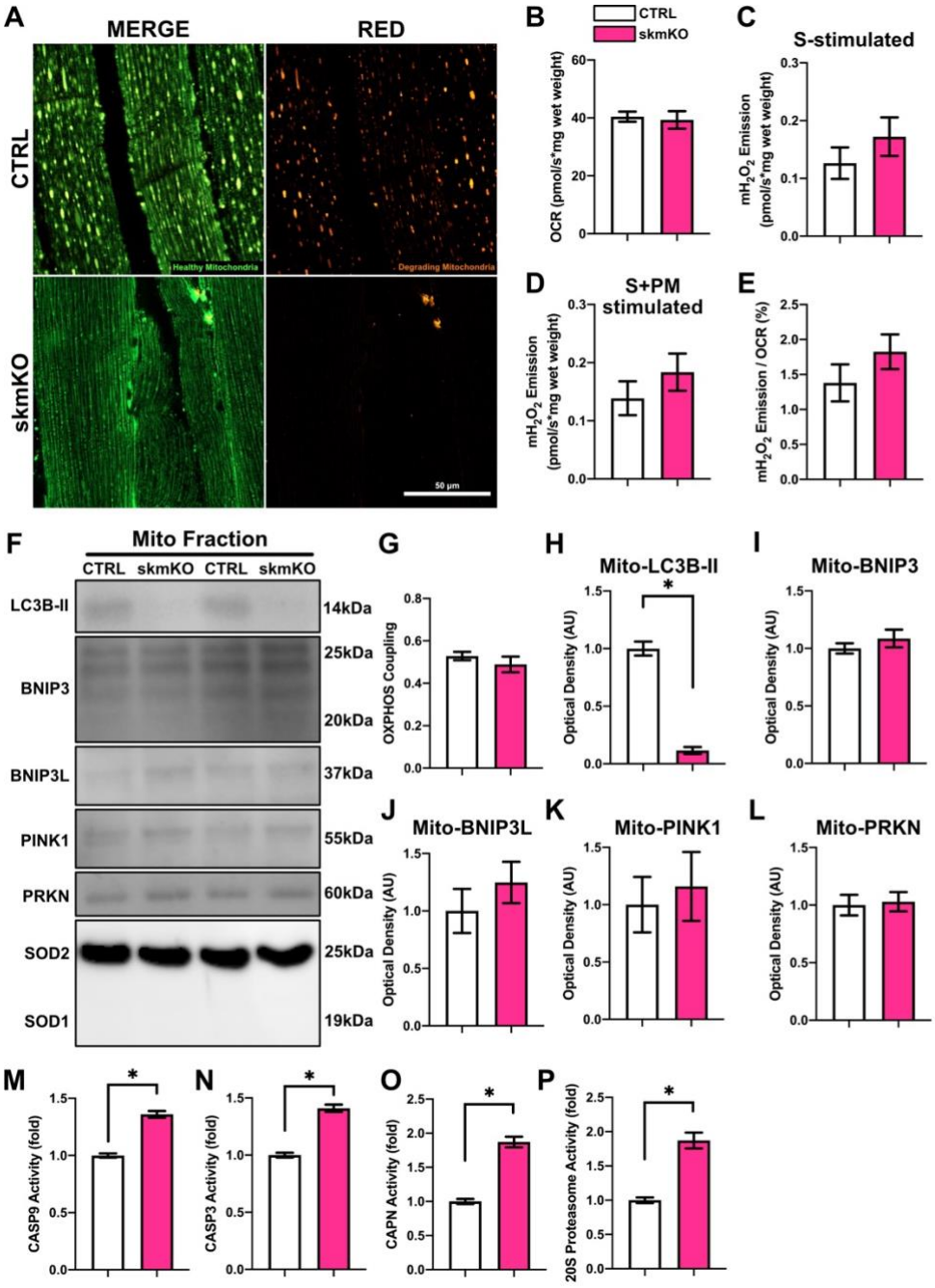


Figure 7: Postnatal development-associated changes in mitophagy and mitochondrial function in young autophagy-deficient skeletal muscle. A) Representative confocal images of mitophagic flux from TA muscles of CTRL (*Atg7*$^{f/f}$) or skmKO (*Atg7*$^{f/f}$:ACTA1-Cre) mice crossed with mt-Keima reporter mice (*Atg7*$^{f/f:mt\text{-}Keima}$). Green fluorescence indicates healthy mitochondria. Red fluorescence indicates degrading mitochondria. Scale bar indicates 50 µm. B) Quantification of maximal oxygen consumption rate (i.e., respiration) of permeabilized bundles from TA muscles. Simultaneous quantification of C) succinate-stimulated hydrogen peroxide (H_2O_2) production, and D) succinate + pyruvate/malate-stimulated H_2O_2 production in permeabilized TA muscle bundles. E) Quantification of mitochondrial fraction of electron leak. F) Representative immunoblots of mitochondrial fractions derived from GAS. G) Quantification of oxidative phosphorylation (OXPHOS) coupling. H) Quantification of H) LC3B-II, I) BNIP3, J) BNIP3L, K) PINK1, and L) PRKN from mitochondrial-enriched

fractions. Quantification of M) caspase 9 (CASP9), N) caspase 3 (CASP3), O) calpain (CAPN), and P) 20S proteasome activities. * $p < 0.05$ compared to CTRL group. n = 4-8 per group.

We observed suppression of select catabolic signaling kinases, including phosphorylated FOXO3A (Ser318/321) and the ratio of phosphorylated to total FOXO3A (Figure 8A-D), as well as AMPK and the ratio of phosphorylated to total AMPK ($p = 0.06$) (Figure 8E-G). Additionally, there was a notable increase in the ratio of phosphorylated to total P70S6K (Figure 8H-J), while phosphorylated AKT1 (Thr308) and the ratio of phosphorylated to total AKT1 was reduced, though not statistically significant (Figure 8K-M). These findings may suggest aberrant feedback and signaling of kinases that regulate catabolism and anabolism in autophagy-deficient mice. Furthermore, we observed reduced levels of ATG7 and LC3B-II, along with an accumulation of SQSTM1, indicating impaired autophagy in skmKO muscles (Figure 9A-B & 9Q-T). Investigation into other mitochondrial remodeling processes revealed potential compensatory responses in biogenesis signaling, as evidenced by elevated TFAM levels, although PPARGC1A levels remained unchanged in P42 skmKO mice compared to CTRL mice (Figure 9C-D). Interestingly, several mitophagy-related molecules including BNIP3, BNIP3L, and PINK1 were significantly suppressed, while PRKN showed no change in P42 skmKO compared to CTRL mice (Figure 9E-H). Regarding mitochondrial dynamics-related proteins, OPA1 and MFN2 levels were suppressed (Figure 9I-J), whereas DNM1L showed no change (Figure 9K). Additionally, we found reduced levels of mitochondrial membrane-related molecules VDAC1 and ANT1 (Figure 9L-M), with no changes observed in other mitochondria-related proteins including CYCS, SOD1, or SOD2 (Figure 9N-P). Overall, these data suggest a complex interplay of impaired autophagy and disrupted mitochondrial homeostasis contributing to altered muscle physiology in young skmKO mice.

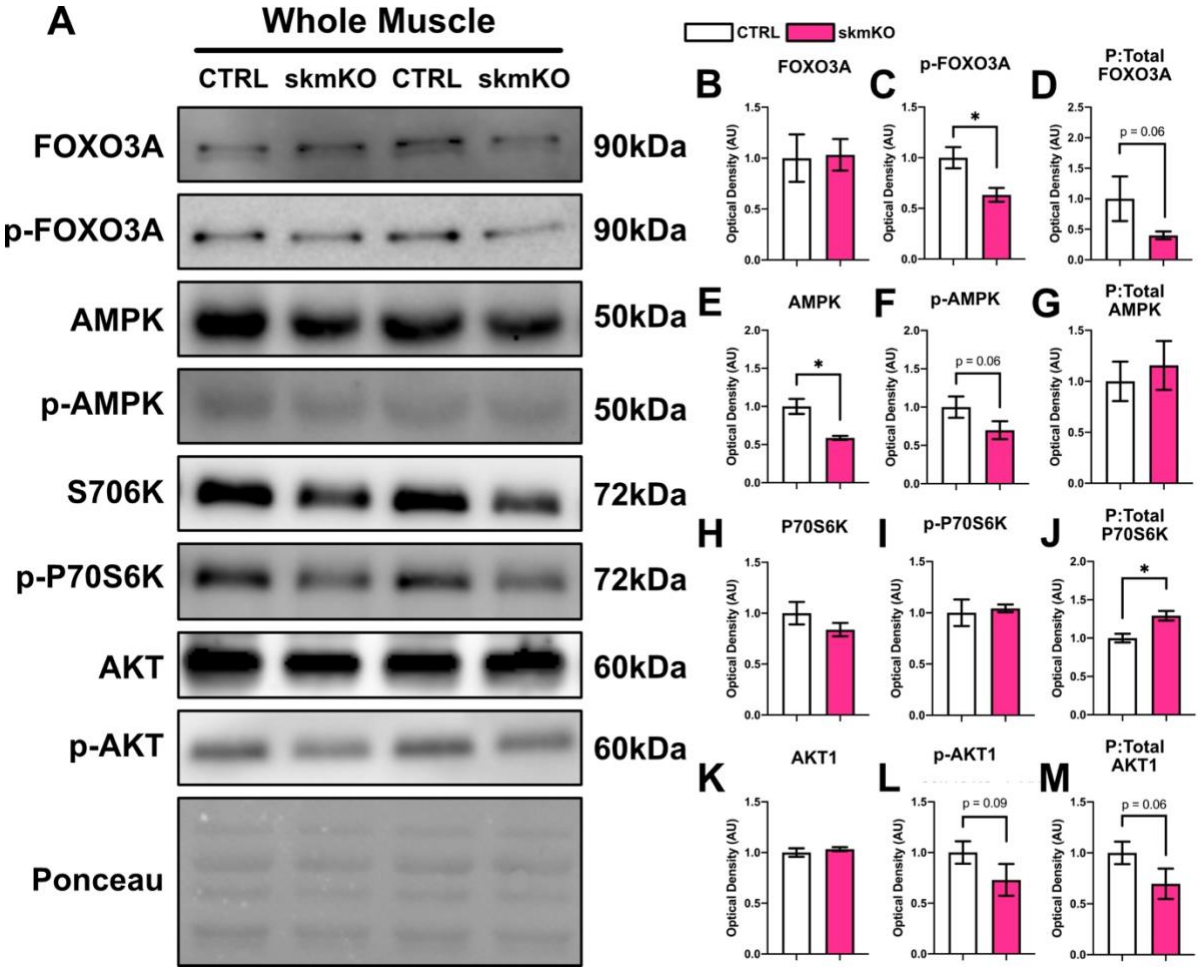


Figure 8: Quantitative analysis of upstream kinases in young autophagy-deficient skeletal muscle. A) Representative immunoblots of whole muscle lysate derived from GAS of CTRL (*Atg7*$^{f/f}$) or skmKO (*Atg7*$^{f/f}$:ACTA1-Cre) mice. Quantitative analysis of B) FOXO3A, C) p-FOXO3A (Ser318/321), D) p:total FOXO3A, E) AMPK, F) p-AMPK (Thr172), G) p:total AMPK, H) P70S6K, I) p-P70S6K (Thr421/424), J) p:total P70S6K, K) AKT1, L) p-AKT1 (Thr308), and M) p:total AKT1 * $p < 0.05$ compared to P7. n = 6 per group.

In summary, our study indicates that constitutive autophagy-deficiency induces specific changes in mitochondrial remodeling. The absence of general negative impact on muscle mass or mitochondrial function may be attributable to the compensatory activation of alternative degradative pathways, such as CASP, CAPN and UPS signaling. These pathways may facilitate the degradation of accumulated cellular debris. Collectively, our findings suggest complex

regulatory mechanisms that balance catabolic and anabolic signaling in the context of autophagy-deficiency during postnatal development.

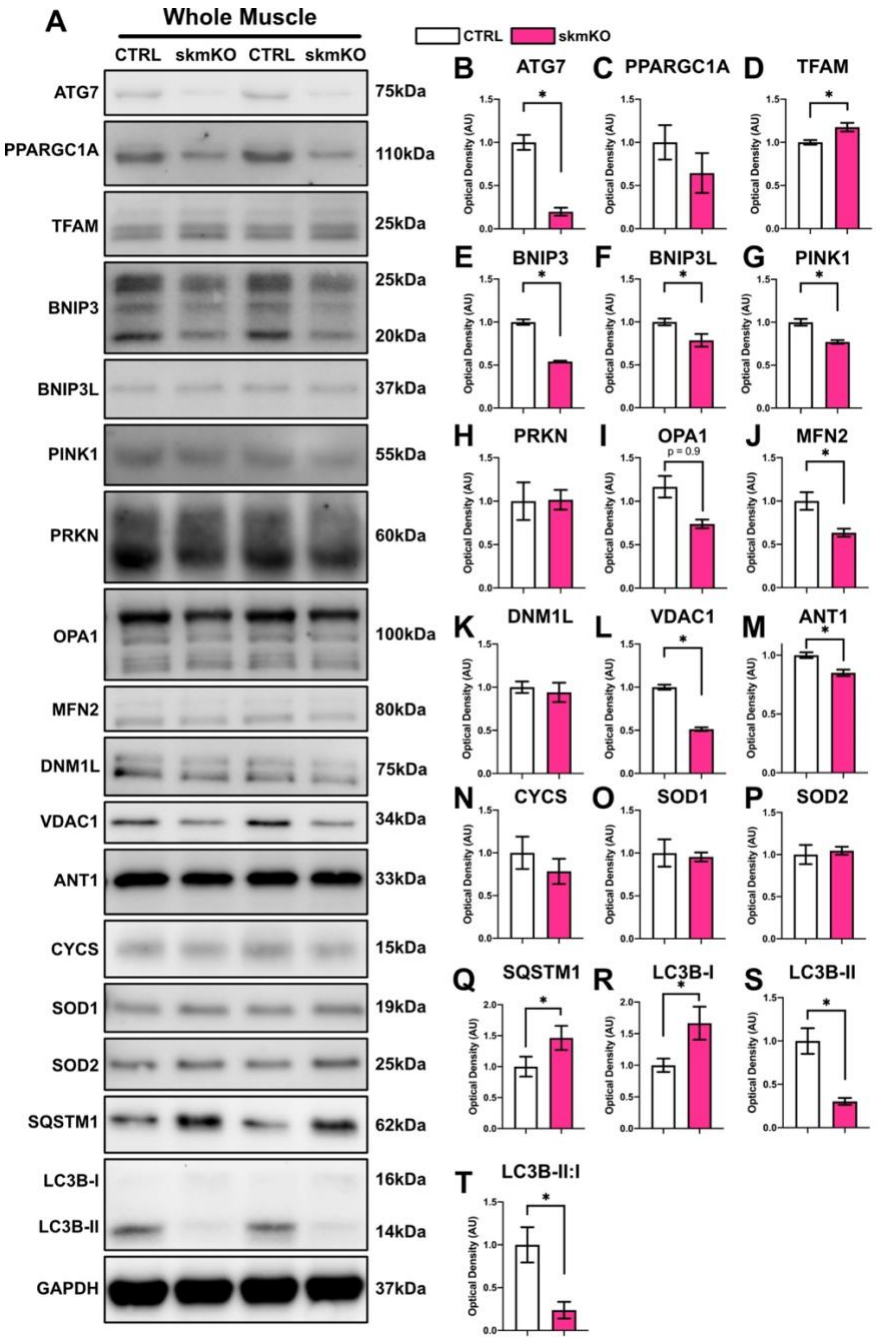


Figure 9: Quantitative analysis of mitochondrial remodeling proteins in young autophagy-deficient skeletal muscle. A) Representative immunoblots of whole muscle lysate derived from GAS of CTRL (P42 *Atg7*$^{f/f}$) or skmKO (P42 *Atg7*$^{f/f}$:ACTA1-Cre) mice. Quantitative analysis of B) ATG7, C) PPARGC1A, D) TFAM, E) BNIP3, F) BNIP3L, G) PINK1, H) PRKN, I) OPA1, J) MFN2, K) DNM1L, L) VDAC1, N) ANT1, N) CYCS, O) SOD1, P) SOD2, Q) SQSTM1, R) LC3B-I, S) LC3B-II, and T) LC3B-II:I. * $p < 0.05$ compared to CTRL. n = 6 per group.

Discussion

Skeletal muscle development is a complex, multi-stage process that coordinates cellular responses to enhance muscle mass and functionality. This developmental progression is closely associated with changes in mitochondrial mass, which parallel patterns of muscle growth (Y. Kim, Yang, et al., 2019). Although several interactions between mitochondrial dynamics and muscle growth have been identified, the specific impacts of mitochondrial remodeling on muscle development are not fully elucidated. The present study focused on the role of mitochondrial remodeling during postnatal skeletal muscle development. We report three key findings: 1) significant mitochondrial remodeling occurs concurrently with postnatal muscle growth, 2) there is a discernible link between muscle growth, mitochondrial function, and mitophagic flux, and 3) autophagy-deficiency can impair muscle strength and signaling pathways, although it does not adversely affect growth in young mice.

Mitochondrial remodeling defines postnatal muscle development

Postnatal development of skeletal muscle involves significant remodeling, characterized by extensive reorganization of both contractile components and cellular organelles. Earlier studies have documented the enhanced formation of t-tubules during this developmental phase (Luff & Atwood, 1971), while others demonstrated expansions in the mitochondrial network, indicating early recognition of the dynamic changes occurring within muscle tissues during postnatal growth (Bakeeva et al., 1978). More contemporary proteomic analyses have provided valuable insights into mitochondrial remodeling during muscle development, though many aspects of the underlying mechanisms and their implications remain elusive (Y. Kim, Yang, et al., 2019). Our RNASeq analyses confirm these findings, providing robust data that complements the proteomic data

previously published (Y. Kim, Yang, et al., 2019). Notably, our study highlights an increase in genes associated with mitochondrial metabolism and a decrease in genes involved in *de novo* muscle formation. This suggests a cellular pivot towards improving mitochondrial efficiency, crucial for meeting the escalated energy demands of growing muscle tissues. A thorough examination of the DEGs from our RNA sequencing analysis identified the mitophagy receptor BNIP3 as a key molecule that was differentially expressed, indicating its potential role in mitochondrial quality control during development. The upregulation of BNIP3 may represent an adaptive response to various metabolic and cellular signaling that occur as muscle tissues mature.

Our RNA sequencing data is complemented by *in vivo* experiments demonstrating progressive muscle growth from P7 to P21, with rapid doubling of both body and muscle mass from P21 to P42. This growth trajectory aligns with previous studies indicating substantial increases in muscle mass, fiber volume, length, and CSA during development (Gokhin et al., 2008; White et al., 2010). Given the heterogeneity of myofibers, we investigated potential shifts in fiber type composition. Contrary to earlier findings that reported a loss of embryonic MYH by P14 and a redistribution of fibers towards MYH IIX and IIB (Gokhin et al., 2008), our results show no significant shift in fiber type from P7 to P42. Although these discrepancies remain unclear, they may be a result of the different mouse strain (i.e., FVB vs. ICR stains). Nonetheless, we observed enhanced mitochondrial function, evidenced by increased oxygen consumption and ROS emission, particularly at P21. This transient increase in ROS may be a crucial step since it is known to activate hypertrophic signals such as MTORC1 (M. Li et al., 2010). Although we did not measure activation of MTORC1 in the present study, we noted an increase in the ratio of phosphorylated to total P70S6K, a downstream effector of MTORC1, which significantly increased starting P21 and remained elevated at P42. Furthermore, the increased mitochondrial ROS emission was also

accompanied by heightened mitophagic flux, similar to previous findings (Frank et al., 2012). Closer examination revealed significantly greater mitochondrial localization of BNIP3, PINK1, and PRKN. Notably, mitochondrial localized BNIP3 exhibited more than a ten-fold increase during development, aligning with both our mitophagy observations and RNA sequencing data. Elevated levels of these mitophagy receptor molecules have been previously documented (Y. Kim, Yang, et al., 2019). To our knowledge, this study is the first to explore potential molecules targeting mitochondria during development, providing new insights into the molecular mechanisms of muscle growth and adaptation. We postulate that the transient elevation in ROS observed at P21 may function as a molecular trigger for the activation of hypertrophic kinases and the induction of mitochondrial remodeling processes such as mitophagy. This cascade of events is proposed to facilitate the development of more efficient mitochondria, thereby meeting the increased energetic demands of growing myofibers.

Prior studies have highlighted significant remodeling of the mitochondrial network during development, transitioning from a "parallel" to a "perpendicular" orientation (Y. Kim, Yang, et al., 2019). This reorganization is believed to support the maturation of the sarcoplasmic reticulum (SR), thereby regulating NADH flux and mitochondrial membrane potential, ultimately enhancing mitochondrial functionality (Y. Kim, Yang, et al., 2019; Luff & Atwood, 1971; Schiaffino & Margreth, 1969; Takekura et al., 2001). In our current investigation utilizing mt-Keima mice to examine mitochondrial morphology, we observed that the mitochondrial network maintained a "parallel" morphology, showing no significant morphological changes. Immunoblot analysis of mitochondrial dynamics proteins revealed stable levels of fusion proteins OPA1 and MFN2, but a noticeable reduction in the fission protein DNM1L at P21 and P42. The reasons behind these specific alterations remain unclear. Potential factors could include genetic differences between our

FVB reporter mouse model and the C57BL/6N strain previously studied (Y. Kim, Yang, et al., 2019), or perhaps limitations in our imaging resolution that preclude detection of subtle or three-dimensional structural changes (Y. Kim, Yang, et al., 2019; Y. Kim et al., 2024). Despite previous findings indicating minimal variation in mitochondrial complex proteins (Y. Kim, Yang, et al., 2019), our results indicate distinct changes during development, specifically a decrease in VDAC1 and an increase in ANT1. This divergence underscores the complexity of mitochondrial adaptations during muscle maturation and highlights the influence of genetic background and methodological approaches on experimental outcomes.

Overall, the remodeling of skeletal muscle during postnatal growth encompasses profound changes in both structural and metabolic components, reflecting intricate adaptations to the demands of growth and function. These findings highlight the ongoing need to further explore the molecular pathways that facilitate these adaptations, enhancing our understanding of muscle development and potentially guiding therapeutic strategies for muscle-related conditions.

Link between muscle growth, mitochondrial function, and mitophagy during development

Traditionally, skeletal muscle research has emphasized growth dynamics; however, recent studies increasingly focus on the degradative mechanisms that complement these processes, particularly autophagy and mitophagy (Leduc-Gaudet et al., 2021; Lei et al., 2024; Rahman & Quadrilatero, 2021b, 2021a). These mechanisms are well-recognized for their activation in response to significant cellular stress, during which they facilitate the removal of damaged cellular material and organelles such as mitochondria (Leduc-Gaudet et al., 2021; Lei et al., 2024; Rahman & Quadrilatero, 2021b, 2021a). Notably, the role of these degradative pathways in regulating development, a fundamentally healthy process, is gaining recognition. Despite the relative scarcity

of studies on the degradative processes during muscle development, emerging evidence from our lab and others underlines the critical role of autophagy and mitophagy during *in vitro* muscle formation. Previous research has demonstrated that inhibiting autophagy or mitophagy through chemical agents or genetic modifications substantially impairs muscle formation *in vitro* (Baechler et al., 2019; McMillan & Quadrilatero, 2014; Sin et al., 2016). One proposed mechanism suggests that deficiencies in autophagy and mitophagy disrupt signaling pathways essential for mitochondrial biogenesis (Baechler et al., 2019; Sin et al., 2016). Our recent observations highlight a significant increase in mitophagic flux concurrent with a reduction in mitochondrial biogenesis signaling, alongside stable levels of mitochondrial-related proteins in developing muscle tissue. These findings suggest that during myogenesis, as opposed to postnatal muscle development, mitochondrial quality control might be predominantly governed through enhanced degradation rather than new mitochondrial synthesis. This shift towards prioritizing mitochondrial integrity via increased mitophagic flux, without alterations in other mitochondrial remodeling processes, may offer insights into the complex interplay of cellular mechanisms driving muscle development.

In the present study, we observed a notable increase in mitochondrial ROS emission at P21, which coincided with enhanced mitochondrial localization of autophagy-related proteins LC3B-II, PINK1, and PRKN. Simultaneously, the mitophagy receptor BNIP3 showed a significant elevation at P42. The onset of increased mitophagic flux beginning at P21 suggests a tightly regulated temporal control of these processes. The role of mitochondrial ROS in triggering mitophagy is well-documented (Schofield & Schafer, 2021), and our findings suggest that the surge in ROS levels may activate PINK1/PRKN-mediated mitophagy during early developmental stages. Afterwards, BNIP3-mediated mitophagy may to become more prominent as the muscle further matures. The underlying cause of the increased ROS production in mice remains uncertain;

it may be related to environmental changes such as weaning, which could introduce metabolic stress, or increased physical activity as the animals develop. Existing studies have explored the impacts of modulating ROS levels. For example, OE of mitochondrial superoxide dismutase (SOD2) and mitochondrial catalase (MCAT) do not exhibit observable developmental defects *in vivo*, indicating a complex balance between ROS production and antioxidant defenses (Heden et al., 2019; Zhuang et al., 2021). However, excessive inhibition of ROS signaling has been shown to impair myogenesis *in vitro* (Rajasekaran et al., 2020), while a loss of antioxidant defenses, such as in SOD2 knockout models during embryonic development, can result in lethality (Y. Li et al., 1995). Furthermore, inducible skeletal muscle-specific SOD2 KO does not seem to impact muscle mass or function in adult mice (Zhuang et al., 2021); however it is unclear if excessive ROS in young animals would impact muscle development by modifying mitochondrial remodeling processes. Our data further suggest that the observed increase in ROS generation and subsequent lipid peroxidation may serve as signaling events for initiating mitophagic flux, which in turn supports postnatal muscle development and enhances mitochondrial function. These findings underscore the importance of precise regulation of mitochondrial quality control mechanisms throughout muscle maturation.

Autophagy-deficiency impairs muscle strength and signaling without affecting overall growth

Autophagy is essential for normal development, playing a critical role in maintaining cellular homeostasis and supporting the rapid changes in tissue composition and energy demands associated with growth. This process facilitates the removal of damaged cellular components and enables adaptation to various stimuli. Impairments in autophagy pathways have been linked to developmental abnormalities and compromised tissue functionality (Collier Jack J. et al., 2021;

Deneubourg et al., 2022; Deng et al., 2021; Kataura et al., 2022). Studies utilizing whole-body autophagy-deficient models have demonstrated early lethality, prompting targeted tissue-specific knockout approaches to better understand the role of autophagy in specific contexts. Notably, some of the first studies using muscle-specific autophagy-deficient models has revealed significant growth defects in young autophagy-deficient mice. For example, previous reports show that animals with muscle-specific autophagy-deficiency exhibited a reduction in body mass from P40 and the disparity continues as the animals age (Masiero et al., 2009). Furthermore, these animals demonstrated a greater loss in muscle size and function after five months of autophagy-deficiency (Masiero et al., 2009). Although this seminal research did not identify developmental defects directly attributable to muscle-specific autophagy-deficiency, it laid the groundwork for subsequent investigations. Our laboratory has built on these findings, showing that defects in autophagy-deficient muscles manifest over time. Specifically, we observed muscle weakness in the soleus muscle at 15 weeks, which was not evident at 5 weeks (Paré et al., 2017). Additionally, we found a significant increase in centralized nuclei in the extensor digitorum longus (EDL) muscle at 15 weeks compared to 5 weeks (Paré et al., 2017). These observations highlight a divergent fiber type/muscle-specific response, and a time-dependent manifestation of defects in autophagy-deficient muscles (Paré et al., 2017). Data from the present study are consistent with our previous work showing no detectable change in body mass, muscle mass, or fiber type distribution in young skmKO animals, yet we noted muscle weakness in these animals (Paré et al., 2017). This reduction in muscle quality may be a result of muscle damage or impairments in contractile ability in the skmKO mice compared to the CTRL (Paré et al., 2017). Nonetheless, these results contrast with findings from other research groups that have reported significant deficits in muscle size and function (Masiero et al., 2009).

Significant remodeling of the mitochondrial network occurs during postnatal muscle development, as documented in various studies (Bakeeva et al., 1978; Y. Kim, Yang, et al., 2019; Y. Kim et al., 2024). Previous research has established that constitutive autophagy-deficiency in muscles lead to the accumulation of abnormal/swollen and dysfunctional mitochondria at 8-weeks of age (Masiero et al., 2009). Our confocal microscopy analyses using autophagy-deficient mt-Keima mice did not reveal any significant changes in mitochondrial morphology. Additionally, we observed no changes in mitochondrial function, such as maximal respiration or ROS emission, despite complete ablation of mitophagic flux. This finding contrasts with other studies reporting significant mitochondrial dysfunction in autophagy-deficient states (Masiero et al., 2009). The apparent absence of defects in our young animal models may be attributed to compensatory degradative mechanisms. For instance, numerous studies have demonstrated an upregulation of apoptotic signaling, ER stress signaling and UPS in an autophagy-deficient state (Baechler et al., 2019; Cuervo et al., 1995; Marshall et al., 2021; McMillan & Quadrilatero, 2014; Paré et al., 2017; Tannous et al., 2008; X. J. Wang et al., 2013). While the UPS can compensate for impaired autophagy-mediated protein degradation, its role is limited to degrading short-lived, soluble proteins and may be transient. The formation of large, insoluble protein aggregates in autophagy-deficient states can lead to cellular dysfunction, potentially explaining the age-related exacerbation of defects observed in our studies (Paré et al., 2017). Moreover, studies have demonstrated that UPS inhibition via MG-132 or Bortezomib treatment can impair mitochondrial function and induce cell death, even when autophagy is functional (Guo & Peng, 2013; Maharjan et al., 2014). This may suggest that the UPS is also an important player in maintaining mitochondrial function; however, the extent to its important during postnatal muscle development is unclear.

Nonetheless, our results also indicated suppressed levels of key molecules involved in mitophagy (BNIP3, BNIP3L, PINK1), mitochondrial fusion (OPA1, MFN2), and mitochondrial membrane integrity (VDAC1, ANT1) in skmKO mice. These findings suggest that alternative pathways may compensate for the loss of mitophagic flux, maintaining mitochondrial function and integrity during early postnatal muscle development. In conclusion, our study highlights the complexity of mitochondrial quality control in muscle development and suggests potential compensatory mechanisms that warrant further investigation. Future research should aim to elucidate the interplay between these pathways and their role in maintaining mitochondrial homeostasis in the context of autophagy-deficiency.

Conclusion

In conclusion, our findings underscore the pivotal role of mitochondrial remodeling in postnatal skeletal muscle development. The significant remodeling observed during this stage indicates that mitochondrial adaptations are closely linked to muscle growth patterns. Our study elucidates the connection between muscle growth, mitochondrial function, and mitophagic flux, highlighting that while autophagy-deficiency can impair muscle strength and signaling, it does not adversely affect overall muscle growth in young mice. These insights contribute to a better understanding of the intricate processes underlying muscle development and suggest that targeting mitochondrial pathways could offer novel therapeutic strategies for muscle-related diseases. Future research should focus on exploring these pathways in greater detail to uncover potential interventions for enhancing muscle function.

Chapter 4: Role of Mitochondrial Remodeling During Immobilization-induced Muscle Atrophy

Project Rationale and Objectives

Skeletal muscle atrophy involves the activation of several degradative pathways, including apoptosis, UPS, autophagy, and mitophagy. Previous studies have characterized the role of mitochondrial remodeling during skeletal muscle atrophy and have noted that it is distinct from muscle formation (i.e., myogenesis) and postnatal development (Borgia et al., 2017; Graham et al., 2018; Triolo et al., 2022; Vainshtein et al., 2015; Yamashita et al., 2021). Recently, the role of mitophagy has been recognized in skeletal muscle atrophy, particularly in denervated and immobilized models (Triolo et al., 2022; Yamashita et al., 2021). Characterizing total mitochondrial proteins and those related to mitophagy offers some insight but does not fully elucidate the process. Additionally, although an increase in mitophagic flux during muscle atrophy is apparent, the underlying mechanisms are still not completely understood.

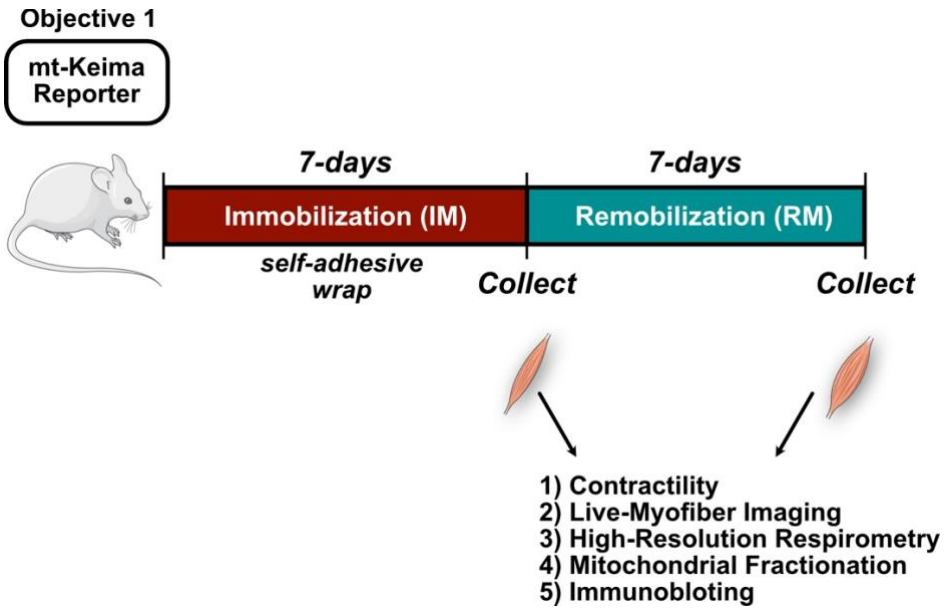
Therefore, the main objectives for Project 3 were:

1. To understand how mitochondrial remodeling processes change in response to hindlimb immobilization and remobilization.
2. To understand how inhibition of ROS signaling or inhibition of the autophagy machinery affects immobilization-atrophy.

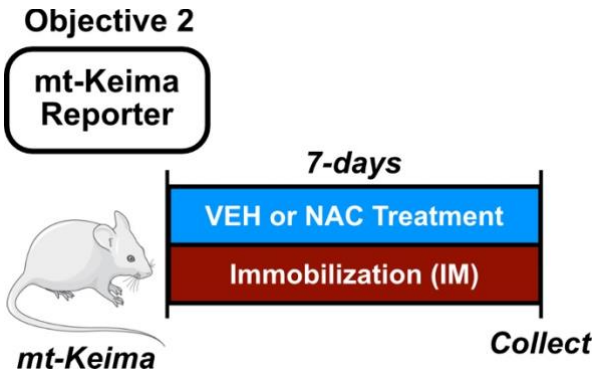
I hypothesized that:

1. Hindlimb immobilization would induce significant mitochondrial defects necessitating mitochondrial fission and mitophagy, while simultaneously suppressing biogenesis. These mitochondrial defects would reverse following hindlimb remobilization.

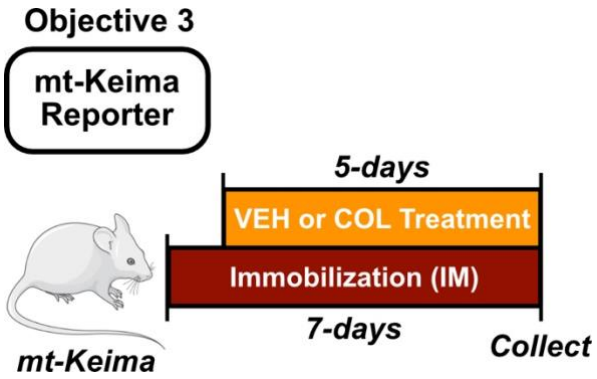
2. Antioxidant treatment would partially preserve mitochondrial function, resulting in partial preservation of muscle mass following hindlimb immobilization. Additionally, the inhibition of the autophagy machinery would exacerbate mitochondrial defects and result in greater muscle atrophy following hindlimb immobilization.



Method Figure 1: Study design for Project 3, Objective 1. Mice from the mt-Keima purebred line were collected after 7-days of immobilization, or 7-days of remobilization. Muscles were collected and analyzed as outlined in the **Material and Methods** section.



Method Figure 2: Study design for Project 3, Objective 2. Mice from the mt-Keima purebred line were collected after 7-days of immobilization. The antioxidant N-acetyl cysteine (NAC) was also be administered during the immobilization phase to limit ROS generation. Muscles were collected and analyzed as outlined in the **Material and Methods** section.



Method Figure 3: Study design for Project 3, Objective 3. Mice from the mt-Keima purebred line were collected after 7-days of immobilization. The autophagy inhibitor colchicine (COL) was also be administered for 5-days during the immobilization phase to limit prevent autophagosome-lysosome fusion. Muscles were collected and analyzed as outlined in the **Material and Methods** section.

Introduction

Skeletal muscle atrophy is characterized as a catabolic state that results in the rapid deterioration of muscle mass and impaired muscle function. Several physiological and pathological conditions can result in skeletal muscle atrophy, including aging, denervation, immobilization, neurodegeneration, and myopathy (Deneubourg et al., 2022; Rahman & Quadrilatero, 2021a; Triolo et al., 2022; Vainshtein et al., 2015; Wohlgemuth et al., 2010). The underlying theme for all these conditions is a reduction in muscular contractions that would otherwise stimulate muscle protein synthesis while simultaneously suppressing proteolysis. The convergence of several molecular signals ultimately results in a shift towards greater protein degradation in myofibers.

Skeletal muscle atrophy occurs by activation of the ubiquitin-proteosome system (UPS), apoptosis, and autophagy. UPS is known to degrade myofibrillar proteins (i.e., actin and myosin) during atrophy, while activation of the intrinsic apoptotic signaling cascade may function to eliminate myonuclei or the entire myofibers (Allen et al., 1997, 1999; Aweida & Cohen, 2021; Leeuwenburgh et al., 2005). Additionally, the role of autophagy has been implicated in the maintenance of muscle mass (Masiero et al., 2009) and in disuse atrophy (Triolo et al., 2022). Autophagy functions to degrade damaged cellular material to allow the recycling of macromolecules to build new proteins. Autophagy can occur in a selective or non-selective manner. With respect to skeletal muscle, the selective degradation of mitochondria, termed mitophagy, has been implicated in maintaining normal function of myofibers (G. K. Sakellariou et al., 2016). Dysfunction or dysregulation of mitophagy has been associated with impaired skeletal muscle function (Rahman & Quadrilatero, 2021a).

Atrophy of myofibers can occur within one week of disuse and is accompanied by elevated mitophagy signaling. Elevated levels of PINK1, PRKN and *Bnip3l* have been reported in immobilized and remobilized skeletal muscles (Deval et al., 2020; C. Kang et al., 2016). Another study demonstrated greater *Bnip3, Bnip3l,* and *Prkn* transcripts from immobilized skeletal muscle (Yamashita et al., 2021). This study also found elevated mitophagic flux in mito-QC reporter animals (Yamashita et al., 2021). Consistent with these findings, elevated mitophagy flux in mt-Keima mice was also recently reported as early as 1-day following denervation (Triolo et al., 2022). Therefore, a clear relationship between mitophagy and disuse atrophy has been established; however, it has yet to be determined whether mitophagy is the driving force for disuse atrophy. The upregulation of mitophagy may be complementary to atrophic conditions, given the lack of energy demand placed on the mitochondria or perhaps due to the intrinsic dysfunction within the mitochondria. Alternatively, mitophagy may serve as an initiating step for atrophy by reducing the bioenergetic status of the myofibers; however, further investigation is required to delineate this relationship.

The purpose of the present study was to understand the role of mitophagy following immobilization and remobilization of skeletal muscle. We further questioned whether inhibition of ROS via antioxidant treatment or autophagy via colchicine treatment could modify mitophagy and immobilization-induced muscle atrophy.

Material and Methods

RNA Sequencing Analysis

Publicly available RNA sequencing datasets were retrieved from the Gene Expression Omnibus (GEO) database (accession number GSE237537). Initial quality control was based on exclusion criteria including adapter contamination and low-quality bases. Gene-level expression was quantified and analyzed using the DESeq2 package in RStudio. Differential expression was determined with an adjusted p-value of <0.05 and a minimum log2 fold change of >1, identifying significantly differentially expressed genes. Enrichment of biological processes and pathways was assessed using the clusterProfiler package, with tests against Gene Ontology (GO) terms. Pathways were considered significantly enriched at a corrected p-value of <0.05. Visualization of the results, including volcano plots, heatmaps, and barplots, were created using GraphPad PRISM software.

Animals

Mt-Keima animals with a FVB background were kindly gifted by Torin Finkel (Sun et al., 2015, 2017). These animals are a valuable tool for studying mitophagy since they express the fluorescent Keima protein conjugated to the COX8 subunit found within complex IV in the IMM. The unique feature of the Keima molecule is its dual-excitation, single-emission fluorescence (i.e., 620 nm), which changes depending on the pH of its environment. Under neutral pH conditions, as found in the cytosol, Keima is excited at 488 nm. In the acidic conditions of the lysosome, where mitochondria are degraded, the excitation shifts to 561 nm. This shift allows for precise monitoring of mitophagy. Additionally, the resistance of this molecule to lysosomal degradation enhances the accuracy of mitophagic flux measurements.

Animals were given free access to food and water. All animal procedures were conducted in accordance with the standards set by the Canadian Council on Animal Care (CCAC) and were approved by the Animal Care Committee (ACC) at the University of Waterloo.

Hindlimb Immobilization and Drug Treatment

Animals were anesthetized under light isoflurane inhalation (~2%). The left hindlimb of each animal was extended and a small (1cm x 3cm) piece of Dermapore tape was wrapped around the ankle and knee joints. An elastic self-adhesive tape (Tensor; 3cm x 5cm) was lightly wrapped on top. One additional layer of medical tape was added on top to secure the self-adhesive tape. All animals regained consciousness after 5 minutes and signs of discomfort were monitored. In a subset of experiments, vehicle (VEH) or N-acetyl-cysteine (NAC; 150mg/kg/day) were injected daily for the duration of the immobilization phase. In another subset of experiments, VEH or colchicine (COL; 0.4mg/kg/day) were injected daily for the final 5-days of the immobilization phase.

Isolation of Skeletal Muscles

The extensor digitorum longus (EDL), tibialis anterior (TA), gastrocnemius (GAS), and quadriceps (QUAD) muscles were rapidly excised from animals. Intact EDL muscle was immediately transferred to Tyrode buffer (121mM NaCl, 5mM KCl, 24mM $NaHCO_3$, 1.8mM $CaCl_2$, 0.4mM NaH_2PO_4, 5.5mM glucose, 0.1mM EDTA, and 0.5mM $MgCl_2$, pH 7.3) at room temperature for contractility measurements. One TA was stored in BIOPS buffer (2.77mM CaK_2EGTA, 7.23mM K_2EGTA, 5.77mM Na_2ATP, 6.56mM $MgCl_2$-$6H_2O$, 20mM taurine, 15mM Na_2PCr, 20mM imidazole, 0.5mM DTT, 50mM K-MES) on ice until use for respirometry and

confocal imaging. The contralateral, TA muscles were embedded in OCT compounds (Tissue Tek), frozen in isopentane cooled by liquid nitrogen and stored at -80°C for fiber type analyses. The GAS and QUAD muscles were cut in half and snap frozen for immunoblot analyses, while the other half was stored in PBS-EDTA solution (10mM EDTA in 1X PBS, pH 7.4) on ice for mitochondrial fractionation.

Live Myofiber Imaging and Mitophagy Flux Analysis

The TA muscle was manually separated into small bundles in BIOPS buffer on ice. Bundles were rapidly transferred to #1 coverslips and carefully separated to allow maximal contact of muscle bundle to the coverslip. A thin layer of 0.8% agarose gel was placed on top of the bundles to prevent movement during imaging. Five to ten fields consisting of 3-5 myofibers were imaged on a Zeiss LSM 800 confocal microscope at 63X magnification. Individual excitation wavelengths were used to minimize overlap between fluorescent channels. An excitation wavelength of 488nm was used to determine healthy mitochondria (pH ~7; green), whereas an excitation wavelength of 561nm was used to determine mitochondria undergoing mitophagy (pH ~4; red). Emission wavelengths remained the same at 620nm. Puncta count and size were determined in each field using the automated Particle Analysis function in ImageJ.

High-Resolution Respirometry with Simultaneous ROS Measurements

The TA muscle was separated under a stereomicroscope into bundles using very fine tipped forceps in ice-cold BIOPS buffer. Bundles were permeabilized in 50μg/ml of saponin in 1.5ml BIOPS buffer for 30 minutes on ice with gentle rocking. Muscle bundles (1-3mg) were then transferred to 1.5ml of buffer Z (105mM K-MES, 30mM KCl, 1mM EGTA, 10mM K_2HPO_4, 5mM

$MgCl_2$-$6H_2O$, 5mg/ml BSA, pH 7.1) to wash prior to respirometry experiments. Oxygen consumption and mitochondrial hydrogen peroxide (mH_2O_2) emission was determined in buffer Z supplemented with 10μM blebbistatin, 10μM Amplex Red, 5U/ml horseradish peroxidase, and 10U/ml superoxide dismutase using an Oxygraph-2K equipped with a LED2 fluorometry module. Experiments were conducted at 37°C in a 2ml chamber that was hyperoxygenated to ~350uM. Reverse electron flow was determined with the addition of 10mM succinate, followed by 5mM pyruvate and 2.5mM malate. Maximal coupled respiration was stimulated with the addition of 5mM ADP. Cytochrome C was added to ensure outer membrane integrity. mH_2O_2 emission was calibrated from a standard curve established with the same reaction conditions.

Mitochondrial Fractionation

GAS and QUAD muscles were chopped on a stainless-steel board using a razor for one minute. The tissue was transferred back into the same tube containing 5ml of PBS with 10mM EDTA (PBS-EDTA solution) and centrifuged at 500g for 5 minutes. The supernatant was discarded, and the muscles were digested in 0.05% trypsin in PBS-EDTA solution for 5 minutes on ice. The trypsin solution was removed by centrifugation at 500g for 5 minutes. Digested muscles were resuspended in mitochondrial isolation buffer (100mM KCl, 50mM MOPS, 5mM $MgSO_4$-$7H_2O$, 1mM EGTA, 2mg/ml BSA, pH 7.4) and homogenized using a Teflon homogenizer equipped on a drill press set to 200rpm for 5-10 strokes. The homogenized tissue was subjected to low-speed centrifugation (~700 x g) to pellet large debris and the supernatant was transferred to ultracentrifuge tubes and spun at 10,000g for 15 minutes at 4°C. The resulting pellet constituted the mitochondrial pellet and was resuspended in mitochondrial isolation buffer without BSA before being transferred to 1.5ml microcentrifuge tubes and spun at 10,000g for 5 minutes. The

resulting pellet was washed and centrifuged three times in mitochondrial isolation buffer without BSA to remove any cytosolic protein. After the final spin, the supernatant was aspirated, and the pellets were frozen in liquid nitrogen.

Immunoblotting

Snap frozen muscle samples were divided into 20-30mg portions and stored in separate tubes. Muscle samples were crushed into a powder using a liquid nitrogen-cooled pestle and mortar and transferred to 1.5ml tubes containing 5 volumes of lysis buffer (20mM HEPES, 10mM NaCl, 1.5mM $MgCl_2$, 1mM DTT, 20% glycerol, 0.1% Triton-X100, pH 7.4) with protease inhibitor. Mitochondrial enriched fractions were resuspended in lysis buffer with protease inhibitor and sonicated at 40 Hz for 10 seconds on ice to dissolve any membranal structures. Protein content was determined using a BCA protein assay. Equal protein was loaded and separated using 8-12% SDS-PAGE, transferred on to PVDF membranes, and blocked with 2-5% non-fat milk powder in TBS-T at room temperature for 1 hour. Membranes were briefly rinsed and incubated overnight in primary antibodies against: BNIP3 (#3769, Cell Signaling), BNIP3L (#12396, Cell Signaling), MAP1LC3B/LC3B (#2775, Cell Signaling), GAPDH (#2118, Cell Signaling), OPA1 (#80471, Cell Signaling), MFN2 (#9482, Cell Signaling), DNM1L (#8570, Cell Signaling), SQSTM1 (PM045, MBL), PINK1 (sc-33796, Santa Cruz), PRKN (sc-32282, Santa Cruz), VDAC1 (sc-390996, Santa Cruz), ANT1 (sc-9299, Santa Cruz), CYCS (sc-13256, Santa Cruz), TFAM (sc-166965, Santa Cruz), BAX (sc-526, Santa Cruz), BCL2 (sc-7382, Santa Cruz), ACT (S2066; Sigma), PPARGC1A (ST1202, Sigma), SOD1 (SOD-101, Stressogen), SOD1 (SOD-110, Stressogen), and 4HNE (ab46545). Following incubation, membranes were washed, and appropriate horseradish peroxidase-conjugated secondary antibody was applied at room

temperature for 1 hour. Bands were visualized using ECL substrate on a ChemiDoc Imaging System.

Caspase, Calpain, and Proteasomal Activity Assay

To measure caspase (CASP), calpain (CAPN) and proteasomal activities, whole-cell lysates were collected as above in the absence of protease inhibitors. Samples were incubated in duplicates with 20μM of Ac-DEVD-AFC for CASP3 or Ac-LEHD-AFC for CASP9 in assay buffer (20 mM HEPES pH 7.4, 10 mM DTT, and 10% glycerol). For CAPN activity, samples were incubated in duplicates with 20μM of Suc-LLVY-AMC and Z-LL-CHO inhibitor in assay buffer for 2 hours at 30°C. For 20S proteasomal activity, samples were incubated in duplicates with 20μM of Suc-LLVY-AMC and MG-132 inhibitor in proteasome assay buffer (50mM Tris/HCl, 25mM KCl, 10mM NaCl, 1mM $MgCl_2$; pH 7.5) for 1 hour at 30°C. Fluorescence measurements were performed at room temperature using a Cytation 5 Imaging Multi-Mode Reader. The AFC probe was measured with excitation and emission wavelengths at 400 and 505 nm, respectively. The AMC probe was measured with excitation and emission wavelengths at 360 and 440 nm, respectively. The fluorescence values were normalized to protein concentration of samples and expressed as fold changes in fluorescence.

Immunofluorescence Fiber Type Analysis

Ten-micron cryosections were cut, mounted onto microscope slides and maintained at -20°C until staining. For staining, slides were dried at room temperature, circumscribed with a hydrophobic pen and blocked using 10% goat serum in PBS. Slides were incubated at room temperature with antibodies against type IIA (SC-71, DSHB), type IIX (6H1, DSHB), and

dystrophin (MANDYS1, DSHB) for 2 hours. Slides were washed three times with PBS and incubated at room temperature with appropriate secondary antibodies. Following incubation with secondary antibodies, slides were washed three times and mounted with Fluoromount mounting medium. Fiber cross-sectional area (CSA) and fiber counts was quantified using ImageJ.

Skeletal Muscle Contractility

Intact EDL muscles were placed in a 25°C bath of oxygenated Tyrode solution. Muscles were placed between two platinum electrodes driven by a biphasic stimulator. Muscle stimulation occurred at varying frequencies from 10 to 150 Hz. After the stimulation protocol, a fatigue protocol was performed by stimulating at 70 Hz for 350ms every 2 seconds for a total of 5 minutes. The number of contractions to reduce force by 50% was used as an index of fatigue. Data was analyzed using Dynamic Muscle Control Data Acquisition software (Aurora Scientific). Specifically, peak isometric force amplitudes (mN) were determined across the range of stimulation frequencies and normalized to muscle mass.

Statistics

Statistical analyses were performed in GraphPad PRISM. T-tests were performed to compare changes in functional parameters between control (CTRL) and immobilized (IM) or remobilized muscle (RM). T-tests were also performed to compare VEH to treatment in immobilized muscle. An alpha value of 0.05 was assigned for all analyses.

Results

Immobilization-induced muscle atrophy upregulates cellular stress signaling genes and downregulates mitochondria-related genes

Immobilization-induced muscle atrophy initiates profound mitochondrial remodeling within skeletal muscle, that trigger structural and functional changes of the myofiber. These adaptations include alterations in mitochondrial density, morphology, and oxidative capacity, which collectively influence myofiber integrity and contractile function (Mirzoev, 2020; Sandri, 2013; Sartori et al., 2021). Concurrent shifts in the molecular profile of proteins associated with mitochondrial biogenesis, mitophagy, and mitochondrial dynamics underscore the intricate regulatory mechanisms governing cellular responses to disuse (Triolo et al., 2022; Vainshtein et al., 2015; F. Wang et al., 2023; Xu et al., 2022; Yamashita et al., 2021). Understanding these mitochondrial adaptations is pivotal for devising strategies to preserve muscle mass and function during periods of immobilization.

To better understand the changes in mitochondrial remodeling processes during immobilization-induced atrophy, we started with a broad RNA-Seq analysis using a publicly available dataset from the GEO database (GSE237537). From this dataset, approximately 55,000 genes were processed and filtered prior to analysis. Differential expression analysis, conducted using DESeq2, identified 92 differentially expressed genes (DEGs) between the immobilized (IM) and control (CTRL) groups ($p < 0.05$; Figure 1A-C). Among these DEGs, several genes associated with cellular stress signaling were upregulated (e.g., *Fbxo32* and *Gadd45a*), while muscle-related genes were downregulated (e.g., *Myl2* and *Myl3*) in the IM group compared to CTRL (Figure 1C). Notably, no DEGs directly associated with mitochondrial remodeling, particularly in terms of mitochondrial biogenesis, mitophagy, or mitochondrial dynamics were observed.

Gene ontology (GO) analysis of this gene pool revealed significant upregulation in genes related to autophagy and the UPS, with little upregulation of mitochondrial-related genes (Figure 1D). Conversely, there was significant downregulation of genes associated with mitochondria, autophagy, and UPS (Figure 1D). Detailed analysis of the top upregulated biological processes and cellular components revealed a greater number of genes associated with degradative pathways, including apoptosis and UPS (Figure 1E-F). Among the major downregulated biological processes and cellular components were genes associated with myofiber development/remodeling and mitochondrial function (Figure 1E-F). Overall, this analysis highlighted significant changes in gene expression profiles due to immobilization, with a notable upregulation of genes associated with degradative processes and a downregulation of genes related to mitochondrial components.

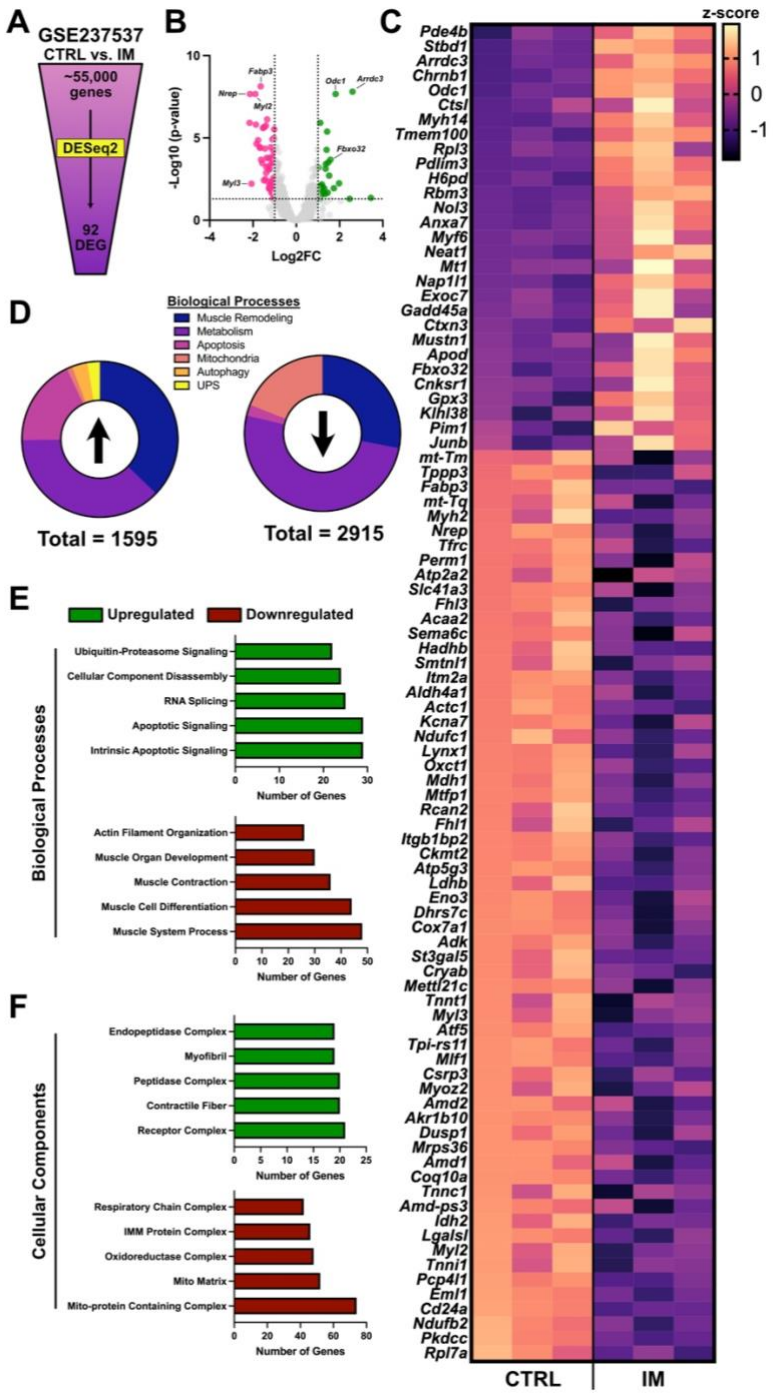


Figure 1: RNA sequencing analysis of control (CTRL) and immobilized (IM) gastrocnemius muscle. A) Representative visualization of genes analyzed from the publicly available Gene Expression Omnibus database (Accession ID: GSE237537). B) Volcano plot displaying differential gene expression in skeletal muscle. The horizontal line delineates a significance threshold of $p < 0.05$. Vertical lines mark a z-score change greater than Log2. Green labels indicate upregulated differentially expressed genes (DEGs), while red labels indicate downregulated DEGs. C) List of all 92 DEGs identified by DESeq2 analysis. D) Gene ontology analyses and donut graph outputs summarizing changes in genes associated with five major remodeling processes: muscle remodeling, metabolism, apoptosis, mitochondria, autophagy, and the ubiquitin proteasome system (UPS). A total

of 1595 genes related to these processes are upregulated while 2915 genes related to these processes are downregulated. E) Gene ontology analyses output of the number of genes linked to the top five upregulated (green) and downregulated (red) biological processes. F) Gene ontology analyses output of the number of genes linked to the top five upregulated (green) and downregulated (red) cellular components. CTRL indicates control animals (i.e., no intervention). IM indicates animals collected following 7-days of immobilization. n = 3 per group.

Hindlimb immobilization leads to greater mitochondrial ROS emission, increased mitophagic flux, and atrophy of all myofibers

To further our understanding, we investigated physiological adaptations in myofibers using a hindlimb bandage model for 7-days to induce immobilization-induced atrophy, followed by a 7-day remobilization period to assess recovery dynamics (Figure 2A). Our findings indicated that IM led to approximately 20% decrease in the relative muscle mass of major hindlimb muscles including the tibialis anterior (TA), gastrocnemius (GAS), and quadriceps (QUAD) muscles, but not the smaller extensor digitorum longus (EDL) muscle compared to CTRL (Figure 2B-F). The reductions in the larger muscle mass were persisted even after 7-days of remobilization (Figure 2B-F). Functional assessments revealed a significant decrease in muscle force and fatiguability in both IM (-66% and -40%, respectively) and RM (-22% and -12%, respectively) EDL muscles compared to CTRL (Figure 2G-I). While RM muscles showed some improvement in force and fatiguability compared to IM muscles, only 88% recovery was achieved relative to CTRL (Figure 2G-I). Detailed fiber type analysis revealed a specific decline in the CSA of type IIA fibers during the IM phase (-27%; $p < 0.05$), which normalized upon RM (Figure 2J-K). However, the mean CSA of type IIX and IIB fibers remained reduced (-22% to -28%; $p < 0.05$) in both phases (Figure 2J-K), indicating a fiber type-specific susceptibility to IM, particularly affecting fibers with faster contractile properties and greater glycolytic phenotype. Furthermore, we observed a shift in fiber type distribution, with an increase in type IIB fibers and a decrease in type IIX fibers during IM, which reverted to initial levels after remobilization (Figure 2L). To explore the mechanisms behind

immobilization-induced muscle atrophy and its connection to mitochondrial quality, we analyzed mitophagic flux in mt-Keima reporter mice. Our results demonstrated a significant increase in mitophagic puncta count in IM (3-fold) and RM (2-fold) muscles compared to CTRL, indicating an enhanced rate of mitophagy; albeit no changes in average mitophagic puncta size was observed (Figure 2M-O). This indicates that immobilization-induced muscle atrophy is closely linked to the activation of mitophagy.

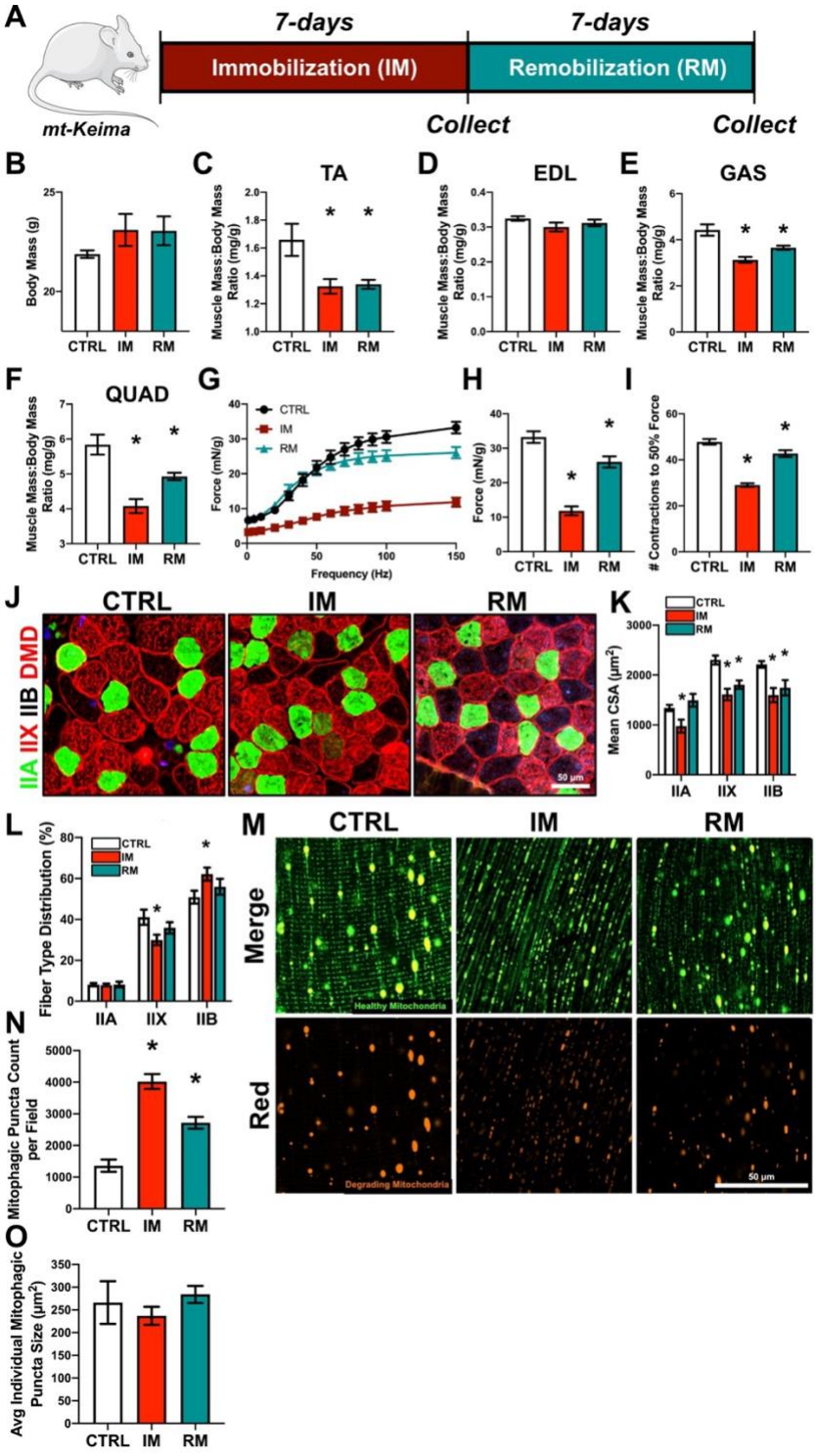


Figure 2: Immobilization- and remobilization-induced changes in skeletal muscle structure and mitophagic flux. A) Representative visualization of immobilization and remobilization protocol. B) Body mass of control (CTRL), immobilized (IM) and remobilized (RM) animals. Normalized skeletal muscle mass measurements of C) tibialis anterior (TA), D) extensor digitorum longus, E) gastrocnemius (GAS), and F) quadriceps (QUAD). G) Force-frequency graph of EDL muscles from CTRL, IM and RM animals. H) Peak force development derived from force-frequency curve. I) Fatigue index measurement of EDL muscle (greater value indicates more fatigue-

resistance). J) Representative immunofluorescent images of TA muscles from CTRL, IM and RM animals. Samples were stained with antibodies specific for individual myosin heavy chain isoforms: type IIA (green), type IIX (red), type IIB (unstained), and dystrophin (red). Scale bars indicate 50 μm. K-L) Quantification of mean cross-sectional area (CSA) and distribution of type IIA, IIX, and IIB myofibers. M) Representative confocal images of mitophagic flux from TA muscles of mt-Keima reporter mice. Green fluorescence indicates healthy mitochondria. Red fluorescence indicates degrading mitochondria. Scale bar indicates 50 μm. N) Quantification of mitophagic (i.e., red) puncta count per field. O) Quantification of average individual mitophagic puncta size. * $p < 0.05$ compared to CTRL group. n = 5-8 per group.

Mitophagy is upregulated in response to various mitochondrial stressors such as excessive reactive oxygen species (ROS) production or a decline in mitochondrial membrane potential. To assess functional changes in mitochondria resulting from IM and subsequent RM, we measured several parameters indicative of mitochondrial function. Our results show significant reductions in maximal mitochondrial respiration capacity (i.e., oxygen consumption rate [OCR]) in IM myofibers compared to CTRL (-25%; $p < 0.05$; Figure 3B). This decrease was accompanied by increased mitochondrial hydrogen peroxide (mH_2O_2) production when stimulated by succinate (+48%; $p < 0.05$; Figure 3C-D). Additionally, we observed increased fraction of electron leak (+66%; $p < 0.05$; Figure 3E), which is indicative of inefficient electron transport. Together, these findings suggest that IM induces substantial impairments in mitochondrial function, likely contributing to the observed muscle atrophy and changes in myofiber composition.

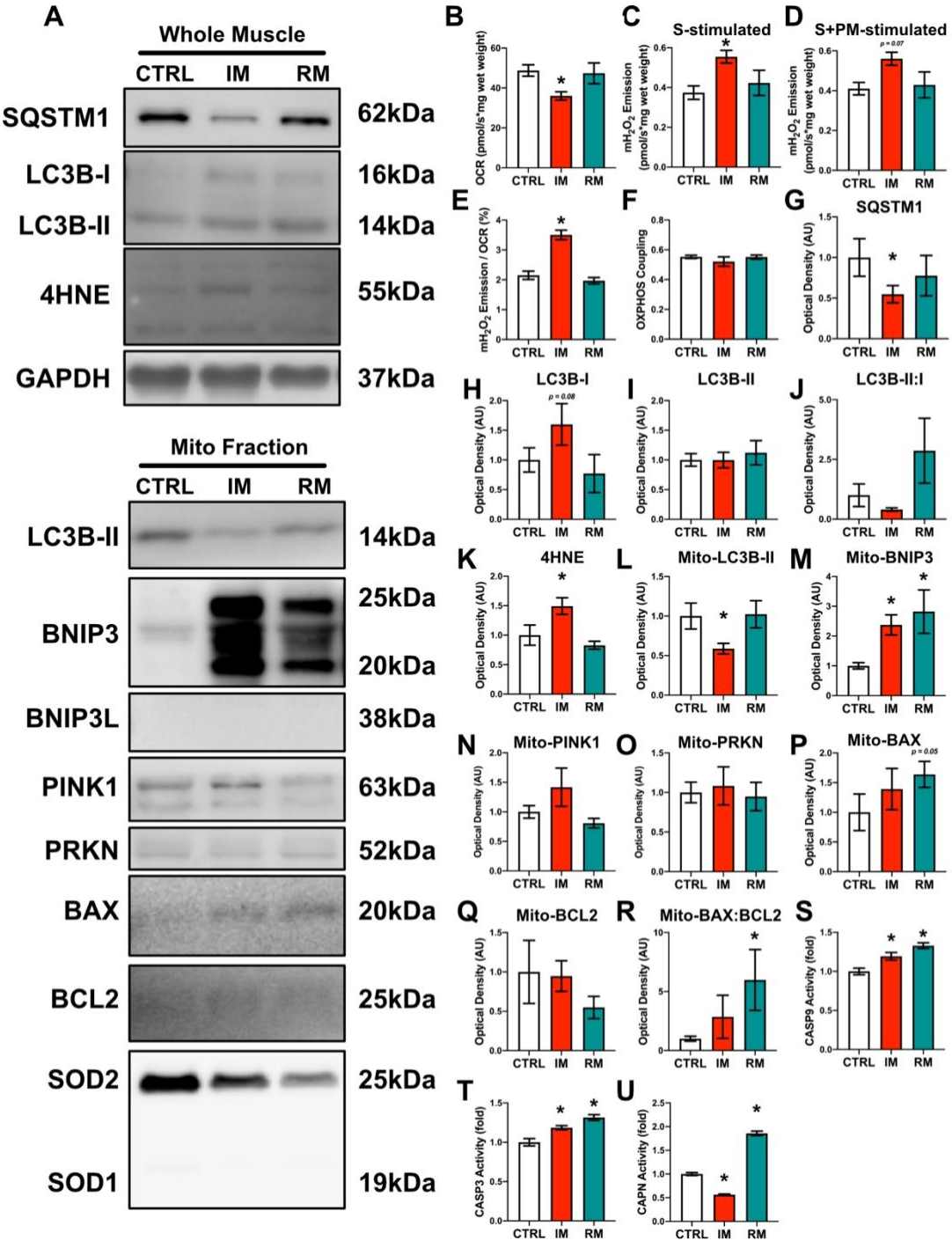


Figure 3: Quantitative analysis of autophagy and mitophagy proteins in IM and RM muscles. A) Representative immunoblots of whole muscle lysate and mitochondrial fractions derived from GAS and QUAD. B) Quantification of maximal oxygen consumption rate (i.e., respiration) of permeabilized bundles from TA muscles. Simultaneous quantification of C) succinate-stimulated hydrogen peroxide (H_2O_2) production, and D) succinate + pyruvate/malate-stimulated H_2O_2 production in permeabilized TA muscle bundles. E) Quantification of mitochondrial fraction of electron leak. F) Quantification of oxidative phosphorylation (OXPHOS) coupling. Quantitative analysis of G) SQSTM1, H) LC3B-I, I) LC3B-II, J) LC3B-II:I, and K) 4HNE from whole muscle lysate. Quantitative analysis of L) LC3B-II, M) BNIP3, N) PINK1, O) PRKN, P) BAX, Q) BCL2, and R)

BAX:BCL2 from mitochondrial-enriched fractions. Quantitative analysis of S) CASP9 activity, T) CASP3 activity, and U) CAPN activity. * $p < 0.05$ compared to CTRL group. n = 6-8 per group.

Mitochondrial localization of BNIP3 and activation of intrinsic apoptotic signaling define immobilization-induced atrophy

To investigate the molecular mechanisms driving mitophagic flux following hindlimb immobilization, we conducted immunoblot analyses on whole muscle lysates and mitochondrial-enriched fractions derived from the GAS and QUAD muscles of CTRL, IM, and RM animals. Our results demonstrated a decrease in the autophagic cargo protein SQSTM1 (-46%; $p < 0.05$), while the autophagy recognition protein LC3B showed little variation, suggesting a differential regulation of autophagic components in response to immobilization (Figure 3A & G-J). In addition, we observed increased lipid peroxidation in IM muscles, as evidenced by a 50% increase in 4-hydroxynonenal (4HNE), which coincided with increased mH_2O_2 emission (Figure 3K). At the mitochondrial level, there was a noticeable reduction in lipidated LC3B-II in IM muscles (Figure 3L). Conversely, mitochondrial localization of the mitophagy receptor BNIP3 was significantly elevated in both IM (+130%; $p < 0.05$) and RM (+180%; $p < 0.05$) muscles (Figure 3M), suggesting a persistent activation of mitophagy as a response to muscle immobilization and subsequent recovery. However, no significant changes were observed in other mitophagy-related proteins including PINK1 and PRKN within the mitochondrial-enriched fractions (Figure 3N-O).

Considering the observed upregulation of genes linked to intrinsic apoptotic signaling in muscle tissues, we examined the involvement of key regulators of mitochondrial outer membrane permeabilization (MOMP). Our analysis revealed no significant changes in the mitochondrial localization of the pro-apoptotic protein BAX or the anti-apoptotic protein BCL2 (Figure 3P-Q). However, an increased BAX/BCL2 ratio was detected in remobilized muscles, indicative of enhanced MOMP and potential susceptibility to mitochondrial apoptotic signaling during the RM

phase (Figure 3R). Further exploration into the downstream signals of intrinsic apoptotic pathways showed 20-30% elevation in caspase 9 (CASP9) and caspase 3 (CASP3) activities in both IM and RM muscles compared to CTRL (Figure 3S-T). This suggests a sustained activation of apoptotic signaling following muscle immobilization and during the recovery phase. Additionally, our results indicated a suppression of calpain (CAPN) activity in IM muscles (-44%; $p < 0.05$; Figure 3U). In contrast, CAPN activity was significantly higher in RM muscles (+85%; $p < 0.05$), possibly reflecting a recovery response associated with muscle remodeling. Collectively, these findings illustrate that immobilization-induced muscle atrophy not only impaired mitochondrial function and heightened mitophagy but also modify apoptotic and proteolytic signaling pathways.

Immobilization suppresses mitochondrial biogenesis and fusion signals, while upregulating key mitophagy molecules

To elucidate the impact of the immobilization-remobilization protocol on mitochondrial remodeling, we analyzed the expression of key mitochondrial proteins involved in biogenesis, mitophagy, and mitochondrial dynamics through immunoblotting. Our findings indicate that IM led to a reduction in the levels of the mitochondrial biogenesis and fusion proteins, including PPARGC1A (also known as PGC-1α; -28%; $p < 0.05$), OPA1 (-20%; $p < 0.05$), and MFN2 (-28%; $p < 0.05$; Figure 4A-B & H-I). Notably, PPARGC1A and MFN2 levels returned to baseline upon remobilization; however, OPA1 levels remained depressed (-10%; $p < 0.05$). Additionally, IM induced an upregulation in the mitophagy-associated proteins BNIP3 (+170%; $p < 0.05$) and PRKN (+70%; $p < 0.05$), without modifying PINK1 or BNIP3L levels (Figure 4D-G). Importantly, BNIP3 levels remained elevated during the remobilization phase (+130%; $p < 0.05$), while PRKN levels reverted to baseline, suggesting differential regulation of mitophagy during the recovery

process. Moreover, we assessed other mitochondrial markers including the mitochondrial biogenesis marker TFAM (Figure 4C), the fission protein dynamin-1-like protein (DNM1L) (Figure 4J), and various mitochondrial-related proteins such as voltage-dependent anion channel 1 (VDAC1), adenine nucleotide translocator 1 (ANT1), cytochrome c (CYCS), and superoxide dismutase 2 (SOD2) (Figure 4K-O). These proteins showed minimal fluctuations throughout the IM and RM phases, suggesting a stable expression under the conditions tested. Taken together, our findings demonstrate that IM induces significant changes in gene expression and physiological adaptations at the myofiber and mitochondrial levels.

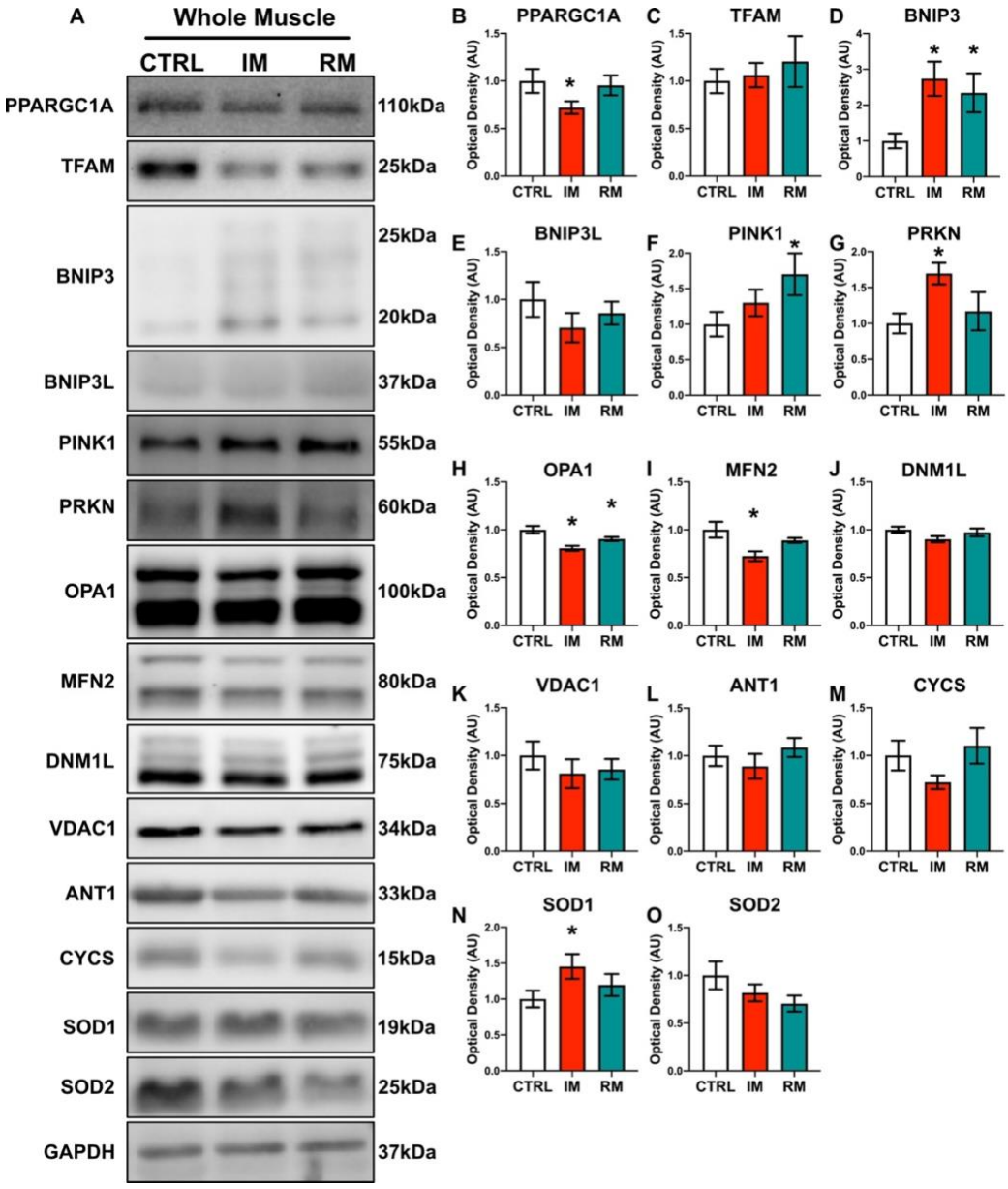


Figure 4: Quantitative analysis of mitochondrial remodeling proteins in IM and RM muscles. A) Representative immunoblots of whole muscle lysate derived from GAS and QUAD. Quantitative analysis of B) PPARGC1A, C) TFAM, D) BNIP3, E) BNIP3L, F) PINK1, G) PRKN, H) OPA1, I) MFN2, J) DNM1L, K) VDAC1, L) ANT1, M) CYCS, N) SOD1, O) SOD2. * $p < 0.05$ compared to CTRL group. n = 8 per group.

NAC treatment during immobilization suppresses mitophagic flux and exacerbates atrophy of type IIX and IIB myofibers

Given the observed impairments in mitochondrial function and the activation of stress responses such as mitophagy and mitochondria-mediated CASP signaling likely due to oxidative

stress, we hypothesized that antioxidant treatment could mitigate these detrimental effects in IM muscles. We tested this hypothesis by administering daily treatments of the antioxidant N-acetylcysteine (NAC) to animals throughout the IM period (Figure 5A). Contrary to our expectations, NAC treatment did not modify body mass nor preserve relative muscle mass of TA, GAS, and QUAD muscles (Figure 5B-E). No changes in absolute muscle mass were observed (data not shown). Surprisingly, NAC treatment during IM led to even greater reductions in the mean CSA of type IIX (-24%; $p < 0.05$) and IIB (-39%; $p < 0.05$) myofibers in the TA, with no changes observed in the overall fiber type distribution (Figure 5F-H). Furthermore, NAC treatment significantly attenuated mitophagy, as evidenced by suppressed mitophagic puncta count (-20%; $p < 0.05$) and average individual puncta size (-33%; $p < 0.05$; Figure 5I-K). These findings suggest that while antioxidant treatment can influence aspects of mitochondrial quality control, it does not necessarily counteract all the adverse effects of IM on myofiber size and may interfere with necessary cellular adaptation processes. It is interesting to note that the reduction in mitophagy was accompanied by significantly greater atrophy of glycolytic fibers in NAC treated animals, marking the first documentation of this phenomenon *in vivo*.

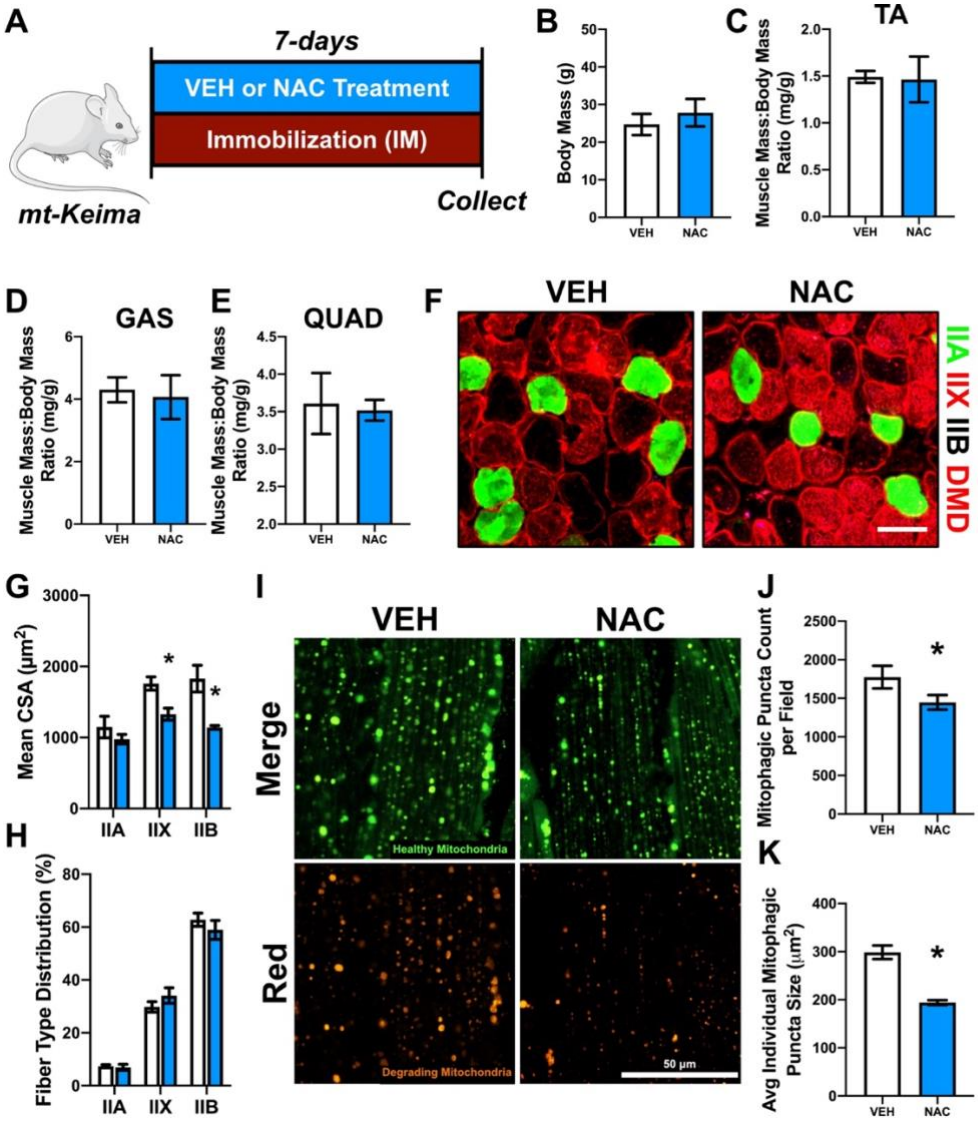


Figure 5: Effect of N-acetyl cysteine (NAC) treatment on immobilized muscles. A) Representative visualization of immobilization and NAC treatment protocol. B) Body mass of vehicle (VEH) and NAC treated animals. Normalized skeletal muscle mass measurements of C) tibialis anterior (TA), D) gastrocnemius (GAS), and E) quadriceps (QUAD). F) Representative immunofluorescent images of TA muscles from VEH and NAC treated immobilized animals. Samples were stained with antibodies specific for individual myosin heavy chain isoforms: type IIA (green), type IIX (red), type IIB (unstained), and dystrophin (DMD, red). Scale bars indicate 50 μm. G-H) Quantification of mean cross-sectional area (CSA) and distribution of type IIA, IIX, and IIB myofibers. I) Representative confocal images of mitophagic flux from TA muscles of immobilized mt-Keima reporter mice treated with VEH or NAC. Green fluorescence indicates healthy mitochondria. Red fluorescence indicates degrading mitochondria. Scale bar indicates 50 μm. J) Quantification of mitophagic (i.e., red) puncta count per field. K) Quantification of average individual mitophagic puncta size. * $p < 0.05$ compared to VEH group. n = 5-8 per group.

Given the significant alterations at the mitochondrial level, particularly with respect to mH_2O_2 emission and oxidative stress following IM, we questioned whether NAC treatment would alleviate some of the defects observed at the mitochondria level. Using high-resolution respirometry, we observed an increase in maximal mitochondrial respiration (+36%; $p < 0.05$) and a reduction in mH_2O_2 emission (-44%; $p < 0.05$) and electron leak fraction from NAC-treated IM muscles (-70%; $p < 0.05$; Figure 6B-E). We also conducted immunoblot analyses on whole muscle lysates and mitochondrial-enriched fractions from NAC-treated IM animals. These assays revealed no changes in SQSTM1, LC3B-I, LC3B-II, but a partial but non-significant reduction in the LC3B-II:I ratio (Figure 6A & G-J). Interestingly, the reduction in ROS generation and slight reduction in LC3B-II:I ratio ($p = 0.08$) was not accompanied by a change in 4HNE (Figure 6K). Additionally, no observable changes in the mitochondrial localization of LC3B-II or the mitophagy receptor BNIP3 were observed following NAC treatment (Figure 6L-M).

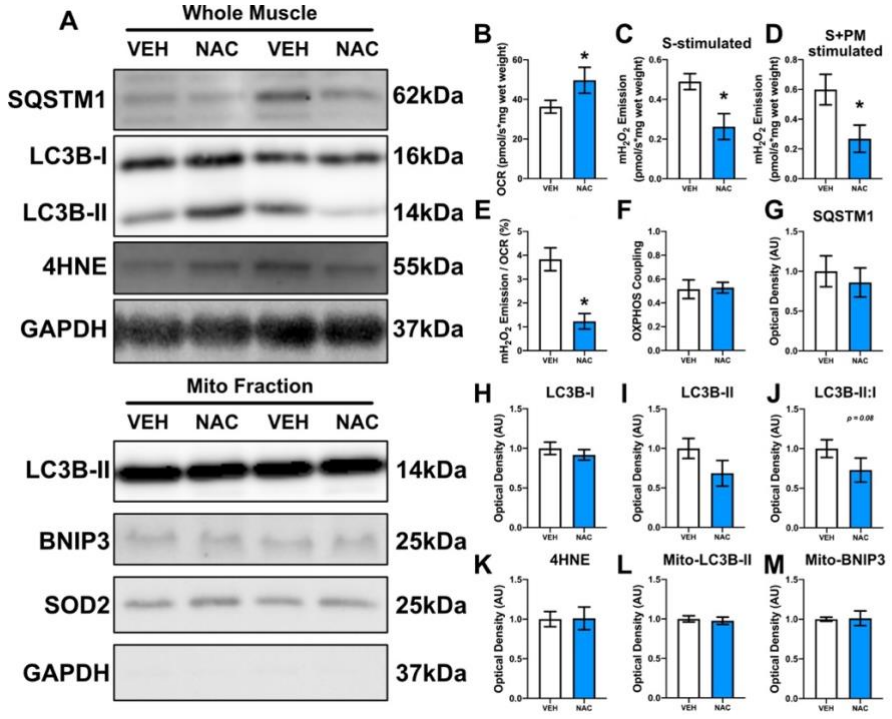


Figure 6: Quantitative analysis of autophagy and mitophagy proteins in VEH and NAC treated immobilized muscles. A) Representative immunoblots of whole muscle lysate and mitochondrial fractions derived from GAS and QUAD. B) Quantification of maximal oxygen consumption rate (i.e., respiration) of permeabilized bundles

from TA muscles. Simultaneous quantification of C) succinate-stimulated hydrogen peroxide (H_2O_2) production, and D) succinate + pyruvate/malate-stimulated H_2O_2 production in permeabilized TA muscle bundles. E) Quantification of mitochondrial fraction of electron leak. F) Quantification of oxidative phosphorylation (OXPHOS) coupling. Quantitative analysis of G) SQSTM1, H) LC3B-I, I) LC3B-II, J) LC3B-II:I, and K) 4HNE from whole muscle lysate. Quantitative analysis of L) LC3B-II, and M) BNIP3 from mitochondrial-enriched fractions. * $p < 0.05$ compared to VEH group. n = 5-10 per group.

Further exploration into changes in the mitochondrial remodeling revealed no changes in proteins related to mitochondrial biogenesis (PPARGC1A and TFAM) or mitophagy (BNIP3 and BNIP3L) (Figure 7A-E). However, we observed a reduction in OPA1 (-17%; $p < 0.05$) and DNM1L levels (-33%; $p < 0.05$), while MFN2 remained unchanged (Figure 7F-H); suggesting a selective disruption of mitochondrial fusion and fission processes, potentially impairing mitochondrial dynamics in response to IM. Furthermore, we observed minimal alterations in other mitochondrial-related molecules (VDAC1 and CYCS) and antioxidant enzymes (SOD1 and SOD2), with the exception of ANT1, which exhibited a reduction in NAC-treated mice (-16%; $p < 0.05$; Figure 7I-M). These results indicate that NAC appears to positively influence mitochondrial function during IM, but its impact on broader maintenance of muscle mass remains limited. Taken together, our data demonstrate that while antioxidant treatment can improve mitochondrial function, it simultaneously limits mitophagic flux and exacerbates atrophy of type IIX and IIB fibers.

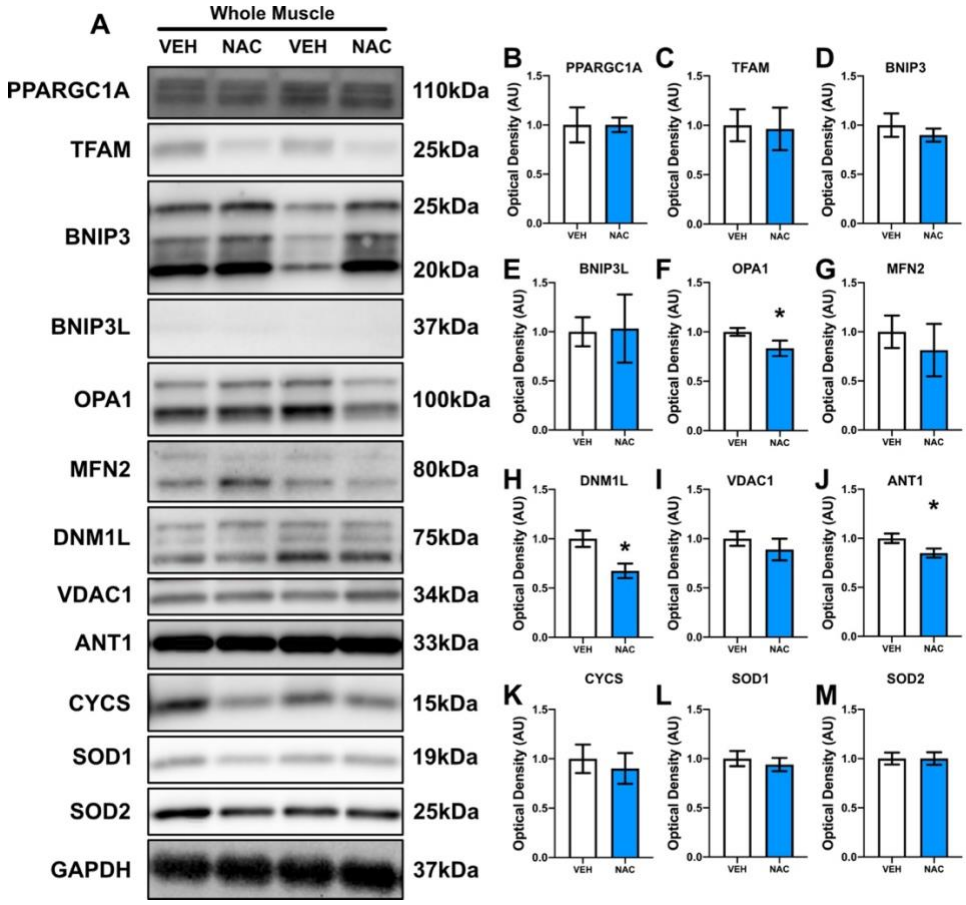


Figure 7: Quantitative analysis of mitochondrial remodeling proteins in VEH and NAC treated immobilized muscles. A) Representative immunoblots of whole muscle lysate derived from GAS and QUAD. Quantitative analysis of B) PPARGC1A, C) TFAM, D) BNIP3, E) BNIP3L, F) OPA1, G) MFN2, H) DNM1L, I) VDAC1, J) ANT1, K) CYCS, L) SOD1, M) SOD2. * $p < 0.05$ compared to VEH group. n = 10 per group.

COL treatment during immobilization inhibits mitophagic flux and exacerbates atrophy of type IIX and IIB myofibers

The improvements in mitochondrial function observed with NAC treatment did not lead to any preservation of muscle mass, highlighting a disconnect between mitochondrial functionality and muscle mass maintenance. However, the concurrent suppression of mitophagic flux and reduction in CSA of type IIX and IIB fibers may suggest that mitophagy is essential for maintaining the normal function of these fibers. To further investigate this, we explored the effects of pharmacologically inhibiting mitophagy on muscle and mitochondrial parameters following IM.

Due to the absence of specific inhibitors of mitophagy, we utilized colchicine (COL), a known inhibitor of microtubule polymerization, to broadly inhibit the autophagy machinery. Mt-Keima mice were IM and treated daily with COL starting on the second day of IM (5 total injections) to minimize any potential drug interaction with isoflurane (Figure 8A). COL treatment of IM animals did not modify body mass or normalized TA, GAS and QUAD muscle mass (Figure 8B-E). No changes in absolute muscle mass were observed (data not shown). However, we observed significant reductions in CSA of type IIX (-12%; $p < 0.05$) and IIB (-40%; $p < 0.05$) myofibers in the TA (Figure 8F-G), similar to NAC treated IM animals; indicating that COL treatment exacerbates immobilization-induced atrophy. Interestingly, we also noted a preferential loss of type IIB fibers, as evidenced by a decreased fiber type distribution, along with a compensatory increase in type IIA and IIX fibers (Figure 8H). Furthermore, COL treatment suppressed mitophagic flux as evidenced by a significant reduction in mitophagic puncta count (-88%; $p < 0.05$), though it did not affect average individual puncta size (Figure 8I-K). These findings highlight that inhibition of the autophagy machinery via COL treatment limits mitophagic flux and leads to greater muscle atrophy in IM mice, in a similar manner to NAC treatment.

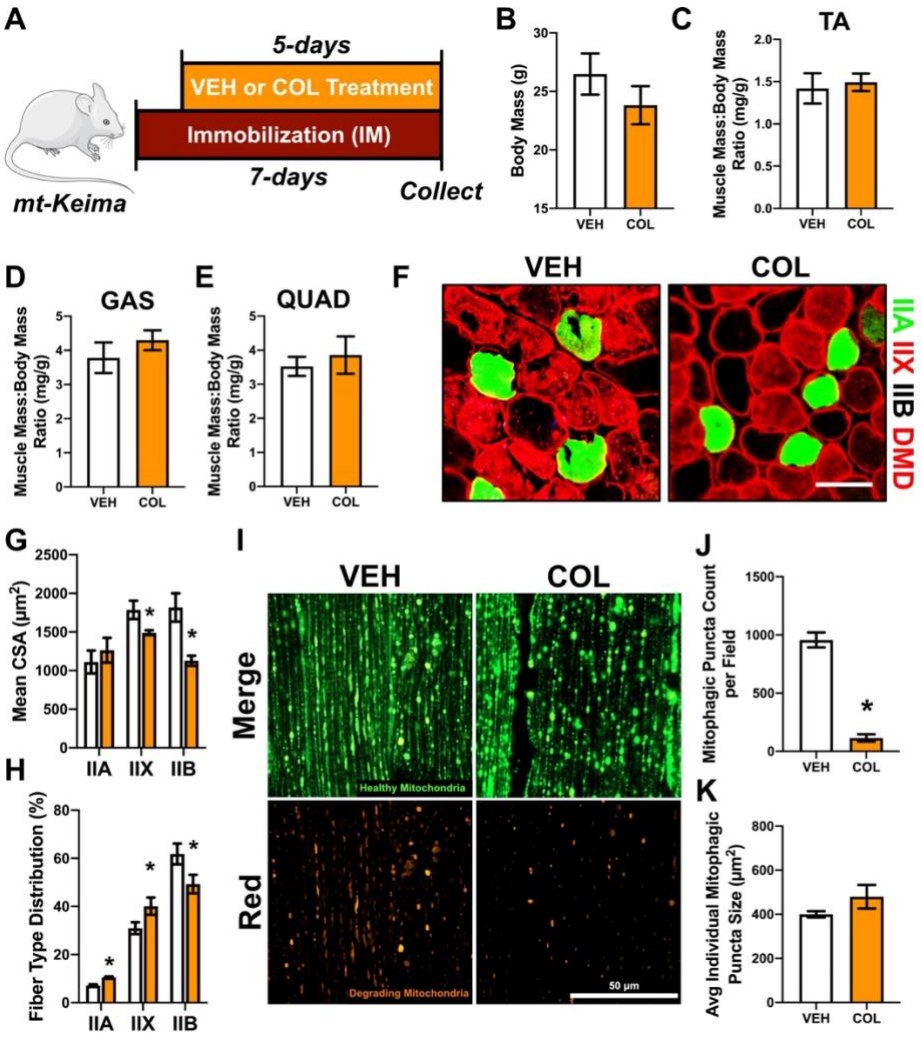


Figure 8: Effect of colchicine (COL) treatment on immobilized muscles. A) Representative visualization of immobilization and COL treatment protocol. B) Body mass of vehicle (VEH) and COL treated animals. Normalized skeletal muscle mass measurements of C) tibialis anterior (TA), D) gastrocnemius (GAS), and E) quadriceps (QUAD). F) Representative immunofluorescent images of TA muscles from VEH and NAC treated immobilized animals. Samples were stained with antibodies specific for individual myosin heavy chain isoforms: type IIA (green), type IIX (red), type IIB (unstained), and dystrophin (DMD, red). Scale bars indicate 50 μm. G-H) Quantification of mean cross-sectional area (CSA) and distribution of type IIA, IIX, and IIB myofibers. I) Representative confocal images of mitophagic flux from TA muscles of immobilized mt-Keima reporter mice treated with VEH or NAC. Green fluorescence indicates healthy mitochondria. Red fluorescence indicates degrading mitochondria. Scale bar indicates 50 μm. J) Quantification of mitophagic (i.e., red) puncta count per field. K) Quantification of average individual mitophagic puncta size. * $p < 0.05$ compared to VEH group. n = 4-8 per group.

COL treatment in IM animals resulted in significant mitochondrial dysfunction, as evidenced by decreased maximal respiration (-45%; $p < 0.05$), mH_2O_2 emission (-53%; $p < 0.05$), electron leak (-31%; $p < 0.05$), and impaired OXPHOS coupling efficiency (-30%; $p < 0.05$; Figure

9B-F). Immunoblot analyses further supported these findings, showing an accumulation of the autophagy marker SQSTM1 (+170%; $p < 0.05$; Figure 9G), LC3B-I (+87%; $p < 0.05$), LC3B-II (+63%; $p < 0.05$), and lipid peroxidation marker 4HNE (+100%; $p < 0.05$; Figure 9H-K). Despite these changes, no alterations were observed in mitochondrial-associated LC3B-II, BNIP3, or apoptotic regulators BAX and BCL2 at the mitochondrial level (Figure 9L-O). However, we observed a notable increase in CASP9 (+19%; $p < 0.05$) and CASP3 activities (+21%; $p < 0.05$) in COL treated animals, indicating enhanced mitochondrial-mediated CASP-signaling (Figure 9P-Q). Interestingly, there were no changes in CAPN activity or in the 20S proteasome activity (Figure 9R-S).

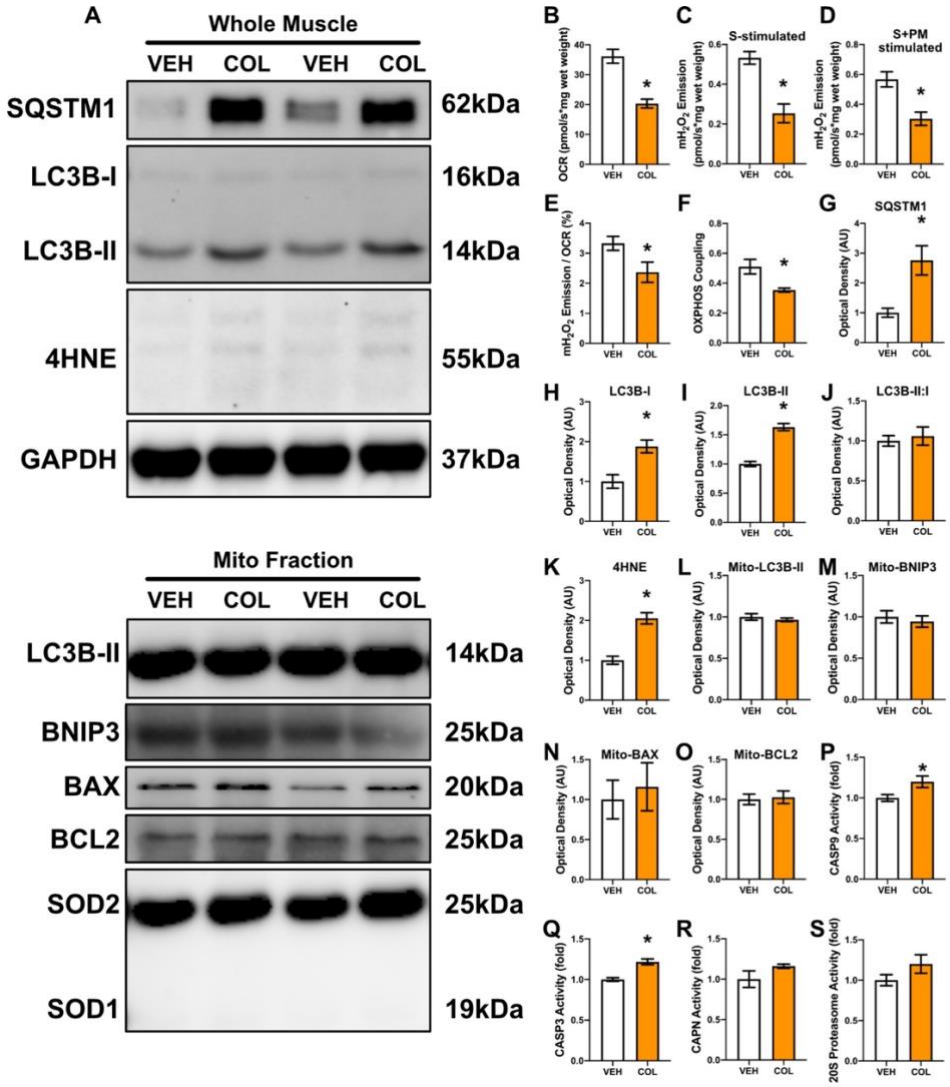


Figure 9: Quantitative analysis of autophagy and mitophagy proteins in VEH and COL treated immobilized muscles. A) Representative immunoblots of whole muscle lysate and mitochondrial fractions derived from GAS. B) Quantification of maximal oxygen consumption rate (i.e., respiration) of permeabilized bundles from TA muscles. Simultaneous quantification of C) succinate-stimulated hydrogen peroxide (H_2O_2) production, and D) succinate + pyruvate/malate-stimulated H_2O_2 production in permeabilized TA muscle bundles. E) Quantification of mitochondrial fraction of electron leak. F) Quantification of oxidative phosphorylation (OXPHOS) coupling. Quantitative analysis of G) SQSTM1, H) LC3B-I, I) LC3B-II, J) LC3B-II:I, and K) 4HNE from whole muscle lysate. Quantitative analysis of L) LC3B-II, M) BNIP3, N) BAX, and O) BCL2 from mitochondrial-enriched fractions. Quantitative analysis of P) CASP9 activity, Q) CASP3 activity, R) CAPN activity, and S) 20S proteasome activity. * $p < 0.05$ compared to VEH group. n = 6-8 per group.

Moreover, COL treatment led to elevated levels of mitochondrial biogenesis and other mitochondrial markers, including total PPARGC1A, TFAM, DNM1L, CYCS, ANT, and SOD1 (Figure 10A-B,H,J-L). This suggests a compensatory response, potentially due to reduced

degradation of these proteins. Conversely, the mitochondrial fusion proteins OPA1 and MFN2 were suppressed in IM muscles treated with COL (Figure 10F-G). Taken together, these findings indicate that COL-induced inhibition of autophagy exacerbates mitochondrial dysfunction and oxidative stress, contributing to increased mitochondrial CASP signaling without impacting proteasomal degradation pathways.

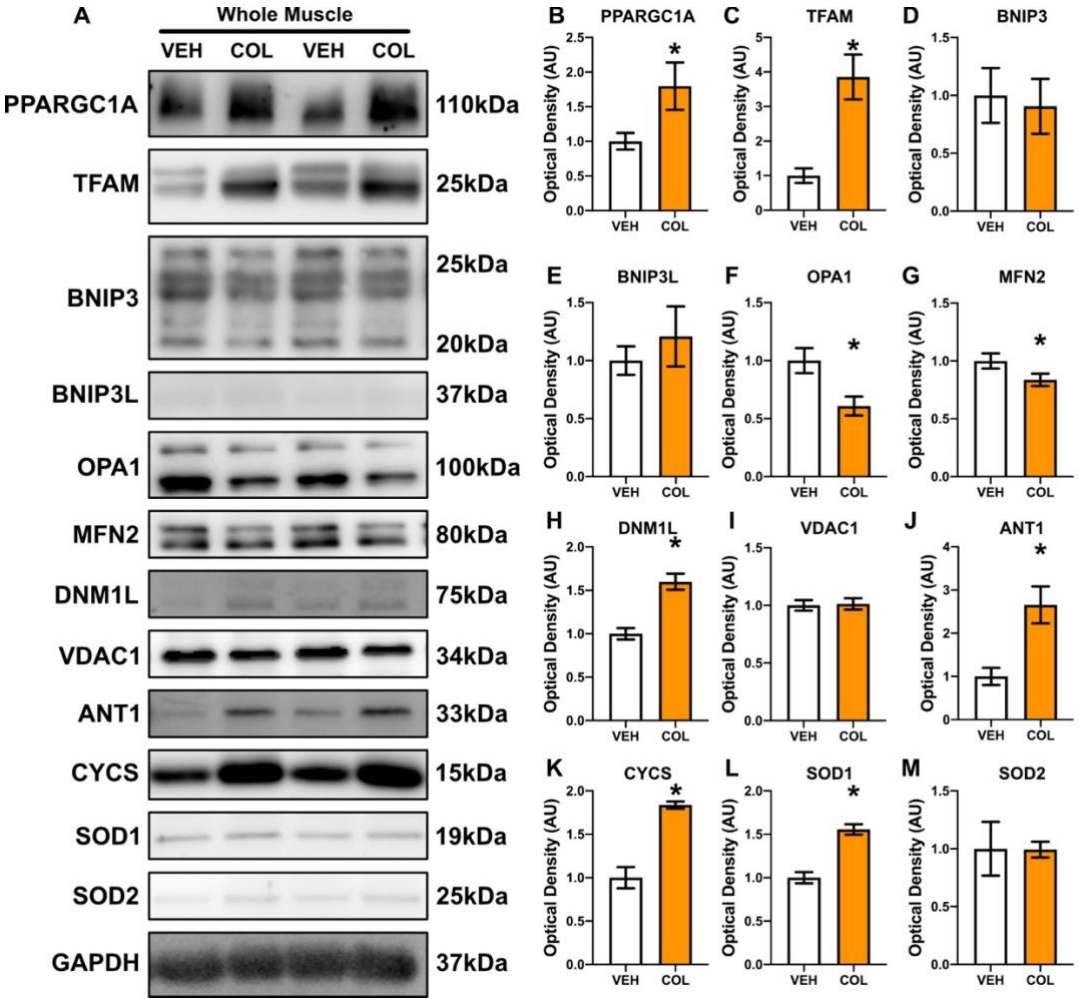


Figure 10: Quantitative analysis of mitochondrial remodeling proteins in VEH and COL treated immobilized muscles. A) Representative immunoblots of whole muscle lysate derived from GAS and QUAD. Quantitative analysis of B) PPARGC1A, C) TFAM, D) BNIP3, E) BNIP3L, F) OPA1, G) MFN2, H) DNM1L, I) VDAC1, J) ANT1, K) CYCS, L) SOD1, M) SOD2. * $p < 0.05$ compared to VEH group. n = 6 per group.

Discussion

Skeletal muscle disuse atrophy is characterized by a significant loss of muscle mass and strength. The pathophysiology of disuse atrophy involves complex molecular mechanisms, predominantly characterized by a decrease in muscle protein synthesis and an increase in protein degradation (Mirzoev, 2020; Sandri, 2013; Sartori et al., 2021). These changes are also associated with alterations in mitochondrial mass and function (Hyatt & Powers, 2021; Muller et al., 2007; Petrick et al., 2023; Triolo et al., 2022; Yajid et al., 1998). Recent research has implicated mitochondrial remodeling, particularly mitophagy, in disuse atrophy (Triolo et al., 2022; F. Wang et al., 2023; Yamashita et al., 2021), though the exact mechanisms and role of mitophagy in the atrophy process remain unclear. In the present study, we found that: 1) immobilization-induced atrophy is accompanied by mitochondrial localization of BNIP3 and enhanced mitophagic flux, 2) antioxidant treatment of immobilized animals partially reduced mitophagy and caused greater atrophy, and 3) inhibition of the autophagic machinery and mitophagic flux negatively impacts mitochondrial function leading to exacerbated myofiber atrophy.

Impact of hindlimb immobilization on mitochondrial remodeling

Immobilization-induced muscle atrophy results in significant structural remodeling, characterized by the extensive degradation of contractile filaments and other cellular components (Pellegrino et al., 2011; Plotkin et al., 2024). This structural remodeling is primarily attributed to a molecular shift from growth-promoting to degradation-signaling pathways (Pellegrino et al., 2011). Key molecular pathways such as PI3K-AKT-MTORC1 are involved in this process, regulating transcription factors like FOXO3A, and subsequently influencing the expression of proteolytic genes such as tripartite motif containing 63 (*Trim63)* and F-box protein 32 (*Fbxo32)*

(Atherton et al., 2016; K.-H. Lin et al., 2021; Stitt et al., 2004; Wu et al., 2023). To make matters worse, activation of other degradative pathways like apoptosis also occurs during disuse atrophy. In fact, proteomic analyses have highlighted significant mitochondrial remodeling in IM human vastus lateralis muscles, showing downregulation of genes related to mitochondrial organization and metabolism, and upregulation of genes linked to apoptosis and ubiquitination (Deane et al., 2021). These findings corroborate our RNA sequencing results, which demonstrate an increase in differentially expressed genes (DEGs) associated with cellular stress responses (i.e., UPS and apoptosis), and a decrease in DEGs linked to muscle contraction, mitochondrial function, and metabolism. Gene ontology analyses further support these findings, indicating an upregulation of genes related to UPS and apoptotic signaling, and a downregulation of genes involved in myofiber organization and mitochondrial function. The consistency of our RNA sequencing results with findings from human studies (Deane et al., 2021) emphasizes the relevance of our research to understanding human muscle atrophy. By paralleling human data, our work confirms the universal nature of the molecular mechanisms driving muscle atrophy across different species while also enhancing the applicability of our models.

Our RNA sequencing results are bolstered by *in vivo* experiments that illustrate progressive muscle loss in IM animals, with partial recovery following RM. Notably, 7-days of IM led to considerable muscle loss and weakness, coupled with increased mitophagic flux, which corroborate prior findings (Yamashita et al., 2021). The observed increases in mitophagy flux from the present study align with those seen in other types of disuse atrophy, such as denervation. For instance, denervation-induced disuse atrophy is reported to enhance mitophagic flux within just 24 hours (Triolo et al., 2022). Comparatively, denervation induces atrophy and mitophagic flux more rapidly than IM (Triolo et al., 2022; Xu et al., 2022). Additionally, our findings suggest a

fiber type specific response to immobilization-induced atrophy; specifically, types IIX and IIB fibers undergo significant atrophy and do not fully recover following RM. In contrast, type IIA fibers seem to regain their original size upon remobilization, potentially due to differences in phenotypic parameters like recruitment patterns or their inherently greater oxidative capacity (Bloemberg & Quadrilatero, 2012; Rahman et al., 2024). For example, our previous work found that oxidative muscles exhibit lower autophagic flux (Paré et al., 2017), potentially moderating the extent of remodeling in response to atrophic stimuli like IM. Overall, the current data confirm a consistent association between muscle atrophy and mitophagic flux in both IM and subsequent RM phases.

We observed mitochondrial dysfunction characterized by reduced maximal respiration, increased mitochondrial ROS emission, and a higher fraction of electron leak, which aligns with elevated lipid peroxidation. These dysfunctions correlate with findings from other studies utilizing disuse atrophy models that also report impaired mitochondrial function, including lower OCR and greater ROS emission (Hyatt & Powers, 2021; Muller et al., 2007; Petrick et al., 2023; Triolo et al., 2022; Yajid et al., 1998). The elevated mitophagic flux observed may be a compensatory response activated by mitochondrial dysfunction, aiming to mitigate further damage to the myofibers. Although changes in autophagy recognition or cargo molecules were not pronounced in whole muscle lysates or mitochondrial-enriched fractions, the previously discussed increased flux indicates active mitochondrial degradation. Notably, we detected significant mitochondrial localization of BNIP3 in IM animals, persisting even after 7-days of remobilization, which is consistent with previous work (F. Wang et al., 2023). Previous studies have also identified upregulation of mitophagy-related molecules such as PINK1 and PRKN and their transcripts (Deval et al., 2020; C. Kang et al., 2016; Yamashita et al., 2021), but this is the first observation

of BNIP3 in the mitochondrial fraction. BNIP3 may influence several mitochondrial parameters, including bioenergetics, mitophagic flux, and apoptosis (Chakraborti et al., 2002; Choi et al., 2016; Rikka et al., 2011). As we explored other BH3-containing molecules, we observed increased BAX:BCL2 ratio in mitochondrial fractions from remobilized muscles, suggesting MOMP opening during this phase. Moreover, elevated activities of CASP9 and CASP3 in both IM and RM muscles underscore the role of mitochondrial apoptotic signaling in the observed muscle atrophy and dysfunction.

Enhancements in degradative pathways are associated with significant changes in molecular signaling, which also govern mitochondrial biogenesis and dynamics. Previous studies have reported a suppression of PPARGC1A, the master regulator of mitochondrial biogenesis, in IM muscles (Cannavino et al., 2015; C. Kang et al., 2016; Sandri et al., 2006). Consistent with these findings, our results demonstrate a reduction in PPARGC1A, indicating diminished mitochondrial biogenesis signaling. This reduction likely stems from the decreased energy demands of IM muscles, which diminish the requirement for new mitochondria formation. Intriguingly, PPARGC1A OE has been shown to mitigate muscle atrophy associated with disuse conditions such as IM and denervation (Cannavino et al., 2015; C. Kang et al., 2016; Sandri et al., 2006). Furthermore, changes in mitochondrial dynamics have been observed, with some studies noting an increase in DNM1L, indicative of mitochondrial fission or fragmentation following disuse (Cannavino et al., 2014; Romanello et al., 2010; Romanello & Sandri, 2010), although this was not universally observed (Petrick et al., 2023; Xu et al., 2022). While our data did not reveal alterations in DNM1L expression in IM muscle, we noted a decrease in OPA1 and MFN2 levels following IM, suggesting a potential shift towards mitochondrial fragmentation. It is possible that DNM1L levels change soon after the onset of disuse, as increased DNM1L levels has been detected

as early as three days following IM, along with reduced *Opa1* and *Mfn1/2* transcripts (Cannavino et al., 2014, 2015). The increased mitophagic flux in response to IM suggests that a shift in mitochondrial dynamics towards fission might occur early in the process to facilitate efficient mitochondrial degradation.

NAC treatment suppresses mitophagy flux and worsens immobilization-induced muscle atrophy

It is noteworthy that mitophagic flux increases in parallel with muscle atrophy during IM. Accompanying this increase, we observed enhanced mitochondrial dysfunction, as evidenced by elevated mitochondrial ROS emission and increased lipid peroxidation. Given the established role of ROS in promoting muscle atrophy, we explored the potential benefits of modulating ROS signaling during IM to preserve muscle mass and mitochondrial function. However, our experiments using NAC did not demonstrate any preservation of muscle mass, aligning with previous findings that show limited efficacy of some antioxidant treatment in maintaining muscle mass (Farid et al., 2005; Petrick et al., 2023). In contrast to these findings, other research groups employing more potent antioxidants, such as vitamin E and mitochondrial-targeted antioxidants, have reported partial or complete preservation of muscle mass (Appell et al., 1997; Demiryürek & Babül, 2004; Kondo et al., 1992; Servais et al., 2007). Interestingly, our data revealed selective atrophy in type IIX and IIB myofibers following NAC treatment, which was associated with reduced mitophagic flux. To our knowledge, this is the first report of specific atrophy in type IIX and IIB fibers in IM muscles. In the mouse TA muscles, type IIX fibers constitute approximately 30% and type IIB fibers about 60% of the total fibers. A 24% to 40% reduction in CSA of these fibers highlights the significant muscle atrophy resulting from NAC treatment. Evaluating changes in CSA provides a more accurate measure of muscle atrophy compared to muscle mass, which can

be influenced by fluid accumulation. The observed reduction in CSA of these fibers, coupled with decreased mitophagic flux suggests an interaction between mitophagic flux and myofiber size regulation. Exploring the use of a more potent antioxidant could be intriguing, particularly to assess whether it not only preserves muscle mass but also modulates mitophagic flux.

Further investigation into the effects of NAC treatment in IM muscle on mitochondrial function has demonstrated improvements in maximal respiration and reductions in mitochondrial ROS emission. Although mitochondrial function improved, there were no significant changes in the markers of autophagy, including the mitochondrial localization of LC3B-II and BNIP3 in IM muscles. This is similar to a previous study that found NAC treatment was insufficient to alter fasting-induced lipidation of LC3 (Qi et al., 2014). This would suggest that while NAC can enhance mitochondrial respiratory capacity and reduce oxidative stress, it does not significantly impact the autophagic processes involved in mitochondrial quality control in the context of muscle IM. Nonetheless, our observations indicate that while NAC limits mitophagic flux, it does not affect the localization of autophagic and mitophagic proteins at the mitochondria. It is possible that alterations in the redox state induced by NAC might interfere with the molecular interactions necessary for cargo recognition at the mitochondrial level or could potentially impair the autophagy machinery through other mechanisms. However, when examining the total content of proteins involved in mitochondrial remodeling, we observed no significant changes in mitochondrial biogenesis, dynamics, or general mitochondrial-related proteins. These findings indicate that ROS signaling is essential for mitophagy, acting to prevent excessive muscle atrophy. Conversely, reducing ROS signaling through NAC treatment suppresses mitophagic flux and exacerbates muscle atrophy in IM muscles.

COL treatment disrupts mitochondrial proteostasis, activates degradative pathways, and contributes to greater atrophy of immobilized muscles

Our data reveal that muscle atrophy coincides with increased mitophagy. Although treatment with NAC seems to moderately suppress this mitophagic activity and enhance mitochondrial function, it does not prevent the reduction in muscle mass. Intrigued by these findings, we investigated the effects of autophagy/mitophagy inhibition through multiple injections of colchicine. Colchicine treatment substantially reduced mitophagic flux but did not significantly alter overall muscle mass. However, we noted a consistent decrease in the CSA of type IIX and IIB fibers and observed a shift in fiber type distribution towards a slower contracting phenotype. Specifically, we observed a greater number of type IIA and IIX fibers and a loss of type IIB fibers. It is important to note that the selective loss of type IIB fibers, accompanied by a 40% reduction in their CSA, clearly indicates significant muscle atrophy in colchicine treated animals following IM. Previous research has demonstrated that autophagy-deficiency exacerbate muscle loss in models of denervation, intensifying atrophic signaling due to disrupted proteostasis and the accumulation of protein aggregates such as SQSTM1 and ubiquitin (Masiero et al., 2009). Although the mechanisms of muscle loss in denervation and immobilization-induced atrophy are similar, denervation typically results in a more profound loss of muscle mass (Masiero et al., 2009; Triolo et al., 2022; Xu et al., 2022). While earlier studies have shown significant atrophy in autophagy-deficient muscles, our results differ. We observe selective atrophy primarily in fast glycolytic myofibers. Considering we previous found that fast/glycolytic muscles are particularly vulnerable to autophagy-deficiency (Paré et al., 2017), we propose that the reduction in IIX and IIB fiber CSA and the shift in fiber type distribution represent adaptive responses to compromised proteostasis in these fibers.

Colchicine treatment during the immobilization phase markedly impaired mitochondrial function, as evidenced by a decrease in maximal respiration, increased mitochondrial ROS emission, and reduced coupling efficiency. Furthermore, colchicine administration in IM muscles led to enhanced lipid peroxidation. This finding aligns with previous work (Buch et al., 2020) that reported compromised mitochondrial function characterized by diminished maximal respiration and elevated ROS production following two days of colchicine treatment. Interestingly, our experiments demonstrated a reduction in ROS generation, which may be linked to mitochondrial membrane damage. This association is supported by the observed decline in all measured mitochondrial functional parameters, indicating compromised mitochondrial integrity. This damage, likely resulting from the accumulation of cellular debris and augmented stress signaling due to immobilization, might interfere with normal mitochondrial ROS production mechanisms.

Additionally, our analysis revealed an accumulation of SQSTM1, LC3B-I, and LC3B-II with colchicine treatment in whole muscle lysates, yet no discernible changes were observed in the mitochondrial localization of proteins associated with autophagy or mitophagy. Moreover, studies have consistently reported an accumulation of autophagy-related molecules like LC3B-II in whole muscle lysates and mitochondrial fractions of animals treated with colchicine for 1-2 days (Carter et al., 2018; Y. Kim, Triolo, et al., 2019; Paré et al., 2017; Triolo et al., 2022; Vainshtein et al., 2015). We hypothesize that prolonged inhibition (i.e., 5-days) of microtubule polymerization might also reduce the efficiency of targeting mitochondria. In other words, although mitochondria continue to be tagged by mitophagy-related proteins like BNIP3, they are not efficiently targeted by autophagosomes, resulting in inadequate removal. Previous research has demonstrated that BNIP3 is induced in autophagy-deficient models, suggesting its role in activating CASP and initiating mitochondrial apoptotic signaling (Masiero et al., 2009). While no changes were detected

in the mitochondrial localization of apoptotic molecules in colchicine-treated animals, we observed elevated CASP9 and CASP3 activities, indicating the activation of alternative stress responses in an autophagy-deficient state. This phenomenon has been previously documented *in vitro* by our group (Baechler et al., 2019; McMillan & Quadrilatero, 2014).

Following colchicine treatment in IM muscles, we observed significant changes indicative of altered mitochondrial dynamics. Notably, there was an accumulation of PPARGC1A and TFAM, suggesting an enhancement of mitochondrial biogenesis signaling. Additionally, we detected increased levels of DNM1L along with decreased levels of OPA1 and MFN2, suggesting a shift toward increased mitochondrial fission. These findings partially corroborate previous research that reported elevated DNM1L protein levels after 2-days of colchicine treatment (Ju et al., 2016). While our confocal microscopy analysis did not reveal any major changes in mitochondrial morphology, it is possible that higher resolution imaging techniques might uncover subtle alterations. Furthermore, although no significant changes were observed in the levels of the mitophagy receptors BNIP3 and BNIP3L, there were elevations in IMM molecules ANT1 and CYCS. Collectively, these results suggest that colchicine treatment may significantly influence mitochondrial biogenesis and dynamics in IM muscle tissues.

Mitophagy protects against immobilization-induced muscle atrophy

Mitophagy plays an essential role in mitigating the deleterious effects of mitochondrial damage. Damaged mitochondria often exhibit reduced ATP production and elevated ROS emission, leading to cellular dysfunction (Van Houten et al., 2006). By clearing damaged mitochondria, mitophagy helps maintain cellular homeostasis and prevents oxidative stress, which can trigger cell death. This is particularly vital in post-mitotic cells, such as skeletal muscle

cells/fibers that accumulate cellular damage over time. The significance of mitophagy extends to various muscle-specific conditions, including denervation, spinal cord injuries, muscular dystrophies, and the aging process (Rahman & Quadrilatero, 2021a, 2021b). In the case of disuse atrophy, increased autophagy and mitophagy signaling along with heightened mitophagic flux have been reported (Triolo et al., 2022; Vainshtein et al., 2015; F. Wang et al., 2023; Yamashita et al., 2021). The current study investigated whether mitophagy acts as a protective mechanism against muscle atrophy or contributes to greater atrophy by reducing the overall mitochondrial pool. Our findings reveal that direct inhibition of autophagy using colchicine, or indirect suppression of mitophagy with NAC, both resulted in significant atrophy in glycolytic fibers, specifically type IIX and IIB. Moreover, despite their differing impacts on mitochondrial function, with NAC enhancing mitochondrial function and colchicine impairing mitochondrial function, the end result was a similar degree of muscle atrophy. This observation likely relates to the observed reduction in mitophagic flux, suggesting that maintaining mitophagic activity is crucial for preserving muscle integrity, regardless of the initial mitochondrial condition. Interestingly, enhancing mitophagic flux with treatments like urolithin A in rodents has been shown to improve muscle function, as evidenced by increased grip strength, maximal running distance, upregulated mitophagy-related genes (i.e., *Bnip3*, *Pink1*, *Prkn*, *Becn1*), and increased CSA in *mdx* mouse muscle (Luan et al., 2021; Ryu et al., 2016). Randomized clinical trials in humans supplementing urolithin A have found elevated markers of mitochondrial function, PRKN levels, and overall muscle performance (Andreux et al., 2019; Faitg et al., 2024; S. Liu et al., 2022; Singh et al., 2022). Nonetheless, accumulating data suggests that promoting mitophagy could potentially counteract muscle atrophy in IM conditions, highlighting the need for further research. Overall,

our findings provide conclusive evidence of the necessity of mitophagy in limiting atrophy in IM muscle.

Conclusion

In conclusion, the present study reveals key insights into the molecular and physiological adaptations associated with immobilization-induced skeletal muscle atrophy. We found that mitochondrial dysfunction and increased mitophagic activity are associated with muscle atrophy, highlighting a complex interplay between mitochondrial damage and the autophagic removal of dysfunctional mitochondria. Our results demonstrate that mitophagy acts as a protective mechanism against excessive atrophy in immobilized muscles. Inhibiting mitophagic flux, either through antioxidant treatment or by blocking autophagic processes, exacerbates muscle atrophy. These findings emphasize the importance of balanced mitochondrial quality control and overall mitochondrial remodeling in maintaining muscle function during periods of disuse. Future studies may wish to target nuanced aspects of mitochondrial remodeling to try and enhance the coordination between these processes during disuse atrophy. This could involve developing targeted therapies that modulate these processes without impairing overall cellular function, potentially leading to more effective strategies against immobilization-induced muscle atrophy.

Chapter 5: Summary and Conclusion

Perspective

This thesis investigated the crucial role of mitochondrial remodeling during skeletal muscle formation, postnatal muscle development, and atrophy. These stages reflect the various phases our muscles undergo throughout life. We utilized diverse experimental models, including cell and animal models, to explore complex biological processes such as autophagy, mitophagy, mitochondrial dynamics, biogenesis, and apoptosis. These processes are integral to muscle physiology but are poorly understood in the aforementioned stages. In a cell model of muscle formation (i.e., myogenesis), we manipulated the genetic expression of key molecules involved in mitochondrial dynamics, mitophagy, and biogenesis. This approach is particularly valuable for studying muscle formation that occurs *in utero*, where direct observation and manipulation are challenging. Additionally, we utilized a unique reporter model containing a mitochondria-targeted fluorescent molecule (mt-Keima) that changes fluorescence based on the pH of its environment. This model enabled us to address fundamental yet unexplored questions regarding the role of mitophagy during postnatal development and immobilization-induced atrophy. We employed several different methodologies, including the investigation of overall signaling and mitochondrial targeting, to better understand how these processes interact in the context of postnatal development and atrophy. Furthermore, we conducted experiments where different compounds were administered to animals to alter specific pathways like ROS and autophagy signaling. These experiments provided further insights into mitochondrial remodeling in muscle physiology.

Chapter 2 Summary

The major aims and hypotheses of Chapter 2 were:

1. To determine the regulatory role of mitochondrial fission on mitophagy and biogenesis during myogenesis. I hypothesized that upregulation of mitochondrial fission would accelerate mitophagy, subsequently signaling the activation of mitochondrial biogenesis to enhance differentiation, while suppression of mitochondrial fission would reduce mitophagy and biogenesis, leading to impaired myogenic differentiation.
2. To determine if the overexpression of mitophagy or biogenesis markers were sufficient in rescuing defects in myogenesis that were accompanied by a lack of mitochondrial fission. I hypothesized that the overexpression of mitophagy receptor BNIP3 would fail to differentiate cells in a fission-deficient state, while overexpression of biogenesis protein PPARGC1A would partially restore myogenic differentiation in fission-deficient cells by enhancing mitochondrial content and function.
3. To determine if the overexpression of mitochondrial fission proteins DNM1L signals mitochondrial biogenesis independent of BNIP3-mediated mitophagy. I hypothesized that the overexpression of DNM1L would fail to signal mitochondrial biogenesis in BNIP3-deficient cells, leading to failed myogenic differentiation.

Major Findings:

1. Overexpression of DNM1L increased mitochondrial network fragmentation and enhanced mitophagic flux during myogenic differentiation of C2C12 cells. DNM1L OE did not adversely affect the process of myogenesis but resulted in smaller myotubes. Despite these changes, DNM1L OE did not alter levels of proteins involved in mitochondrial turnover such as PPARGC1A, BNIP3, BNIP3L, and PINK1.
2. Knockdown of DNM1L limited mitochondrial network fragmentation and subsequent mitophagic flux during myogenic differentiation of C2C12 cells. DNM1L knockdown significantly impeded myogenesis and was associated with elevated mitochondrial apoptotic signaling, evidenced by increased activities of CASP9 and CASP3. Furthermore, DNM1L knockdown diminished mitochondrial biogenesis and mitophagy signaling, as indicated by reduced levels of PPARGC1A, BNIP3, and PINK1.
3. Overexpression of BNIP3 promoted mitophagy flux in fission-deficient cells (i.e., DNM1L KD). While BNIP3 OE reduced mitochondrial apoptotic signaling (CASP9 and CASP3 activities), it did not impact myogenesis in fission-deficient cells. Notably, BNIP3 OE suppressed PPARGC1A levels without affecting other mitophagy- or mitochondrial-related proteins.
4. Overexpression of PPARGC1A exacerbated myogenic defects in fission-deficient cells, independently of any increase in mitophagy- or mitochondrial-related protein levels.
5. DNM1L OE in *Bnip3*$^{-/-}$ cells increased mitochondrial fragmentation and mitophagic flux. This OE was also associated with reductions in MPTP opening, and activities of CASP9 and CASP3. However, it failed to restore myogenesis or modify mitochondrial remodeling signaling in *Bnip3*$^{-/-}$ cells.

Chapter 3 Summary

The major aims and hypotheses of Chapter 3 were:

1. To characterize mitochondrial remodeling during postnatal development of skeletal muscle. I hypothesized that postnatal development would be accompanied by an initial stage of mitochondrial turnover via mitophagy followed by biogenesis and formation of higher functioning mitochondria in skeletal muscle.
2. To determine the role of autophagy/mitophagy-deficiency on mitochondrial remodeling during postnatal development. I hypothesized that *Atg7*-deficiency would prevent the initiation of mitophagy and biogenesis during postnatal development, leading to incomplete maturation of the mitochondrial network and significant mitochondrial dysfunction.

Major Findings:

1. RNA sequencing analyses revealed that BNIP3 was the only gene differentially expressed and related to mitochondrial remodeling during postnatal development. Postnatal development was characterized by an upregulation of genes associated with metabolism and a downregulation of genes associated with cell growth and differentiation.
2. *In vivo* experiments demonstrated significant increases in body mass, muscle mass, and myofiber CSA, with a notable doubling occurring from P21 to P42.
3. Mitochondria continued to mature during postnatal development as evidenced by increased maximal respiration and reduced electron leak. This was accompanied by elevated mitophagic flux and increased mitochondrial localization of autophagy and mitophagy proteins, including LC3B-II, BNIP3, PINK1, and PRKN.
4. There was a decline in phosphorylated to total AMPK and an increase in phosphorylated to total P70S6K, suggesting divergent changes in signaling pathways with greater signaling of anabolism during postnatal development.
5. Postnatal development of skeletal muscle showed reduced mitochondrial biogenesis signaling (i.e., PARGC1A and TFAM), alongside increased mitophagy signaling (i.e., BNIP3) and a potential shift in mitochondrial morphology towards mitochondrial fusion, indicated by increased OPA1 and reduced DNM1L.
6. Skeletal muscle-specific *Atg7* knockout (skmKO) mice exhibited no changes in body mass, muscle mass or mitochondrial function compared to controls; however, they displayed compensatory hypertrophy of type IIX fibers. In these mice, mitophagic flux was ablated, but this did not correspond with alterations in mitochondrial function.
7. We observed a compensatory activation of enzymes corresponding to alternative degradative pathways including CASP9, CASP3, CAPN, and 20S Proteasome.
8. There were observed reductions in phosphorylated to total FOXO3A and an elevation in phosphorylated to total P70S6K in skmKO mice compared to controls.
9. Consistent reductions in proteins related to mitophagy (i.e., BNIP3, BNIP3L, PINK1), mitochondrial fusion (i.e., OPA1, MFN2), and other mitochondrial-associated proteins (i.e., VDAC1, ANT1) were observed in skmKO mice compared to controls.

Chapter 4 Summary

The major aims and hypotheses of Chapter 4 were:

1. To understand how mitochondrial remodeling processes change in response to hindlimb immobilization and remobilization. I hypothesized that hindlimb immobilization would induce significant mitochondrial defects necessitating mitochondrial fission and mitophagy, while simultaneously suppressing biogenesis. Additionally, I hypothesized that these mitochondrial defects would reverse following hindlimb remobilization.
2. To understand how inhibition of ROS signaling or inhibition of the autophagy machinery affects atrophy. I hypothesized that antioxidant treatment with NAC would partially preserve mitochondrial function, resulting in partial preservation of muscle mass following hindlimb immobilization. Additionally, I hypothesized that complete inhibition of the autophagy machinery with COL would exacerbate mitochondrial defects and result in greater muscle atrophy following hindlimb immobilization.

Major Findings:

1. Hindlimb immobilization led to an upregulation of genes associated with protein degradation, specifically those linked to UPS and apoptosis, alongside a downregulation of genes involved in muscle development and mitochondrial components.
2. Immobilization induced atrophy across large musculature of the hindlimb, which was partially reversed upon remobilization. Notably, type IIA fibers recovered following remobilization, whereas type IIX and IIB fibers did not.
3. There was an increase in mitophagic flux following immobilization that remained elevated even after remobilization. Concurrently, there was a reduction in mitochondrial function, evidenced by decreased maximal respiration and increased ROS emission. The mitochondrial localization of the mitophagy receptor BNIP3 was also noted during immobilization and remobilization phases.
4. Immobilization was associated with enhanced mitochondrial apoptotic signaling, specifically through the activities of CASP9 and CASP3. Additionally, there was increased mitophagy signaling coupled with suppressed mitochondrial biogenesis signaling.
5. During the immobilization phase, NAC treatment resulted in greater atrophy of type IIX and IIB fibers. However, it suppressed mitophagic flux, enhanced mitochondrial function, and reduced ROS emission without significantly modifying mitochondrial remodeling markers or the localization of autophagy/mitophagy-related molecules.
6. COL treatment during immobilization caused atrophy of type IIX and IIB fibers. COL inhibited mitophagic flux and did not alter mitochondrial tagging with mitophagy or apoptosis molecules. Following immobilization and COL treatment, we observed mitochondrial apoptotic signaling and the accumulation of several biogenesis and mitochondria-related molecules.

Broad Summary

Over the past three decades, the study of cellular remodeling has emerged as a major area of interest within the scientific community, reflecting its fundamental role in modulating cellular structure and function in response to diverse stimuli. Cellular remodeling induces profound changes in morphology and function, pivotal for regulating cell fate through a balance of growth and degradative signals (Bloemberg & Quadrilatero, 2019; Y. Kim, Yang, et al., 2019; Rahman & Quadrilatero, 2021b). A major component of this remodeling is mitochondrial remodeling through mechanisms like fission, fusion, mitophagy and biogenesis, which are especially relevant in post-mitotic tissues such as skeletal muscle. Skeletal muscle mitochondria undergo extensive remodeling across various physiological and pathological states (Rahman & Quadrilatero, 2021b, 2021a, 2022). The controlled remodeling of the mitochondrial network is crucial for regulating processes like myogenesis, postnatal muscle growth, and muscle atrophy.

The function of mitochondrial remodeling varies across different physiological states. This thesis explored the role of mitochondrial remodeling processes in skeletal muscle throughout the lifespan. During embryonic development, skeletal muscle arises from unspecialized stem cells that activate, proliferate, differentiate, and fuse to form nascent myofibers (Dumont, Wang, et al., 2015; Hawke & Garry, 2001). This energetically demanding process involves a transition from a state of low mitochondrial function to one characterized by enhanced respiration and OXPHOS capacity (Barbieri et al., 2011; Robinson et al., 2019; Sin et al., 2016; Vertel & Fischman, 1977). This renewal process necessitates the remodeling and enrichment of the mitochondrial pool through mitophagy, which depends on mitochondrial fission. We demonstrated this using a genetic knockdown of the fission protein DNM1L. Our findings indicated that downstream processes such as mitophagy and mitochondrial biogenesis can occur independent of mitochondrial fission;

however, this is insufficient for myogenesis. Additionally, we found that BNIP3 is required for myogenic differentiation and its function may extend beyond its role in mitophagy. Thus, the sequential process of mitochondrial fission, mitophagy, and biogenesis was essential for renewing mitochondria in myoblasts, facilitating myotube formation. In this context, mitophagy was proposed as a mechanism for the removal of immature mitochondria.

During postnatal muscle growth, there was an observed increase in mitophagic flux alongside a reduction in mitochondrial biogenesis signaling as development progresses from neonatal to late-adolescent stages. While this may seem contradictory to earlier studies that suggested a shift towards increased mitochondrial biogenesis signaling and network morphological changes (Y. Kim et al., 2024; Y. Kim, Yang, et al., 2019), the overall enhancement of mitochondrial function implies maturation of the mitochondrial network. Initially, it was hypothesized that increased mitophagy during postnatal development would occur first to facilitate the removal of immature mitochondria and biogenesis would occur later to promote formation of higher functioning mitochondria. To our surprise, the opposite was the case: biogenesis signaling declined while mitophagic flux and signaling increased throughout the developmental process. Interestingly, *Atg7* knockout completely ablated mitophagy flux, without affecting muscle growth or mitochondrial function. The capacity of the mitochondrial network to mature independently of mitophagy may be attributable to intrinsic mitochondrial changes. One such change could be cristae remodeling, which can enhance mitochondrial efficiency without directly involving mitophagy (Cogliati et al., 2013; Gomes et al., 2011; Patten et al., 2014). In addition, the activation of alternative degradative pathways including mitochondrial apoptotic signaling, ER stress signaling, and UPS signaling may assist in the remodeling of the mitochondrial network. The compensatory activation of these alternative degradative pathways have been observed in our lab

and by other groups (Baechler et al., 2019; Cuervo et al., 1995; Marshall et al., 2021; McMillan & Quadrilatero, 2014; Paré et al., 2017; Tannous et al., 2008; X. J. Wang et al., 2013). Nonetheless, the dynamic changes within the mitochondrial network and compensatory activation of alternative degradative pathways may temporarily protect it; however, this protection is likely finite. Over time, the cumulative damage to the mitochondrial network could lead to whole-tissue dysfunction, as noted in previous studies (Masiero et al., 2009; Paré et al., 2017). In the context of postnatal development, it appears that the maturation of the mitochondrial network can occur independently of mitophagy, although the precise mechanisms behind this remain unclear.

In the hindlimb immobilization model, mitochondrial remodeling played a distinct role compared to previous *in vitro* and developmental models. This divergence is attributed to the experiments being conducted on skeletal muscle from mature mice. Immobilization-induced atrophy was accompanied by increased mitophagy and reduced biogenesis signaling. The reduction in mitochondrial biogenesis signaling likely reflected diminished energetic demand, while increased mitophagy protects against further mitochondrial damage. Interestingly, while the mitochondrial defects returned to normal following remobilization, mitophagic flux remained elevated potentially to aid in the removal of dysfunctional mitochondria that accumulated during the immobilization phase. Further investigation with treatments like NAC or COL resulted in atrophy of type IIX and IIB fibers. Atrophy of these fibers correlated with reduced mitophagic flux but not mitochondrial function since NAC enhanced mitochondrial function whereas COL reduced mitochondrial function. It is crucial to acknowledge that ROS have been previously implicated as a signaling mechanism promoting muscle atrophy (Powers et al., 2012). Additionally, previous studies have not conclusively determined whether mitophagy exacerbates or mitigates muscle atrophy (Triolo et al., 2022; Vainshtein et al., 2015; F. Wang et al., 2023; Yamashita et al., 2021).

Our data clearly demonstrate that mitophagy is essential for preventing excessive atrophy, with a reduction in mitophagic activity correlating with increased atrophy in immobilized muscles. This evidence underscores the vital role of mitophagy in preserving glycolytic myofibers from atrophy caused by immobilization.

The nuanced interpretation of data emphasises the importance of context when assessing the roles and impacts of mitochondrial dynamics within various muscle conditions, highlighting how different cellular and tissue conditions can affect the functional outcomes of mitochondrial remodeling.

Mitochondrial Fission Regulates Mitophagy and Biogenesis

Mitochondrial fission is an important preliminary step to mitophagy and plays a vital role in maintaining cellular function by ensuring the efficient removal of damaged or dysfunctional mitochondria. Fission divides the mitochondrial network into smaller fragments, which facilitates the selective recognition and sequestration of these fragments by autophagosomes (Song et al., 2015; Twig & Shirihai, 2011). Essentially, a hyperfused mitochondrial network poses a physical challenge for the autophagy machinery, making it difficult to target and degrade the mitochondria efficiently (Song et al., 2015; Twig & Shirihai, 2011). Conversely, a fragmented mitochondrial network allows for more effective degradation by autophagic processes.

In this thesis, we provide robust evidence that mitochondrial fission precedes mitophagy *in vitro* during myogenesis, aligning with numerous previous studies (Burman et al., 2017; Gomes et al., 2011). The process of mitochondrial fission is primarily accomplished by the protein DNM1L, which localizes to mitochondria by binding to adaptor molecules on the OMM to facilitate fission. Our genetic manipulations of DNM1L expression revealed that its loss significantly reduced mitophagic flux, whereas its overexpression enhanced mitophagic flux during myogenesis. These alterations result in either the complete cessation of myogenic differentiation/fusion or the atrophy of myotubes. Similar effects have been reported by other research groups, where suppression of DNM1L GTPase activity, either through chemical inhibitors or dominant negative mutations of DNM1L, inhibits myotube formation (B. Kim et al., 2013). This inhibition is presumed to be due to the disruption of mitophagy and mitochondrial biogenesis (B. Kim et al., 2013). Intriguingly, our data also indicate that loss of DNM1L depresses levels of other mitochondrial remodeling signaling molecules like BNIP3 and PPARGC1A, supporting the idea that fission regulates mitophagy and biogenesis.

Shifting focus to skeletal muscle tissue, which is distinct from myoblasts, we observe an interesting pattern. DNM1L levels decreased shortly after the weaning of the animals and coincided with increased body and muscle mass. While the reasons for this trend are unclear, it does not rule out the possibility that DNM1L continues to localize at the mitochondrial level to induce some degree of mitochondrial fission. In the context of muscle atrophy, previous reports have indicated increased mitochondrial fission, especially during the early stages of disuse (Cannavino et al., 2014; Romanello et al., 2010; Romanello & Sandri, 2010). Although we did not observe significant changes in DNM1L levels, we found reduced levels of OPA1 and MFN2 following immobilization that was in line with previous mRNA data (Cannavino et al., 2015), suggesting a shift towards greater mitochondrial fission. However, due to the lack of super-resolution imaging, we cannot conclusively confirm this phenomenon. Nevertheless, in the context of immobilization-induced atrophy, the potential shift towards greater mitochondrial fission would coincide with increased mitophagic flux, underscoring the complex interplay between mitochondrial fission and mitophagy in different muscle states.

Temporal Modulation of Mitochondrial Remodeling in Skeletal Muscle

Mitochondrial remodeling encompasses a suite of highly dynamic processes including fission, fusion, mitophagy, and biogenesis. These processes are critical for cellular adaptation and survival. These processes are temporally regulated to meet changing cellular energy and metabolic demands, respond to environmental stresses, and maintain cellular homeostasis. Fission and fusion dynamically modulate mitochondrial morphology and distribution, optimizing function and energy distribution (Song et al., 2015; Twig & Shirihai, 2011). Mitophagy prevents the accumulation of dysfunctional organelles and is integral to cellular quality control (Rahman & Quadrilatero, 2021b, 2021a). Concurrently, mitochondrial biogenesis replenishes the mitochondrial population, sustaining the capacity for energy production (Rahman & Quadrilatero, 2021b, 2021a). The precise temporal coordination of these activities is important for maintaining efficient energy production and supporting cellular function.

This thesis provides evidence to support the idea that mitochondrial remodeling mechanisms likely occur in a specific temporal manner. In studying temporal changes during *in vitro* myogenic differentiation, we observed significant mitochondrial remodeling shortly after differentiation as shown by increased mitochondrial fragmentation and mitophagic flux. Previous research, including work from our lab and others have demonstrated dramatic increases in markers of fission, autophagy, and mitophagy during differentiation, such as DNM1L, ATG7, LC3B, and BNIP3 at the early stages of myogenic differentiation (Baechler et al., 2019; Bloemberg & Quadrilatero, 2016; B. Kim et al., 2013; Sin et al., 2016). Subsequently, these studies reported greater OPA1, TFAM, COX4, mtDNA, and nuclear localization of PPARGC1A at the latter stages of myogenic differentiation (Baechler et al., 2019; Sin et al., 2016). Disruption of any of these remodeling processes negatively impacts the subsequent remodeling process. Unpublished data

from our group also found that premature overactivation of autophagic and mitophagic flux via genetic OE or chemical enhancement significantly inhibits myogenesis. These findings would suggest that a precise magnitude and temporal balance of autophagy and mitophagy is essential for optimal myogenic differentiation. The data presented in this thesis further supports the critical role of each remodeling process during differentiation. For instance, DNM1L KD experiments that show substantial reductions in mitophagic flux, mitophagy signaling, and biogenesis signaling. Moreover, the temporal regulation of mitochondrial remodeling processes is essential for normal differentiation, and genetically altering these processes does not compensate for their regulatory roles.

In the context of growing and atrophying muscle, the temporal role of mitochondrial remodeling processes differs. Previous studies have reported elevated mitophagy and biogenesis-related proteins during postnatal development (Y. Kim, Yang, et al., 2019); however, our findings partially diverge. We observed increased mitophagic flux accompanied by reduced mitochondrial biogenesis signaling during postnatal development. While the reasons for this are unclear, enhanced mitochondrial function is evident as muscle matures in young animals. The observed reduction in DNM1L levels during muscle development may suggest a temporal aspect in the maturation of the mitochondrial network into a more complex structure as previously shown by FIB-SEM imaging (Y. Kim et al., 2024). During immobilization-induced atrophy in mature muscle, we noted distinct elevation in mitophagic flux, reductions in mitochondrial biogenesis signaling, and a shift towards mitochondrial fission. Some studies have suggested DNM1L-mediated mitochondrial fission occurs shortly following disuse as a preceding step for mitophagy and as an adaptive response to reduced energy demand; however, there is no general consensus (Cannavino et al., 2015; Petrick et al., 2023; Romanello et al., 2010; Romanello & Sandri, 2010;

Xu et al., 2022). Our investigation was limited to a single time point which may have missed earlier fission events (i.e., < 7-days). Nonetheless, we observed a recovery in PPARGC1A, MFN2, and PRKN levels, indicating normalization of select mitochondrial remodeling molecules during the remobilization phase.

Apparent Elevation of Mitophagy in Muscle Growth and Atrophy

Mitophagy plays a critical role in cellular function by eliminating damaged or redundant mitochondria, thus preventing negative downstream consequences. While evidently a degradative mechanism, mitophagy has been implicated in both growth-promoting and atrophic conditions in muscle tissue, highlighting a potential paradox.

During muscle growth, mitophagy is essential for maintaining a pool of functional mitochondria, thereby optimizing energy production to support anabolic processes. A previous study has shown that muscle-specific *Atg7* knockout, which subsequently limits mitophagy, negatively impacts muscle mass (Masiero et al., 2009). This suggests the necessity of both autophagy and mitophagy in muscle maintenance (Masiero et al., 2009). While the detailed mechanisms by which autophagy and mitophagy contribute to hypertrophy in mature muscle remain unclear, the findings in this thesis reveal that mitophagic flux increases consistently throughout the postnatal growth phase. Intriguingly, our observations suggest that the loss of autophagy via muscle-specific *Atg7* deletion does not detrimentally affect postnatal muscle development, suggesting that autophagy/mitophagy may not be essential for postnatal growth per se. Instead, we propose that other mechanisms compensate to protect against muscle defects during postnatal development. However, this protective effect is short lived since defects emerge as the animals age (Paré et al., 2017).

Conversely, elevated levels of autophagy and mitophagy have been documented in response to muscle disuse conditions, such as immobilization and denervation. This thesis corroborates previous studies, demonstrating an increase in mitophagic flux accompanying disuse atrophy (Triolo et al., 2022; F. Wang et al., 2023; Yamashita et al., 2021). Interestingly, inhibition of autophagy through NAC or colchicine treatment resulted in detrimental effects on mitochondrial

function and exacerbates atrophy in glycolytic IIX and IIB myofibers. These findings suggest a protective role of mitophagy in atrophic conditions, aimed at preserving mitochondrial integrity against defects that arise during periods of disuse.

Therefore, the seemingly paradoxical increase in mitophagic flux in both growth and atrophy can be contextualized as a reflection of its adaptive roles in different physiological states. During postnatal growth, the increase in mitophagic activity may be related to the heightened movement and energy demands of growing tissues, necessitating efficient mitochondrial turnover. In contrast, during muscle atrophy, elevated mitophagy serves a protective function, safeguarding mitochondrial function against the stresses induced by disuse. This perspective helps to resolve the apparent paradoxical role of mitophagy in skeletal muscle tissue, emphasizing its context-dependent functionality in maintaining or adapting mitochondrial networks according to the specific demands of the cell/myofibers.

The Recurring Role of BNIP3 in Muscle Growth and Atrophy

BNIP3 is a critical regulator of both cellular survival and cell death, notably in cardiac and skeletal muscle tissues. As a member of the BCL2 family, BNIP3 is distinguished by its atypical BH3 domain, a LIR motif, and an essential transmembrane domain (J. Zhang & Ney, 2009). In the cytosol, BNIP3 triggers signaling cascades that lead to programmed cell death or autophagy. BNIP3 can form homodimers or heterodimers with other BCL2 family members, influencing its biological functions (Ray et al., 2000; Sulistijo & MacKenzie, 2009). Notably, BNIP3 disrupts the BCL2-BECN1 complex by binding to BCL2, which releases BECN1 and initiates autophagy (Bellot et al., 2009). Furthermore, BNIP3 may activate autophagy through its interaction with and inhibition of RHEB, a known suppressor of autophagy (Y. Li et al., 2007). When localized to the mitochondria, BNIP3 influences mitochondrial functionality and dynamics significantly. Its transmembrane domain enables anchoring to the mitochondrial outer membrane, where it can promote MOMP through interactions with pro-apoptotic molecules like BAX and BAK1 (Hendgen-Cotta et al., 2017). The LIR motif of BNIP3 interacts directly with lipidated LC3B-II on autophagosomes, facilitating efficient mitophagy by bypassing the need for adaptor or cargo recognition molecules (Hanna et al., 2012; R.-Y. Shi et al., 2014). Moreover, the role of BNIP3 in mitochondrial fission, underscored by its involvement in recruiting DNM1L, highlights its impact on mitochondrial morphology (Lee et al., 2011). These mechanisms underline the numerous roles of BNIP3 in maintaining mitochondrial integrity and responding to cellular stress.

In this thesis, BNIP3 has demonstrated a recurring role in various stages including muscle formation, postnatal growth, and atrophy. In cellular studies, the importance of BNIP3 in differentiation is increasingly recognized. For instance, upregulation of BNIP3 has been observed in adipocyte differentiation (Choi et al., 2016), and similarly during myogenic differentiation

(Baechler et al., 2019). Previous findings from our group confirm that myogenic differentiation is severely impaired in the absence of BNIP3 (Baechler et al., 2019), aligning with the cell data presented in this thesis and indicating the importance of this molecule. Furthermore, we discovered that despite increases in mitochondrial fission and mitophagic flux, myogenic differentiation remains hindered in *Bnip3*$^{-/-}$ cells, suggesting that the role of BNIP3 extends beyond mitophagy. BNIP3 may potentially influence myogenic regulatory factors or other signaling pathways; however, the specific mechanisms remain unclear.

BNIP3 continues to play a role throughout the lifespan of muscle, particularly during postnatal development and atrophy in mature muscles. Previous studies have indicated a gradual increase in BNIP3 levels during postnatal development (Y. Kim, Yang, et al., 2019), which coincides with our observations. Data from this thesis found that mitochondrial localization of BNIP3 increases markedly (>10 fold) compared to other markers such as PINK1 and PRKN during the postnatal developmental period. This may signify a greater impact of BNIP3 on mitophagy during development compared to other mitophagy molecules. Nonetheless, in conditions of muscle atrophy, BNIP3 levels are consistently elevated, particularly in immobilized and subsequently remobilized muscles (F. Wang et al., 2023), mirroring our findings of significantly greater mitochondrial localization of BNIP3 in these conditions. It is important to note that BNIP3 continues to tag skeletal muscle mitochondria even when autophagy/mitophagy is inhibited or completely ablated. This suggests that BNIP3 may also play a role in regulating other aspects of mitochondrial function, such as bioenergetics. These insights highlight role of BNIP3 in muscle physiology, emphasizing its role during *in vitro* myogenesis and *in vivo* muscle adaptation across various stages of life. Further investigation through genetic manipulation of BNIP3 levels may provide deeper insights into its effects on muscle formation, postnatal growth, and atrophy.

Relevance to Human Physiology

While our study did not directly investigate mitochondrial remodeling in humans, the findings offer significant insights into human physiology. This thesis explored mitochondrial remodeling within the contexts of myogenesis, postnatal growth, and muscle atrophy, highlighting the commonalities between human and rodent models during these physiological stages. Thorough investigation of myogenesis *in utero* presents numerous challenges, leading researchers to frequently utilize *in vitro* cell models. These models facilitate the study of fundamental cellular processes such as growth and differentiation within a controlled environment. For instance, mutations in the human DNM1L gene and knockout models of DNM1L in rodents both result in early lethality, underscoring the critical role of this protein and the process of mitochondrial fission during embryonic development (Bauer et al., 2023; Favaro et al., 2019; Tezze et al., 2017; Wakabayashi et al., 2009). Moreover, DNM1L mutations result in mitochondrial fission-deficiency and is complicated to study with respect to human myogenesis. It is important to note that the process of myogenesis shares several similarities between human and rodents (Mierzejewski et al., 2020). Nonetheless, to better isolate and elucidate these complex mechanisms, *in vitro* experiments are pivotal. Our research contributes to this understanding by highlighting how disruptions in mitochondrial fission underlie certain pathological conditions, leading to failed muscle cell differentiation. Moreover, we have identified that mitochondrial fission must occur before other remodeling processes such as mitophagy and biogenesis for normal myogenesis. These findings imply that targeting mitochondrial remodeling processes that are downstream to fission, like mitophagy, may not yield effective therapeutic outcomes in cells that display dysregulated fission. Instead, strategies that restore mitochondrial fission appear more promising as a primary target, especially in the context of myogenesis.

Studying postnatal muscle development offers critical insights into the unique and rapid mitochondrial remodeling that occurs during this growth phase. Unlike traditional muscle hypertrophy, which occurs gradually, the postnatal growth phase is marked by a rapid rate of muscle growth that is not replicated at any other time. This period is critical for understanding the progression of various mitochondrial diseases and myopathies, which often worsen with age. While our research did not target any specific disease, we successfully characterized and documented the alterations in mitochondrial remodeling during this phase. Additionally, we elucidated the role of autophagy, which has been previously established as crucial for maintaining muscle mass during development (Masiero et al., 2009). This knowledge is particularly valuable as there is a growing body of evidence suggesting that enhancing mitophagy could be beneficial in treating certain juvenile diseases. For instance, activation of mitophagy with urolithin A treatment in rodent models of Duchenne's muscular dystrophy, a degenerative myopathy characterized by severe muscle damage, has been shown to improve several functional parameters including grip strength, maximum running distance, and fiber size (Luan et al., 2021; Ryu et al., 2016). The potential therapeutic application of urolithin A extends beyond Duchenne muscular dystrophy and may be relevant in other juvenile diseases; however, these applications have not been fully explored. By understanding these complex mechanisms in greater detail, we hope to improve the design of therapeutics for neonatal and juvenile conditions, potentially leading to more effective treatment strategies tailored to the unique needs of these growth phases.

Studying the changes associated with disuse atrophy provides crucial insights applicable to a broad demographic, particularly as it affects individuals who become inactive due to factors such as aging, injury, hospitalization, or lifestyle changes. This inactivity often leads to significant loss of muscle mass. Using the hindlimb immobilization model in mice, which closely mimics the

rapid muscle atrophy observed in humans following bedrest (Belavý et al., 2009; Dirks et al., 2016; LeBlanc et al., 1997; Marusic et al., 2021), we have been able to investigate the relationship between muscle atrophy and mitochondrial remodeling processes. Previous studies have indicated that disuse correlates with increased mitochondrial degradation, prompting us to further explore this phenomenon. Our research findings demonstrate that mitophagy is significantly upregulated during muscle atrophy and that attempts to inhibit mitophagy, either through antioxidant treatment or suppression of autophagic machinery, exacerbated the condition. This suggests that mitophagy plays a crucial protective role, possibly by adapting the bioenergetic status of the muscle to the reduced physiological demands, a mechanism also observed in human models of immobilization (Belavý et al., 2009; Dirks et al., 2016; LeBlanc et al., 1997; Marusic et al., 2021). Thus, understanding and manipulating this process is essential to developing interventions that mitigate the effects of disuse atrophy.

Limitations

In this thesis, we have endeavored to minimize the inherent limitations of our experimental design; however, complete elimination of all constraints is not feasible. One notable limitation arises from the use of a complete BNIP3 knockout model in cell studies. While this model has been effectively employed in previous research (Baechler et al., 2019), the prolonged absence of BNIP3 may lead to phenotypic and/or behaviour changes in the long term. Using a transient knockout model could potentially mitigate the long-term cellular changes caused by BNIP3 deficiency. Additionally, our experiments were exclusively conducted on C2C12 murine myoblasts, which may limit the applicability of our findings to human physiology. It is crucial to recognize that the direct applicability of our findings to human studies may be limited due to significant differences between human and rodent muscle tissues, including their fiber type composition, metabolic phenotype, and recruitment patterns. These disparities necessitate careful consideration and further validation before extrapolating our results to humans (Rahman et al., 2024).

Future Directions

This thesis has elucidated several fundamental aspects of mitochondrial remodeling within the contexts of myogenesis, postnatal muscle development, and disuse atrophy, thereby setting the stage for future research. Our studies have consistently identified BNIP3 as a potential mediator in mitochondrial remodeling both *in vitro* and *in vivo*. While we have determined some of the molecular targets of mitochondrial pathways, the discovery of BNIP3 as a pivotal factor opens new avenues for exploration. Some cell studies have found that BNIP3 can exist as either a monomer or a dimer (Ray et al., 2000; Sulistijo & MacKenzie, 2009), which could potentially influence mitochondrial remodeling during muscle development and atrophy. Additionally, BNIP3 contains multiple phosphorylation sites, which have been shown to regulate its function in various mammalian cells (He et al., 2020). The role of these post-translational modifications in skeletal muscle differentiation, postnatal development, and atrophy remains unclear and warrants further investigation.

Our cellular studies showed that mitophagy can occur independently of BNIP3. We observed that increasing mitochondrial fission enhanced mitophagic flux in *Bnip3*$^{-/-}$ cells; however, this did not restore their differentiation capabilities. Future research should investigate alternative proteins that could regulate mitophagy in the absence of BNIP3. Mitophagy-related molecules such as FUNDC1, BCL2L13, BNIP3L, or certain RAB-related proteins may regulate mitophagic flux independent of BNIP3. The observation that *Bnip3*$^{-/-}$ impairs differentiation without completely ablated mitophagic indicates that its role may extend beyond just mitophagy. BNIP3 might also affect interactions with other critical molecular players in muscle development, including MRFs or growth-signaling molecules like RHEB, which activates the MTORC1 pathway to promote growth.

In the postnatal development study of this thesis, RNA-Seq analyses revealed significant changes in genes regulating metabolism. Although the study of metabolism is beyond the scope of this thesis, it is noteworthy for future exploration to better understand postnatal development and possible interaction with mitochondrial remodeling processes. Our findings show elevated BNIP3 levels in mature versus neonatal muscles, although it remains uncertain whether this elevation is due to increased muscle maturation or mitochondrial network complexity, or if BNIP3 directly drives these developmental changes. Notably, no studies to date have examined BNIP3 knockout in developing muscles to assess its role in mitochondrial remodeling.

Our studies on disuse atrophy have uncovered an imbalance in mitochondrial remodeling processes, characterized by elevated mitophagic flux and suppressed PPARGC1A signaling, both of which are linked to mitochondrial dysfunction. Future investigations may wish to utilize small molecule modulators, such as ZLN005, or apply muscle-targeted genetic approaches to manipulate these pathways in the context of immobilization-induced atrophy. Additionally, our findings highlight fiber type-specific atrophy, particularly in groups treated with antioxidants and colchicine. This underscores the importance of conducting detailed fiber-specific analyses to better understand these subtleties and explore the impact of atrophic stimuli on different muscles, each with distinct fiber type compositions and metabolic phenotypes (Rahman et al., 2024).

Conclusion

This thesis collectively demonstrates that the regulation of mitochondrial fission, mitophagy, and biogenesis are crucial for efficient muscle cell differentiation and overall muscle function. Specifically, mitochondrial fission serves as a critical initiation point for subsequent remodeling processes essential for myogenic differentiation. Our findings indicate that disruptions in mitochondrial fission impede mitophagy and biogenesis, thereby affecting the entire sequence of mitochondrial renewal and ultimately impairing myogenic differentiation. These defects associated with fission deficiency cannot be overcome by overexpressing mitophagy or biogenesis-related molecules. During postnatal skeletal muscle development, we observe significant mitochondrial remodeling, characterized by increased mitophagic flux, reduced biogenesis signaling, and enhanced mitochondrial function. This illustrates the relationship between mitochondrial function, muscle growth, and mitophagic flux, highlighting that while deficits in autophagic processes can undermine muscle strength and signaling pathways, they do not necessarily hinder overall muscle growth in young mice. The absence of a negative phenotype in our study may be attributed to the upregulation of alternative degradative pathways, such as the UPS. This adaptation could potentially compensate for the suppression of autophagy and mitophagy in our models. In response to immobilization-induced muscle atrophy, there is a complex interplay between mitochondrial dysfunction and increased mitophagic activity. Treatment with antioxidants to reduce ROS signaling improved mitochondrial function in immobilized muscles but exacerbated muscle atrophy. Conversely, treatments that reduced mitophagic activity worsened muscle atrophy, emphasizing the need for a balanced approach to mitochondrial quality control. These insights suggest that targeted therapeutic strategies aimed at enhancing the coordination between mitochondrial remodeling processes could optimize skeletal

muscle function. Such strategies would ideally involve stabilizing mitochondrial fission and fusion processes, ensuring efficient mitophagic clearance of damaged, dysfunctional, or immature mitochondria, and promoting mitochondrial biogenesis to maintain a healthy mitochondrial network in skeletal muscle cells and tissues.

References

Adhihetty, P. J., Ljubicic, V., Menzies, K. J., & Hood, D. A. (2005). Differential susceptibility of subsarcolemmal and intermyofibrillar mitochondria to apoptotic stimuli. *American Journal of Physiology. Cell Physiology*, *289*(4), C994–C1001. https://doi.org/10.1152/ajpcell.00031.2005

Aerts, L., Craessaerts, K., De Strooper, B., & Morais, V. A. (2015). PINK1 kinase catalytic activity is regulated by phosphorylation on serines 228 and 402. *The Journal of Biological Chemistry*, *290*(5), 2798–2811. https://doi.org/10.1074/jbc.M114.620906

Alexandre, A., Reynafarje, B., & Lehninger, A. L. (1978). Stoichiometry of vectorial H+ movements coupled to electron transport and to ATP synthesis in mitochondria. *Proceedings of the National Academy of Sciences*, *75*(11), 5296–5300. https://doi.org/10.1073/pnas.75.11.5296

Allen, D. L., Linderman, J. K., Roy, R. R., Bigbee, A. J., Grindeland, R. E., Mukku, V., & Edgerton, V. R. (1997). Apoptosis: A mechanism contributing to remodeling of skeletal muscle in response to hindlimb unweighting. *The American Journal of Physiology*, *273*(2 Pt 1), C579-587. https://doi.org/10.1152/ajpcell.1997.273.2.C579

Allen, D. L., Roy, R. R., & Edgerton, V. R. (1999). Myonuclear domains in muscle adaptation and disease. *Muscle & Nerve*, *22*(10), 1350–1360. https://doi.org/10.1002/(SICI)1097-4598(199910)22:10<1350::AID-MUS3>3.0.CO;2-8

Altmann, R. (1894). *Die Elementarorganismen und ihre Beziehungen zu den Zellen*. Veit.

Andreux, P. A., Blanco-Bose, W., Ryu, D., Burdet, F., Ibberson, M., Aebischer, P., Auwerx, J., Singh, A., & Rinsch, C. (2019). The mitophagy activator urolithin A is safe and induces a molecular

signature of improved mitochondrial and cellular health in humans. *Nature Metabolism*, *1*(6), 595–603. https://doi.org/10.1038/s42255-019-0073-4

Appell, H. J., Duarte, J. A., & Soares, J. M. (1997). Supplementation of vitamin E may attenuate skeletal muscle immobilization atrophy. *International Journal of Sports Medicine*, *18*(3), 157–160. https://doi.org/10.1055/s-2007-972612

Atherton, P. J., Greenhaff, P. L., Phillips, S. M., Bodine, S. C., Adams, C. M., & Lang, C. H. (2016). Control of skeletal muscle atrophy in response to disuse: Clinical/preclinical contentions and fallacies of evidence. *American Journal of Physiology. Endocrinology and Metabolism*, *311*(3), E594-604. https://doi.org/10.1152/ajpendo.00257.2016

Aweida, D., & Cohen, S. (2021). Breakdown of Filamentous Myofibrils by the UPS–Step by Step. *Biomolecules*, *11*(1), 110. https://doi.org/10.3390/biom11010110

Bachman, J. F., & Chakkalakal, J. V. (2022). Insights into muscle stem cell dynamics during postnatal development. *The FEBS Journal*, *289*(10), 2710–2722. https://doi.org/10.1111/febs.15856

Baechler, B. L., Bloemberg, D., & Quadrilatero, J. (2019). Mitophagy regulates mitochondrial network signaling, oxidative stress, and apoptosis during myoblast differentiation. *Autophagy*, *15*(9), 1606–1619. https://doi.org/10.1080/15548627.2019.1591672

Bakeeva, L. E., Chentsov, Yu. S., & Skulachev, V. P. (1978). Mitochondrial framework (reticulum mitochondriale) in rat diaphragm muscle. *Biochimica et Biophysica Acta (BBA) - Bioenergetics*, *501*(3), 349–369. https://doi.org/10.1016/0005-2728(78)90104-4

Baker, D. J., & Hepple, R. T. (2006). Elevated caspase and AIF gene expression correlate with progression of sarcopenia during aging in male F344BN rats. *Experimental Gerontology*, *41*(11), 1149–1156. https://doi.org/10.1016/j.exger.2006.08.007

Baldelli, S., Aquilano, K., & Ciriolo, M. R. (2014). PGC-1α buffers ROS-mediated removal of mitochondria during myogenesis. *Cell Death & Disease*, *5*(11), e1515. https://doi.org/10.1038/cddis.2014.458

Ban, T., Ishihara, T., Kohno, H., Saita, S., Ichimura, A., Maenaka, K., Oka, T., Mihara, K., & Ishihara, N. (2017). Molecular basis of selective mitochondrial fusion by heterotypic action between OPA1 and cardiolipin. *Nature Cell Biology*, *19*(7), 856–863. https://doi.org/10.1038/ncb3560

Barbieri, E., Battistelli, M., Casadei, L., Vallorani, L., Piccoli, G., Guescini, M., Gioacchini, A. M., Polidori, E., Zeppa, S., Ceccaroli, P., Stocchi, L., Stocchi, V., & Falcieri, E. (2011). Morphofunctional and Biochemical Approaches for Studying Mitochondrial Changes during Myoblasts Differentiation. *Journal of Aging Research*, *2011*. https://doi.org/10.4061/2011/845379

Bauer, B. L., Rochon, K., Liu, J. C., Ramachandran, R., & Mears, J. A. (2023). Disease-associated mutations in Drp1 have fundamentally different effects on the mitochondrial fission machinery. *Human Molecular Genetics*, *32*(12), 1975–1987. https://doi.org/10.1093/hmg/ddad029

Belavý, D. L., Miokovic, T., Armbrecht, G., Richardson, C. A., Rittweger, J., & Felsenberg, D. (2009). Differential atrophy of the lower-limb musculature during prolonged bed-rest. *European*

Journal of Applied Physiology, *107*(4), 489–499. https://doi.org/10.1007/s00421-009-1136-0

Bellot, G., Garcia-Medina, R., Gounon, P., Chiche, J., Roux, D., Pouysségur, J., & Mazure, N. M. (2009). Hypoxia-induced autophagy is mediated through hypoxia-inducible factor induction of BNIP3 and BNIP3L via their BH3 domains. *Molecular and Cellular Biology*, *29*(10), 2570–2581. https://doi.org/10.1128/MCB.00166-09

Bernardi, P., Rasola, A., Forte, M., & Lippe, G. (2015). The Mitochondrial Permeability Transition Pore: Channel Formation by F-ATP Synthase, Integration in Signal Transduction, and Role in Pathophysiology. *Physiological Reviews*, *95*(4), 1111–1155. https://doi.org/10.1152/physrev.00001.2015

Bernardini, J. P., Lazarou, M., & Dewson, G. (2017). Parkin and mitophagy in cancer. *Oncogene*, *36*(10), Article 10. https://doi.org/10.1038/onc.2016.302

Berry, E. A., Guergova-Kuras, M., Huang, L. S., & Crofts, A. R. (2000). Structure and function of cytochrome bc complexes. *Annual Review of Biochemistry*, *69*, 1005–1075. https://doi.org/10.1146/annurev.biochem.69.1.1005

Beutner, G., Alavian, K. N., Jonas, E. A., & Porter, G. A. (2017). The Mitochondrial Permeability Transition Pore and ATP Synthase. *Handbook of Experimental Pharmacology*, *240*, 21–46. https://doi.org/10.1007/164_2016_5

Bleck, C. K. E., Kim, Y., Willingham, T. B., & Glancy, B. (2018). Subcellular connectomic analyses of energy networks in striated muscle. *Nature Communications*, *9*(1), Article 1. https://doi.org/10.1038/s41467-018-07676-y

Bloemberg, D., & Quadrilatero, J. (2012). Rapid Determination of Myosin Heavy Chain Expression in Rat, Mouse, and Human Skeletal Muscle Using Multicolor Immunofluorescence Analysis. *PLoS ONE*, *7*(4). https://doi.org/10.1371/journal.pone.0035273

Bloemberg, D., & Quadrilatero, J. (2016). Effect of mitochondrial fission inhibition on C2C12 differentiation. *Data in Brief*, *7*, 634–640. https://doi.org/10.1016/j.dib.2016.02.070

Bloemberg, D., & Quadrilatero, J. (2019). Autophagy, apoptosis, and mitochondria: Molecular integration and physiological relevance in skeletal muscle. *American Journal of Physiology-Cell Physiology*, *317*(1), C111–C130. https://doi.org/10.1152/ajpcell.00261.2018

Borgia, D., Malena, A., Spinazzi, M., Desbats, M. A., Salviati, L., Russell, A. P., Miotto, G., Tosatto, L., Pegoraro, E., Sorarù, G., Pennuto, M., & Vergani, L. (2017). Increased mitophagy in the skeletal muscle of spinal and bulbar muscular atrophy patients. *Human Molecular Genetics*, *26*(6), 1087–1103. https://doi.org/10.1093/hmg/ddx019

Bratton, S. B., Lewis, J., Butterworth, M., Duckett, C. S., & Cohen, G. M. (2002). XIAP inhibition of caspase-3 preserves its association with the Apaf-1 apoptosome and prevents CD95- and Bax-induced apoptosis. *Cell Death & Differentiation*, *9*(9), 881–892. https://doi.org/10.1038/sj.cdd.4401069

Bravo-San Pedro, J. M., Kroemer, G., & Galluzzi, L. (2017). Autophagy and Mitophagy in Cardiovascular Disease. *Circulation Research*, *120*(11), 1812–1824. https://doi.org/10.1161/CIRCRESAHA.117.311082

Brooks, N. E., & Myburgh, K. H. (2014). Skeletal muscle wasting with disuse atrophy is multi-dimensional: The response and interaction of myonuclei, satellite cells and signaling pathways. *Frontiers in Physiology*, *5*, 99. https://doi.org/10.3389/fphys.2014.00099

Bruni, F., Polosa, P. L., Gadaleta, M. N., Cantatore, P., & Roberti, M. (2010). Nuclear respiratory factor 2 induces the expression of many but not all human proteins acting in mitochondrial DNA transcription and replication. *The Journal of Biological Chemistry*, *285*(6), 3939–3948. https://doi.org/10.1074/jbc.M109.044305

Buch, B. T., Halling, J. F., Ringholm, S., Gudiksen, A., Kjøbsted, R., Olsen, M. A., Wojtaszewski, J. F. P., & Pilegaard, H. (2020). Colchicine treatment impairs skeletal muscle mitochondrial function and insulin sensitivity in an age-specific manner. *FASEB Journal: Official Publication of the Federation of American Societies for Experimental Biology*, *34*(6), 8653–8670. https://doi.org/10.1096/fj.201903113RR

Buck, M. D., O'Sullivan, D., Klein Geltink, R. I., Curtis, J. D., Chang, C.-H., Sanin, D. E., Qiu, J., Kretz, O., Braas, D., van der Windt, G. J. W., Chen, Q., Huang, S. C.-C., O'Neill, C. M., Edelson, B. T., Pearce, E. J., Sesaki, H., Huber, T. B., Rambold, A. S., & Pearce, E. L. (2016). Mitochondrial Dynamics Controls T Cell Fate through Metabolic Programming. *Cell*, *166*(1), 63–76. https://doi.org/10.1016/j.cell.2016.05.035

Buckingham, M., Bajard, L., Chang, T., Daubas, P., Hadchouel, J., Meilhac, S., Montarras, D., Rocancourt, D., & Relaix, F. (2003). The formation of skeletal muscle: From somite to limb. *Journal of Anatomy*, *202*(1), 59–68. https://doi.org/10.1046/j.1469-7580.2003.00139.x

Burman, J. L., Pickles, S., Wang, C., Sekine, S., Vargas, J. N. S., Zhang, Z., Youle, A. M., Nezich, C. L., Wu, X., Hammer, J. A., & Youle, R. J. (2017). Mitochondrial fission facilitates the

selective mitophagy of protein aggregates. *The Journal of Cell Biology*, *216*(10), 3231–3247. https://doi.org/10.1083/jcb.201612106

Caffin, F., Prola, A., Piquereau, J., Novotova, M., David, D. j., Garnier, A., Fortin, D., Alavi, M. v., Veksler, V., Ventura-Clapier, R., & Joubert, F. (2013). Altered skeletal muscle mitochondrial biogenesis but improved endurance capacity in trained OPA1-deficient mice. *The Journal of Physiology*, *591*(23), 6017–6037. https://doi.org/10.1113/jphysiol.2013.263079

Camara, A. K. S., Zhou, Y., Wen, P.-C., Tajkhorshid, E., & Kwok, W.-M. (2017). Mitochondrial VDAC1: A Key Gatekeeper as Potential Therapeutic Target. *Frontiers in Physiology*, *8*. https://www.frontiersin.org/articles/10.3389/fphys.2017.00460

Cannavino, J., Brocca, L., Sandri, M., Bottinelli, R., & Pellegrino, M. A. (2014). PGC1-α over-expression prevents metabolic alterations and soleus muscle atrophy in hindlimb unloaded mice. *The Journal of Physiology*, *592*(Pt 20), 4575–4589. https://doi.org/10.1113/jphysiol.2014.275545

Cannavino, J., Brocca, L., Sandri, M., Grassi, B., Bottinelli, R., & Pellegrino, M. A. (2015). The role of alterations in mitochondrial dynamics and PGC-1α over-expression in fast muscle atrophy following hindlimb unloading. *The Journal of Physiology*, *593*(Pt 8), 1981–1995. https://doi.org/10.1113/jphysiol.2014.286740

Carnio, S., LoVerso, F., Baraibar, M. A., Longa, E., Khan, M. M., Maffei, M., Reischl, M., Canepari, M., Loefler, S., Kern, H., Blaauw, B., Friguet, B., Bottinelli, R., Rudolf, R., & Sandri, M. (2014). Autophagy impairment in muscle induces neuromuscular junction degeneration

and precocious aging. *Cell Reports*, *8*(5), 1509–1521. https://doi.org/10.1016/j.celrep.2014.07.061

Carter, H. N., Kim, Y., Erlich, A. T., Zarrin-khat, D., & Hood, D. A. (2018). Autophagy and mitophagy flux in young and aged skeletal muscle following chronic contractile activity. *The Journal of Physiology*, *596*(16), Article 16. https://doi.org/10.1113/JP275998

Chakraborti, T., Das, S., Mandal, M., Mandal, A., & Chakraborti, S. (2002). Role of Ca2+-Dependent Metalloprotease-2 in Stimulating Ca2+ATPase Activity Under Peroxynitrite Treatment in Bovine Pulmonary Artery Smooth Muscle Membrane. *IUBMB Life*, *53*(3), 167–173. https://doi.org/10.1080/15216540212337

Chan, J. Y., Kwong, M., Lu, R., Chang, J., Wang, B., Yen, T. S. B., & Kan, Y. W. (1998). Targeted disruption of the ubiquitous CNC-bZIP transcription factor, Nrf-1, results in anemia and embryonic lethality in mice. *The EMBO Journal*, *17*(6), 1779–1787. https://doi.org/10.1093/emboj/17.6.1779

Chang, N. C. (2020). Autophagy and Stem Cells: Self-Eating for Self-Renewal. *Frontiers in Cell and Developmental Biology*, *8*. https://www.frontiersin.org/articles/10.3389/fcell.2020.00138

Chaugule, V. K., Burchell, L., Barber, K. R., Sidhu, A., Leslie, S. J., Shaw, G. S., & Walden, H. (2011). Autoregulation of Parkin activity through its ubiquitin-like domain. *The EMBO Journal*, *30*(14), 2853–2867. https://doi.org/10.1038/emboj.2011.204

Chen, H., Detmer, S. A., Ewald, A. J., Griffin, E. E., Fraser, S. E., & Chan, D. C. (2003). Mitofusins Mfn1 and Mfn2 coordinately regulate mitochondrial fusion and are essential for

embryonic development. *The Journal of Cell Biology*, *160*(2), 189–200. https://doi.org/10.1083/jcb.200211046

Chen, H., Vermulst, M., Wang, Y. E., Chomyn, A., Prolla, T. A., McCaffery, J. M., & Chan, D. C. (2010). Mitochondrial Fusion Is Required for mtDNA Stability in Skeletal Muscle and Tolerance of mtDNA Mutations. *Cell*, *141*(2), 280–289. https://doi.org/10.1016/j.cell.2010.02.026

Chen, H.-C., Kanai, M., Inoue-Yamauchi, A., Tu, H.-C., Huang, Y., Ren, D., Kim, H., Takeda, S., Reyna, D. E., Chan, P. M., Ganesan, Y. T., Liao, C.-P., Gavathiotis, E., Hsieh, J. J., & Cheng, E. H. (2015). An interconnected hierarchical model of cell death regulation by the BCL-2 family. *Nature Cell Biology*, *17*(10), 1270–1281. https://doi.org/10.1038/ncb3236

Cho, B., Cho, H. M., Jo, Y., Kim, H. D., Song, M., Moon, C., Kim, H., Kim, K., Sesaki, H., Rhyu, I. J., Kim, H., & Sun, W. (2017). Constriction of the mitochondrial inner compartment is a priming event for mitochondrial division. *Nature Communications*, *8*(1), Article 1. https://doi.org/10.1038/ncomms15754

Choi, J. W., Jo, A., Kim, M., Park, H. S., Chung, S. S., Kang, S., & Park, K. S. (2016). BNIP3 is essential for mitochondrial bioenergetics during adipocyte remodelling in mice. *Diabetologia*, *59*(3), 571–581. https://doi.org/10.1007/s00125-015-3836-9

Cogliati, S., Frezza, C., Soriano, M. E., Varanita, T., Quintana-Cabrera, R., Corrado, M., Cipolat, S., Costa, V., Casarin, A., Gomes, L. C., Perales-Clemente, E., Salviati, L., Fernandez-Silva, P., Enriquez, J. A., & Scorrano, L. (2013). Mitochondrial cristae shape determines respiratory chain supercomplexes assembly and respiratory efficiency. *Cell*, *155*(1), 160–171. https://doi.org/10.1016/j.cell.2013.08.032

Cogswell, A. M., Stevens, R. J., & Hood, D. A. (1993). Properties of skeletal muscle mitochondria isolated from subsarcolemmal and intermyofibrillar regions. *The American Journal of Physiology*, *264*(2 Pt 1), C383-389. https://doi.org/10.1152/ajpcell.1993.264.2.C383

Collier Jack J., Guissart Claire, Oláhová Monika, Sasorith Souphatta, Piron-Prunier Florence, Suomi Fumi, Zhang David, Martinez-Lopez Nuria, Leboucq Nicolas, Bahr Angela, Azzarello-Burri Silvia, Reich Selina, Schöls Ludger, Polvikoski Tuomo M., Meyer Pierre, Larrieu Lise, Schaefer Andrew M., Alsaif Hessa S., Alyamani Suad, … Taylor Robert W. (2021). Developmental Consequences of Defective ATG7-Mediated Autophagy in Humans. *New England Journal of Medicine*, *384*(25), 2406–2417. https://doi.org/10.1056/NEJMoa1915722

Cuervo, A. M., Palmer, A., Rivett, A. J., & Knecht, E. (1995). Degradation of proteasomes by lysosomes in rat liver. *European Journal of Biochemistry*, *227*(3), 792–800. https://doi.org/10.1111/j.1432-1033.1995.tb20203.x

Deane, C. S., Willis, C. R. G., Phillips, B. E., Atherton, P. J., Harries, L. W., Ames, R. M., Szewczyk, N. J., & Etheridge, T. (2021). Transcriptomic meta-analysis of disuse muscle atrophy vs. Resistance exercise-induced hypertrophy in young and older humans. *Journal of Cachexia, Sarcopenia and Muscle*, *12*(3), 629–645. https://doi.org/10.1002/jcsm.12706

Deas, E., Plun-Favreau, H., Gandhi, S., Desmond, H., Kjaer, S., Loh, S. H. Y., Renton, A. E. M., Harvey, R. J., Whitworth, A. J., Martins, L. M., Abramov, A. Y., & Wood, N. W. (2011). PINK1 cleavage at position A103 by the mitochondrial protease PARL. *Human Molecular Genetics*, *20*(5), 867–879. https://doi.org/10.1093/hmg/ddq526

Demiryürek, S., & Babül, A. (2004). Effects of vitamin E and electrical stimulation on the denervated rat gastrocnemius muscle malondialdehyde and glutathione levels. *The International Journal of Neuroscience*, *114*(1), 45–54. https://doi.org/10.1080/00207450490249374

Demontis, F., & Perrimon, N. (2010). FOXO/4E-BP Signaling in Drosophila Muscles Regulates Organism-wide Proteostasis during Aging. *Cell*, *143*(5), 813–825. https://doi.org/10.1016/j.cell.2010.10.007

Deneubourg, C., Ramm, M., Smith, L. J., Baron, O., Singh, K., Byrne, S. C., Duchen, M. R., Gautel, M., Eskelinen, E.-L., Fanto, M., & Jungbluth, H. (2022). The spectrum of neurodevelopmental, neuromuscular and neurodegenerative disorders due to defective autophagy. *Autophagy*, *18*(3), 496–517. https://doi.org/10.1080/15548627.2021.1943177

Deng, Z., Zhou, X., Lu, J.-H., & Yue, Z. (2021). Autophagy deficiency in neurodevelopmental disorders. *Cell & Bioscience*, *11*, 214. https://doi.org/10.1186/s13578-021-00726-x

Deval, C., Calonne, J., Coudy-Gandilhon, C., Vazeille, E., Bechet, D., Polge, C., Taillandier, D., Attaix, D., & Combaret, L. (2020). Mitophagy and Mitochondria Biogenesis Are Differentially Induced in Rat Skeletal Muscles during Immobilization and/or Remobilization. *International Journal of Molecular Sciences*, *21*(10), Article 10. https://doi.org/10.3390/ijms21103691

Dirks, M. L., Wall, B. T., van de Valk, B., Holloway, T. M., Holloway, G. P., Chabowski, A., Goossens, G. H., & van Loon, L. J. C. (2016). One Week of Bed Rest Leads to Substantial Muscle

Atrophy and Induces Whole-Body Insulin Resistance in the Absence of Skeletal Muscle Lipid Accumulation. *Diabetes*, *65*(10), Article 10. https://doi.org/10.2337/db15-1661

Distefano, G., Standley, R. A., Dubé, J. J., Carnero, E. A., Ritov, V. B., Stefanovic-Racic, M., Toledo, F. G. S., Piva, S. R., Goodpaster, B. H., & Coen, P. M. (2017). Chronological Age Does not Influence Ex-vivo Mitochondrial Respiration and Quality Control in Skeletal Muscle. *The Journals of Gerontology. Series A, Biological Sciences and Medical Sciences*, *72*(4), 535–542. https://doi.org/10.1093/gerona/glw102

Dumont, N. A., Bentzinger, C. F., Sincennes, M.-C., & Rudnicki, M. A. (2015). Satellite Cells and Skeletal Muscle Regeneration. *Comprehensive Physiology*, *5*(3), 1027–1059. https://doi.org/10.1002/cphy.c140068

Dumont, N. A., Wang, Y. X., & Rudnicki, M. A. (2015). Intrinsic and extrinsic mechanisms regulating satellite cell function. *Development (Cambridge, England)*, *142*(9), 1572–1581. https://doi.org/10.1242/dev.114223

Durcan, T. M., & Fon, E. A. (2015). The three 'P's of mitophagy: PARKIN, PINK1, and post-translational modifications. *Genes & Development*, *29*(10), 989–999. https://doi.org/10.1101/gad.262758.115

Eisner, V., Csordás, G., & Hajnóczky, G. (2013). Interactions between sarco-endoplasmic reticulum and mitochondria in cardiac and skeletal muscle – pivotal roles in Ca2+ and reactive oxygen species signaling. *Journal of Cell Science*, *126*(14), 2965–2978. https://doi.org/10.1242/jcs.093609

Enari, M., Sakahira, H., Yokoyama, H., Okawa, K., Iwamatsu, A., & Nagata, S. (1998). A caspase-activated DNase that degrades DNA during apoptosis, and its inhibitor ICAD. *Nature*, *391*(6662), 43–50. https://doi.org/10.1038/34112

Faitg, J., D'Amico, D., Rinsch, C., & Singh, A. (2024). Mitophagy Activation by Urolithin A to Target Muscle Aging. *Calcified Tissue International*, *114*(1), 53–59. https://doi.org/10.1007/s00223-023-01145-5

Farid, M., Reid, M. B., Li, Y.-P., Gerken, E., & Durham, W. J. (2005). Effects of dietary curcumin or N-acetylcysteine on NF-kappaB activity and contractile performance in ambulatory and unloaded murine soleus. *Nutrition & Metabolism*, *2*, 20. https://doi.org/10.1186/1743-7075-2-20

Favaro, G., Romanello, V., Varanita, T., Andrea Desbats, M., Morbidoni, V., Tezze, C., Albiero, M., Canato, M., Gherardi, G., De Stefani, D., Mammucari, C., Blaauw, B., Boncompagni, S., Protasi, F., Reggiani, C., Scorrano, L., Salviati, L., & Sandri, M. (2019). DRP1-mediated mitochondrial shape controls calcium homeostasis and muscle mass. *Nature Communications*, *10*(1), 2576. https://doi.org/10.1038/s41467-019-10226-9

Fischer, F., Hamann, A., & Osiewacz, H. D. (2012). Mitochondrial quality control: An integrated network of pathways. *Trends in Biochemical Sciences*, *37*(7), 284–292. https://doi.org/10.1016/j.tibs.2012.02.004

Franco-Iborra, S., Vila, M., & Perier, C. (2018). Mitochondrial Quality Control in Neurodegenerative Diseases: Focus on Parkinson's Disease and Huntington's Disease. *Frontiers in Neuroscience*, *12*. https://www.frontiersin.org/articles/10.3389/fnins.2018.00342

Frank, M., Duvezin-Caubet, S., Koob, S., Occhipinti, A., Jagasia, R., Petcherski, A., Ruonala, M. O., Priault, M., Salin, B., & Reichert, A. S. (2012). Mitophagy is triggered by mild oxidative stress in a mitochondrial fission dependent manner. *Biochimica et Biophysica Acta (BBA) - Molecular Cell Research*, *1823*(12), 2297–2310. https://doi.org/10.1016/j.bbamcr.2012.08.007

Friedman, J. R., Mourier, A., Yamada, J., McCaffery, J. M., & Nunnari, J. (2015). MICOS coordinates with respiratory complexes and lipids to establish mitochondrial inner membrane architecture. *eLife*, *4*. https://doi.org/10.7554/eLife.07739

Friedman, J. R., & Nunnari, J. (2014). Mitochondrial form and function. *Nature*, *505*(7483), 335–343. https://doi.org/10.1038/nature12985

Fröhlich, C., Grabiger, S., Schwefel, D., Faelber, K., Rosenbaum, E., Mears, J., Rocks, O., & Daumke, O. (2013). Structural insights into oligomerization and mitochondrial remodelling of dynamin 1-like protein. *The EMBO Journal*, *32*(9), 1280–1292. https://doi.org/10.1038/emboj.2013.74

Galluzzi, L., Vitale, I., Aaronson, S. A., Abrams, J. M., Adam, D., Agostinis, P., Alnemri, E. S., Altucci, L., Amelio, I., Andrews, D. W., Annicchiarico-Petruzzelli, M., Antonov, A. V., Arama, E., Baehrecke, E. H., Barlev, N. A., Bazan, N. G., Bernassola, F., Bertrand, M. J. M., Bianchi, K., … Kroemer, G. (2018). Molecular mechanisms of cell death: Recommendations of the Nomenclature Committee on Cell Death 2018. *Cell Death and Differentiation*, *25*(3), 486–541. https://doi.org/10.1038/s41418-017-0012-4

García-Prat, L., Martínez-Vicente, M., Perdiguero, E., Ortet, L., Rodríguez-Ubreva, J., Rebollo, E., Ruiz-Bonilla, V., Gutarra, S., Ballestar, E., Serrano, A. L., Sandri, M., & Muñoz-Cánoves, P.

(2016). Autophagy maintains stemness by preventing senescence. *Nature*, *529*(7584), 37–42. https://doi.org/10.1038/nature16187

Garcia-Vallve, S. (2004). Contribution of each complex of the mitochondrial respiratory chain in the generation of the proton-motive force. *Biochemistry and Molecular Biology Education*, *32*(1), 17–19. https://doi.org/10.1002/bmb.2004.494032010308

Gattazzo, F., Laurent, B., Relaix, F., Rouard, H., & Didier, N. (2020). Distinct Phases of Postnatal Skeletal Muscle Growth Govern the Progressive Establishment of Muscle Stem Cell Quiescence. *Stem Cell Reports*, *15*(3), 597–611. https://doi.org/10.1016/j.stemcr.2020.07.011

Giovarelli, M., Zecchini, S., Martini, E., Garrè, M., Barozzi, S., Ripolone, M., Napoli, L., Coazzoli, M., Vantaggiato, C., Roux-Biejat, P., Cervia, D., Moscheni, C., Perrotta, C., Parazzoli, D., Clementi, E., & De Palma, C. (2020). Drp1 overexpression induces desmin disassembling and drives kinesin-1 activation promoting mitochondrial trafficking in skeletal muscle. *Cell Death & Differentiation*, *27*(8), 2383–2401. https://doi.org/10.1038/s41418-020-0510-7

Glancy, B., Hartnell, L. M., Malide, D., Yu, Z.-X., Combs, C. A., Connelly, P. S., Subramaniam, S., & Balaban, R. S. (2015). Mitochondrial reticulum for cellular energy distribution in muscle. *Nature*, *523*(7562), 617–620. https://doi.org/10.1038/nature14614

Gleyzer, N., & Scarpulla, R. C. (2011). PGC-1-related coactivator (PRC), a sensor of metabolic stress, orchestrates a redox-sensitive program of inflammatory gene expression. *The Journal of Biological Chemistry*, *286*(46), 39715–39725. https://doi.org/10.1074/jbc.M111.291575

Gokhin, D. S., Ward, S. R., Bremner, S. N., & Lieber, R. L. (2008). Quantitative analysis of neonatal skeletal muscle functional improvement in the mouse. *The Journal of Experimental Biology*, *211*(Pt 6), 837–843. https://doi.org/10.1242/jeb.014340

Gomes, L. C., Benedetto, G. D., & Scorrano, L. (2011). During autophagy mitochondria elongate, are spared from degradation and sustain cell viability. *Nature Cell Biology*, *13*(5), Article 5. https://doi.org/10.1038/ncb2220

Gouspillou, G., Godin, R., Piquereau, J., Picard, M., Mofarrahi, M., Mathew, J., Purves-Smith, F. M., Sgarioto, N., Hepple, R. T., Burelle, Y., & Hussain, S. N. A. (2018). Protective role of Parkin in skeletal muscle contractile and mitochondrial function. *The Journal of Physiology*, *596*(13), 2565–2579. https://doi.org/10.1113/JP275604

Graham, Z. A., Harlow, L., Bauman, W. A., & Cardozo, C. P. (2018). Alterations in mitochondrial fission, fusion, and mitophagic protein expression in the gastrocnemius of mice after a sciatic nerve transection. *Muscle & Nerve*, *58*(4), 592–599. https://doi.org/10.1002/mus.26197

Greene, A. W., Grenier, K., Aguileta, M. A., Muise, S., Farazifard, R., Haque, M. E., McBride, H. M., Park, D. S., & Fon, E. A. (2012). Mitochondrial processing peptidase regulates PINK1 processing, import and Parkin recruitment. *EMBO Reports*, *13*(4), 378–385. https://doi.org/10.1038/embor.2012.14

Guo, N., & Peng, Z. (2013). MG132, a proteasome inhibitor, induces apoptosis in tumor cells. *Asia-Pacific Journal of Clinical Oncology*, *9*(1), 6–11. https://doi.org/10.1111/j.1743-7563.2012.01535.x

Gustafsson, A. B., & Gottlieb, R. A. (2007). Bcl-2 family members and apoptosis, taken to heart. *American Journal of Physiology. Cell Physiology*, *292*(1), C45-51. https://doi.org/10.1152/ajpcell.00229.2006

H. Dehkordi, M., Tashakor, A., O'Connell, E., & Fearnhead, H. O. (2020). Apoptosome-dependent myotube formation involves activation of caspase-3 in differentiating myoblasts. *Cell Death & Disease*, *11*(5), 1–12. https://doi.org/10.1038/s41419-020-2502-4

Hanna, R. A., Quinsay, M. N., Orogo, A. M., Giang, K., Rikka, S., & Gustafsson, Å. B. (2012). Microtubule-associated protein 1 light chain 3 (LC3) interacts with Bnip3 protein to selectively remove endoplasmic reticulum and mitochondria via autophagy. *The Journal of Biological Chemistry*, *287*(23), 19094–19104. https://doi.org/10.1074/jbc.M111.322933

Hawke, T. J., & Garry, D. J. (2001). Myogenic satellite cells: Physiology to molecular biology. *Journal of Applied Physiology*, *91*(2), 534–551.

He, Y.-L., Gong, S.-H., Cheng, X., Zhao, M., Zhao, T., Zhao, Y.-Q., Fan, M., Zhu, L.-L., & Wu, L.-Y. (2020). BNIP3 phosphorylation by JNK1/2 promotes mitophagy via enhancing its stability under hypoxia. *bioRxiv*, 2020.08.27.271270. https://doi.org/10.1101/2020.08.27.271270

Heden, T. D., Johnson, J. M., Ferrara, P. J., Eshima, H., Verkerke, A. R. P., Wentzler, E. J., Siripoksup, P., Narowski, T. M., Coleman, C. B., Lin, C.-T., Ryan, T. E., Reidy, P. T., de Castro Brás, L. E., Karner, C. M., Burant, C. F., Maschek, J. A., Cox, J. E., Mashek, D. G., Kardon, G., … Funai, K. (2019). Mitochondrial PE potentiates respiratory enzymes to amplify skeletal muscle aerobic capacity. *Science Advances*, *5*(9), eaax8352. https://doi.org/10.1126/sciadv.aax8352

Hendgen-Cotta, U. B., Esfeld, S., Rudi, K., Miinalainen, I., Klare, J. P., & Rassaf, T. (2017). Cytosolic BNIP3 Dimer Interacts with Mitochondrial BAX Forming Heterodimers in the Mitochondrial Outer Membrane under Basal Conditions. *International Journal of Molecular Sciences*, *18*(4), 687. https://doi.org/10.3390/ijms18040687

Heo, J.-M., Ordureau, A., Paulo, J. A., Rinehart, J., & Harper, J. W. (2015). The PINK1-PARKIN Mitochondrial Ubiquitylation Pathway Drives a Program of OPTN/NDP52 Recruitment and TBK1 Activation to Promote Mitophagy. *Molecular Cell*, *60*(1), 7–20. https://doi.org/10.1016/j.molcel.2015.08.016

Holloszy, J. O. (1967). Biochemical Adaptations in Muscle: EFFECTS OF EXERCISE ON MITOCHONDRIAL OXYGEN UPTAKE AND RESPIRATORY ENZYME ACTIVITY IN SKELETAL MUSCLE. *Journal of Biological Chemistry*, *242*(9), 2278–2282. https://doi.org/10.1016/S0021-9258(18)96046-1

Hong, X., Isern, J., Campanario, S., Perdiguero, E., Ramírez-Pardo, I., Segalés, J., Hernansanz-Agustín, P., Curtabbi, A., Deryagin, O., Pollán, A., González-Reyes, J. A., Villalba, J. M., Sandri, M., Serrano, A. L., Enríquez, J. A., & Muñoz-Cánoves, P. (2022). Mitochondrial dynamics maintain muscle stem cell regenerative competence throughout adult life by regulating metabolism and mitophagy. *Cell Stem Cell*, *29*(9), 1298-1314.e10. https://doi.org/10.1016/j.stem.2022.07.009

Hoppeler, H., Lüthi, P., Claassen, H., Weibel, E. R., & Howald, H. (1973). The ultrastructure of the normal human skeletal muscle. *Pflügers Archiv*, *344*(3), 217–232. https://doi.org/10.1007/BF00588462

Hoque, A., Sivakumaran, P., Bond, S. T., Ling, N. X. Y., Kong, A. M., Scott, J. W., Bandara, N., Hernández, D., Liu, G.-S., Wong, R. C. B., Ryan, M. T., Hausenloy, D. J., Kemp, B. E., Oakhill, J. S., Drew, B. G., Pébay, A., & Lim, S. Y. (2018). Mitochondrial fission protein Drp1 inhibition promotes cardiac mesodermal differentiation of human pluripotent stem cells. *Cell Death Discovery*, *4*(1), 1–13. https://doi.org/10.1038/s41420-018-0042-9

Hyatt, H. W., & Powers, S. K. (2021). Mitochondrial Dysfunction Is a Common Denominator Linking Skeletal Muscle Wasting Due to Disease, Aging, and Prolonged Inactivity. *Antioxidants*, *10*(4), Article 4. https://doi.org/10.3390/antiox10040588

Iguchi, M., Kujuro, Y., Okatsu, K., Koyano, F., Kosako, H., Kimura, M., Suzuki, N., Uchiyama, S., Tanaka, K., & Matsuda, N. (2013). Parkin-catalyzed ubiquitin-ester transfer is triggered by PINK1-dependent phosphorylation. *The Journal of Biological Chemistry*, *288*(30), 22019–22032. https://doi.org/10.1074/jbc.M113.467530

Inoue-Yamauchi, A., & Oda, H. (2012). Depletion of mitochondrial fission factor DRP1 causes increased apoptosis in human colon cancer cells. *Biochemical and Biophysical Research Communications*, *421*(1), 81–85. https://doi.org/10.1016/j.bbrc.2012.03.118

Ishihara, N., Eura, Y., & Mihara, K. (2004). Mitofusin 1 and 2 play distinct roles in mitochondrial fusion reactions via GTPase activity. *Journal of Cell Science*, *117*(26), 6535–6546. https://doi.org/10.1242/jcs.01565

Jin, S. M., Lazarou, M., Wang, C., Kane, L. A., Narendra, D. P., & Youle, R. J. (2010). Mitochondrial membrane potential regulates PINK1 import and proteolytic destabilization by PARL. *The Journal of Cell Biology*, *191*(5), 933–942. https://doi.org/10.1083/jcb.201008084

Ju, J.-S., Jeon, S.-I., Park, J.-Y., Lee, J.-Y., Lee, S.-C., Cho, K.-J., & Jeong, J.-M. (2016). Autophagy plays a role in skeletal muscle mitochondrial biogenesis in an endurance exercise-trained condition. *The Journal of Physiological Sciences: JPS*, *66*(5), 417–430. https://doi.org/10.1007/s12576-016-0440-9

Kang, C., Yeo, D., & Ji, L. L. (2016). Muscle immobilization activates mitophagy and disrupts mitochondrial dynamics in mice. *Acta Physiologica (Oxford, England)*, *218*(3), 188–197. https://doi.org/10.1111/apha.12690

Kang, S. W. S., Haydar, G., Taniane, C., Farrell, G., Arias, I. M., Lippincott-Schwartz, J., & Fu, D. (2016). AMPK Activation Prevents and Reverses Drug-Induced Mitochondrial and Hepatocyte Injury by Promoting Mitochondrial Fusion and Function. *PloS One*, *11*(10), e0165638. https://doi.org/10.1371/journal.pone.0165638

Kappler, L., Hoene, M., Hu, C., von Toerne, C., Li, J., Bleher, D., Hoffmann, C., Böhm, A., Kollipara, L., Zischka, H., Königsrainer, A., Häring, H.-U., Peter, A., Xu, G., Sickmann, A., Hauck, S. M., Weigert, C., & Lehmann, R. (2019). Linking bioenergetic function of mitochondria to tissue-specific molecular fingerprints. *American Journal of Physiology. Endocrinology and Metabolism*, *317*(2), E374–E387. https://doi.org/10.1152/ajpendo.00088.2019

Kataura, T., Sedlackova, L., Otten, E. G., Kumari, R., Shapira, D., Scialo, F., Stefanatos, R., Ishikawa, K., Kelly, G., Seranova, E., Sun, C., Maetzel, D., Kenneth, N., Trushin, S., Zhang, T., Trushina, E., Bascom, C. C., Tasseff, R., Isfort, R. J., … Korolchuk, V. I. (2022). Autophagy promotes cell survival by maintaining NAD levels. *Developmental Cell*, *57*(22), 2584-2598.e11. https://doi.org/10.1016/j.devcel.2022.10.008

Kerr, J. S., Adriaanse, B. A., Greig, N. H., Mattson, M. P., Cader, M. Z., Bohr, V. A., & Fang, E. F. (2017). Mitophagy and Alzheimer's Disease: Cellular and Molecular Mechanisms. *Trends in Neurosciences*, *40*(3), 151–166. https://doi.org/10.1016/j.tins.2017.01.002

Khosravi, S., & Harner, M. E. (2020). The MICOS complex, a structural element of mitochondria with versatile functions. *Biological Chemistry*, *401*(6–7), 765–778. https://doi.org/10.1515/hsz-2020-0103

Kim, B., Kim, J.-S., Yoon, Y., Santiago, M. C., Brown, M. D., & Park, J.-Y. (2013). Inhibition of Drp1-dependent mitochondrial division impairs myogenic differentiation. *American Journal of Physiology. Regulatory, Integrative and Comparative Physiology*, *305*(8), R927-938. https://doi.org/10.1152/ajpregu.00502.2012

Kim, H., Rafiuddin-Shah, M., Tu, H.-C., Jeffers, J. R., Zambetti, G. P., Hsieh, J. J.-D., & Cheng, E. H.-Y. (2006). Hierarchical regulation of mitochondrion-dependent apoptosis by BCL-2 subfamilies. *Nature Cell Biology*, *8*(12), 1348–1358. https://doi.org/10.1038/ncb1499

Kim, Y., Parry, H. A., Willingham, T. B., Alspaugh, G., Lindberg, E., Combs, C. A., Knutson, J. R., Bleck, C. K. E., & Glancy, B. (2024). Reorganization of mitochondria-organelle interactions during postnatal development in skeletal muscle. *The Journal of Physiology*, *602*(5), 891–912. https://doi.org/10.1113/JP285014

Kim, Y., Triolo, M., Erlich, A. T., & Hood, D. A. (2019). Regulation of autophagic and mitophagic flux during chronic contractile activity-induced muscle adaptations. *Pflügers Archiv - European Journal of Physiology*, *471*(3), 431–440. https://doi.org/10.1007/s00424-018-2225-x

Kim, Y., Yang, D. S., Katti, P., & Glancy, B. (2019). Protein composition of the muscle mitochondrial reticulum during postnatal development. *The Journal of Physiology*, *597*(10), 2707–2727. https://doi.org/10.1113/JP277579

Kleele, T., Rey, T., Winter, J., Zaganelli, S., Mahecic, D., Perreten Lambert, H., Ruberto, F. P., Nemir, M., Wai, T., Pedrazzini, T., & Manley, S. (2021). Distinct fission signatures predict mitochondrial degradation or biogenesis. *Nature*, *593*(7859), Article 7859. https://doi.org/10.1038/s41586-021-03510-6

Koentjoro, B., Park, J.-S., & Sue, C. M. (2017). Nix restores mitophagy and mitochondrial function to protect against PINK1/Parkin-related Parkinson's disease. *Scientific Reports*, *7*, 44373. https://doi.org/10.1038/srep44373

Kondapalli, C., Kazlauskaite, A., Zhang, N., Woodroof, H. I., Campbell, D. G., Gourlay, R., Burchell, L., Walden, H., Macartney, T. J., Deak, M., Knebel, A., Alessi, D. R., & Muqit, M. M. K. (2012). PINK1 is activated by mitochondrial membrane potential depolarization and stimulates Parkin E3 ligase activity by phosphorylating Serine 65. *Open Biology*, *2*(5), 120080. https://doi.org/10.1098/rsob.120080

Kondo, H., Miura, M., Kodama, J., Ahmed, S. M., & Itokawa, Y. (1992). Role of iron in oxidative stress in skeletal muscle atrophied by immobilization. *Pflugers Archiv: European Journal of Physiology*, *421*(2–3), 295–297. https://doi.org/10.1007/BF00374844

Kraft, C. S., LeMoine, C. M. R., Lyons, C. N., Michaud, D., Mueller, C. R., & Moyes, C. D. (2006). Control of mitochondrial biogenesis during myogenesis. *American Journal of Physiology. Cell Physiology*, *290*(4), C1119-1127. https://doi.org/10.1152/ajpcell.00463.2005

Kraus, F., & Ryan, M. T. (2017). The constriction and scission machineries involved in mitochondrial fission. *Journal of Cell Science*, *130*(18), 2953–2960. https://doi.org/10.1242/jcs.199562

Kroemer, G., Galluzzi, L., & Brenner, C. (2007). Mitochondrial membrane permeabilization in cell death. *Physiological Reviews*, *87*(1), 99–163. https://doi.org/10.1152/physrev.00013.2006

Kubli, D. A., & Gustafsson, Å. B. (2012). Mitochondria and Mitophagy: The Yin and Yang of Cell Death Control. *Circulation Research*, *111*(9), 1208–1221. https://doi.org/10.1161/CIRCRESAHA.112.265819

Kühlbrandt, W. (2015). Structure and function of mitochondrial membrane protein complexes. *BMC Biology*, *13*(1), 89. https://doi.org/10.1186/s12915-015-0201-x

Kumar, R., & Reichert, A. S. (2021). Common Principles and Specific Mechanisms of Mitophagy from Yeast to Humans. *International Journal of Molecular Sciences*, *22*(9), Article 9. https://doi.org/10.3390/ijms22094363

Kuwana, T., Bouchier-Hayes, L., Chipuk, J. E., Bonzon, C., Sullivan, B. A., Green, D. R., & Newmeyer, D. D. (2005). BH3 domains of BH3-only proteins differentially regulate Bax-mediated mitochondrial membrane permeabilization both directly and indirectly. *Molecular Cell*, *17*(4), 525–535. https://doi.org/10.1016/j.molcel.2005.02.003

Lai, L., Leone, T. C., Zechner, C., Schaeffer, P. J., Kelly, S. M., Flanagan, D. P., Medeiros, D. M., Kovacs, A., & Kelly, D. P. (2008). Transcriptional coactivators PGC-1alpha and PGC-lbeta control overlapping programs required for perinatal maturation of the heart. *Genes & Development*, *22*(14), 1948–1961. https://doi.org/10.1101/gad.1661708

Lampert, M. A., Orogo, A. M., Najor, R. H., Hammerling, B. C., Leon, L. J., Wang, B. J., Kim, T., Sussman, M. A., & Gustafsson, Å. B. (2019). BNIP3L/NIX and FUNDC1-mediated mitophagy is required for mitochondrial network remodeling during cardiac progenitor cell differentiation. *Autophagy*, *15*(7), 1182–1198. https://doi.org/10.1080/15548627.2019.1580095

Lazarou, M., Jin, S. M., Kane, L. A., & Youle, R. J. (2012). Role of PINK1 binding to the TOM complex and alternate intracellular membranes in recruitment and activation of the E3 ligase Parkin. *Developmental Cell*, *22*(2), 320–333. https://doi.org/10.1016/j.devcel.2011.12.014

Lazarou, M., Sliter, D. A., Kane, L. A., Sarraf, S. A., Wang, C., Burman, J. L., Sideris, D. P., Fogel, A. I., & Youle, R. J. (2015). The ubiquitin kinase PINK1 recruits autophagy receptors to induce mitophagy. *Nature*, *524*(7565), 309–314. https://doi.org/10.1038/nature14893

LeBlanc, A., Rowe, R., Evans, H., West, S., Shackelford, L., & Schneider, V. (1997). Muscle atrophy during long duration bed rest. *International Journal of Sports Medicine*, *18 Suppl 4*, S283-285. https://doi.org/10.1055/s-2007-972726

LeBleu, V. S., O'Connell, J. T., Gonzalez Herrera, K. N., Wikman, H., Pantel, K., Haigis, M. C., de Carvalho, F. M., Damascena, A., Domingos Chinen, L. T., Rocha, R. M., Asara, J. M., & Kalluri, R. (2014). PGC-1α mediates mitochondrial biogenesis and oxidative phosphorylation in cancer cells to promote metastasis. *Nature Cell Biology*, *16*(10), Article 10. https://doi.org/10.1038/ncb3039

Leduc-Gaudet, J.-P., Hussain, S. N. A., Barreiro, E., & Gouspillou, G. (2021). Mitochondrial Dynamics and Mitophagy in Skeletal Muscle Health and Aging. *International Journal of Molecular Sciences*, *22*(15), Article 15. https://doi.org/10.3390/ijms22158179

Lee, Y., Lee, H.-Y., Hanna, R. A., & Gustafsson, Å. B. (2011). Mitochondrial autophagy by Bnip3 involves Drp1-mediated mitochondrial fission and recruitment of Parkin in cardiac myocytes. *American Journal of Physiology - Heart and Circulatory Physiology*, *301*(5), H1924–H1931. https://doi.org/10.1152/ajpheart.00368.2011

Leeuwenburgh, C., Gurley, C. M., Strotman, B. A., & Dupont-Versteegden, E. E. (2005). Age-related differences in apoptosis with disuse atrophy in soleus muscle. *American Journal of Physiology-Regulatory, Integrative and Comparative Physiology*, *288*(5), R1288–R1296. https://doi.org/10.1152/ajpregu.00576.2004

Lei, Y., Gan, M., Qiu, Y., Chen, Q., Wang, X., Liao, T., Zhao, M., Chen, L., Zhang, S., Zhao, Y., Niu, L., Wang, Y., Zhu, L., & Shen, L. (2024). The role of mitochondrial dynamics and mitophagy in skeletal muscle atrophy: From molecular mechanisms to therapeutic insights. *Cellular & Molecular Biology Letters*, *29*(1), 59. https://doi.org/10.1186/s11658-024-00572-y

Lelliott, C. J., Medina-Gomez, G., Petrovic, N., Kis, A., Feldmann, H. M., Bjursell, M., Parker, N., Curtis, K., Campbell, M., Hu, P., Zhang, D., Litwin, S. E., Zaha, V. G., Fountain, K. T., Boudina, S., Jimenez-Linan, M., Blount, M., Lopez, M., Meirhaeghe, A., … Vidal-Puig, A. (2006). Ablation of PGC-1beta results in defective mitochondrial activity, thermogenesis, hepatic function, and cardiac performance. *PLoS Biology*, *4*(11), e369. https://doi.org/10.1371/journal.pbio.0040369

Leone, T. C., Lehman, J. J., Finck, B. N., Schaeffer, P. J., Wende, A. R., Boudina, S., Courtois, M., Wozniak, D. F., Sambandam, N., Bernal-Mizrachi, C., Chen, Z., Holloszy, J. O., Medeiros, D. M., Schmidt, R. E., Saffitz, J. E., Abel, E. D., Semenkovich, C. F., & Kelly, D. P. (2005). PGC-1alpha deficiency causes multi-system energy metabolic derangements: Muscle dysfunction, abnormal weight control and hepatic steatosis. *PLoS Biology*, *3*(4), e101. https://doi.org/10.1371/journal.pbio.0030101

Letai, A., Bassik, M. C., Walensky, L. D., Sorcinelli, M. D., Weiler, S., & Korsmeyer, S. J. (2002). Distinct BH3 domains either sensitize or activate mitochondrial apoptosis, serving as prototype cancer therapeutics. *Cancer Cell*, *2*(3), 183–192. https://doi.org/10.1016/s1535-6108(02)00127-7

Li, M., Zhao, L., Liu, J., Liu, A., Jia, C., Ma, D., Jiang, Y., & Bai, X. (2010). Multi-mechanisms are involved in reactive oxygen species regulation of mTORC1 signaling. *Cellular Signalling*, *22*(10), 1469–1476. https://doi.org/10.1016/j.cellsig.2010.05.015

Li, Y., Huang, T.-T., Carlson, E. J., Melov, S., Ursell, P. C., Olson, J. L., Noble, L. J., Yoshimura, M. P., Berger, C., Chan, P. H., Wallace, D. C., & Epstein, C. J. (1995). Dilated cardiomyopathy and neonatal lethality in mutant mice lacking manganese superoxide dismutase. *Nature Genetics*, *11*(4), 376–381. https://doi.org/10.1038/ng1295-376

Li, Y., Wang, Y., Kim, E., Beemiller, P., Wang, C.-Y., Swanson, J., You, M., & Guan, K.-L. (2007). Bnip3 mediates the hypoxia-induced inhibition on mammalian target of rapamycin by interacting with Rheb. *The Journal of Biological Chemistry*, *282*(49), 35803–35813. https://doi.org/10.1074/jbc.M705231200

Liang, H., & Ward, W. F. (2006). PGC-1α: A key regulator of energy metabolism. *Advances in Physiology Education*, *30*(4), 145–151. https://doi.org/10.1152/advan.00052.2006

Lin, J., Wu, P.-H., Tarr, P. T., Lindenberg, K. S., St-Pierre, J., Zhang, C.-Y., Mootha, V. K., Jäger, S., Vianna, C. R., Reznick, R. M., Cui, L., Manieri, M., Donovan, M. X., Wu, Z., Cooper, M. P., Fan, M. C., Rohas, L. M., Zavacki, A. M., Cinti, S., … Spiegelman, B. M. (2004). Defects in adaptive energy metabolism with CNS-linked hyperactivity in PGC-1alpha null mice. *Cell*, *119*(1), 121–135. https://doi.org/10.1016/j.cell.2004.09.013

Lin, K.-H., Wilson, G. M., Blanco, R., Steinert, N. D., Zhu, W. G., Coon, J. J., & Hornberger, T. A. (2021). A deep analysis of the proteomic and phosphoproteomic alterations that occur in skeletal muscle after the onset of immobilization. *The Journal of Physiology*, *599*(11), 2887–2906. https://doi.org/10.1113/JP281071

Lira, V. A., Okutsu, M., Zhang, M., Greene, N. P., Laker, R. C., Breen, D. S., Hoehn, K. L., & Yan, Z. (2013). Autophagy is required for exercise training-induced skeletal muscle adaptation and improvement of physical performance. *FASEB Journal: Official Publication of the Federation of American Societies for Experimental Biology*, *27*(10), 4184–4193. https://doi.org/10.1096/fj.13-228486

Liu, J., Liu, W., Li, R., & Yang, H. (2019). Mitophagy in Parkinson's Disease: From Pathogenesis to Treatment. *Cells*, *8*(7). https://doi.org/10.3390/cells8070712

Liu, K., Zhao, Q., Sun, H., Liu, L., Wang, C., Li, Z., Xu, Y., Wang, L., Zhang, L., Zhang, H., Chen, Q., & Zhao, T. (2022). BNIP3 (BCL2 interacting protein 3) regulates pluripotency by modulating mitochondrial homeostasis via mitophagy. *Cell Death & Disease*, *13*(4), 334. https://doi.org/10.1038/s41419-022-04795-9

Liu, S., D'Amico, D., Shankland, E., Bhayana, S., Garcia, J. M., Aebischer, P., Rinsch, C., Singh, A., & Marcinek, D. J. (2022). Effect of Urolithin A Supplementation on Muscle Endurance and Mitochondrial Health in Older Adults: A Randomized Clinical Trial. *JAMA Network Open*, *5*(1), e2144279. https://doi.org/10.1001/jamanetworkopen.2021.44279

Luan, P., D'Amico, D., Andreux, P. A., Laurila, P.-P., Wohlwend, M., Li, H., Imamura de Lima, T., Place, N., Rinsch, C., Zanou, N., & Auwerx, J. (2021). Urolithin A improves muscle function by inducing mitophagy in muscular dystrophy. *Science Translational Medicine*, *13*(588), eabb0319. https://doi.org/10.1126/scitranslmed.abb0319

Luff, A. R., & Atwood, H. L. (1971). Changes in the sarcoplasmic reticulum and transverse tubular system of fast and slow skeletal muscles of the mouse during postnatal development. *The Journal of Cell Biology*, *51*(21), 369–383. https://doi.org/10.1083/jcb.51.2.369

Madeira, V. M. C. (2012). Overview of Mitochondrial Bioenergetics. In C. M. Palmeira & A. J. Moreno (Eds.), *Mitochondrial Bioenergetics: Methods and Protocols* (pp. 1–6). Humana Press. https://doi.org/10.1007/978-1-61779-382-0_1

Maharjan, S., Oku, M., Tsuda, M., Hoseki, J., & Sakai, Y. (2014). Mitochondrial impairment triggers cytosolic oxidative stress and cell death following proteasome inhibition. *Scientific Reports*, *4*(1), 5896. https://doi.org/10.1038/srep05896

Marshall, R. S., Li, F., Gemperline, D. C., Book, A. J., & Vierstra, R. D. (2021). Autophagic Degradation of the 26S Proteasome Is Mediated by the Dual ATG8/Ubiquitin Receptor RPN10 in Arabidopsis. *Molecular Cell*, *81*(9), 2053. https://doi.org/10.1016/j.molcel.2021.03.026

Marusic, U., Narici, M., Simunic, B., Pisot, R., & Ritzmann, R. (2021). Nonuniform loss of muscle strength and atrophy during bed rest: A systematic review. *Journal of Applied Physiology*, *131*(1), 194–206. https://doi.org/10.1152/japplphysiol.00363.2020

Masiero, E., Agatea, L., Mammucari, C., Blaauw, B., Loro, E., Komatsu, M., Metzger, D., Reggiani, C., Schiaffino, S., & Sandri, M. (2009). Autophagy is required to maintain muscle mass. *Cell Metabolism*, *10*(6), 507–515. https://doi.org/10.1016/j.cmet.2009.10.008

Matsuda, N., Sato, S., Shiba, K., Okatsu, K., Saisho, K., Gautier, C. A., Sou, Y.-S., Saiki, S., Kawajiri, S., Sato, F., Kimura, M., Komatsu, M., Hattori, N., & Tanaka, K. (2010). PINK1 stabilized by mitochondrial depolarization recruits Parkin to damaged mitochondria and activates latent Parkin for mitophagy. *The Journal of Cell Biology*, *189*(2), 211–221. https://doi.org/10.1083/jcb.200910140

McClung, J. M., Judge, A. R., Powers, S. K., & Yan, Z. (2010). P38 MAPK links oxidative stress to autophagy-related gene expression in cachectic muscle wasting. *American Journal of Physiology - Cell Physiology*, *298*(3), C542. https://doi.org/10.1152/ajpcell.00192.2009

McMillan, E. M., & Quadrilatero, J. (2014). Autophagy is required and protects against apoptosis during myoblast differentiation. *The Biochemical Journal*, *462*(2), 267–277. https://doi.org/10.1042/BJ20140312

Mears, J. A., Lackner, L. L., Fang, S., Ingerman, E., Nunnari, J., & Hinshaw, J. E. (2011). Conformational changes in Dnm1 support a contractile mechanism for mitochondrial fission. *Nature Structural & Molecular Biology*, *18*(1), 20–26. https://doi.org/10.1038/nsmb.1949

Meissner, C., Lorenz, H., Weihofen, A., Selkoe, D. J., & Lemberg, M. K. (2011). The mitochondrial intramembrane protease PARL cleaves human Pink1 to regulate Pink1 trafficking. *Journal of Neurochemistry*, *117*(5), 856–867. https://doi.org/10.1111/j.1471-4159.2011.07253.x

Mierzejewski, B., Archacka, K., Grabowska, I., Florkowska, A., Ciemerych, M. A., & Brzoska, E. (2020). Human and mouse skeletal muscle stem and progenitor cells in health and disease. *Seminars in Cell & Developmental Biology*, *104*, 93–104. https://doi.org/10.1016/j.semcdb.2020.01.004

Minai, L., Martinovic, J., Chretien, D., Dumez, F., Razavi, F., Munnich, A., & Rötig, A. (2008). Mitochondrial respiratory chain complex assembly and function during human fetal development. *Molecular Genetics and Metabolism*, *94*(1), 120–126. https://doi.org/10.1016/j.ymgme.2007.12.007

Mirzoev, T. M. (2020). Skeletal Muscle Recovery from Disuse Atrophy: Protein Turnover Signaling and Strategies for Accelerating Muscle Regrowth. *International Journal of Molecular Sciences*, *21*(21), Article 21. https://doi.org/10.3390/ijms21217940

Mofarrahi, M., Guo, Y., Haspel, J. A., Choi, A. M. K., Davis, E. C., Gouspillou, G., Hepple, R. T., Godin, R., Burelle, Y., & Hussain, S. N. A. (2013). Autophagic flux and oxidative capacity of skeletal muscles during acute starvation. *Autophagy*, *9*(10), 1604–1620. https://doi.org/10.4161/auto.25955

Morales, P. E., Monsalves-Álvarez, M., Tadinada, S. M., Harris, M. P., Ramírez-Sagredo, A., Ortiz-Quintero, J., Troncoso, M. F., De Gregorio, N., Calle, X., Pereira, R. O., Lira, V. A., Espinosa, A., Abel, E. D., & Lavandero, S. (2021). Skeletal muscle type-specific mitochondrial adaptation to high-fat diet relies on differential autophagy modulation. *FASEB Journal:*

Official Publication of the Federation of American Societies for Experimental Biology, *35*(10), e21933. https://doi.org/10.1096/fj.202001593RR

Morita, M., Prudent, J., Basu, K., Goyon, V., Katsumura, S., Hulea, L., Pearl, D., Siddiqui, N., Strack, S., McGuirk, S., St-Pierre, J., Larsson, O., Topisirovic, I., Vali, H., McBride, H. M., Bergeron, J. J., & Sonenberg, N. (2017). mTOR Controls Mitochondrial Dynamics and Cell Survival via MTFP1. *Molecular Cell*, *67*(6), 922-935.e5. https://doi.org/10.1016/j.molcel.2017.08.013

Moyes, C. D., Mathieu-Costello, O. A., Tsuchiya, N., Filburn, C., & Hansford, R. G. (1997). Mitochondrial biogenesis during cellular differentiation. *The American Journal of Physiology*, *272*(4 Pt 1), C1345-1351. https://doi.org/10.1152/ajpcell.1997.272.4.C1345

Muller, F. L., Song, W., Jang, Y. C., Liu, Y., Sabia, M., Richardson, A., & Van Remmen, H. (2007). Denervation-induced skeletal muscle atrophy is associated with increased mitochondrial ROS production. *American Journal of Physiology. Regulatory, Integrative and Comparative Physiology*, *293*(3), R1159-1168. https://doi.org/10.1152/ajpregu.00767.2006

Narendra, D. P., Jin, S. M., Tanaka, A., Suen, D.-F., Gautier, C. A., Shen, J., Cookson, M. R., & Youle, R. J. (2010). PINK1 Is Selectively Stabilized on Impaired Mitochondria to Activate Parkin. *PLOS Biology*, *8*(1), e1000298. https://doi.org/10.1371/journal.pbio.1000298

Neel, B. A., Zong, H., Backer, J. M., & Pessin, J. E. (2015). Identification of Atypical Peri-Nuclear Multivesicular Bodies in Oxidative and Glycolytic Skeletal Muscle of Aged and Pompe's Disease Mouse Models. *Frontiers in Physiology*, *6*, 393. https://doi.org/10.3389/fphys.2015.00393

Nielsen, J., Gejl, K. D., Hey-Mogensen, M., Holmberg, H., Suetta, C., Krustrup, P., Elemans, C. P. H., & Ørtenblad, N. (2017). Plasticity in mitochondrial cristae density allows metabolic

capacity modulation in human skeletal muscle. *The Journal of Physiology*, *595*(9), 2839–2847. https://doi.org/10.1113/JP273040

Novak, I., Kirkin, V., McEwan, D. G., Zhang, J., Wild, P., Rozenknop, A., Rogov, V., Löhr, F., Popovic, D., Occhipinti, A., Reichert, A. S., Terzic, J., Dötsch, V., Ney, P. A., & Dikic, I. (2010). Nix is a selective autophagy receptor for mitochondrial clearance. *EMBO Reports*, *11*(1), 45–51. https://doi.org/10.1038/embor.2009.256

Ogborn, D. I., McKay, B. R., Crane, J. D., Safdar, A., Akhtar, M., Parise, G., & Tarnopolsky, M. A. (2015). Effects of age and unaccustomed resistance exercise on mitochondrial transcript and protein abundance in skeletal muscle of men. *American Journal of Physiology-Regulatory, Integrative and Comparative Physiology*, *308*(8), R734–R741. https://doi.org/10.1152/ajpregu.00005.2014

Okatsu, K., Oka, T., Iguchi, M., Imamura, K., Kosako, H., Tani, N., Kimura, M., Go, E., Koyano, F., Funayama, M., Shiba-Fukushima, K., Sato, S., Shimizu, H., Fukunaga, Y., Taniguchi, H., Komatsu, M., Hattori, N., Mihara, K., Tanaka, K., & Matsuda, N. (2012). PINK1 autophosphorylation upon membrane potential dissipation is essential for Parkin recruitment to damaged mitochondria. *Nature Communications*, *3*, 1016. https://doi.org/10.1038/ncomms2016

Okatsu, K., Uno, M., Koyano, F., Go, E., Kimura, M., Oka, T., Tanaka, K., & Matsuda, N. (2013). A dimeric PINK1-containing complex on depolarized mitochondria stimulates Parkin recruitment. *The Journal of Biological Chemistry*, *288*(51), 36372–36384. https://doi.org/10.1074/jbc.M113.509653

Ong, S.-B., Subrayan, S., Lim, S. Y., Yellon, D. M., Davidson, S. M., & Hausenloy, D. J. (2010). Inhibiting mitochondrial fission protects the heart against ischemia/reperfusion injury. *Circulation*, *121*(18), 2012–2022. https://doi.org/10.1161/CIRCULATIONAHA.109.906610

Ørtenblad, N., Nielsen, J., Boushel, R., Söderlund, K., Saltin, B., & Holmberg, H.-C. (2018). The Muscle Fiber Profiles, Mitochondrial Content, and Enzyme Activities of the Exceptionally Well-Trained Arm and Leg Muscles of Elite Cross-Country Skiers. *Frontiers in Physiology*, *9*. https://www.frontiersin.org/articles/10.3389/fphys.2018.01031

Osellame, L. D., Singh, A. P., Stroud, D. A., Palmer, C. S., Stojanovski, D., Ramachandran, R., & Ryan, M. T. (2016). Cooperative and independent roles of the Drp1 adaptors Mff, MiD49 and MiD51 in mitochondrial fission. *Journal of Cell Science*, *129*(11), 2170–2181. https://doi.org/10.1242/jcs.185165

Papanicolaou, K. N., Khairallah, R. J., Ngoh, G. A., Chikando, A., Luptak, I., O'Shea, K. M., Riley, D. D., Lugus, J. J., Colucci, W. S., Lederer, W. J., Stanley, W. C., & Walsh, K. (2011). Mitofusin-2 maintains mitochondrial structure and contributes to stress-induced permeability transition in cardiac myocytes. *Molecular and Cellular Biology*, *31*(6), 1309–1328. https://doi.org/10.1128/MCB.00911-10

Paré, M. F., Baechler, B. L., Fajardo, V. A., Earl, E., Wong, E., Campbell, T. L., Tupling, A. R., & Quadrilatero, J. (2017). Effect of acute and chronic autophagy deficiency on skeletal muscle apoptotic signaling, morphology, and function. *Biochimica Et Biophysica Acta. Molecular Cell Research*, *1864*(4), 708–718. https://doi.org/10.1016/j.bbamcr.2016.12.015

Patten, D. A., Wong, J., Khacho, M., Soubannier, V., Mailloux, R. J., Pilon-Larose, K., MacLaurin, J. G., Park, D. S., McBride, H. M., Trinkle-Mulcahy, L., Harper, M.-E., Germain, M., & Slack, R. S. (2014). OPA1-dependent cristae modulation is essential for cellular adaptation to metabolic demand. *The EMBO Journal*, *33*(22), 2676–2691. https://doi.org/10.15252/embj.201488349

Pellegrino, M. A., Desaphy, J.-F., Brocca, L., Pierno, S., Camerino, D. C., & Bottinelli, R. (2011). Redox homeostasis, oxidative stress and disuse muscle atrophy. *The Journal of Physiology*, *589*(Pt 9), 2147–2160. https://doi.org/10.1113/jphysiol.2010.203232

Petrick, H. L., Handy, R. M., Vachon, B., Frangos, S. M., Holwerda, A. M., Gijsen, A. P., Senden, J. M., van Loon, L. J. C., & Holloway, G. P. (2023). Dietary nitrate preserves mitochondrial bioenergetics and mitochondrial protein synthesis rates during short-term immobilization in mice. *The Journal of Physiology*. https://doi.org/10.1113/JP284701

Picard, M., Gentil, B. J., McManus, M. J., White, K., St. Louis, K., Gartside, S. E., Wallace, D. C., & Turnbull, D. M. (2013). Acute exercise remodels mitochondrial membrane interactions in mouse skeletal muscle. *Journal of Applied Physiology*, *115*(10), 1562–1571. https://doi.org/10.1152/japplphysiol.00819.2013

Picard, M., McManus, M. J., Csordás, G., Várnai, P., Dorn II, G. W., Williams, D., Hajnóczky, G., & Wallace, D. C. (2015). Trans-mitochondrial coordination of cristae at regulated membrane junctions. *Nature Communications*, *6*(1), Article 1. https://doi.org/10.1038/ncomms7259

Picard, M., White, K., & Turnbull, D. M. (2013). Mitochondrial morphology, topology, and membrane interactions in skeletal muscle: A quantitative three-dimensional electron

microscopy study. *Journal of Applied Physiology (Bethesda, Md.: 1985)*, *114*(2), 161–171. https://doi.org/10.1152/japplphysiol.01096.2012

Plotkin, D. L., Mattingly, M. L., Anglin, D. A., Michel, J. M., Godwin, J. S., McIntosh, M. C., Bergamasco, J. G. A., Scarpelli, M. C., Angleri, V., Taylor, L. W., Willoughby, D. S., Mobley, C. B., Kavazis, A. N., Ugrinowitsch, C., Libardi, C. A., & Roberts, M. D. (2024). Skeletal muscle myosin heavy chain protein fragmentation as a potential marker of protein degradation in response to resistance training and disuse atrophy. *bioRxiv: The Preprint Server for Biology*, 2024.05.24.595789. https://doi.org/10.1101/2024.05.24.595789

Ploumi, C., Daskalaki, I., & Tavernarakis, N. (2017). Mitochondrial biogenesis and clearance: A balancing act. *The FEBS Journal*, *284*(2), 183–195. https://doi.org/10.1111/febs.13820

Popov, D. V., Lysenko, E. A., Kuzmin, I. V., Vinogradova, V., & Grigoriev, A. I. (2015). Regulation of PGC-1α Isoform Expression in Skeletal Muscles. *Acta Naturae*, *7*(1), 48–59.

Powers, S. K., Smuder, A., & Judge, A. (2012). Oxidative stress and disuse muscle atrophy: Cause or consequence? *Current Opinion in Clinical Nutrition and Metabolic Care*, *15*(3), 240–245. https://doi.org/10.1097/MCO.0b013e328352b4c2

Qi, Z., He, Q., Ji, L., & Ding, S. (2014). Antioxidant Supplement Inhibits Skeletal Muscle Constitutive Autophagy rather than Fasting-Induced Autophagy in Mice. *Oxidative Medicine and Cellular Longevity*, *2014*, 315896. https://doi.org/10.1155/2014/315896

Rahman, F. A., Baechler, B. L., & Quadrilatero, J. (2024). Key considerations for investigating and interpreting autophagy in skeletal muscle. *Autophagy*, 1–12. https://doi.org/10.1080/15548627.2024.2373676

Rahman, F. A., & Quadrilatero, J. (2021a). Emerging role of mitophagy in myoblast differentiation and skeletal muscle remodeling. *Seminars in Cell & Developmental Biology*. https://doi.org/10.1016/j.semcdb.2021.11.026

Rahman, F. A., & Quadrilatero, J. (2021b). Mitochondrial network remodeling: An important feature of myogenesis and skeletal muscle regeneration. *Cellular and Molecular Life Sciences: CMLS*, *78*(10), 4653–4675. https://doi.org/10.1007/s00018-021-03807-9

Rahman, F. A., & Quadrilatero, J. (2022). Mitochondrial Apoptotic Signaling Involvement in Remodeling During Myogenesis and Skeletal Muscle Atrophy. *Seminars in Cell & Developmental Biology*. https://doi.org/10.1016/j.semcdb.2022.01.011

Rajasekaran, N. S., Shelar, S. B., Jones, D. P., & Hoidal, J. R. (2020). Reductive stress impairs myogenic differentiation. *Redox Biology*, *34*, 101492. https://doi.org/10.1016/j.redox.2020.101492

Ramachandran, R. (2018). Mitochondrial dynamics: The dynamin superfamily and execution by collusion. *Seminars in Cell & Developmental Biology*, *76*, 201–212. https://doi.org/10.1016/j.semcdb.2017.07.039

Ramos, E. S., Motori, E., Brüser, C., Kühl, I., Yeroslaviz, A., Ruzzenente, B., Kauppila, J. H. K., Busch, J. D., Hultenby, K., Habermann, B. H., Jakobs, S., Larsson, N.-G., & Mourier, A. (2019). Mitochondrial fusion is required for regulation of mitochondrial DNA replication. *PLOS Genetics*, *15*(6), e1008085. https://doi.org/10.1371/journal.pgen.1008085

Ray, R., Chen, G., Vande Velde, C., Cizeau, J., Park, J. H., Reed, J. C., Gietz, R. D., & Greenberg, A. H. (2000). BNIP3 Heterodimerizes with Bcl-2/Bcl-XL and Induces Cell Death Independent of a Bcl-2 Homology 3 (BH3) Domain at Both Mitochondrial and Nonmitochondrial Sites*.

Journal of Biological Chemistry, *275*(2), 1439–1448. https://doi.org/10.1074/jbc.275.2.1439

Redpath, C. J., Khalil, M. B., Drozdzal, G., Radisic, M., & McBride, H. M. (2013). Mitochondrial Hyperfusion during Oxidative Stress Is Coupled to a Dysregulation in Calcium Handling within a C2C12 Cell Model. *PLOS ONE*, *8*(7), e69165. https://doi.org/10.1371/journal.pone.0069165

Remels, A. H. V., Langen, R. C. J., Schrauwen, P., Schaart, G., Schols, A. M. W. J., & Gosker, H. R. (2010). Regulation of mitochondrial biogenesis during myogenesis. *Molecular and Cellular Endocrinology*, *315*(1–2), 113–120. https://doi.org/10.1016/j.mce.2009.09.029

Rikka, S., Quinsay, M. N., Thomas, R. L., Kubli, D. A., Zhang, X., Murphy, A. N., & Gustafsson, Å. B. (2011). Bnip3 impairs mitochondrial bioenergetics and stimulates mitochondrial turnover. *Cell Death and Differentiation*, *18*(4), 721–731. https://doi.org/10.1038/cdd.2010.146

Rimbaud, S., Garnier, A., & Ventura-Clapier, R. (2009). Mitochondrial biogenesis in cardiac pathophysiology. *Pharmacological Reports*, *61*(1), 131–138. https://doi.org/10.1016/S1734-1140(09)70015-5

Ristevski, S., O'Leary, D. A., Thornell, A. P., Owen, M. J., Kola, I., & Hertzog, P. J. (2004). The ETS transcription factor GABPalpha is essential for early embryogenesis. *Molecular and Cellular Biology*, *24*(13), 5844–5849. https://doi.org/10.1128/MCB.24.13.5844-5849.2004

Robinson, M. M., Sather, B. K., Burney, E. R., Ehrlicher, S. E., Stierwalt, H. D., Franco, M. C., & Newsom, S. A. (2019). Robust intrinsic differences in mitochondrial respiration and H2O2

emission between L6 and C2C12 cells. *American Journal of Physiology-Cell Physiology*, *317*(2), C339–C347. https://doi.org/10.1152/ajpcell.00343.2018

Romanello, V., Guadagnin, E., Gomes, L., Roder, I., Sandri, C., Petersen, Y., Milan, G., Masiero, E., Del Piccolo, P., Foretz, M., Scorrano, L., Rudolf, R., & Sandri, M. (2010). Mitochondrial fission and remodelling contributes to muscle atrophy. *The EMBO Journal*, *29*(10), 1774–1785. https://doi.org/10.1038/emboj.2010.60

Romanello, V., & Sandri, M. (2010). Mitochondrial biogenesis and fragmentation as regulators of muscle protein degradation. *Current Hypertension Reports*, *12*(6), 433–439. https://doi.org/10.1007/s11906-010-0157-8

Rowe, G. C., Jiang, A., & Arany, Z. (2010). PGC-1 coactivators in cardiac development and disease. *Circulation Research*, *107*(7), 825–838. https://doi.org/10.1161/CIRCRESAHA.110.223818

Rudrappa, S. S., Wilkinson, D. J., Greenhaff, P. L., Smith, K., Idris, I., & Atherton, P. J. (2016). Human Skeletal Muscle Disuse Atrophy: Effects on Muscle Protein Synthesis, Breakdown, and Insulin Resistance—A Qualitative Review. *Frontiers in Physiology*, *0*. https://doi.org/10.3389/fphys.2016.00361

Ruprecht, J. J., & Kunji, E. R. S. (2020). The SLC25 Mitochondrial Carrier Family: Structure and Mechanism. *Trends in Biochemical Sciences*, *45*(3), 244–258. https://doi.org/10.1016/j.tibs.2019.11.001

Russ, D. W., Krause, J., Wills, A., & Arreguin, R. (2012). “SR stress” in mixed hindlimb muscles of aging male rats. *Biogerontology*, *13*(5), 547–555. https://doi.org/10.1007/s10522-012-9399-y

Ryu, D., Mouchiroud, L., Andreux, P. A., Katsyuba, E., Moullan, N., Nicolet-Dit-Félix, A. A., Williams, E. G., Jha, P., Lo Sasso, G., Huzard, D., Aebischer, P., Sandi, C., Rinsch, C., & Auwerx, J. (2016). Urolithin A induces mitophagy and prolongs lifespan in C. elegans and increases muscle function in rodents. *Nature Medicine*, *22*(8), 879–888. https://doi.org/10.1038/nm.4132

Saikumar, P., Dong, Z., Mikhailov, V., Denton, M., Weinberg, J. M., & Venkatachalam, M. A. (1999). Apoptosis: Definition, mechanisms, and relevance to disease. *The American Journal of Medicine*, *107*(5), 489–506. https://doi.org/10.1016/s0002-9343(99)00259-4

Sakahira, H., Enari, M., & Nagata, S. (1998). Cleavage of CAD inhibitor in CAD activation and DNA degradation during apoptosis. *Nature*, *391*(6662), 96–99. https://doi.org/10.1038/34214

Sakellariou, G. K., Pearson, T., Lightfoot, A. P., Nye, G. A., Wells, N., Giakoumaki, I. I., Vasilaki, A., Griffiths, R. D., Jackson, M. J., & McArdle, A. (2016). Mitochondrial ROS regulate oxidative damage and mitophagy but not age-related muscle fiber atrophy. *Scientific Reports*, *6*(1), 33944. https://doi.org/10.1038/srep33944

Sakellariou, P., O'Neill, A., Mueller, A. L., Stadler, G., Wright, W. E., Roche, J. A., & Bloch, R. J. (2016). Neuromuscular electrical stimulation promotes development in mice of mature human muscle from immortalized human myoblasts. *Skeletal Muscle*, *6*. https://doi.org/10.1186/s13395-016-0078-6

Salem, A. F., Whitaker-Menezes, D., Howell, A., Sotgia, F., & Lisanti, M. P. (2012). Mitochondrial biogenesis in epithelial cancer cells promotes breast cancer tumor growth and confers autophagy resistance. *Cell Cycle*, *11*(22), 4174–4180. https://doi.org/10.4161/cc.22376

Sandoval, H., Thiagarajan, P., Dasgupta, S. K., Schumacher, A., Prchal, J. T., Chen, M., & Wang, J. (2008). Essential role for Nix in autophagic maturation of erythroid cells. *Nature*, *454*(7201), 232–235. https://doi.org/10.1038/nature07006

Sandri, M. (2013). Protein breakdown in muscle wasting: Role of autophagy-lysosome and ubiquitin-proteasome. *The International Journal of Biochemistry & Cell Biology*, *45*(10), 2121–2129. https://doi.org/10.1016/j.biocel.2013.04.023

Sandri, M., Lin, J., Handschin, C., Yang, W., Arany, Z. P., Lecker, S. H., Goldberg, A. L., & Spiegelman, B. M. (2006). PGC-1alpha protects skeletal muscle from atrophy by suppressing FoxO3 action and atrophy-specific gene transcription. *Proceedings of the National Academy of Sciences of the United States of America*, *103*(44), 16260–16265. https://doi.org/10.1073/pnas.0607795103

Sarraf, S. A., Raman, M., Guarani-Pereira, V., Sowa, M. E., Huttlin, E. L., Gygi, S. P., & Harper, J. W. (2013). Landscape of the PARKIN-dependent ubiquitylome in response to mitochondrial depolarization. *Nature*, *496*(7445), 372–376. https://doi.org/10.1038/nature12043

Sartori, R., Romanello, V., & Sandri, M. (2021). Mechanisms of muscle atrophy and hypertrophy: Implications in health and disease. *Nature Communications*, *12*(1), 330. https://doi.org/10.1038/s41467-020-20123-1

Schiaffino, S., & Margreth, A. (1969). Coordinated development of the sarcoplasmic reticulum and T system during postnatal differentiation of rat skeletal muscle. *The Journal of Cell Biology*, *41*(3), 855–875. https://doi.org/10.1083/jcb.41.3.855

Schofield, J. H., & Schafer, Z. T. (2021). Mitochondrial Reactive Oxygen Species and Mitophagy: A Complex and Nuanced Relationship. *Antioxidants & Redox Signaling*, *34*(7), 517–530. https://doi.org/10.1089/ars.2020.8058

Schreiber, S. N., Emter, R., Hock, M. B., Knutti, D., Cardenas, J., Podvinec, M., Oakeley, E. J., & Kralli, A. (2004). The estrogen-related receptor alpha (ERRalpha) functions in PPARgamma coactivator 1alpha (PGC-1alpha)-induced mitochondrial biogenesis. *Proceedings of the National Academy of Sciences of the United States of America*, *101*(17), 6472–6477. https://doi.org/10.1073/pnas.0308686101

Schreiber, S. N., Knutti, D., Brogli, K., Uhlmann, T., & Kralli, A. (2003). The transcriptional coactivator PGC-1 regulates the expression and activity of the orphan nuclear receptor estrogen-related receptor alpha (ERRalpha). *The Journal of Biological Chemistry*, *278*(11), 9013–9018. https://doi.org/10.1074/jbc.M212923200

Schultz, B. E., & Chan, S. I. (2001). Structures and proton-pumping strategies of mitochondrial respiratory enzymes. *Annual Review of Biophysics and Biomolecular Structure*, *30*, 23–65. https://doi.org/10.1146/annurev.biophys.30.1.23

Schumacker, P. T., Gillespie, M. N., Nakahira, K., Choi, A. M. K., Crouser, E. D., Piantadosi, C. A., & Bhattacharya, J. (2014). Mitochondria in lung biology and pathology: More than just a powerhouse. *American Journal of Physiology-Lung Cellular and Molecular Physiology*, *306*(11), L962–L974. https://doi.org/10.1152/ajplung.00073.2014

Schwarten, M., Mohrlüder, J., Ma, P., Stoldt, M., Thielmann, Y., Stangler, T., Hersch, N., Hoffmann, B., Merkel, R., & Willbold, D. (2009). Nix directly binds to GABARAP: A possible

crosstalk between apoptosis and autophagy. *Autophagy*, *5*(5), 690–698. https://doi.org/10.4161/auto.5.5.8494

Schweers, R. L., Zhang, J., Randall, M. S., Loyd, M. R., Li, W., Dorsey, F. C., Kundu, M., Opferman, J. T., Cleveland, J. L., Miller, J. L., & Ney, P. A. (2007). NIX is required for programmed mitochondrial clearance during reticulocyte maturation. *Proceedings of the National Academy of Sciences*, *104*(49), 19500–19505. https://doi.org/10.1073/pnas.0708818104

Schwerzmann, K., Hoppeler, H., Kayar, S. R., & Weibel, E. R. (1989). Oxidative capacity of muscle and mitochondria: Correlation of physiological, biochemical, and morphometric characteristics. *Proceedings of the National Academy of Sciences*, *86*(5), 1583–1587. https://doi.org/10.1073/pnas.86.5.1583

Seo, J. Y., Park, J., Yu, M. R., Kim, Y. S., Ha, H., & Lee, H. B. (2009). Positive feedback loop between plasminogen activator inhibitor-1 and transforming growth factor-beta1 during renal fibrosis in diabetes. *American Journal of Nephrology*, *30*(6), 481–490. https://doi.org/10.1159/000242477

Servais, S., Letexier, D., Favier, R., Duchamp, C., & Desplanches, D. (2007). Prevention of unloading-induced atrophy by vitamin E supplementation: Links between oxidative stress and soleus muscle proteolysis? *Free Radical Biology & Medicine*, *42*(5), 627–635. https://doi.org/10.1016/j.freeradbiomed.2006.12.001

Sgarbi, G., Matarrese, P., Pinti, M., Lanzarini, C., Ascione, B., Gibellini, L., Dika, E., Patrizi, A., Tommasino, C., Capri, M., Cossarizza, A., Baracca, A., Lenaz, G., Solaini, G., Franceschi, C., Malorni, W., & Salvioli, S. (2014). Mitochondria hyperfusion and elevated autophagic

activity are key mechanisms for cellular bioenergetic preservation in centenarians. *Aging (Albany NY)*, *6*(4), 296–310.

Shi, G., Lee, J. R., Grimes, D. A., Racacho, L., Ye, D., Yang, H., Ross, O. A., Farrer, M., McQuibban, G. A., & Bulman, D. E. (2011). Functional alteration of PARL contributes to mitochondrial dysregulation in Parkinson's disease. *Human Molecular Genetics*, *20*(10), 1966–1974. https://doi.org/10.1093/hmg/ddr077

Shi, R.-Y., Zhu, S.-H., Li, V., Gibson, S. B., Xu, X.-S., & Kong, J.-M. (2014). BNIP3 interacting with LC3 triggers excessive mitophagy in delayed neuronal death in stroke. *CNS Neuroscience & Therapeutics*, *20*(12), 1045–1055. https://doi.org/10.1111/cns.12325

Shiba-Fukushima, K., Imai, Y., Yoshida, S., Ishihama, Y., Kanao, T., Sato, S., & Hattori, N. (2012). PINK1-mediated phosphorylation of the Parkin ubiquitin-like domain primes mitochondrial translocation of Parkin and regulates mitophagy. *Scientific Reports*, *2*, 1002. https://doi.org/10.1038/srep01002

Sin, J., Andres, A. M., Taylor, D. J. R., Weston, T., Hiraumi, Y., Stotland, A., Kim, B. J., Huang, C., Doran, K. S., & Gottlieb, R. A. (2016). Mitophagy is required for mitochondrial biogenesis and myogenic differentiation of C2C12 myoblasts. *Autophagy*, *12*(2), 369–380. https://doi.org/10.1080/15548627.2015.1115172

Singh, A., D'Amico, D., Andreux, P. A., Fouassier, A. M., Blanco-Bose, W., Evans, M., Aebischer, P., Auwerx, J., & Rinsch, C. (2022). Urolithin A improves muscle strength, exercise performance, and biomarkers of mitochondrial health in a randomized trial in middle-aged adults. *Cell Reports Medicine*, *3*(5), 100633. https://doi.org/10.1016/j.xcrm.2022.100633

Song, M., Mihara, K., Chen, Y., Scorrano, L., & Dorn, G. W. (2015). Mitochondrial fission and fusion factors reciprocally orchestrate mitophagic culling in mouse hearts and cultured fibroblasts. *Cell Metabolism*, *21*(2), 273–286. https://doi.org/10.1016/j.cmet.2014.12.011

Sonoda, J., Mehl, I. R., Chong, L.-W., Nofsinger, R. R., & Evans, R. M. (2007). PGC-1beta controls mitochondrial metabolism to modulate circadian activity, adaptive thermogenesis, and hepatic steatosis. *Proceedings of the National Academy of Sciences of the United States of America*, *104*(12), 5223–5228. https://doi.org/10.1073/pnas.0611623104

Spinelli, J. B., & Haigis, M. C. (2018). The Multifaceted Contributions of Mitochondria to Cellular Metabolism. *Nature Cell Biology*, *20*(7), 745–754. https://doi.org/10.1038/s41556-018-0124-1

Stitt, T. N., Drujan, D., Clarke, B. A., Panaro, F., Timofeyva, Y., Kline, W. O., Gonzalez, M., Yancopoulos, G. D., & Glass, D. J. (2004). The IGF-1/PI3K/Akt pathway prevents expression of muscle atrophy-induced ubiquitin ligases by inhibiting FOXO transcription factors. *Molecular Cell*, *14*(3), 395–403. https://doi.org/10.1016/s1097-2765(04)00211-4

Suen, D.-F., Norris, K. L., & Youle, R. J. (2008). Mitochondrial dynamics and apoptosis. *Genes & Development*, *22*(12), 1577–1590. https://doi.org/10.1101/gad.1658508

Sulistijo, E. S., & MacKenzie, K. R. (2009). Structural Basis for Dimerization of the BNIP3 Transmembrane Domain,. *Biochemistry*, *48*(23), 5106–5120. https://doi.org/10.1021/bi802245u

Sun, N., Malide, D., Liu, J., Rovira, I. I., Combs, C. A., & Finkel, T. (2017). A fluorescence-based imaging method to measure in vitro and in vivo mitophagy using mt-Keima. *Nature Protocols*, *12*(8), Article 8. https://doi.org/10.1038/nprot.2017.060

Sun, N., Yun, J., Liu, J., Malide, D., Liu, C., Rovira, I. I., Holmström, K. M., Fergusson, M. M., Yoo, Y. H., Combs, C. A., & Finkel, T. (2015). Measuring In Vivo Mitophagy. *Molecular Cell*, *60*(4), 685–696. https://doi.org/10.1016/j.molcel.2015.10.009

Takahashi, M., & Hood, D. A. (1996). Protein Import into Subsarcolemmal and Intermyofibrillar Skeletal Muscle Mitochondria: DIFFERENTIAL IMPORT REGULATION IN DISTINCT SUBCELLULAR REGIONS *. *Journal of Biological Chemistry*, *271*(44), 27285–27291. https://doi.org/10.1074/jbc.271.44.27285

Takekura, H., Fujinami, N., Nishizawa, T., Ogasawara, H., & Kasuga, N. (2001). Eccentric exercise-induced morphological changes in the membrane systems involved in excitation-contraction coupling in rat skeletal muscle. *The Journal of Physiology*, *533*(Pt 2), 571–583. https://doi.org/10.1111/j.1469-7793.2001.0571a.x

Tannous, P., Zhu, H., Nemchenko, A., Berry, J. M., Johnstone, J. L., Shelton, J. M., Miller, F. J., Rothermel, B. A., & Hill, J. A. (2008). Intracellular protein aggregation is a proximal trigger of cardiomyocyte autophagy. *Circulation*, *117*(24), 3070–3078. https://doi.org/10.1161/CIRCULATIONAHA.107.763870

Tatsuta, T., & Langer, T. (2008). Quality control of mitochondria: Protection against neurodegeneration and ageing. *The EMBO Journal*, *27*(2), 306–314. https://doi.org/10.1038/sj.emboj.7601972

Tezze, C., Romanello, V., Desbats, M. A., Fadini, G. P., Albiero, M., Favaro, G., Ciciliot, S., Soriano, M. E., Morbidoni, V., Cerqua, C., Loefler, S., Kern, H., Franceschi, C., Salvioli, S., Conte, M., Blaauw, B., Zampieri, S., Salviati, L., Scorrano, L., & Sandri, M. (2017). Age-Associated Loss of OPA1 in Muscle Impacts Muscle Mass, Metabolic Homeostasis, Systemic Inflammation, and Epithelial Senescence. *Cell Metabolism*, *25*(6), 1374-1389.e6. https://doi.org/10.1016/j.cmet.2017.04.021

Tondera, D., Czauderna, F., Paulick, K., Schwarzer, R., Kaufmann, J., & Santel, A. (2005). The mitochondrial protein MTP18 contributes to mitochondrial fission in mammalian cells. *Journal of Cell Science*, *118*(14), 3049–3059. https://doi.org/10.1242/jcs.02415

Touvier, T., De Palma, C., Rigamonti, E., Scagliola, A., Incerti, E., Mazelin, L., Thomas, J.-L., D'Antonio, M., Politi, L., Schaeffer, L., Clementi, E., & Brunelli, S. (2015). Muscle-specific Drp1 overexpression impairs skeletal muscle growth via translational attenuation. *Cell Death & Disease*, *6*, e1663. https://doi.org/10.1038/cddis.2014.595

Triolo, M., Slavin, M., Moradi, N., & Hood, D. A. (2022). Time-dependent changes in autophagy, mitophagy and lysosomes in skeletal muscle during denervation-induced disuse. *The Journal of Physiology*, *600*(7), 1683–1701. https://doi.org/10.1113/JP282173

Trumpower, B. L. (1990). The protonmotive Q cycle. Energy transduction by coupling of proton translocation to electron transfer by the cytochrome bc1 complex. *The Journal of Biological Chemistry*, *265*(20), 11409–11412.

Tubbs, E., Chanon, S., Robert, M., Bendridi, N., Bidaux, G., Chauvin, M.-A., Ji-Cao, J., Durand, C., Gauvrit-Ramette, D., Vidal, H., Lefai, E., & Rieusset, J. (2018). Disruption of Mitochondria-Associated Endoplasmic Reticulum Membrane (MAM) Integrity Contributes to Muscle

Insulin Resistance in Mice and Humans. *Diabetes*, *67*(4), 636–650. https://doi.org/10.2337/db17-0316

Twig, G., & Shirihai, O. S. (2011). The Interplay Between Mitochondrial Dynamics and Mitophagy. *Antioxidants & Redox Signaling*, *14*(10), 1939–1951. https://doi.org/10.1089/ars.2010.3779

Vainshtein, A., Desjardins, E. M., Armani, A., Sandri, M., & Hood, D. A. (2015). PGC-1α modulates denervation-induced mitophagy in skeletal muscle. *Skeletal Muscle*, *5*(1), 9. https://doi.org/10.1186/s13395-015-0033-y

Van Houten, B., Woshner, V., & Santos, J. H. (2006). Role of mitochondrial DNA in toxic responses to oxidative stress. *DNA Repair*, *5*(2), 145–152. https://doi.org/10.1016/j.dnarep.2005.03.002

VanderVeen, B. N., Fix, D. K., & Carson, J. A. (2017, July 13). *Disrupted Skeletal Muscle Mitochondrial Dynamics, Mitophagy, and Biogenesis during Cancer Cachexia: A Role for Inflammation* [Review Article]. Oxidative Medicine and Cellular Longevity; Hindawi. https://doi.org/10.1155/2017/3292087

Vertel, B. M., & Fischman, D. A. (1977). Mitochondrial development during myogenesis. *Developmental Biology*, *58*(2), 356–371. https://doi.org/10.1016/0012-1606(77)90097-5

Vianna, C. R., Huntgeburth, M., Coppari, R., Choi, C. S., Lin, J., Krauss, S., Barbatelli, G., Tzameli, I., Kim, Y.-B., Cinti, S., Shulman, G. I., Spiegelman, B. M., & Lowell, B. B. (2006). Hypomorphic mutation of PGC-1beta causes mitochondrial dysfunction and liver insulin resistance. *Cell Metabolism*, *4*(6), 453–464. https://doi.org/10.1016/j.cmet.2006.11.003

Wakabayashi, J., Zhang, Z., Wakabayashi, N., Tamura, Y., Fukaya, M., Kensler, T. W., Iijima, M., & Sesaki, H. (2009). The dynamin-related GTPase Drp1 is required for embryonic and brain development in mice. *The Journal of Cell Biology*, *186*(6), 805–816. https://doi.org/10.1083/jcb.200903065

Wang, F., Zhou, T., Zhou, C. X., Zhang, Q. B., Wang, H., & Zhou, Y. (2023). The worsening of skeletal muscle atrophy induced by immobilization at the early stage of remobilization correlates with BNIP3-dependent mitophagy. *BMC Musculoskeletal Disorders*, *24*, 632. https://doi.org/10.1186/s12891-023-06759-2

Wang, X. J., Yu, J., Wong, S. H., Cheng, A. S. L., Chan, F. K. L., Ng, S. S. M., Cho, C. H., Sung, J. J. Y., & Wu, W. K. K. (2013). A novel crosstalk between two major protein degradation systems: Regulation of proteasomal activity by autophagy. *Autophagy*, *9*(10), 1500–1508. https://doi.org/10.4161/auto.25573

White, R. B., Biérinx, A.-S., Gnocchi, V. F., & Zammit, P. S. (2010). Dynamics of muscle fibre growth during postnatal mouse development. *BMC Developmental Biology*, *10*(1), 21. https://doi.org/10.1186/1471-213X-10-21

Willingham, T. B., Ajayi, P. T., & Glancy, B. (2021). Subcellular Specialization of Mitochondrial Form and Function in Skeletal Muscle Cells. *Frontiers in Cell and Developmental Biology*, *9*. https://www.frontiersin.org/articles/10.3389/fcell.2021.757305

Wohlgemuth, S. E., Seo, A. Y., Marzetti, E., Lees, H. A., & Leeuwenburgh, C. (2010). Skeletal muscle autophagy and apoptosis during aging: Effects of calorie restriction and life-long exercise. *Experimental Gerontology*, *45*(2), 138–148. https://doi.org/10.1016/j.exger.2009.11.002

Wu, K.-C., Lin, H.-W., Chu, P.-C., Li, C.-I., Kao, H.-H., Lin, C.-H., & Cheng, Y.-J. (2023). A non-invasive mouse model that recapitulates disuse-induced muscle atrophy in immobilized patients. *Scientific Reports*, *13*(1), 22201. https://doi.org/10.1038/s41598-023-49732-8

Xu, Z., Fu, T., Guo, Q., Zhou, D., Sun, W., Zhou, Z., Chen, X., Zhang, J., Liu, L., Xiao, L., Yin, Y., Jia, Y., Pang, E., Chen, Y., Pan, X., Fang, L., Zhu, M., Fei, W., Lu, B., & Gan, Z. (2022). Disuse-associated loss of the protease LONP1 in muscle impairs mitochondrial function and causes reduced skeletal muscle mass and strength. *Nature Communications*, *13*(1), Article 1. https://doi.org/10.1038/s41467-022-28557-5

Yajid, F., Mercier, J. G., Mercier, B. M., Dubouchaud, H., & Préfaut, C. (1998). Effects of 4 wk of hindlimb suspension on skeletal muscle mitochondrial respiration in rats. *Journal of Applied Physiology (Bethesda, Md.: 1985)*, *84*(2), 479–485. https://doi.org/10.1152/jappl.1998.84.2.479

Yamano, K., Matsuda, N., & Tanaka, K. (2016). The ubiquitin signal and autophagy: An orchestrated dance leading to mitochondrial degradation. *EMBO Reports*, *17*(3), 300–316. https://doi.org/10.15252/embr.201541486

Yamano, K., & Youle, R. J. (2011). Coupling mitochondrial and cell division. *Nature Cell Biology*, *13*(9), 1026–1027. https://doi.org/10.1038/ncb2334

Yamano, K., & Youle, R. J. (2013). PINK1 is degraded through the N-end rule pathway. *Autophagy*, *9*(11), 1758–1769. https://doi.org/10.4161/auto.24633

Yamashita, S.-I., Kyuuma, M., Inoue, K., Hata, Y., Kawada, R., Yamabi, M., Fujii, Y., Sakagami, J., Fukuda, T., Furukawa, K., Tsukamoto, S., & Kanki, T. (2021). Mitophagy reporter mouse

analysis reveals increased mitophagy activity in disuse-induced muscle atrophy. *Journal of Cellular Physiology*. https://doi.org/10.1002/jcp.30404

Yeo, D., Kang, C., Gomez-Cabrera, M. C., Vina, J., & Ji, L. L. (2019). Intensified mitophagy in skeletal muscle with aging is downregulated by PGC-1alpha overexpression in vivo. *Free Radical Biology and Medicine*, *130*, 361–368. https://doi.org/10.1016/j.freeradbiomed.2018.10.456

Ying, Z., Liu, Z., Xiang, G., Xin, Y., Wang, J., & Liu, X. (2021). Protocols for analysis of mitochondrial permeability transition pore opening in mouse somatic cell reprogramming. *STAR Protocols*, *2*(2), 100568. https://doi.org/10.1016/j.xpro.2021.100568

Youle, R. J., & Karbowski, M. (2005). Mitochondrial fission in apoptosis. *Nature Reviews Molecular Cell Biology*, *6*(8), Article 8. https://doi.org/10.1038/nrm1697

Youle, R. J., & van der Bliek, A. M. (2012). Mitochondrial fission, fusion, and stress. *Science (New York, N.Y.)*, *337*(6098), 1062–1065. https://doi.org/10.1126/science.1219855

Zechner, C., Lai, L., Zechner, J. F., Geng, T., Yan, Z., Rumsey, J. W., Collia, D., Chen, Z., Wozniak, D. F., Leone, T. C., & Kelly, D. P. (2010). Total skeletal muscle PGC-1 deficiency uncouples mitochondrial derangements from fiber type determination and insulin sensitivity. *Cell Metabolism*, *12*(6), 633–642. https://doi.org/10.1016/j.cmet.2010.11.008

Zhang, J., & Ney, P. A. (2009). Role of BNIP3 and NIX in cell death, autophagy, and mitophagy. *Cell Death and Differentiation*, *16*(7), 939–946. https://doi.org/10.1038/cdd.2009.16

Zhang, T., Xue, L., Li, L., Tang, C., Wan, Z., Wang, R., Tan, J., Tan, Y., Han, H., Tian, R., Billiar, T. R., Tao, W. A., & Zhang, Z. (2016). BNIP3 Protein Suppresses PINK1 Kinase Proteolytic

Cleavage to Promote Mitophagy. *The Journal of Biological Chemistry*, *291*(41), 21616–21629. https://doi.org/10.1074/jbc.M116.733410

Zhou, J., Li, G., Zheng, Y., Shen, H.-M., Hu, X., Ming, Q.-L., Huang, C., Li, P., & Gao, N. (2015). A novel autophagy/mitophagy inhibitor liensinine sensitizes breast cancer cells to chemotherapy through DNM1L-mediated mitochondrial fission. *Autophagy*, *11*(8), 1259–1279. https://doi.org/10.1080/15548627.2015.1056970

Zhu, Y., Massen, S., Terenzio, M., Lang, V., Chen-Lindner, S., Eils, R., Novak, I., Dikic, I., Hamacher-Brady, A., & Brady, N. R. (2013). Modulation of serines 17 and 24 in the LC3-interacting region of Bnip3 determines pro-survival mitophagy versus apoptosis. *The Journal of Biological Chemistry*, *288*(2), 1099–1113. https://doi.org/10.1074/jbc.M112.399345

Zhuang, A., Yang, C., Liu, Y., Tan, Y., Bond, S. T., Walker, S., Sikora, T., Laskowski, A., Sharma, A., de Haan, J. B., Meikle, P. J., Shimizu, T., Coughlan, M. T., Calkin, A. C., & Drew, B. G. (2021). SOD2 in skeletal muscle: New insights from an inducible deletion model. *Redox Biology*, *47*, 102135. https://doi.org/10.1016/j.redox.2021.102135